NEW OPTICAL SENSING SYSTEM APPLIED TO TAUT WIRE BASED STRAIGHTNESS MEASUREMENT

BY

OLEG BORISOV

A thesis submitted to the University of Huddersfield in partial fulfilment of the requirements for the degree of Doctor of Philosophy

The University of Huddersfield
May 2015

ABSTRACT

In modern manufacturing industry, precision components are typically produced on Computer Numerical Controlled (CNC) machine tools which translate their accuracy onto machined parts. This accuracy is affected by a set of different motion errors caused by inherent imperfections in the design and build of the machine, variations in the local environment such as temperature, the cutting process itself and human factors. The reduction of these effects is achieved primarily through design improvements and error compensation techniques. The latter requires detailed knowledge about the existing errors in order to deal with them effectively.

This thesis describes a novel sensor system for measurement of errors caused by deviation in the straightness of Cartesian axes present in the structural loop of most machine tools. Currently there are very few methods available to measure straightness directly, each having advantages and disadvantages when considering simplicity, accuracy and affordability. The proposed system uses a taut wire reference with a novel sensor, a two-point technique for reference error cancellation and software to enable fast and accurate measurement of straightness between any two points of the measured machine's working volume.

The standout features of the sensing system include ultra-low cost and high performance when compared with existing state-of-the-art systems. It is capable of measuring a straightness error as low as 3µm and takes only 2s of dwell time between readings, while laser interferometer requires 4s to perform averaging when measuring the same error. Existing taut wire microscopy is limited by 10-20µm of measured error depending on optics quality and manual reading takes at least 5s to minimise the human error. Setup time is also different – the new system saves 15 minutes time on 2m axis and more on longer lengths compared the laser due to simpler reference alignment procedure.

Theoretical analysis and practical implementation are followed by detailed performance evaluation experiments carried out under typical manufacturing conditions comprising different machine tools, different axes, measured errors, environmental effects and alternative measuring equipment. Tests cover aspects of accuracy, repeatability and overall system stability providing a complete picture of the system's capability and the method's potential which is also supported by uncertainty analysis. In addition to defining setup and measuring procedures, a user-friendly software interface is described and its main units are explained with respect to overall measurement efficiency and setup fault detection.

ACKNOWLEDGEMENTS

The author would like to thank Dr Simon Fletcher, Dr Andrew P Longstaff and Prof. Alan Myers for supervising the project, providing all necessary support and guidance during the work which could not have been completed without the knowledge and experience that was shared.

Thanks also to my brother Alexander for his valuable advice regarding electronics, parts machining and assembly of the instrument, provided to support the work.

CONTENTS

FIGURE, TABLE AND EQUATION LIST

Equations:

CHAPTER 1 | MACHINE TOOL CALIBRATION APPROACH

1.1 PREAMBLE

Manufacturing industry in the modern world plays a role of extreme importance. It is more or less involved in almost any of human's activities as those always require material objects which have been somehow manufactured and produced in numbers which could not be possible without the use of a variety of automated machinery.

Manufacturing typically involves processing raw materials in some way to produce components. This process is often achieved using automated precision machinery such as metal cutting machines including lathes, milling and drilling machines, Electrical Discharge Machines (EDMs) and many other types.

Being complex, expensive and industry determinative, such machines are characterised by their features and capability. These include the metal removal method, spindle speeds and power, internal workspace volume, number of axes, performance (accuracy and repeatability) and sometimes flexibility and modularity. As is true in industry in general, end users of machines demand more capability and features as they endeavour to improve quality and reduce costs.

One of the most important characteristics of a machine tool is the ability to produce components accurately and efficiently i.e. with stable and high level of shape and dimensional quality. The more accurate the machine tool is the more accurate components it can be used to produce. This gives many advantages to the whole manufacturing process, such as:

1. Reduced tolerances enabling more accurate assemblies resulting in improved performance.
2. Simplification of assembly reducing its selective phase.
3. Reduction of scrap and rework amount.
4. Reduction in the number of machine tools needed for cutting a single part.

All of the above increase demand for ever more accurate machine tools as a key factor of an efficient manufacturing process.

Traditionally, the first approach to increase the accuracy was design improvement. More rigid foundations, manually scraped guide ways, special cooling systems did increase the level of accuracy but with additional cost, including maintenance and dedication to a certain finishing operations only.

The knowledge that costs can rise considerably as tolerances reduce, gave way to an alternative approach based on keeping available design but using it with higher efficiency. The principle here is not reducing the errors caused by the design, wear, environmental and cutting conditions but compensating them, applying counter-motions through feed drives. The hardware remains the same and considerable investments may be avoided.

Error compensation can be active or pre-calibrated. In the first case additional hardware and software is used to enhance the machine's controller so that during finishing cutting stage the axes move according to a part program containing all necessary corrections to minimise motion errors. The correction data is usually obtained by probing the part before machining. Active compensation can offer very accurate results and considers the majority of error sources but there are disadvantages such as necessity to adapt the compensation system to machines interface which might restrict the system's application on another machine, extra time needed for probing and probe errors that can be caused by swarf on the surface of the workpiece when small particles of the material interfere with probe as it slides over the measured surface.

Pre-calibrated compensation differs in that the errors are calculated from measurements of a variable other than the actual distortion between the tool and workpiece. For example, a system developed at the University of Huddersfield by Postlethwaite [1] uses standard laser calibration data produced by Renishaw laser software package (linear, angular, straightness and squareness). This data is transformed into a table of error values corresponding to axis position (error map). A computer running CNC-compatible software is connected to machine's controller, the software uses error map to generate the correction values which are then fed into the CNC to modify the motion commands sent directly to the feed drives.

This kind of compensation requires knowledge of the machine tool errors which is normally obtained by measuring them with the help of existing measurement equipment and methods. Consequently, the success of compensation strongly depends on how accurately the individual errors have been measured and how well the produced error map corresponds to the machine's structure [2]. In some cases separately measured errors can influence each other and their functions can crosstalk, therefore a great care is recommended during error map synthesis.

The error map uses large number of different factors which can be measured separately or together, forming three major groups: thermal, non-rigid and geometric errors.

1.1.1 Machine tool errors

Thermal errors are caused by inevitable distortions of machine's structure due to temperature changes. The main sources of heat are environmental temperature variations, internal heat generation and radiant heating. Resulting errors become significant as machine mechanical specifications improve and tolerances tighten. Thermal problem is complex [3] and normally addressed in many different ways, which can be categorised into: minimising heat generation or heat effect, and error compensation. Despite being large, thermal errors can be successfully reduced by temperature control systems and intermittent re-datuming. Fletcher *et al* [4] discusses a simplified error model for a small vertical milling machine. This model was validated during a random duty cycle of the spindle. The author reports that position independent thermal error in Y-axis direction reduced from 71μm to 7.5μm (≈90%) and Z-axis error reduced from 14 to 3.5 (≈75%). Position dependent thermal error result is even better – 27μm reduced to 2μm which is a reduction of 91%. Both results confirm successful application of thermal error compensation technique.

Non-rigid body errors occur due to loading of the machine structural elements [5, 6]. The causes can be movement of machine axes, workpiece weight, cutting load, variable tool weight and insufficient fixture stiffness. These factors all contribute to deformations within the machine and lead to inaccuracies which are generally thought of as the smallest part of total error.

Geometrical errors are generally described in the way of three translational and three rotational motions along a single axis. Translational errors are known as linear positioning error and two straightness errors (vertical and horizontal), and rotational as roll pitch and yaw. Increasing the number of linked axes causes additional error components to arise: for example for a 3-axis machine these are three squareness errors between the nominally perpendicular axes. This results in a total of 21 error components. To increase machine capability, it is common to add one or two rotary axes. Considering the case of a 5-axis machine tools, the total number of errors increases to 39 according to Bohez [7].

Typically, geometric errors have the most effect on machine tool accuracy [8]: they originate from mechanical imperfections in the structure and its assembly and therefore always present, even in a perfect environment and with negligible cutting forces, resulting in shape and dimensional artefacts on machined parts and predominantly limiting their accuracy.

The six degrees-of-freedom (DoF, Figure 1) for Cartesian and rotary axes are described in detail in international standards [9].

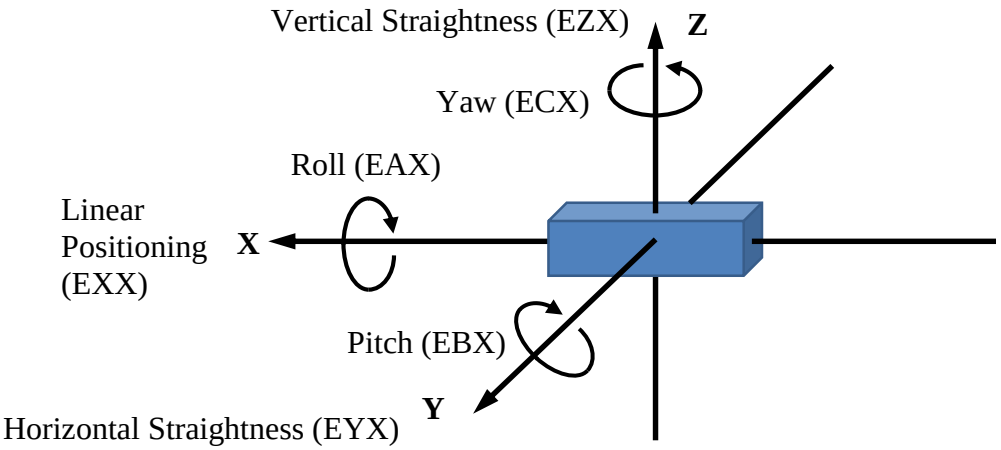

Figure 1. Six degrees of freedom of a moving object

Two of the unwanted DoF are described as straightness motion error of any linear axis which directly influence the straightness and flatness of surfaces as well as the form, location and orientation of geometric features of the workpiece produced.

Measuring the straightness motion of axes is of importance for machine tool accuracy assessment but the methodology and equipment currently available have disadvantages which will be discussed in the next chapter thereby providing motivation for the alternative solution.

1.2 INTRODUCTION TO STRAIGHTNESS

The measurement of straightness is prolific in dimensional measurement and it is important to understand its definition when developing a new measuring system and/or strategy. The Oxford English Dictionary [10] defines the word “straightness” as “quality of being straight, in various senses of the adjective”. Word “straight” according to the same source has two meanings: “Extended at full length” and “Not crooked; free from curvature, bending, or angularity curvature, bending, or angularity”. Applied to a line it sounds as “…uniform in direction throughout its length”.

Normally straightness characterises a line connecting two points. The shortest possible one is absolutely straight, all others are less straight. The longer the line, the less straight it is.

The geometric entity in Figure 2a is a straight line, while the three others are clearly not straight. Commonly straightness is being measured for lines which have bending angle less than 90 degrees (Figure 2 b-c). If it is greater (Figure 2d), then determining a straightness of such a line becomes meaningless.

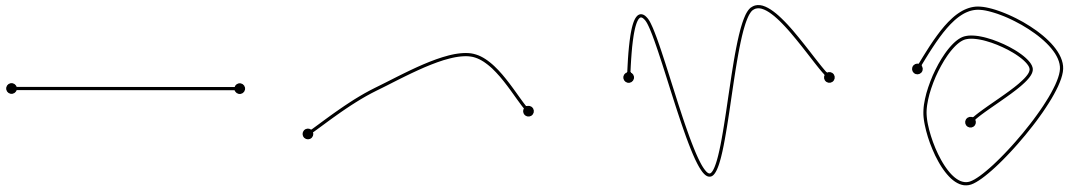

Figure 2. Line examples with change in linearity

The degree of straightness is determined by measuring maximum distance between two parallel straight lines which encompass the intended measured line in the direction of measurement. Location of those two lines affects the result and depends on background of the measurement. For machine tools, straightness measurement is explained by the International Standard ISO230-1 [9] in two ways: straightness of a line on a plane (a) and in space (b):

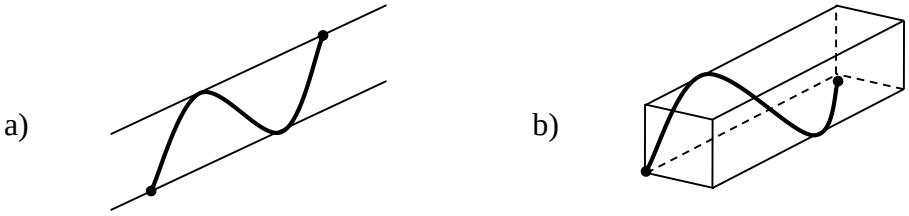

Figure 3. Straightness in plane and in space

In both cases depicted in Figure 3 measurement involves a representative line which specifies the direction of two parallel straight lines used to determine the level of straightness of a target line. It is recommended to position the representative line so that it connects the end points of the measured line, as shown in Figure 4 (dashed):

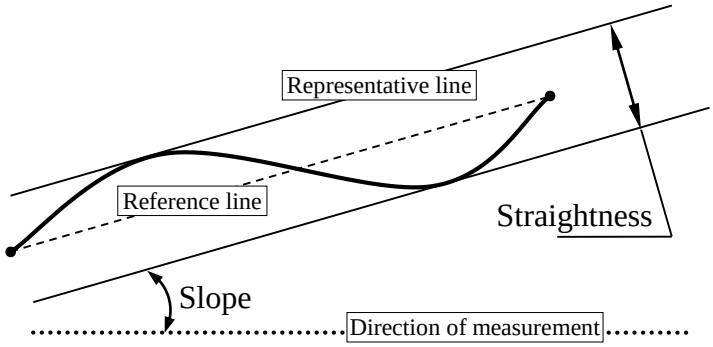

Figure 4. Positioning of a representative line

Alternatively, least squares fitting is used to obtain a representative line; due to relying on more points it gives more consistent results compared to end point fitting and is recommended by ISO standard [9]. It is important for side by side comparison of multiple straightness profiles obtained from various methods.

When it comes to measurement practice, the fourth line, called a reference line is used (Figure 4, dotted). It is a material or optical reference that is either straight (relative to the measured line) or has a known profile unless a reversal technique [9] is used which requires reference stability. It might be a straightedge, a laser beam, or a taut wire.

There is always an angular difference between representative and reference lines which is called "slope". Generally it is recommended to minimise the slope angle by positioning the reference line so that readings on both ends of the measured line are within a recommended range depending on the instrument. In case of laser interferometer slope error has to be less than 20 microns for short range (axes up to 4m) measurements and the reasons for such a requirement is a necessity to maintain high level of received signal, keep positioning along the measured axis at maximum and avoid translation of slope error into measured straightness error. Therefore, slope elimination normally precedes the measurement.

1.2.1 Measurement methodology

The aforementioned ISO standard [9] describes methods of measuring straightness. All of them involve measuring angles or displacements which are dependent of each other. Using straightedge artefacts as a reference for another surface of similar length can be measured using a linear displacement sensor attached to the spindle and contacting the reference surface while the axis moves along it. The advantages of this method are simplicity, low cost and relatively high accuracy due to reversal techniques allowing minimisation of imperfections in the straightedge itself [9]. The main disadvantage is that the measured surface length should not exceed the length of a reference artefact used. It can become impractical to have very long artefacts due to their weight, cost and stability.

Optical instruments such as alignment telescopes, alignment lasers and laser interferometers do not have the aforementioned restrictions in terms of measuring length. Telescopes and alignment laser methods suitable for angular measurements are based on visual inspection of the displacement of a light source, moving along the measured axis against optics, mounted on a machine. The problem here is that measurement accuracy depends on beam pointing stability and the optical path greatly affected by inhomogeneity in the interfacial air, particularly in case of long strokes or changing temperature conditions [2]. (beam deviation of 50μm in 10m of travel in a vertical temperature gradient of 1K/m, pointing error of nearly 2 arc-sec, Estler [11], more in section 2.3)

Using a laser interferometer for measuring straightness potentially enables higher accuracy due to the use of a stable wavelength as the reference and automated data capture. The setup can be more complicated – an example is shown in Figure 5.

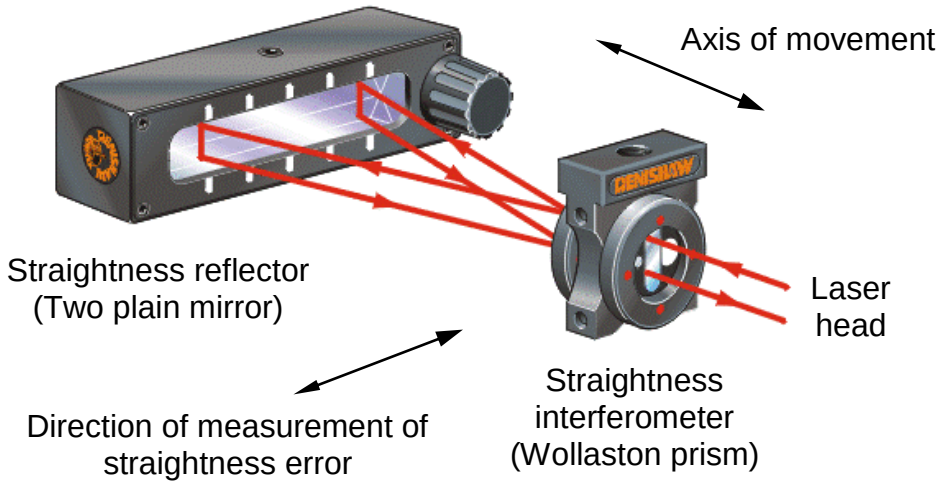

Figure 5. Measuring straightness with a laser (adopted from Renishaw)

A laser beam is split by the moving optics, one branch considered as a reference, another – as measured one. Both are reflected back to the laser device and compared.

Such a setup implements an error cancellation principle according to which, due to their proximity, factors affecting both laser beams after the splitter are subtracted from each other, theoretically leaving just the systematic measured value. However, in practice this is only partially effective as the error caused by noise is random. This is exacerbated when long range optics are used (for measurements between 4 and 20m) where the sensitivity to air turbulence in increases greatly (Figure 6, regular workshop with no temperature control [12]). ISO 230 part 1, section 8.2.2.5 [9] recommends drift tests before measurements.

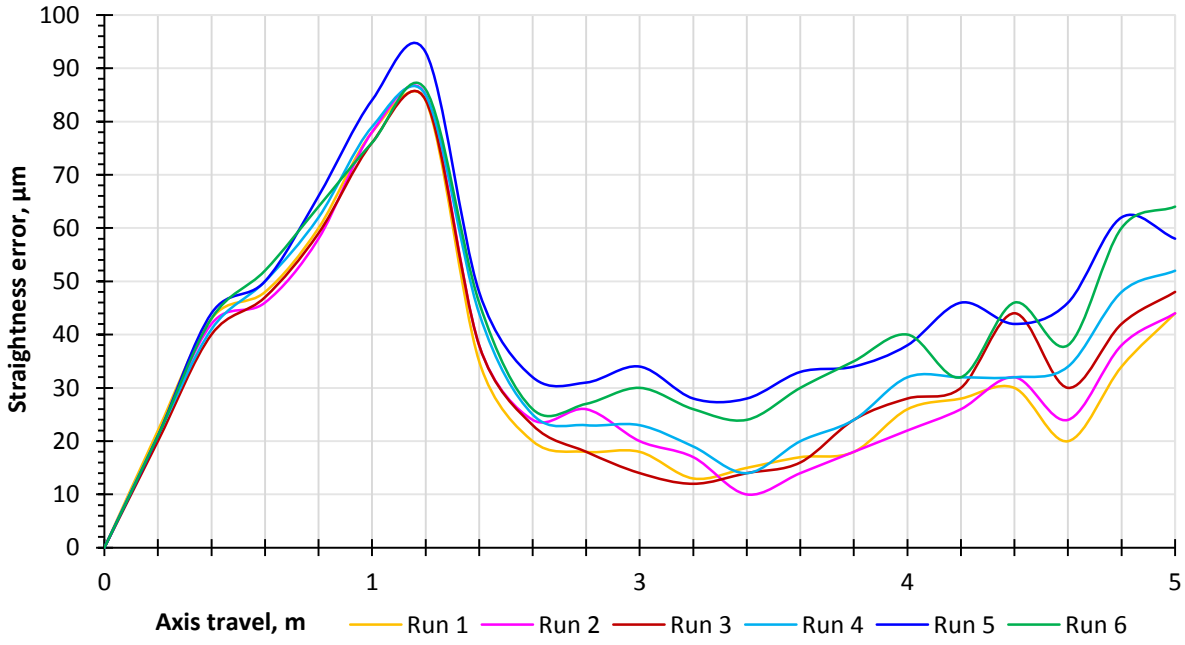

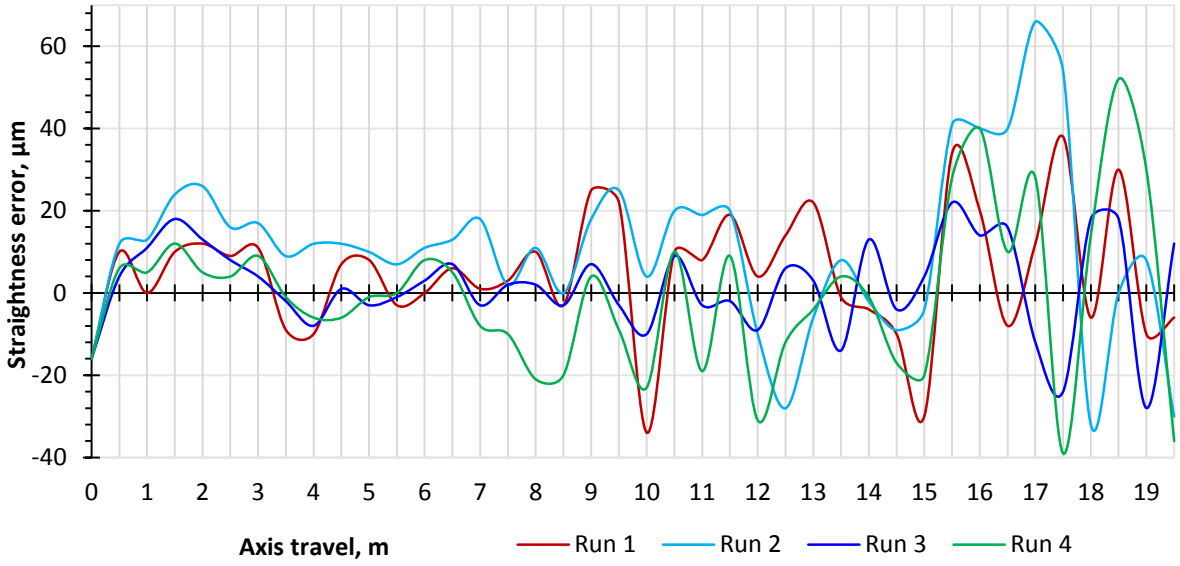

Figure 6. Straightness laser measurements of 5m and 20m axes

Another method for straightness measurement of components utilises the direction of the gravitational vector as a reference. Using an electronic level, the angular change of a surface, e.g. a guide way, in relation to the gravity field of the earth is observed. By integrating the angle over the stepwise displacement of the level along the surface, the straightness of the surface can be evaluated. However, it often more difficult to know the precise integration distance because it relates to the spacing between the contacting points (feet) of the guiding systems and is therefore not recommended.

Yellowhair *et al* [13] analysed measurement errors of precision electronic levels and names two main sources of error: environmental (thermal) drift and random noise. These two are considered unavoidable and can contaminate the result.

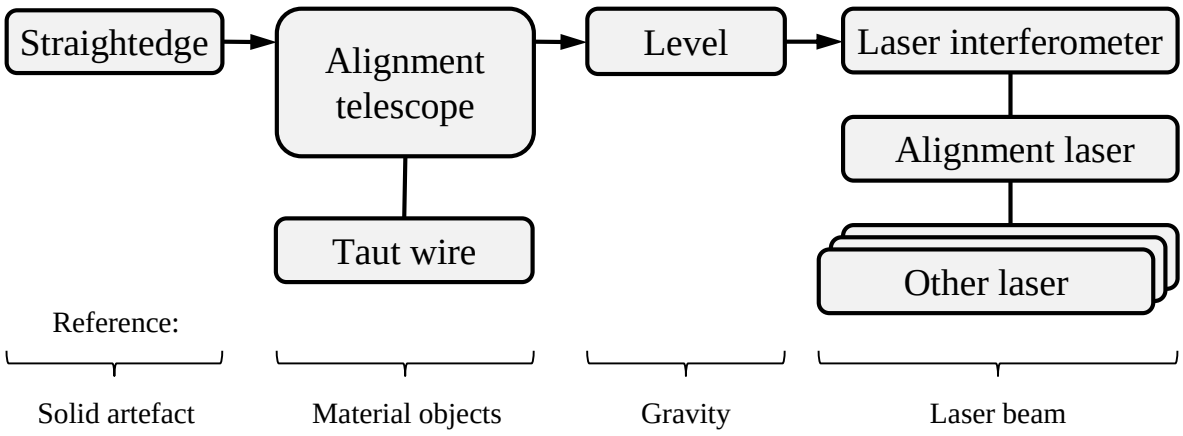

Figure 7. Direct methods of straightness measurement

All up to date direct measurement methods are summarised in Figure 7. These are grouped by reference which is a wire, stretched between two points in case of the taut wire method. It involves manual operations with a microscope [9], making it prone to human error, time consuming and suitable for large machines due to the high magnitude of measured error.

1.2.2 Importance of straightness measurement

Within some manufacturing environments it has been evidenced that measurement of all the contributors to volumetric performance is often not completed. Positioning measurements using laser interferometers were the most common with additional angular measurements either with the additional optics required for angular measurement using the laser or with precision inclinometers. Similarly squareness measurements using the Renishaw Ballbar or artefacts were common and generally the measured errors were easy to reduce by mechanical adjustment. The least frequently measured have been straightness errors. In most cases where the laser interferometer was the primary instrument for measuring the machines, the reasons were either that the additional optics were not purchased due to cost or/and the set-up was difficult and time-consuming.

As a faster alternative to conventional laser interferometer-based linear, angle and straightness measurements arose – group of diagonal tests (including vector and step diagonal methods [14], [15]). Chapman in his paper [16] discusses limitations of those methods coming to a conclusion that they are suitable for machines with significant volumetric error only, otherwise providing unreliable results not justifying potential savings in test time. Ibaraki *et al* state that environmental uncertainty of those methods is also high [17].

Where artefacts were used, a limited axial range was the only but significant drawback. (Here and after, term “axial range” will be used to indicate a longevity of the axis, straightness of which could be measured using an instrument. Standards do not provide a specific definition of this parameter, therefore, “axial range” is suggested).

Even if direct measurement is successfully applied this might not be sufficient as often such methods are not efficient when individual errors need to be measured for remedial work on the axis or synthesis models and associated equipment are not suitable or available for the machine. Then machine tool capability assessment should involve geometry tests including straightness. It is not only because straightness of axes is reflected on the machined surfaces with shape tolerances, but also for determining volumetric performance [9] or when applying compensation, it is important to include all main errors as partial measurement can give a false output or reduce the accuracy due to a number of errors cancelling each other out.

1.2.3 Thesis structure

The next chapter will describe the work which has been published on machine tool measurements: starting from different approaches to accuracy assessment, it will involve all main factors affecting machine tool's accuracy, pointing out the place and importance of straightness measurement. The aim of this project will be formulated.

Chapter three will discuss the development of the proposed measuring system starting from design requirements and corresponding straightness reference and continuing to the exact implementation and basic tests to confirm the choice of materials, sensors and basic setup technique. After that reference error cancellation will be discussed including catenary and wire diameter variation effects, finishing with sensor calibration to equalise and linearize multiple sensor output.

The next two chapters, fourth and fifth, will contain the actual test results on different machines, when the system is compared against the industrial laser interferometer in different environmental conditions, on axes of different lengths and different measured error values. This will provide validation data for the new system, show its capability and practical performance.

Chapter six will present an uncertainty analysis of straightness measurement with both tools, summarising the data from measurement errors assessment and then the data flow processing will be discussed explaining all operations needed to convert the signal from the measuring head to straightness error reporting. This will also include preliminary checks for setup validation.

The last, seventh, chapter, will bring all the results together and make conclusions on the work done, suggesting the directions of further development.

CHAPTER 2 PREVIOUS WORK ON MACHINE TOOL CALIBRATION

Achieving the required accuracy level is often a challenge because there are a large number of factors affecting it. Florussen *et al* [18] name four groups of errors responsible for deviations in a tool path of any machine:

1. Geometrical errors in the guide way systems.
2. Finite stiffness of the structural loop under static load.
3. Thermal behaviour.
4. Dynamic behaviour of the machine.

The first three are called quasi-static and defined as sources causing errors in the relative location between the tool and the work piece that are varying slowly in time and are related to the structure of the machine tool itself. These quasi-static errors account for the largest part (about 70%) of the errors attributable to the machine [19]. Dynamic errors are considered to have an effect mostly on machined surface roughness rather than on its dimensions when spindle speeds are optimised (otherwise cutting force error will dominate [20]).

Here and after geometrical error will be discussed mostly as it is highly systematic (produced by stiff structure), effective under any load and during any machine operation in any part of the working volume.

Finite stiffness of the structural loop has a different effect on accuracy depending on load and is usually more difficult to measure and improve.

Thermal behaviour can be highly non-linear due to multiple heat sources and variable specific heat capacity of the different structural elements. However, various modelling methods, typically using temperature measurement, have been applied successfully to compensate thermal errors. Measuring methods are well defined and described in ISO 230 part 3 [21] which can generally be applied to most machines.

The work done on measurement and compensation of geometric errors will be discussed in the next three sections gradually focusing on straightness error measurement as a main subject of this research project.

2.1 ACCURACY ASSESSEMENT

There are two approaches to volumetric error assessment of the machine: *direct measurement* and *error synthesis* method [22]. In the first case all or most of the geometric errors are measured together i.e. it is the direct measurement of their combined effect that is measured, using tools such as artefacts, ballbars and laser trackers. Alternatively, various equipment, some of which have already been mentioned, is used to measure each geometric error component separately and the volumetric error is synthesised using a model of the machine. In both cases one of the main outcomes is the determination of the volumetric accuracy which takes into account all geometric errors in every point of machine's working volume [22] to provide a good indication of the machines production capability. Both approaches have their own advantages and disadvantages and both are widely used in industry.

Referring to geometric error components, positioning errors are the most common to measure and to control. Most machine tools have some form of electronic compensation to automatically reduce this error.

Straightness error measurement will be discussed separately further in the third part of the literature review. Angular errors can be measured using optics. For example, Huang *et al* [23] propose a method based on internal reflection within a prism. This relatively simple low cost solution comprises a laser diode as a light source, two beam splitters, two prisms and two photodiodes (Figure 8). The method is based on measuring reflected light which changes with angular displacement. Main challenge here is a compensation of nonlinearity error of reflected laser beam as a reaction on angular displacement. A differential method of linearization is described: two photodiodes are used and both work in opposite sides of their sensitivity area. The average of both signals is taken which ensures subtraction of nonlinear parts of both.

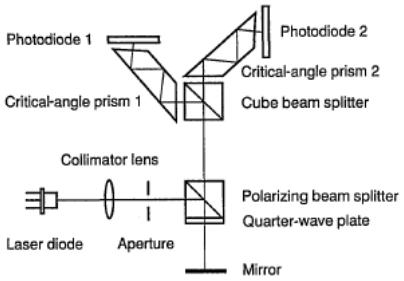

Figure 8. Optical layout of the prototype sensor

A potential limitation of this method is the necessity to have two identical prisms as well sensors. The difference that may occur can limit the accuracy of measurement, the paper

does not address that, limiting possible error sources by angular displacement of the laser beam in the plane perpendicular to the measurement plane and beam divergence only.

A complete measurement approach is presented by Rahman *et al* [24]: in which a laser interferometer is used to find roll, pitch, yaw and positioning errors of multi-axis machine tools, and with a linear comparator – positioning, straightness and squareness errors. Volumetric error is then calculated using homogenous transformation matrices and approximation of measured error in one part of machine's working volume to all the rest of it. The method relies on interpolation of error values which assumes even error distribution in the workspace – that might not be the case. Also the model is suitable for simple 3-axis machines only and cannot be applied to more complicated structures.

A simpler and less computationally intensive method is described by S. Fletcher *et al* [22]. The machine tool geometric model is constructed by adding the effects of each contributing error by studying the machine geometry and applying a simple measurement protocol. Errors, measured separately with Abbe offset and sign taken into account, are added together giving a total (volumetric) error. In order to determine the volumetric performance anywhere in the volume, a vector difference method is used to compare all the errors which gives a result that is independent of the measuring set-up i.e. where the measurement are datumed (typically the machine reference position). It is recommended to use software and simplified model to deal with high density of points in the working volume.

Direct measurement of volumetric error can be achieved using laser trackers or sequential multilateration such as the commercial systems such as the Etalon LaserTracer [25]. Models are available for most of 3 and 5-axis machines. Such equipment is usually very expensive and therefore research into using a telescoping double ballbar, a low cost device typically used for quick check circularity measurements, to obtain volumetric error has been prolific and is reviewed here.

Pahk *et al* [26] discuss volumetric error models for column-type and horizontal machining centres. Input data for polynomial based models is obtained from circular tests performed using a 150mm telescoping ballbar. Positional errors, straightness and angular components are calculated from measured circular patterns. Both models are validated by subtracting calculated error values from original raw data plots to obtain circles with reduced residual error.

Two measurement methods using the ballbar are proposed by Wang and Ehmann [27]. The first one, based on triangulation principle, requires positioning a ballbar three times within the working volume to get sufficient information for calculating positioning errors of

the machine in every point of its working volume. A significant disadvantage here is the ballbar length limitation – as the spindle is not moving, it needs to be connected with three points on the table using ballbars of different lengths which may have different accuracy. The second method called "single socket" uses three points in the volume which can be located close to each other i.e. within the range of one ballbar. Although easier and more flexible, this method requires special location of the ballbar and is more sensitive to its own error. The exact amount of self-induced error is uncertain as no accuracy estimation or experimental tests have been included.

A universal measurement model for the ballbar is presented by Florussen *et al* [18]; it uses simple and fast length measurements to determine position errors. Only five ballbar positions are required to collect data for all measurement points and estimate geometrical error components in the volume defined by the ballbar's working range. The proposed model showed poor correlation and hence the authors introduce correlation coefficients. Another issue is a poor sensitivity of the method to straightness errors and presence of dominant rotational error. There are some optimisations that can be applied to the model to improve repeatability however predicted and measured results do not always match.

Laser interferometry is a commonly used method of determining individual geometric error components which has also been applied in direct measurement strategies. The ISO 230 part 6 standard [28] provides instructions that have been used for estimating volumetric accuracy from face and body diagonal tests which are relatively quick to perform but they cannot provide an unambiguous description of the magnitude of the individual contributing error components affecting the tool point in each axis direction [15, 29].

Chen *et al* [14] introduce a simplified diagonal laser test. Only 15 length measurements are sufficient to calculate all 21 geometric errors of a Cartesian 3-axis machine using the model proposed. The method shows good correlation with traditional measurements and is less time consuming due to the decreased number of intermediate measurements. The measurement of lengths only can further decrease measurement uncertainty compared to a system including straightness and angular measurements as these typically have higher levels of uncertainty.

A further attempt to reduce the number of tests for complete volumetric assessment using the synthesis method is made by Fan *et al* [14]. Three parallel laser beams are used together with corresponding optics to measure all six errors of a moving stage at once. This makes the process significantly faster and less affected by environmental temperature changes compared to a set of separate tests. The system, potentially being simpler and lower in cost than commercial laser systems, claims to have similar level of accuracy on a short range

(tested up to 200mm) but may not be sufficiently sensitive to measure roll error due to setup limitations as mentioned by authors. Also, its performance depends on the quality of the optics.

Certain amount of research has been done on more complicated, 5-axis machines where taking into account additional axes means large increase in the number of measurements to be made [29]. This gave rise to alternative approaches.

Lei *et al* [30] describe a probe-ball device and a method which combines the basic double ballbar and 3D measuring probe. Practically, it is a probe mounted on the spindle and has a socket at its end. This socket is connected magnetically to a ball mounted on a plate fixed on the machine table. Using different paths of probing the ball, measurement data is collected to fill homogenous transformation matrices which are used to estimate geometric error components. A possible issue is that the measuring probe must be calibrated on the machine prior to any tests which involves a Coordinate Measuring Machine (CMM) which might not be available during practical application.

In the second part of this research, the same authors [31] developed a reduced model based on the aforementioned method to find "non-measurable" errors which cannot be measured using a laser interferometer. These are named as link errors of rotary axes block, main spindle block and tool holder. Unfortunately, there is no explanation of what the author specifically means by those errors as they have not been mentioned in other models of 5-axis machines.

Another approach of testing 5-axis machine tools is proposed by Ibaraki *et al* [32] where a set of machining tests create a test artefact which is then measured on a CMM. Different machining patterns are used to identify kinematic errors of small machines which are particularly useful when other specialist metrology instruments such as laser systems and ballbars are not available or are too large. A similar technique was applied by Cho *et al* [33] in 2002, when error data captured while profiling a test piece provided necessary tool path corrections, with 90% of surface error reduction reported [34].

A disadvantage of the requirement to machine an artefact or test part is that these are dependent on machining conditions and tool wear, cutting force and feed rates. The tests need to be performed very carefully to minimise these effects. Conversely, they may better represent the machine capability as it is under these conditions that a machine normally operates.

2.2 ERROR COMPENSATION

Measurement of machine motion errors is closely linked with their correction and accuracy improvement. Along with acceptance tests and periodic accuracy assessments, data collected from machine measurements is used to overcome design, manufacture and build imperfections which are always present in real life which limit the accuracy that could be achieved [8]. The aforementioned approach of error compensation is completely different in that no attempt is made to avoid the error. Rather, whatever the error is, the same is measured and compensated for, usually electronically. Error compensation could thus be considered a primary method of error reduction in modern machine tools [8] and which can drastically improve geometric accuracy and thermal stability [35, 36 37].

According to Sartori and Zhang [38], error compensation is a software procedure following machine calibration which applies corrections to the measurement system. The word “calibration” generally stands for error measurement which provides information about errors to be compensated on CNC level.

Machine tools and CMMs have similar structure and both need to be accurate, they both benefit from error compensation which historically has been implemented more commonly on CMMs than on CNC machines. This is because a normal CMM is equipped with a versatile software system closely integrated with mechanics and electronics and can account for the errors numerically in the output results from the CMM whereas a machine tool must correct its tool path physically to ensure correct manufacture. In addition, CMM machine models can be simpler as the number of factors affecting accuracy is relatively small i.e. no significant internal heat, reduced loads, negligible probing forces, complicated structural loops and special tools. Also, the error itself lies within a relatively short range.

Since a CNC machine requires both accuracy and repeatability [38], compensation has become more prevalent and sophisticated. Attention on measuring methods to provide the information has also increased.

However, as soon as compensation takes place, the methods of measuring and compensation are similar. Barakat *et al* [39] divide those on to three groups:

1. Methods based on measuring the 21 source errors requiring the use of expensive instruments.
2. Methods based on measuring certain artefacts, which are used as references for calibration.
3. Methods based on kinematic references (e.g. the magnetic ballbar).

The measurements required to provide data for compensation are typically made using laser interferometry systems. They have advantages such as long axial range, accuracy and in many cases efficiency [40]. Nevertheless, alternative laser-based methods have been developed to reduce measurement time and cost.

For instance, an auto-alignment laser interferometer is offered as an alternative to a traditional laser to reduce the time of optical setup [40]. Using optic-fibre cable, the laser head is mounted on the measured machine tool as shown on Figure 9 and can be moved automatically keeping alignment (which was done manually before). Linear displacement tests, performed along several lines, produced by the automatic alignment, allow estimation of all 21 geometric errors of a 3-axis machine. The downside of this method is that it does not allow accurate measurement of straightness over long distances because accumulated positional error used to obtain straightness values becomes significant.

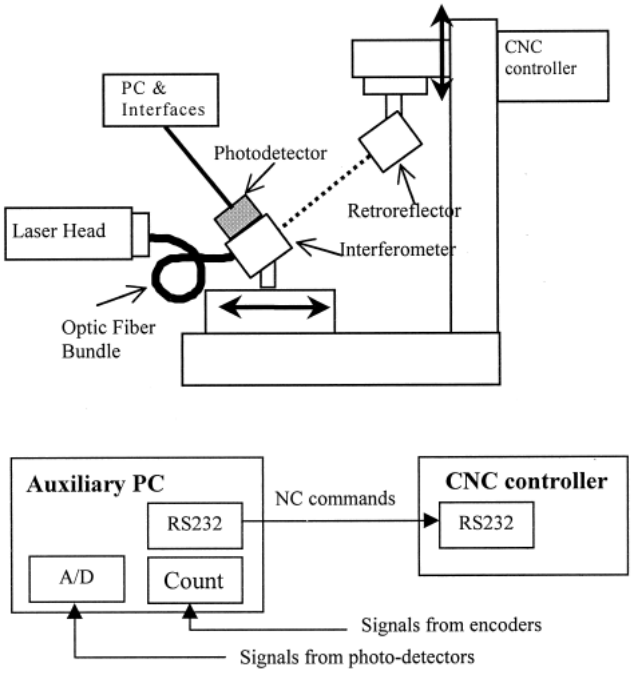

Figure 9. Configuration of the auto-alignment laser interferometer

Ni *et al* [41] replaced the interferometer optic (beam splitter) with custom optical setup consisting of laser emitter and a number of mirrors and photodetectors, installed on a measured axis. Multiple setups of that kind could be used at once, providing simultaneous measurement of all the axis geometric errors. The method was validated on short axes (375mm long) using laser interferometer. The measured error of 9μm was obtained from both methods, though repeatability was not addressed.

Another alternative to laser interferometry aligned with the measured axis is a laser tracker which uses automatic alignment/tracking to cover the entire working volume of the machine without moving the laser source and measure volumetric error. Its calculations are based on a rigid body assumption [2, 24, 30, 31 and 39] (some models incorporating finite stiffness effects are available) and allow estimation of all parametric errors of each axis. Laser tracker measures only two angles, azimuth and elevation, and a distance; the 3D coordinates of an optical reflector typically mounted on the spindle are calculated and then compared against the machine [17, 42 43]. A potential limitation here is the distance dependent accuracy associated with the rotation axes of the devices.

To overcome this issue, a relatively new system named "LaserTRACER" has been developed by NPL and PTB [25]. It measures changes in length only, combining multiple measurements in different positions (sequential multilateration) to calculate the machine error. The accuracy this time is not compromised by mechanical bearings and axes alignment because it uses a high accuracy sphere as an optical reference. The method was shown to have the same level of accuracy achieved by a ball plate artefact (for example, straightness is measured within several microns over 1m length). It is also fast, taking only 2.5 hours to completely measure a 3-axis machine [25]. Unfortunately, the cost of such equipment is very high and might not be justifiable in many cases.

An alternative methodology is proposed by Balsamo *et al* [44]. A standard laser interferometer system with optical set-up for positioning error only is used to reduce cost and set-up time. However, 31 measuring lines are suggested which may limit the potential savings. The method was validated using simulation and its statistical behaviour proved to strongly depend on machine measurement noise level which needs to be very low to get accurate results.

The problems of calibration uncertainty are addressed by Bringmann *et al* [45] and an example of uncertainty prediction for machined work piece is observed: a set of simulated errors of a 5-axis machine is taken many times with random variability within its acceptance protocol ranges added and used to simulate a geometric output on a test piece. Different error magnitudes measured during calibration can be used to predict accuracy changes of the work piece. This fills a gap between machine accuracy and accuracy of a machined component.

Another issue when determining uncertainty of calibration highlighted by Bringmann *et al* [46] is error interdependence as a reason for different measurement results for different axis locations. Modification to a ball plate is discussed – a stand which allows lifting this plate along the vertical axis to measure the same set of errors twice to see the effect of squareness error which was not considered before. This "3D Ball Plate" allows separation of

axis errors in the case of a 3-axis machine. For more complicated structures this approach may not be suitable due to the error interdependencies leading to rise of uncertainty.

An opportunity to decrease time and costs associated with laser measurements was investigated by Fletcher [47]. The feasibility of replacing a stabilised Helium Neon laser source with a number of laser diodes placed in the machine's working volume to facilitate measurement of straightness, linear and rotational errors using parallel multilateration was ascertained. A typical uncertainty of 5μm/m after calibration was simulated. Where this level of accuracy is sufficient, the multiple laser diode setup makes measuring the volumetric error faster, simpler, cheaper and more flexible. The system needs regular calibration to prevent spectral linewidth drift of the diodes to maintain the stated accuracy which makes the use of diodes doubtful when reference interferometer availability is limited. No practical validation has been undertaken so far.

2.3 STRAIGHTNESS MEASUREMENT

Mapping straightness errors of machine axes requires measurement of their lateral displacements along the axis of travel [2]. The error is typically obtained by comparing the axis motion against a straightness reference using a kind of a sensitive indicator.

As mentioned before, the most accurate and popular methods use a laser beam as a straightness reference. There are commercial systems on the market such as laser interferometers manufactured by HP and Renishaw, but being relatively complex and expensive, they provided ground for development of a variety of alternative methods.

International Standard ISO230 part 1 [9] includes the description of straightness measurements using a taut wire and microscope. The setup is shown in Figure 10:

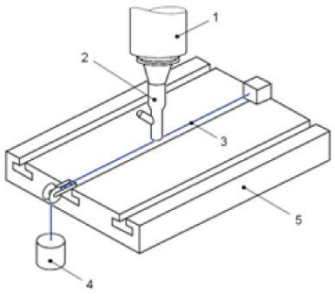

1 spindle
2 microscope
3 taut wire
4 weight
5 table

Figure 10. Straightness error measurement using taut wire and microscope

The standard recommends measuring straightness error in horizontal plane only to avoid the wire catenary contribution to the reference error.

Fan *et al* [48] describe a laser-based system to measure all six motion errors of a linear moving stage. Three laser beams are pointed on a moving retroreflector and redirected to electronic targets. Beams frequency change data is used for measured error estimation. The system measured 8μm straightness error of 200mm axis which was validated using a laser interferometer. Complex optical setup is a disadvantage here, while successful application on longer axes has not been experimentally confirmed.

Fan and Zhao [49] introduce a simple laser test for measuring straightness using a four-quadrant photo detector. No optics is required and the laser beam is relatively short, i.e. never combined or reflected. After calibration using a HP5528 laser interferometer [50, Appendix B], the proposed system shows repeatability within the range of 0.5μm on short axial ranges (100mm). This method is potentially lower in cost as it does not require investment in matched optics (prisms, reflectors).

One more method, claimed to be more sensitive compared to conventional interferometer (HP 5528A) was published by Lin [51]. Replacing a V-shape mirror with a double right-angle prism doubles the receiver response and does not require a matched pair of reflector and interferometer. Also there is no need in aligning the reflector. This makes the device cheaper and easier to use, achieving 1μm repeatability over 200mm range.

Methods combining sensitivity and simplicity of setup are proposed by Feng *et al* [52] and Kuang *et al* [53]. A single mode laser module produces a beam which is returned back by a moving retroreflector, the position of which is measured by a four-quadrant photo detector. Results provided show an accuracy over 1.5m similar to a dual frequency commercial device, but the same time results strongly depend on laser beam drift so a high quality source is required. Furthermore, thicker laser beam is desired and size of the detector has to be increased to improve output linearity. No associated uncertainty analysis is given by the authors.

A solution to measure straightness measuring not linear but angular beam deviation was developed by Zhu [54]. Polarised beam is split four times through prisms and an optical wedge. Four photo detectors measure light intensity which is converted to lateral displacement of optics moving along measured axis.

The method requires calibration to make sensor outputs linear over all measuring range and links all optics used in one system parts of which are not interchangeable. Also the optical wedge needs to be very precise and have certain dimensions which might not be available. Furthermore, optical emitter and receiver mounted on the machine have cables which might affect positioning accuracy and limit measuring range.

The advantage of the method is simplicity of setup and low uncertainty of 1μm on 1m length (after calibration). Maximum 0.5mm measured error range, however, might not be enough on some machines.

Special attention needs to be brought to scalability of straightness measuring methods over varying distance. A comprehensive review of long range measurements was written by Estler *et al* [11]. It was stated that "with a few notable exceptions (such as the use of taut wires for alignment or hydrostatic fluids used for levelling) large-scale metrology is characterised by the transfer of information between the measurement instrumentation and the measured object via light rays propagating in the atmosphere". At the same time, all optical methods which use a light beam or observation over all measured distance, have their accuracy compromised because of the following unavoidable issues:

1. Refraction errors affecting trajectory.
2. Refraction errors affecting wavelength.

Refraction errors are caused by temperature and pressure gradients and represent a major problem [55]. Mostly temperature differences on the way of propagation make light change its trajectory from a straight line to a parabolic one. The amount of resulting error can be large and it is not normally compensated because that would require accurate temperature measurements throughout the working range and large amount of computations. Dual wavelength lasers could be a solution but those are expensive and not readily available.

Possible solution here can be commercial surveying and levelling instrumentation providing off-line refraction corrections based on user input of temperature data. Such corrections are not, however, normally applied in large-scale coordinate metrology using, for example, laser trackers [56]. In very high-accuracy applications such as accelerator alignment these effects can be significant when compared with required tolerances. A horizontal laser beam will deviate from a straight line by about 50μm in 10m of travel in a vertical temperature gradient of 1K/m, with a pointing error of nearly 2 arc-sec. If the beam is scanned upward along a work piece, the refraction error decreases to zero when pointing vertically. The net effect is a vertical distortion in the measured separation of points on the work piece. In the general problem one has to consider horizontal index gradients as well, leading to even greater complexity.

Given the dominant role played by temperature gradients, an obvious approach would be to deploy a large array of temperature sensors, such as thermistors, throughout the working volume of interest in an effort to compute temperature distribution. Many machine tools, for

example, have been so instrumented in an effort to predict their thermal behavior. Despite its relatively straightforward nature, and the availability of low-cost temperature sensors, no such attempt at index of refraction modelling in large-scale coordinate metrology is known.

You *et al* [57] applied Finite Element Analysis (FEA) to model and compensate laser beam bending. A heat source was placed at some position along the propagated beam and its effect on pointing accuracy mostly compensated. To apply compensation correctly, local heat sources must be known and measured which can become problematic considering mostly distributed heat in a workshop, for example, from wall heaters.

In laser interferometry, the corresponding length scale is the wavelength which varies in the air depending on its temperature, pressure and humidity. Most commercial laser systems have special "weather stations" for measuring these parameters enabling software correction. Typically however, the measurement are made only in one or two positions which may not be representative of the total average over the entire axial range.

Air turbulence is prolific in the environments in which these measuring systems are typically used and therefore the changing air density adds random error to the laser beam changing its parameters and pointing stability (this strongly depends on laser source). This error is not systematic and therefore difficult to model and can only be partially compensated through additional test runs and averaging. It takes extra time and because of that other time-dependent errors increase, first of all thermally induced ones.

In addition to these random influences, setup and alignment errors also contribute to the total measurement uncertainty. Knapp [58] states that these are caused by setup procedures and can be in the same order of magnitude as the error being measured, particularly in the case of long range tests. This is where measurements based on optical methods may become unsuitable depending on accuracy requirements.

Estler reports [11] the following test results:

1. In a controlled experiment at NBS (now NIST) the beam from a commercial, high-pointing-stability alignment laser was directed onto a 2-axis lateral effect photodiode detector at a range of 4m. The position of the beam centroid was monitored and showed a radial location wander of about 12μm rms averaged over 40 sec. The amplitude of such turbulence noise increases roughly as $L^{3/2}$ for path length L, so that at a distance of 20m, for example, one would expect a random radial wander (alignment noise) of about 130μm rms.

2. Lateral position noise of 30μm to 40μm rms (10s average) was observed in an uncompensated fringe pattern at a range of 11.5m. Polarization-encoded compensation scheme reduced this noise to a range of 10μm to 15μm rms.
3. In an experiment using a commercial angle interferometer with a distance of about 500mm between the optics, thermal gradients were produced in the beam paths by means of a sealed container of heated water. Peak-to-valley increase in angular noise of about 0.25 arc-sec per Kelvin change in the water temperature was observed.

In typical laboratory or workshop environments, the effects of turbulence on commercial straightness or angle interferometers can be severe. In many cases data averaging becomes absolutely necessary.

Simultaneous measurement at two wavelengths for turbulence compensation in straightness and displacement metrology have been demonstrated but have not been generally applied in large scale coordinate metrology [11].

Magalini and Vetturi [59] completed experiments which confirm a high level of uncertainty due to the environment when using a Hewlett Packard laser interferometer. Measuring straightness of a center lathe axis, using Monte Carlo simulation they calculated an uncertainty of 4μm rising up to 16μm (calculated on the basis of a 95% confidence interval) over 8.5m when metrological laboratory (environmentally controlled conditions) is changed to a production department (environmental weakly controlled conditions). Comparing a precision level (straightness in vertical plane) and taut wire with microscope combination (horizontal plane) with a HP5519A laser interferometer, the authors conclude that laser interferometry does not allow lower uncertainties than the first two methods in weakly controlled environments (mean 105μm for laser system and 85μm – for precision level).

An attempt to increase the effective range of laser measurements was made by Liotto and Wang [60] measuring multiple slopes along the range and calculating lateral displacements from measured angles. The results on 5m (11 μm), 10m (2μm) and 15m (25μm) axial ranges reported to match the ones obtained using a piano wire and a collimator. Certainly suitable for mentioned magnitudes of straightness error, the method cannot be used with the same efficiency on more precise axes because it uses continuous movement and does not allow sufficient dwell time for the laser. Taut wire alternative was stated as having low resolution and time-consuming.

In response to the aforementioned distance related problems, several alternatives to optical methods have been proposed.

Campbell [61] describes a method suitable for lathes where a long steel cylinder is machined with a constant diameter which repeats the straightness profile of main axis, and on zero spindle speed a flat land is cut along its length using a flat-tipped diamond tool. Land path, measured with a LVDT (Linear Variable Differential Transformer) installed instead of the diamond tool, represents a more precise straightness profile free from errors caused by spindle rotation. Based on straightedge reversal principle, this method offers a simple and accurate solution suitable for lathes and possibly some other types of turning machines.

Another specialised method (for miniature machine tools) by Lee and Yang [62] utilises capacitance sensors to measure geometric errors of a linear axis. The small workspace is covered by a machined target acting like a capacitor together with vice it is sliding above. Two horizontal and three vertical sensors are mounted on the target attached to the spindle using an adapter. Straightness, along with angular motion errors, are derived by solving homogeneous transformation matrices. The raw data consists of angles and enables load considerations. The method was tested over a distance of 60mm, measuring a profile having a straightness deviation from 4 to 15 microns depending on axis. Implementation of a recursive compensation technique reduced the measured error to less than 1μm by Lee *et al* [63].

Zang and Liu [64] use capacitive sensors to detect the taut wire used as a reference for straightness measurement of vertical guideways. The signal from capacitive sensor is compared to the one from inductive sensor moved along the measured guideway. Reference error is supposed to be eliminated by wire reversal. The latter here applies to wire slope and position only and does not consider wire diameter inconsistency in the direction of stretching. This limits the accuracy of the method.

A methodology to enhance the use of straightedge artefacts is proposed by Pahk *et al* [65]. A significant limitation of a straightedge is its length determines the axial range and longer artefacts become expensive or impractical. This method expands the suitable axis length by using multiple measurements with partial overlapping. The same part is measured twice to calculate the angle between them and to build a combined profile. The accuracy strongly depends on the number of overlaps and their length. To reduce the accumulated error in each overlap and to reduce the number of overlaps, a longer straightedge is still beneficial.

A method of measuring straightness based on relative displacements was described and applied to long-range measurements [66, 67, 68 and 69]. A machined plate applied along the length of a measured axis was used as a straightness reference. In this case, the accuracy of the reference was taken into consideration in the calculation by using an additional displacement sensor. Because the distance between the pair of sensors is equal to the

increment of axis travel, they can operate together to measure relative displacement at every next point. Adding each displacement value to the previous one, starting from zero, gives the separated lateral error of the measured axis and straightness reference. This technique (also called two-point method) was applied on a 7m long boring machine, when the error was measured along 5m range with increments of 100 or 200mm [67]. Kaman gap sensors (sensitivity 5μm/mV) provided readings of lateral movement in every point of the working range. The method showed good correlation with laser measurements – match within 5μm when measured error was 35μm – and did not suffer from accumulated error using either 50 or 25 increments.

An additional feature of the relative displacement method was investigated by Yin and Li [70]. A dedicated sensor captures gap readings with a different separation which, being chosen properly (both increments do not have common divisor), allows calculation of error values between two adjacent points. This way, if both increments are 5 and 7mm respectively, a resulting resolution of 1mm can be achieved. It can be particularly useful for short-range measurements when number of increments is small. As before, the reference is a long plate. Pitch error is measured using a collimator.

A disadvantage of the method for general calibration work is the necessity of obtaining and mounting a straight artefact on the machine, and then to measure its pitch error to obtain separated straightness values of the axis. This could become an issue in case of a longer axis.

Okuyama *et al* [71] provide a solution to reduce the accumulated error of the two-point method (when the number of increments is large, in this case 133) using weighted addition and inverse filtering calculations to separate cross-axis motion, pitch motion and random error from measured straightness. This approach shows good results with no noticeable accumulation error when measuring 8μm straightness error of 250mm axis with 133 sample points making sampling interval only 2mm which is significantly smaller than the one commonly used and ensures no details of straightness profile remain “hidden” between sampling points.

Hwang *et al* [72] describe an application of the two-point method to ultra-precise guide ways measuring 0.2μm straightness error on 250mm parallel straightedges using capacitive probes (ADE, Microsense 3401). The result is repeatable and confirms the specification of straightedges. This, however, might include the measurement error which has not been tested separately. Also the method requires knowledge of the pitch error which needs to be measured separately using a laser interferometer or similarly capable system.

2.4 CONCLUSIONS ON PAST RESEARCH

2.4.1 Accuracy assessment

1. Ballbar methods are limited by the tool size, repeatability of error estimation and complexity of corresponding models which normally require extensive amount of computations.
2. Laser tests are limited by the number of measurements which are slow due to a complexity of optics setup. Another limitation is accuracy which decreases with distance.
3. Probing methods suffer from limitations in the sizes of the probed artefacts. Also large amount of computations is needed.
4. Machining tests are limited by size of the artefact, machine kinematics and machining conditions.
5. Laser interferometry is the most popular commercially available tool for geometric error measurement in industrial environments.

2.4.2 Error compensation

6. It is often easier to compensate machine errors than avoid them, therefore measurement is important. Most modern CNC systems have the facility to apply geometric compensation and subsequently the number of machines using it is increasing.
7. Various optical methods have been developed that provide efficiency and good axial range but which typically require higher levels of investment in the associated equipment such as precision laser sources and optics. In some cases the accuracy diminishes with measuring distance.
8. Kinematic models are based on rigid body assumptions and totally depend on accuracy of tests involved.

2.4.3 Straightness measurement

9. Most of the straightness measuring methods reviewed are based on optical methods due to the extensibility and relative accuracy of using a laser beam as a reference.

10. Advancements in laser based techniques often require additional equipment (mostly optics) which increases investments which are already high in case of traditional interferometry systems.
11. Laser beam straightness and wavelength stability is greatly affected by air turbulence inducing random changes in refraction index. The adverse effect increases with measurement distance. From the reviewed material, the magnitude of these effects can be significant compared to the accuracy required for machine tool calibration.
12. Lower cost non-laser based methods can be limited in accuracy, range and setup conditions. The application of a taut wire and optical reader is common but it is typically a manual measurement process with associated efficiency and precision issues.
13. Error separation through relative displacement (two-point) method has been applied to surface measurement but due to the nature of straightness reference has not become suitable for general measurement of machine axes.

In summary, it can be concluded that error compensation approach has been accepted as a primary solution to machine tool accuracy enhancement which is evident both by the amount of research carried out in the area and the availability of advanced compensation on modern CNC.

A number of volumetric measurement methods have been reviewed that identify motion errors of the whole machine volume. However, separate measurements are still commonly applied in industrial environments and often are the most appropriate and flexible solutions for measuring machine tools. This means that the methods of individual motion error (positioning, angular, straightness etc.) measurement are important and in demand.

Straightness motion error affects the machine accuracy and therefore the component accuracy. Traditionally it is measured using a laser interferometer or optical alignment systems, the disadvantages of which have been clearly reviewed. There has been a relatively small amount of research done on alternative methods and there is a gap in corresponding knowledge to be filled. The distribution of straightness measuring methods in the scale of accuracy and range is shown in Figure 11:

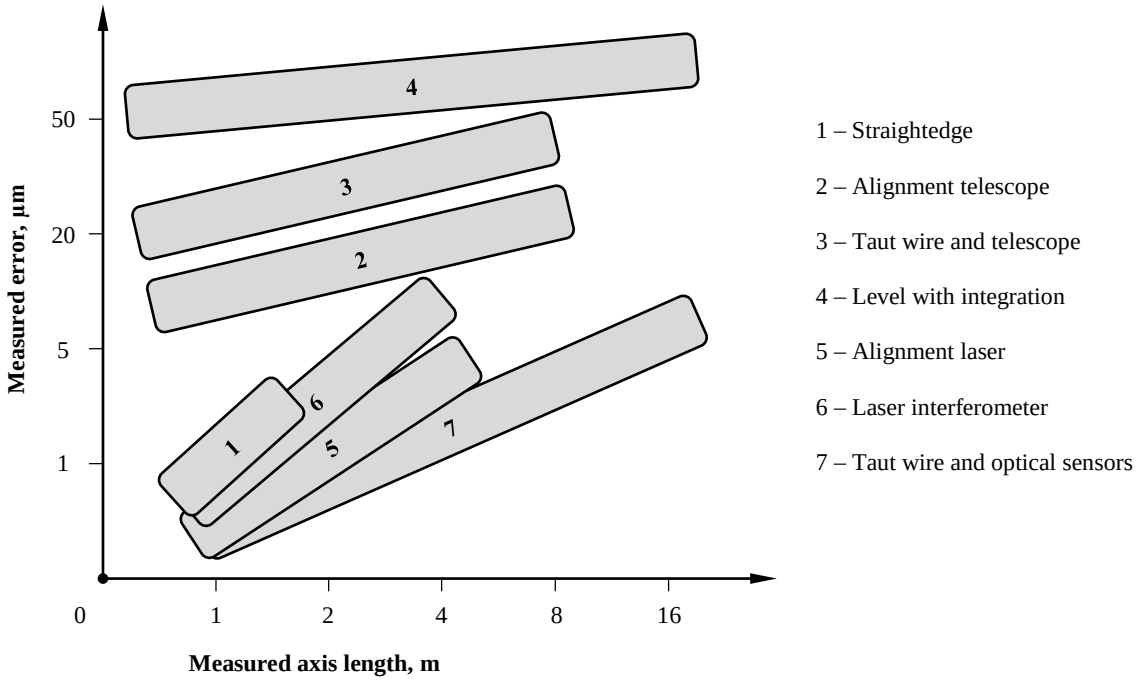

Figure 11. A comparison of straightness measurement methods

The diagram demonstrates the general capability of different measurement methods and the advantage of taut wire reference – stability over the range of axis travel. On the other side, taking readings needs to be improved in terms of speed and accuracy to that of a manually operated microscope. This defines the aim of the work committed:

2.5 RESEARCH AIM

Create a novel system for automated measurement of straightness motion error of machine tool axes.

2.5.1 Objectives

In order to provide a system that would provide significant benefits for industrial use, the following objectives have been identified:

1. Have accuracy comparable to conventional straightness motion error measuring systems, in particular a laser interferometer, not exceeding 2µm.
2. Have high repeatability (<1µm).
3. Utilise easy to understand measurement procedures compatible with current international standards.
4. Incorporate readily available, off-the-shelf, components to ensure reproduction.

5. Have ultra-low cost to be affordable even to small industrial units.
6. Be easily transportable.
7. Be suitable for axes of any orientation.
8. Allow simple and efficient setup on the machine.
9. Be extensible, not limited by the measured axis length.
10. Allow simultaneous measurement in both planes.
11. Not require expensive and rare equipment for calibration.
12. Be resistant to environmental conditions such as temperature gradients, vibrations and air turbulence.
13. Have constant performance over time.

Additional ‘nice-to-have’ objectives have also been considered:

14. Short warm-up time.
15. Possible permanent installation on the machine.
16. Room for functional expansion.

CHAPTER 3 STRAIGHTNESS MEASUREMENT REFERENCE AND SENSOR

According to the aim and objectives stated in the previous chapter, a new tool, dedicated to the measurement of straightness motion error of machine tool axes is to be developed. General information about straightness and its measurement and existing solutions outline the basics of the new system which needs to be implemented as a combination of hardware and software.

This chapter will start by looking in detail at the principle of straightness measurement using a taut wire and the primary limitation of its accuracy. The exact implementation of measurement system will be discussed further, along with requirements to both sensor element and the taut wire which need to be fulfilled to reproduce the system. The technique to overcome wire inaccuracy as a reference will be followed by a calibration procedure, normally preceding straightness measurements, given with the respect to required accuracy of measurement for the target application.

3.1 DETERMINATION OF A STRAIGHTNESS REFERENCE

Structurally, measurement of straightness is always two-dimensional. The first dimension matches the propagation of a measured line, the second is orthogonal to the first and represents straightness error. This means that a straightness reference should ideally be a single-dimensional object. In practice it is possible to achieve only a great difference between one dimension and two other ones. As it was showed in the previous chapter, a light beam has got a wide application as such a reference.

In order to satisfy the target specification related to simplicity in application, availability and affordability, the use of a laser as reference was dismissed. Although laser sources themselves can be inexpensive if they are not stabilised, the associated optics, detectors, electronics etc. add cost and complexity. A requirement of a suitability for long axes with low measurement error increase, earlier discovered to be important, suggests more environmentally stable object. A solid reference was dismissed due to poor portability, convenience and accuracy over long distances. Also, there was limited scope for novel methodology or technology. When considering the taut wire as a reference it clearly possessed the extensibility of an optical system in that traditionally it had been used

successfully on a wide range of axis lengths with manual instrumentation to read the position of the wire. Availability of the wire and simplicity in alignment with an axis are also ideal and so too the affordability, depending of course on the sensing system. The taut wire was therefore analysed.

As an alternative to a beam of light, it has similar dimensional properties but completely different physical nature. Any wire, stretched between two points, provides a straight line between such. This unique behaviour of actually any flexible object affected by at least two forces acting in mutually opposite directions, combines with a simple structure (long and thin cylinder) in case of the wire. Having a relatively constant diameter and cylindrical shape, the wire becomes very much like a line when its diameter value is far less than its length. The only condition required to make this line straight is a force applied to put the wire into tension i.e. if the wire is taut then it is nominally straight.

When a taut wire is positioned along a linear axis of machine tool, it becomes a reference for measuring the straightness of the axis. The next step is to fix an indicator on the moving part of the axis in such a way as to detect lateral displacements orthogonally to the axis.

Any moving axis has six motion errors and if we aim to measure straightness in one or both planes, then the displacement indicator needs to be sensitive to displacements in that direction(s) only i.e. not adversely affected by changes in the transverse directions.

Regardless of axis errors and wire variability, there will always be a “slope” error (explained in section 1.2). It is cumulative, starts from zero, and proportionally increases with axis travel from its beginning to its end. The slope should be minimised on both physical and calculation levels and taken out of the measured straightness error. This is desirable to reduce the magnitude of total measured error so that it does not exceed the sensor’s measuring range and only minimal part of it is used.

The measurement can be done statically where the machine moves specified intervals and stops every time to capture the reading. Alternatively, readings can be taken dynamically which may reduce measurement time. The first method is recommended in the machine tool measurement standards [9] and it provides the opportunity to use filtering or averaging to reduce noise in the data. Dynamic data capture may be useful for quick preliminary assessment of long axes.

After taking readings from the indicator over the full traverse range of the axis, those readings represent a combined straightness of both the reference and the axis. If one of them is known, its subtraction gives the other. Taut wire straightness is normally unique to every piece of it, only its approximate magnitude can be known. This can become an issue on

precise axes, to overcome it, an error cancellation technique might be necessary and will be discussed separately in section 3.4.

3.2 MEASURING HEAD AND THE WIRE

According the measurement strategy described above, a measurement system needs to be designed to implement the theoretical findings. From the project objectives, it is particularly important to make the device from readily available components, maintain simplicity in the design to reduce the need for internal adjustments or precise component parameters. It should be easy to setup and to operate, provide sufficient level of accuracy and repeatability, allow further modifications and reconfiguration.

3.2.1 General design requirements

The system needs to have a separate units for mounting on the machine and for data analysis, connected together to pass the measurement data. The moving unit should be portable and capable of mounting in any orientation on the moving axis, while the wire is suspended along the direction of motion.

The signal from sensors must represent the relative displacement of the axis only, not be affected by the location. It must represent the straightness error of the axis, have sufficient resolution and linearity.

The assembly should be easy to setup and to adjust, allow calibration without repositioning the wire, provide as many sequential measurements as required with consistency and repeatability.

3.2.2 Design details

The measuring head needs to be assembled on an angled metal plate which allows mounting on a spindle, axis or a magnetic base as an intermediate component. The plate should have a main flat surface to fix the displacement sensors, electronic circuit board and standalone components like switches and regulators.

Places for sensors should be in the same plane which is parallel to the mounting plane. The distance between sensors should be fixed and equal to the considered step size or be adjustable.

Sensor circuits should be designed as separate channels and there should be at least two of them (to implement double sensor principle).

Electronic components should have high stability but paired ones do not need to have parameters matching exactly as all channels will be calibrated prior to use.

The electronic circuit should provide power for sensors and deliver the output from them to the signal converter. Also it should implement fine adjustment of at least one channel output signal. It should also produce the signal which can be passed through a shielded cable of several meters length without distortion and contamination by electrical noise.

The sensors need to be capable of detecting the wire position with an accuracy of less than a micron (mainly to prevent accumulated error from being high) and not very sensitive to environmental effects such as ambient light. The sensitivity characteristics of sensors should be roughly linear and covering a typical straightness error range of few hundred microns.

The outer case should be detachable and usable when the wire passes through the device. This will prevent the wire working area from disturbances and will reduce the change of lighting conditions around the sensors during the axis travel.

The converter which receives the signal form the device should have equal or exceeding accuracy and number of channels. It should have averaging, real time monitoring and PC connectivity features.

3.2.3 Optical sensors

A sensing system is required to detect the position of the wire. The detection has to be non-contact to preserve the wire surface profile during the measurement. Commonly, a microscope [9, 59] is used to read wire position on every measurement step. This involves manual operation (therefore it is time consuming) and human error. Automation has been achieved by using video probes along with edge detection software [73]. This is a more complex and expensive solution.

During the investigation, an alternative was identified based on phototransistors. These are typically used in the process industry to detect the presence of objects at high speed. There are many different types available for different applications, here the most suitable for wire detection were chosen.

The sensors in the measuring system are supposed to detect presence of wire in approximately $1mm^3$ of space without contact with it and with accuracy beyond 1µm. The first number represents a maximum measuring error range plus nonlinear margins on both sides. The second one is desired accuracy, which utilises the potential of modern optical sensors. The simplest and cheapest solution would be optical sensor consisting of light emitter and light detector. Any non-transparent object between them would change the amount of emitted light coming in to the detector and the level of current on it.

To achieve that, photomicrosensor devices were taken as a basis. Mostly manufactured by Omron Corporation [74], those multi-purpose components perfectly combine small size, low cost and ease of use. Normally these sensors operate in two states: 1 and 0, standing for "closed" and "open". This indicates presence or absence of an object in the sensor's working area. It might be used for controlling doors, covers, mechanical triggers, mouse wheels or transparency of controlled objects. To fit general purpose application, these sensors are manufactured in different sizes, with different mounting solutions. The work principle is the same and electrical characteristics differ slightly. A variety of different photomicrosensors are different due to the following features:

1. Dimensions.
2. A way of mounting.
3. Number of channels (one or two).
4. Aperture size and orientation.

The most important parts – emitter and detector themselves are always present. This means the sensitivity, which is important for accuracy in our application, depends mostly on aperture shape or position, all the rest is more or less important for mechanical composition of the measuring unit.

The sensors suitable for wire detection should have working area large enough for the wire to be placed inside, safely distant from both emitter and receiver even with significant slope error of the wire. This is satisfied by 3mm of total distance (1mm working area and 1mm on both sides of it).

Figure 12 shows two photomicrosensors ("sensors" from here after), which have dimensions 25×10×6mm, flat surface and two apertures for mounting. The aperture has a rectangular shape and located horizontally (Figure 12 left) or vertically (Figure 12 right). Specifications of both are in in Appendix B, aperture dimensions in Figure 13.

Figure 12. Omron EE-SX1096 and EE-SH3 photomicrosensors

The first option is the most suitable for this measurement application because the horizontal alignment of the sensing area and the wire corresponds to higher output signal sensitivity than if both were crossed.

The measurement relies on the wire being positioned in the sensor partially obscuring the window of the detector reducing the amount of optical energy reaching the detector (Figure 13) changing the light current from the phototransistor which can be converted in to displacement units using a simple resistor circuit and calibration.

It is important that the sensor is sensitive in one direction only, when the wire comes in and comes out, its position between emitter and receiver does not influence the amount of light passing through and therefore, does not affect the output signal. This can be considered as a second order effect and its negligence will be confirmed later, during the tests on a machine (Section 6.1.1).

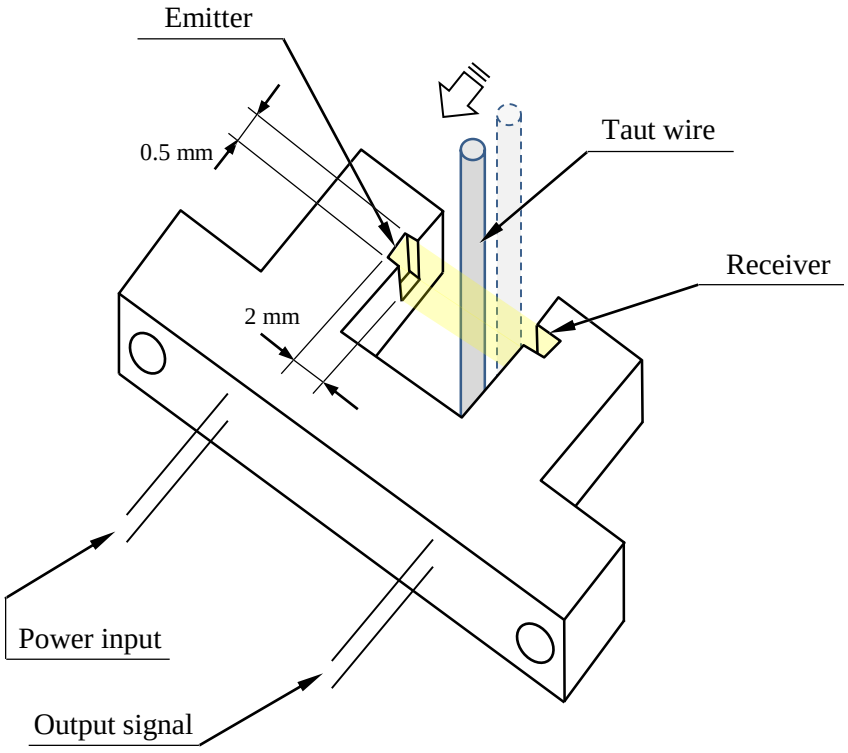

Figure 13. The wire detected by the photomicrosensor

The light produce by the emitter has a wavelength of 940nm which is far beyond the visible spectrum and ensures sensor low susceptibility to ambient light.

It is important to note that the sensors will be used in non-conventional manner, because the wire will be detected gradually on its way across the sensing area. Not only two states “in” and “out” will be detected.

3.2.4 Measuring system design

To measure the wire position in two directions and to implement the error cancellation method described in section 3.4, the system must consist of four sensors, associated electronic circuit board, battery, power on switch and a socket to connect a cable passing analogue signal to a ADC. The circuit is shown in Figure 14. It has four channels every one of which has a basic filter and power loop. A battery was used instead of a power supply unit to reduce fluctuations in the current supplied to the sensor emitters which might affect the result. Later it was replaced with a stabilised power adapter to provide continuously stable output for long test runs.

Ideally the power source should be battery because its current does not have any noise which needs to be filtered otherwise. On the other side, its voltage changes due to discharge, load and temperature, so stabilisation is required.

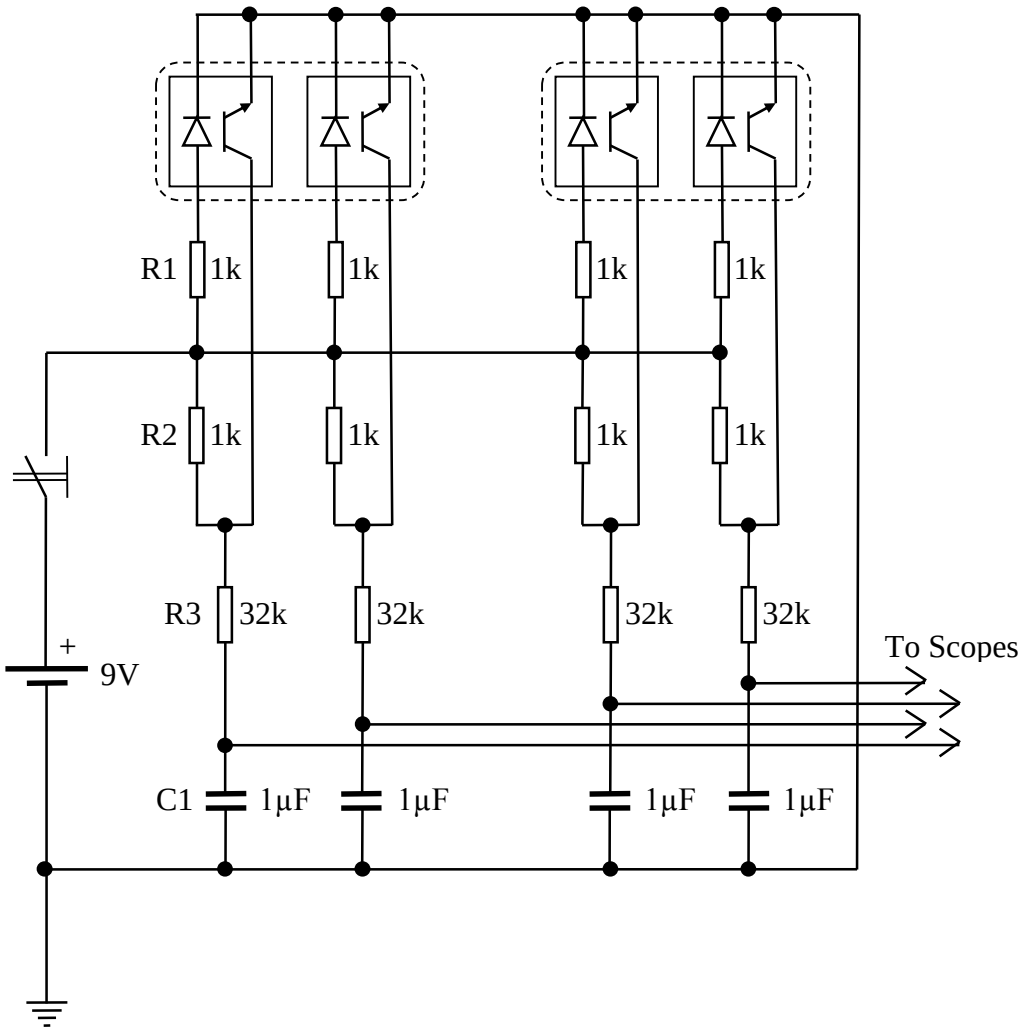

Figure 14. Circuit diagram

The diagram above is based on the reference circuit provided by Omron for their sensors. It has four identical channels operating simultaneously. Resistor R1 reduces the input voltage on emitter which accepts up to 4V according to the specification [75]. Practically it can operate on higher voltage which is desirable for maintaining as high sensitivity of the sensor as possible. Resistor R2 enables minimum output for detector, group R3-C1 serves as chattering prevention unit.

The device layout with dimensions is shown in Figure 15:

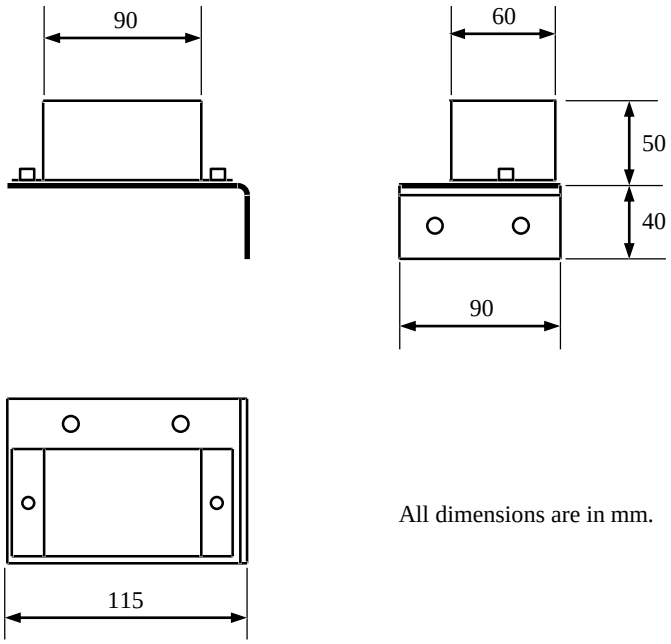

Figure 15. Measuring head layout

Figure 16 and Figure 17 show the whole assembly, from hereinafter named the "measuring head", with and without the outer cover respectively. The wire is shown in red to emphasise its position while it passes through all four sensors, two of which are positioned vertically and two horizontally.

The shape of L-plate was chosen to implement the simplest yet versatile mounting solution when the unit itself is portable and convenient to mount on horizontal and vertical axes without obstructing machine's elements and providing easy access to mounting screws. Apertures in the plate are positioned to match typical magnetic stand square mounts and available adjustment carriages. These apertures are located on both shoulders of the plate so that either vertical or horizontal, table or spindle could be used to attach the head to.

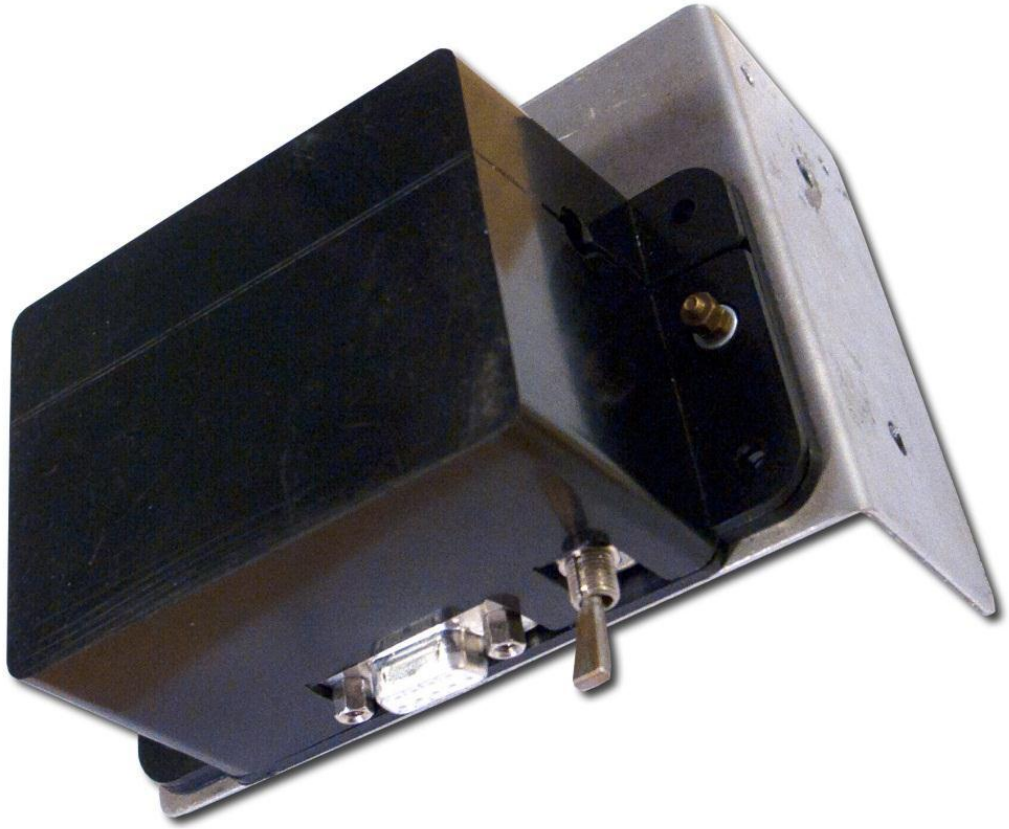

Figure 16. Measuring head with cover

The black plastic cover originated from universal electric boxes, readily available from electronics stores. It was modified to fit the purpose by cutting a slot to pass the wire and an aperture across its working position to prevent contact between the wire and the cover. Also apertures for external components such as connector and power switch were cut with a saw. Attaching the cover on the stage of the system's setup allows protection from light and air disturbances in the area close to the sensors. Also it prevents dust, liquids and other objects coming in contact with the sensors. This is desired to maintain their accuracy.

The circuit board rests on a screw, secured by two nuts, other components are fixed on aluminum support plates, fixed on the base plate through the plastic lid from electric box.

Typical D-type connector was chosen to get reliable connection between the head and the cable transmitting output signals and power for the unit. The cable is supposed to be connected after the head is mounted on the machine, for simplification of the procedure.

Power switch was included to allow switching the head on separately from the power source which can be useful if batteries are used or to keep the power supply unit permanently on, without the need to wait for heating up phase to complete.

The device with cover and battery removed is shown in Figure 17.

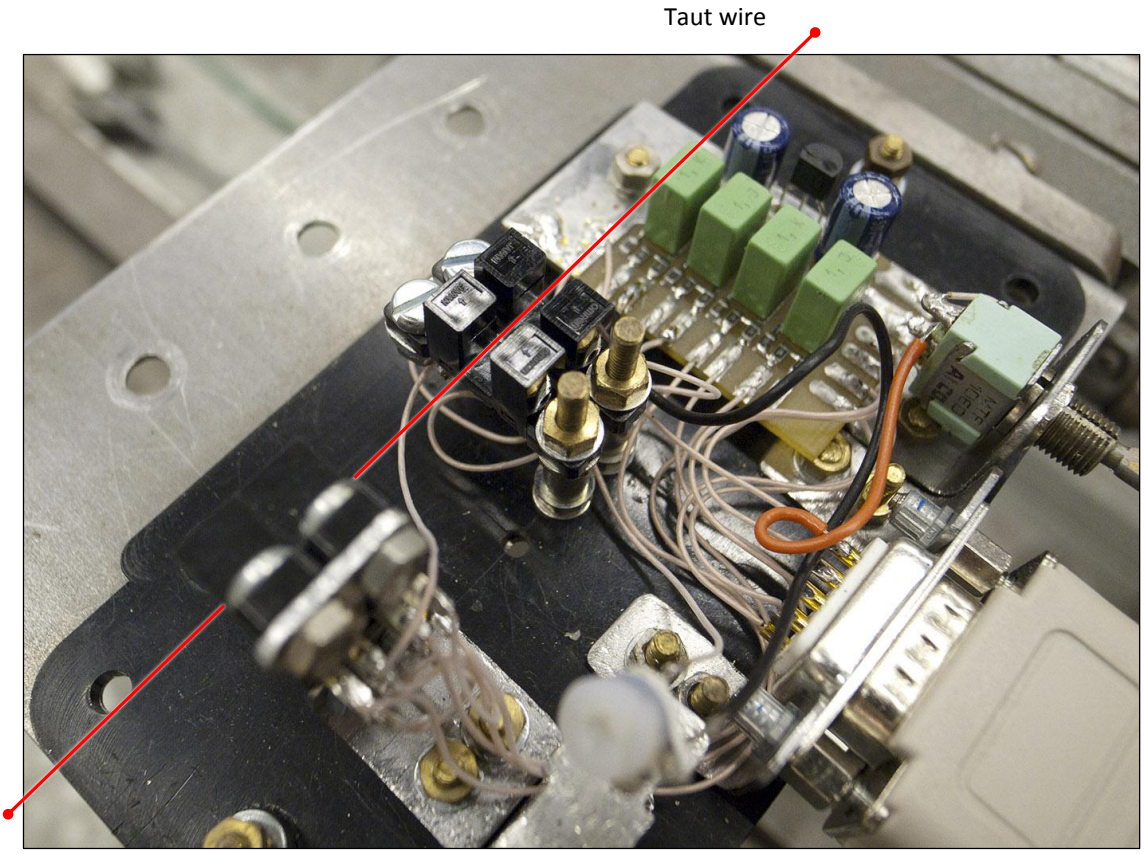

Figure 17. Measuring head (without top cover)

3.2.5 Optical sensor testing

In order to confirm the suitability of the proposed sensors to use with the wire, the sensors were checked for wire detection sensitivity. The result is shown in Figure 18:

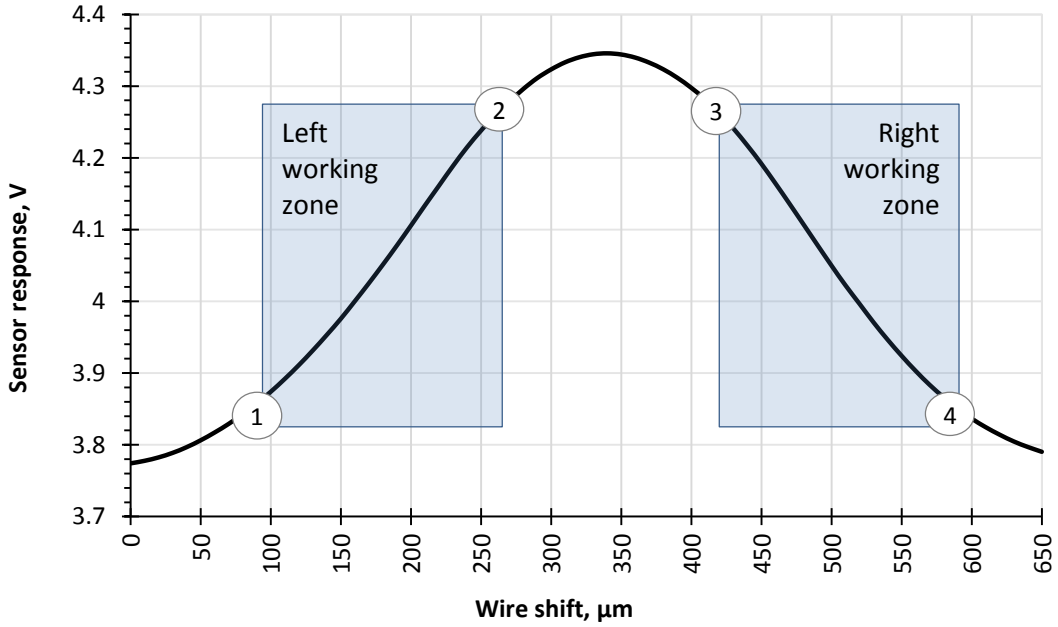

Figure 18. Chart of sensor output voltage variation against wire position

The test was carried out on a stationary axis, with the measuring head moving in the plane where straightness was supposed to be measured. This was done using a micrometer, operated manually, with 10µm increments. The figure demonstrates how one side of the wire reaches the sensing area (1), passes it through (1-2), comes out of it (2), another side of the wire starts leaving the sensing area (3), leaves it completely (4). The lengths of these parts are subject to wire diameter to sensor aperture ratio. In practice, only one side of the wire represents its straightness and is used as a reference therefore only one working zone is used at a time.

The range of the linear working zone is equivalent to a measuring range of 200µm, estimated from Figure 18, which is sufficient to accommodate most machine tool axes straightness motion error, even long range ones. The output is not exactly linear and its deviations from linearity are unique for every sensor however it is systematic and can be removed using a sensor calibration procedure.

As it is shown on the graph above, the sensor sensitivity is about 2mV/µm which is suitable for available Analog-to-Digital Converters (ADC's). The one used in this project, National Instruments (NI) 9239, has an accuracy of ±100ppm maximum (±0.4mV).

3.2.6 Wire sensitivity change due to positioning inside the sensor

It is important to check the effect of changing position of the wire between light emitter and receiver in both directions. A special test was done to measure the change in sensitivity in the measuring direction as the wire moves in the transverse direction.

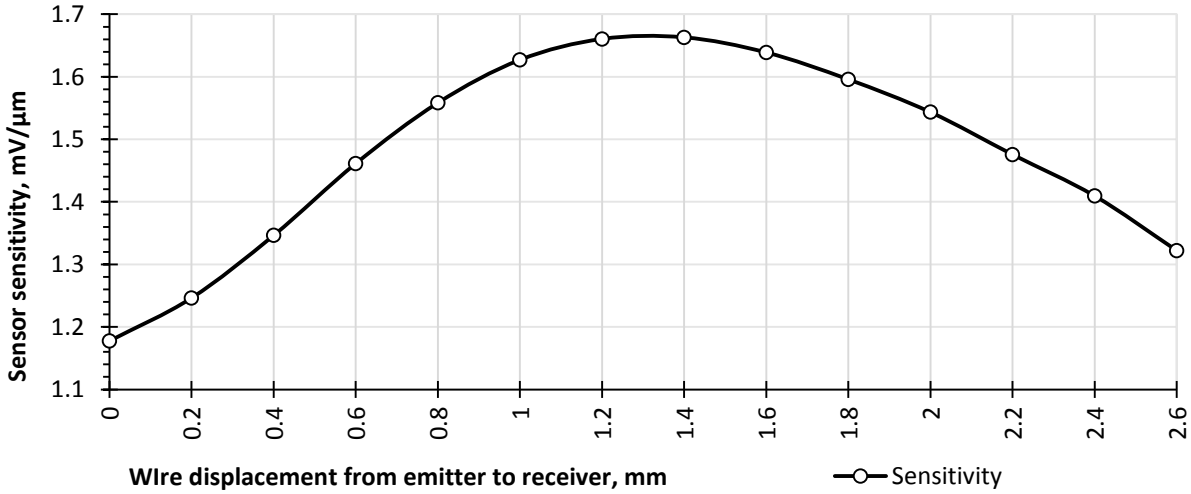

Figure 19. Change of sensitivity of optical sensors due to the wire lateral displacement

The machine again remained stationary, but this time the head was moved using two micrometers set up orthogonal to each other. The sensor head was repositioned so that the

wire passed the sensor right close to its emitter and then the head was moved using 0.2mm increments towards the receiver (horizontally). At every point the sensor's sensitivity was measured (vertically, as to produce Figure 18) and average values of sensitivity obtained from every vertical test obtained are shown together in Figure 19. Every point there represents an average value of sensitivity at every possible position of the wire in horizontal plane.

It can be seen that area in the middle provides the highest sensitivity and the most suitable for measuring. It stays practically the same within 0.6mm which is far more than straightness error would normally be.

3.2.7 Measurement of straightness with taut wire

The taut wire straightness measurement system outline is as shown in Figure 20. The system is mounted on the measured axis so that the wire is positioned parallel to the axis guide and its length, available for measurement is slightly more the length of the axis itself. The system consists of:

1. Piece of wire.
2. Two columns holding the wire.
3. Four fine adjustment carriages.
4. Counterweight, wire clamp and a wire guide wheel.
5. Measuring head.
6. A flexible cable connecting the head with an external ADC.
7. Four channel ADC (NI 9239, specification in Appendix B).
8. PC.

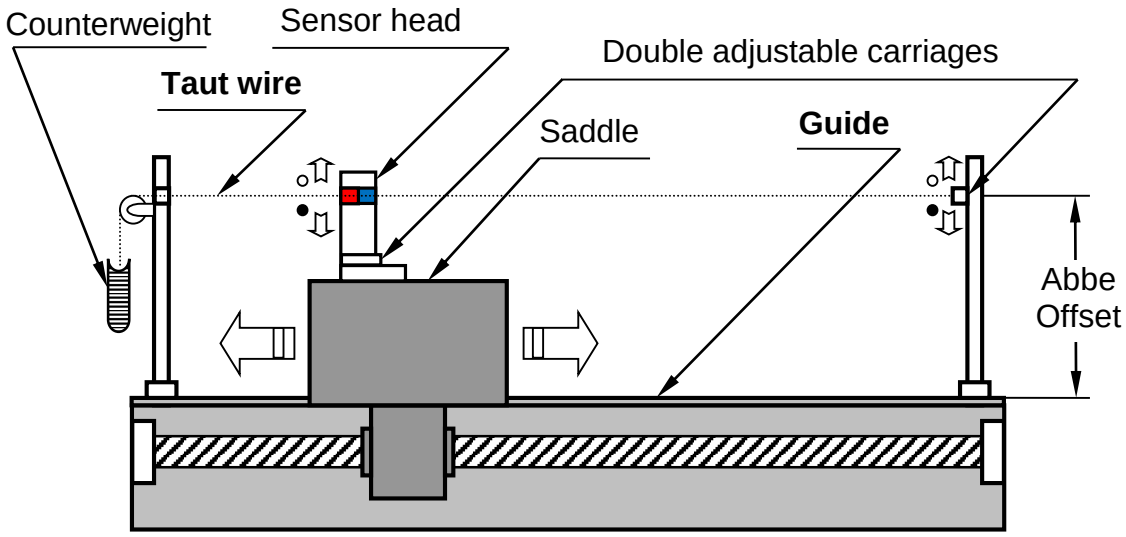

Figure 20. Taut wire measurement system setup layout

The wire is passed through the sensing device which reports the position of the wire while the measured axis moves from its one end to another in certain increments. Signal from the sensor is then converted into lateral displacement values which form axis straightness.

The sensor's sensitivity is determined prior to measurements, using the predefined lateral motion of the sensor. This can be done using a displacement indicator or machine's vertical axis motion. Moving the sensor up or down in known increments and recording corresponding sensor signal change incrementally, a value of sensitivity can be calculated at each point of the sensor's working range.

The wire piece is taken from a roll of readily available *DAIWA Sensor Monofil 0.26mm*, clamped on the right column and put through the left one where it is rolled over the guide wheel and fixed to the counterweight (1.5kg or 15N). Both columns are fixed on the guide way of measured axis and the right one has two fine adjustment carriages (hand-driven, 5mm range, full specification in Appendix B) mounted on it and one on the top of another. This combination allows wire repositioning needed for its alignment with the axis.

The left column has an aperture in it and a guide wheel attached. The counterweight is a hook holding a round plate used to keep a number of standard weights at once.

The measuring head is mounted on two fine adjustment carriages positioned perpendicular to each another in the same way as the two other carriages on the right column. The difference is that these both have integrated micrometre handles facilitating movement of the head with precision control over certain intervals needed for system calibration. Alternatively, a suitable linear displacement sensor can be used for the same purpose.

A cable connects the measuring head to the NI ADC to convert analog signal from the circuit into discrete values and recording on the computer. The same cable can be used to provide power to the measuring head if no battaries are used.

Figure 21 shows both columns and the wire mounted on the single axis test rig.

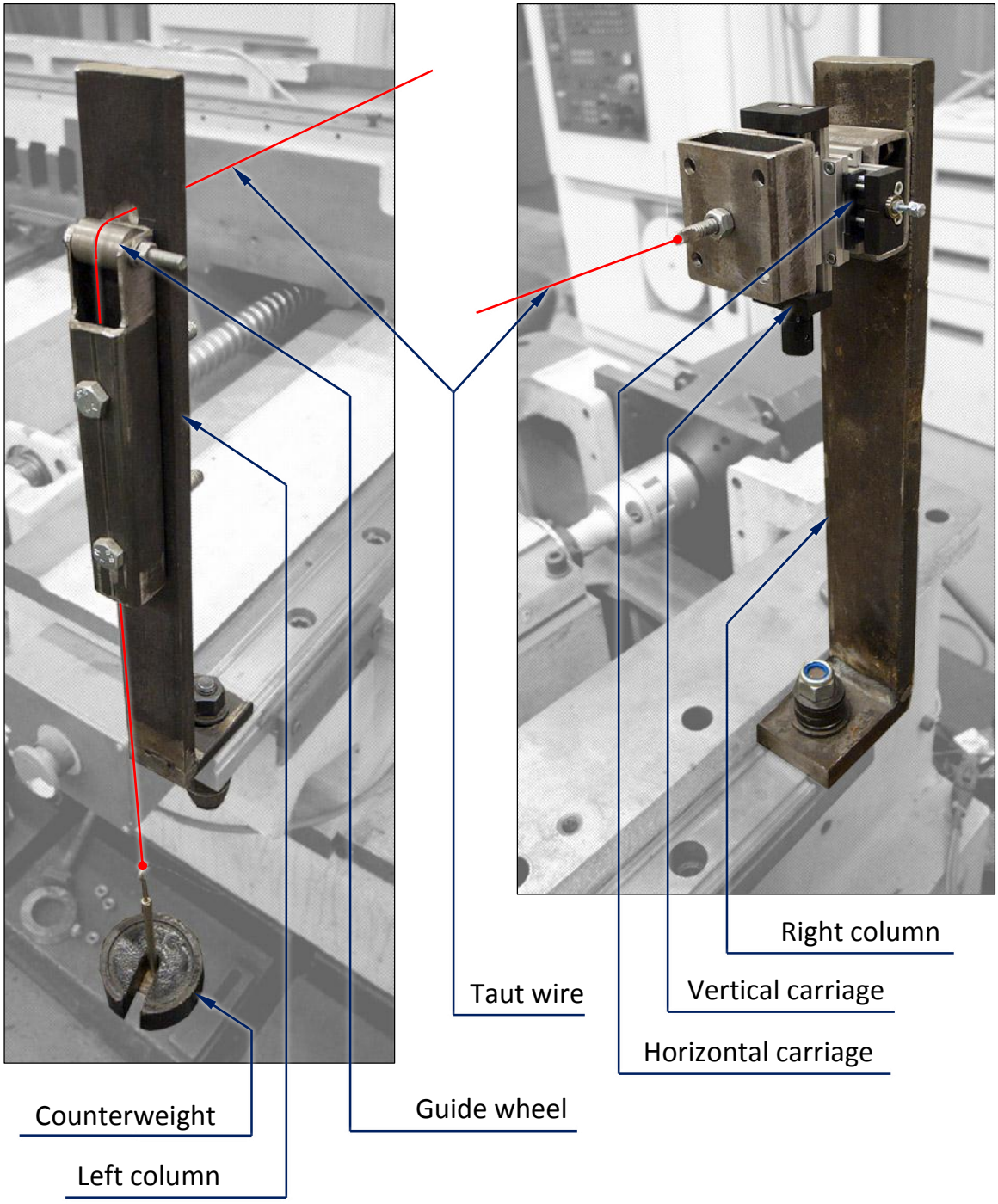

Figure 21. Left and right columns equipped

It demonstrates how the wire is mounted on a machine. In this case the precision test rig is shown in the background, on which both columns are fixed at opposite ends of the right guide way. One end (the right column in Figure 21) is adjustable in two directions using the aforementioned perpendicular carriages while the opposite end has a fixed position. The wire guide wheel has a groove to prevent the wire from moving laterally along its surface while settling and during setup.

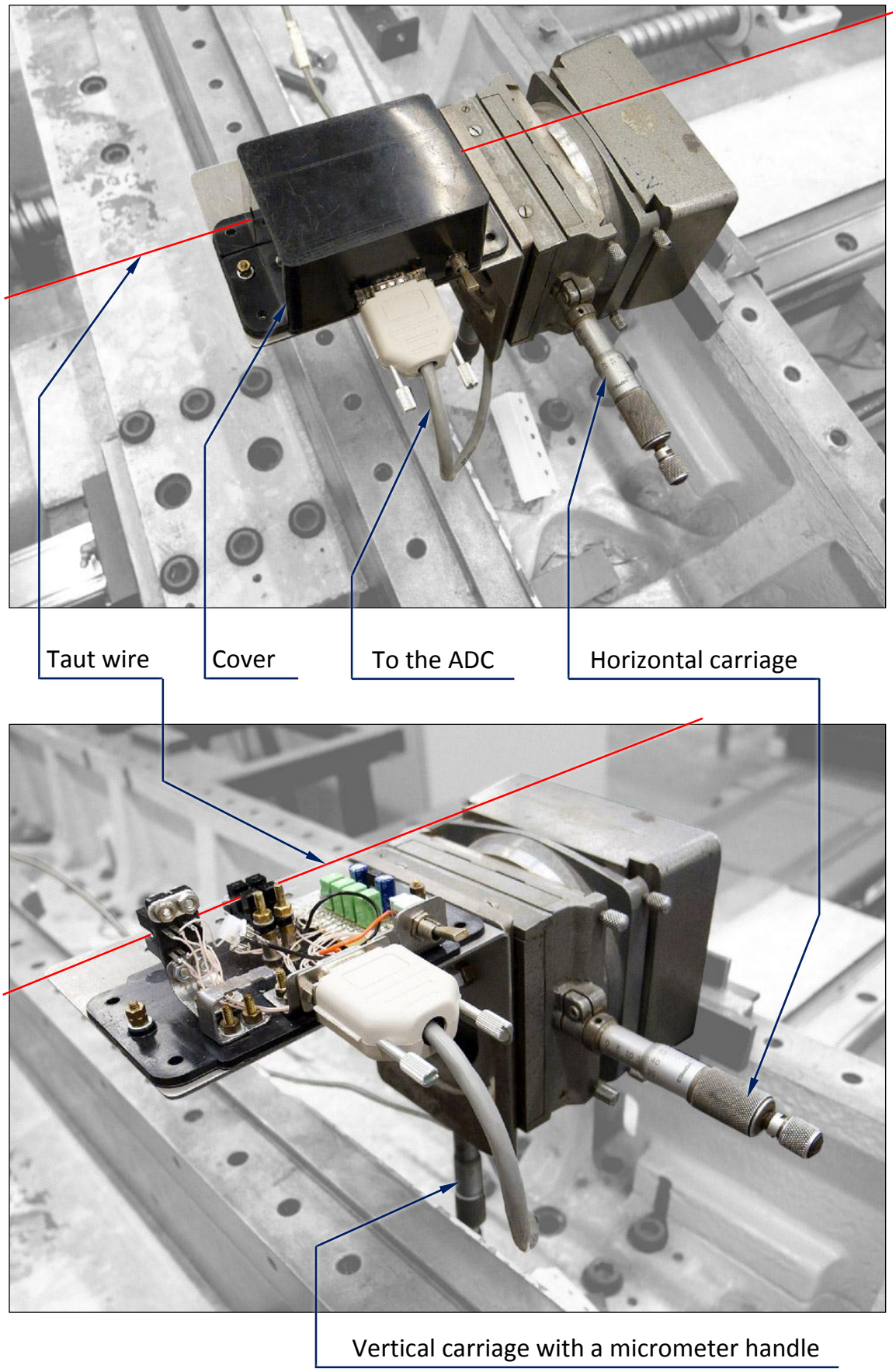

Figure 22. Measuring head with and without the top cover

Figure 22 shows the measuring head mounted on an angled plate, which can be moved so that the wire locates exactly within both sensing regions at once. This actually makes precise alignment of sensor groups within the measuring head unimportant as they can both be aligned to the wire itself. The angled plate is fixed on dual adjustment carriage which is bolted to the moving saddle of the test rig.

The top cover, of the main constituent being a plastic box, can be put in place after the wire has been installed preventing ambient light disturbances.

Although only one sensor from each pair is required to measure the wire position, if sufficient data channels are available, both pairs can work together providing data for averaging to decrease the measurement uncertainty and/or perform straightness measurements in both planes simultaneously.

3.2.8 Wire settling

An important part of taut wire setup is settling the wire. Regardless of wire material and value of tensile force there is a certain period of instability, during which the wire is changing its diameter, tension and becoming unevenly thinner. Depending on wire mechanical properties and condition, this process can take from few minutes to several hours.

While the wire is changing, it cannot be used as a straightness reference, even with error cancellation technique, because the change is considerable. Figure 23 shows two channel log of approximately 10 minutes of a continuous fishing wire test without any machine movement.

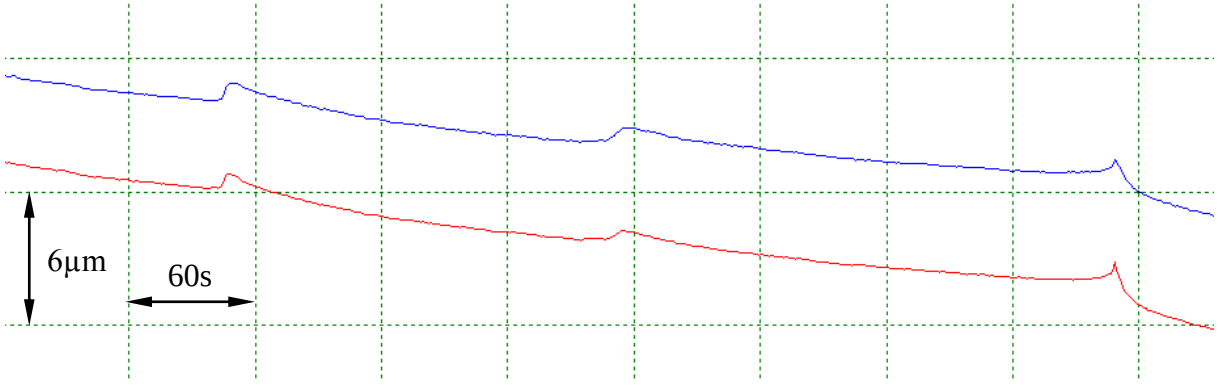

Figure 23. Wire instability after tensile force has been applied

It is clearly visible that wire settling has a complicated order, when short periods of rapid retraction change with long periods of diameter drop. With time retractions become rarer and rarer, drops less and less in magnitude and finally graphs become straight lines.

Error cancellation allows starting the measurement before the wire settles down completely, the only condition is to do measurement runs between retractions. Even if this condition is not fulfilled, it will be obvious from comparison of sequential test runs and necessity to redo the measurement.

As it was said, condition of the wire affects its settling time. The wire which has already been stretched settles several times faster and ideally should be prepared in advance. Typical settling times for the chosen wire are 5-10 minutes or 3-6 minutes for the wire which has been settled once.

3.2.9 Wire considerations

There is a variety of different wires, with different physical properties, price and availability. The question which one is the most suitable for straightness measurement makes necessary some experimental work because related research has not been published yet and there is no relevant information currently available.

The criteria for differencing the wires are the following:

1. Stability.
2. Ability to straighten under tension.
3. Transparency.
4. Diameter uniformity.

Types of readily available wires are:

1. Fishing wire.
2. Metal wire.
3. Sewing thread.

Several different wires were tested in the same conditions, on a half meter distance and axis with few microns straightness error. The tests were simple, using a single sensor and no error cancellation. Taking that the error of the axis remained the same, its value combined with straightness error of each wire could be used for determining wire suitability for measurement. The less was total – the more suitable the wire was considered to be because being closer to an ideal straightness reference.

A laser interferometer was used to measure the straightness of the axis to be taken as a reference for wire measurement results. Figure 24 shows a comparison of four different wires. Thick (0.5mm diameter) fishing wire proved to be not suitable for measurement, the rest of the wires performed on the same level. Steel wire demonstrated worse results after being left

on the machine overnight. This can be explained by slow elastic deformations gradually changing the wire thickness. More flexible wires did not show any significant difference in such a case. Also steel wire diameter uniformity remains very low compared to other wires, regardless of tensile force applied. It was considered not suitable for straightness measurements.

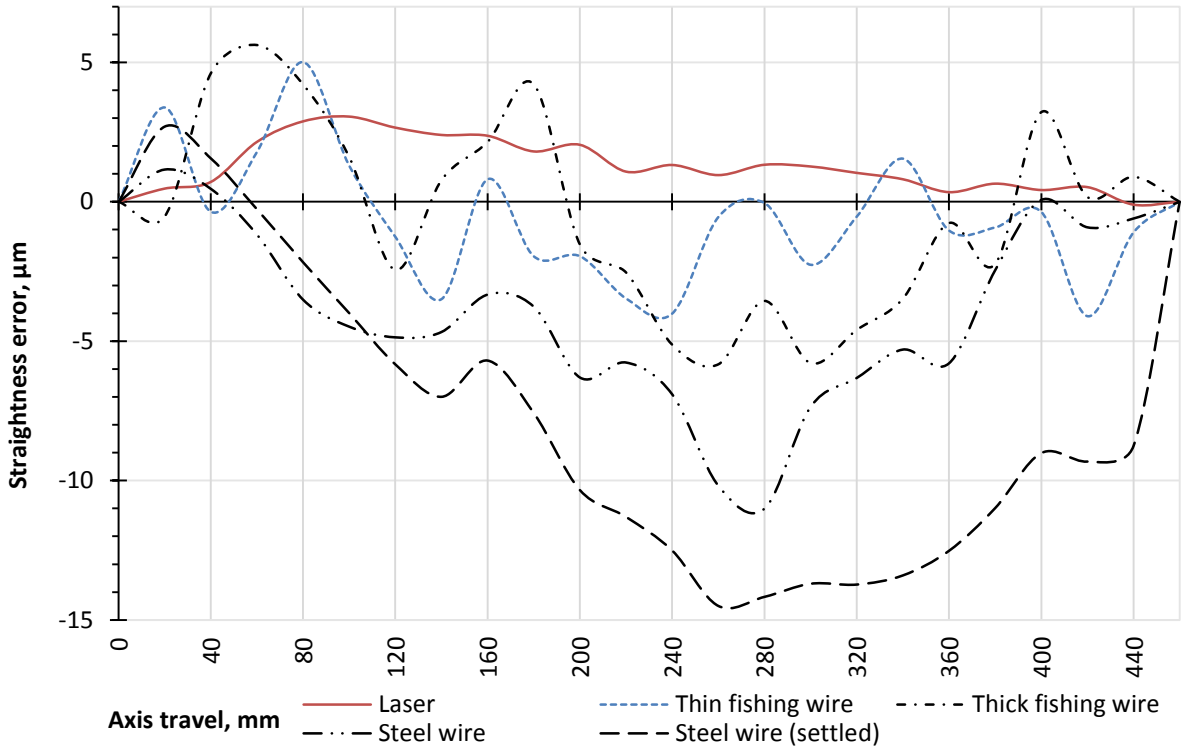

Figure 24. Comparison of different wires, part 1

The next two wires, copper and sewing one, showed very poor results (Figure 25). Even been stretched to their maximum strength, they still have a very large straightness error.

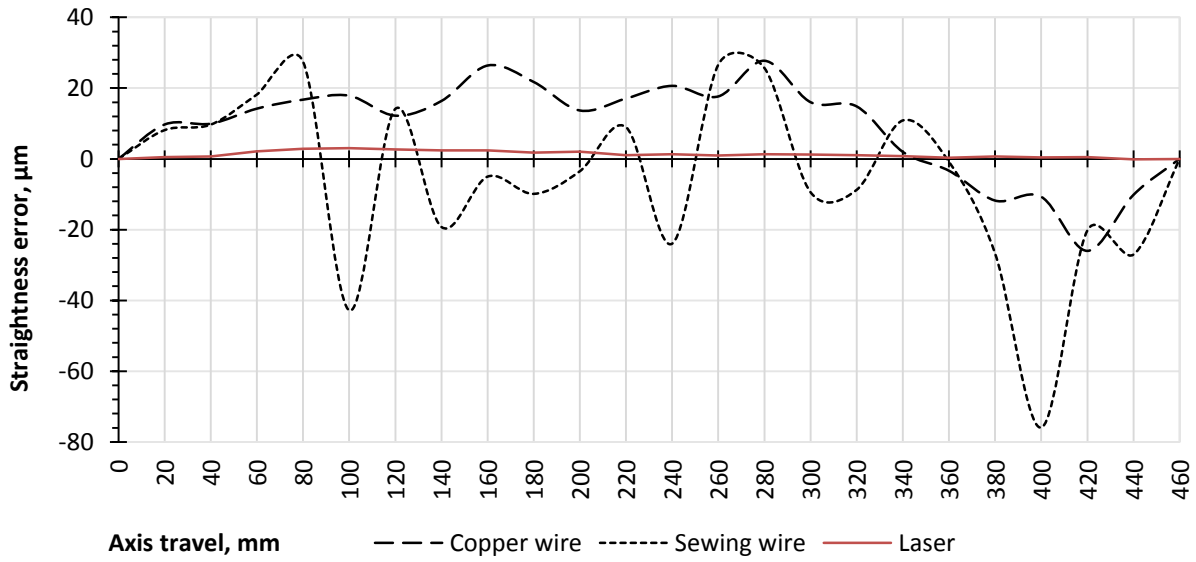

Figure 25. Comparison of different wires, part 2

The decision on results: thin (0.26mm) fishing wire was chosen for all further experiments as having the most consistent diameter and easiest to use.

3.2.10 Counterweight consideration

It is obvious that the tensioning force makes wire straight. A simple experiment was carried out to determine how the fishing wire (chosen previously) straightness depends on specific tensioning forces. Three different weights of 0.1Kg were used and single sensor measurement of the wire straightness was recorded. The results are shown in Figure 26. Signs of initial deformation when the wire was on a roll remain even after stretching. It is clear that increasing the force is better straightening of the wire. The limit here is wire strength – at some point while the tension is increasing, elastic deformation occurs which will change the wire diameter until at some point the wire snaps.

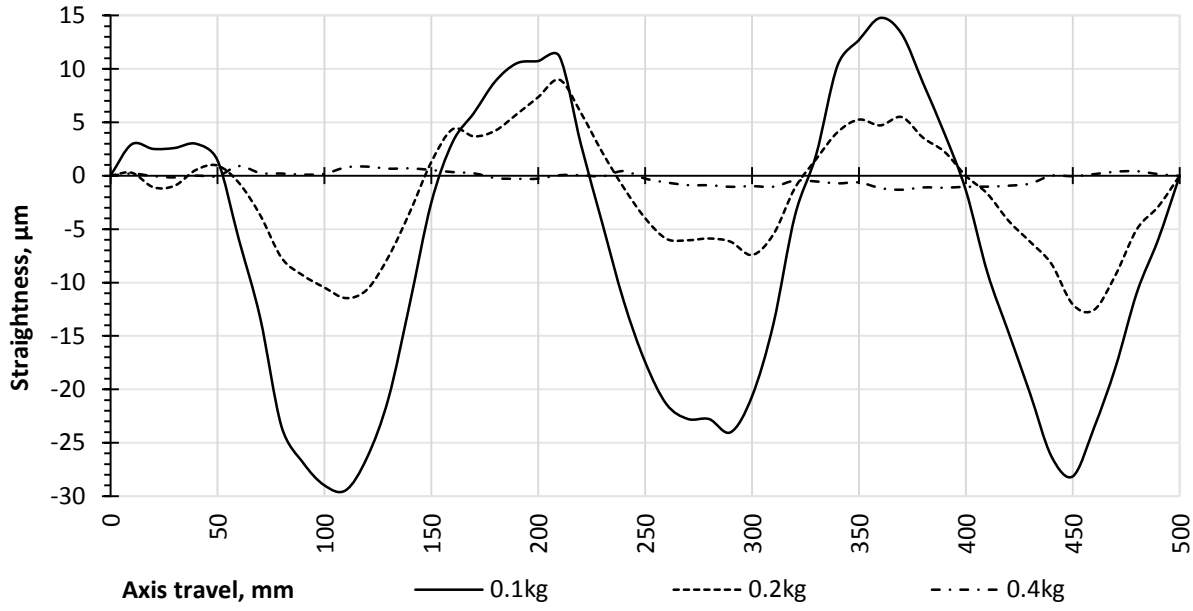

Figure 26. Wire straightness against tensile force provided by the counterweight

Therefore, a general rule for taut wire straightness measurement should be to maintain a balance between force for wire loading and its deformation. Fishing wires are normally rated by the parameter of braking weight, which can be used to obtain the value of counterweight. To avoid potential tearing of the wire or its deformation, approximately 1/3 of maximum load should be used, which is safe in terms of deformation but does not reduce achievable wire straightness because its improvement with increase of tension saturates long before the maximum permissible loading is reached.

Such underloading reduces the probability of overstretching the wire when sudden instabilities in its structure change its straightness profile. This is due to the nature of wire

material deformation. Figure 26 shows the first stage of stretching – up to several microns straightness and very soon after the tensile force has been applied.

The initial condition can look like shown in Figure 27:

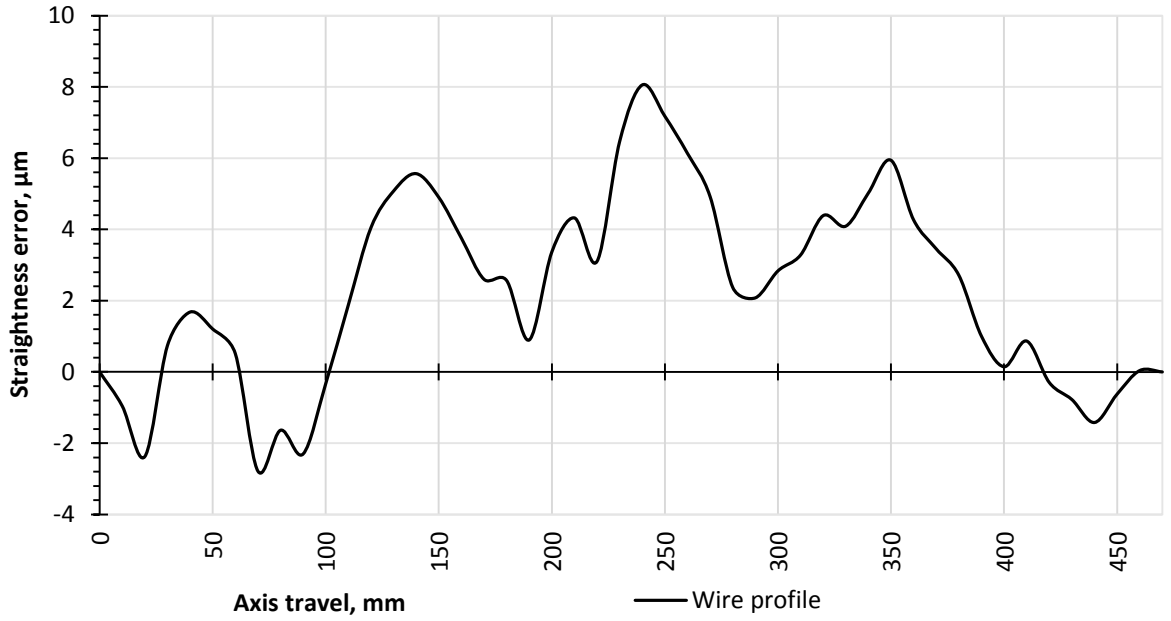

Figure 27. Normally stretched (just settled) wire

After a short time (several minutes for a wire with thickness <0.2mm) relatively flat surface of the wire rapidly changes at some places – dips (or high spikes) appear like the ones shown in Figure 28.

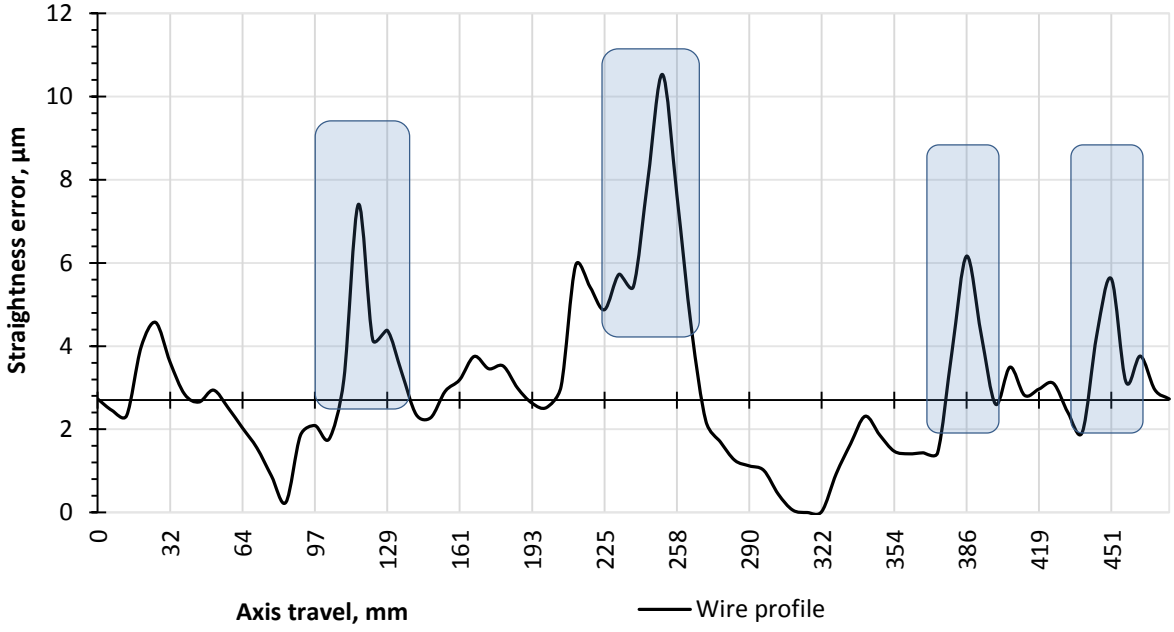

Figure 28. Deformations due to overstretching

These are acceptable for measurements with error cancellation but can be unacceptable in case of single sensor and axis has same or less error than the reference.

3.2.11 Obtaining an increment (step size) value

Separation of the sensors is determined once by using a piece of opaque tape attached to the wire. Detection of the edge of the tape while slowly moving the machine axis gives each sensor a clear and rapid change in readings taken and the difference in machine coordinates of both points gives the measured step size. Ambiguity using this simple method comes from the accuracy of the axis, shape of the tape, speed of motion, etc. During experiments it was in the order of 10µm (based on repeatability of manual operation) which is sufficient because the rate of change in diameter of the fishing wire (including large defects) used is very small, typically 0.1µm/1mm (i.e. only 0.001µm over 10µm).

Normally step size does not need to match the distance between the sensors exactly; a small deviation of ±0.2mm is acceptable according to Figure 29 which shows the result of eight sequential tests with a different movement increment. The measured error remains on the same level.

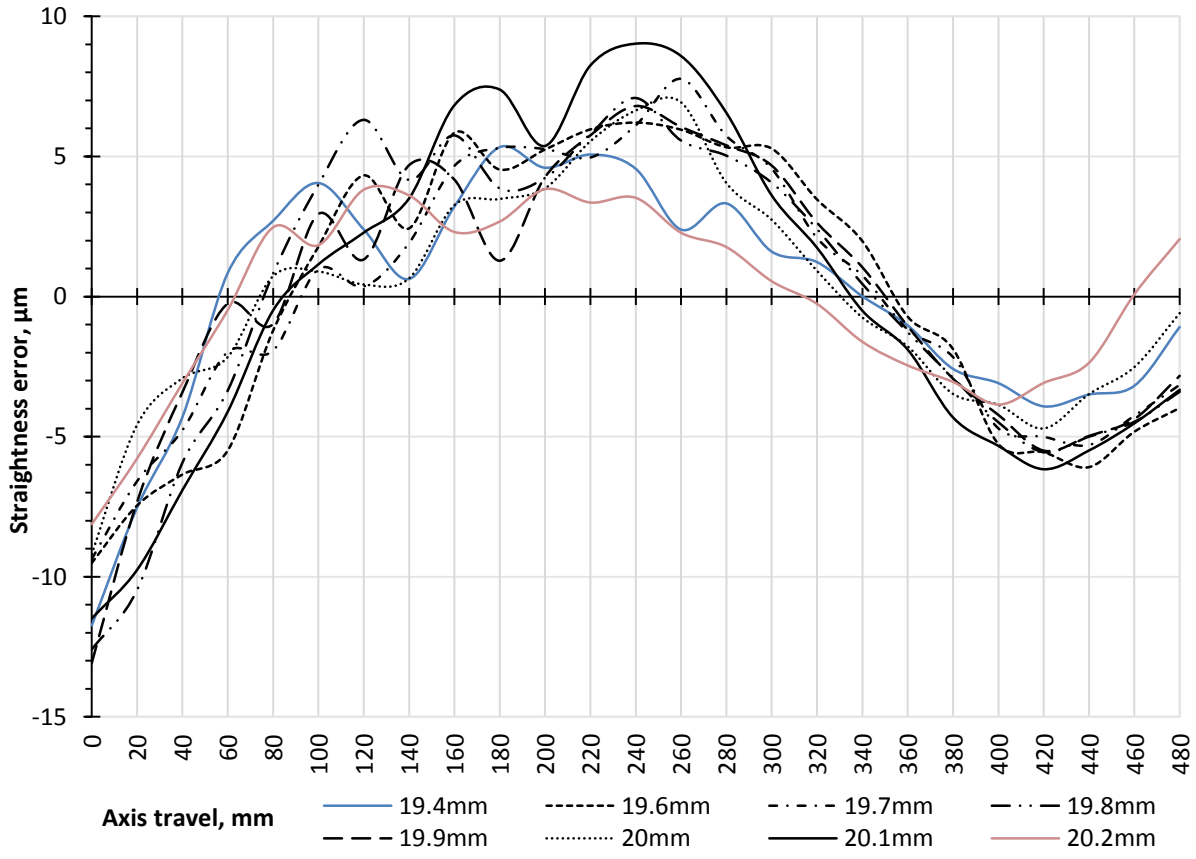

Figure 29. Straightness measurement with a different movement increment

The distance between sensors used to be 19.9mm measured using the method described above. There is no systematic effect produced by distance and step mismatches but the more it is, the greater difference it makes.

3.3 CATENARY COMPENSATION

The longer the measured axis, the longer the wire is needed to measure it. When wire tensile force remains the same as well as its diameter, sag in the wire due to gravity increases with the distance between the stands (wire mounting points). As a result wire sag contributes to straightness reference error potentially limiting the final measurement accuracy of vertical straightness measurement on horizontal axes. This error is systematic and predictable; it is parabolic [76], can be calculated and subtracted from the measurement result.

A simple model of the taut wire is shown in Figure 30.

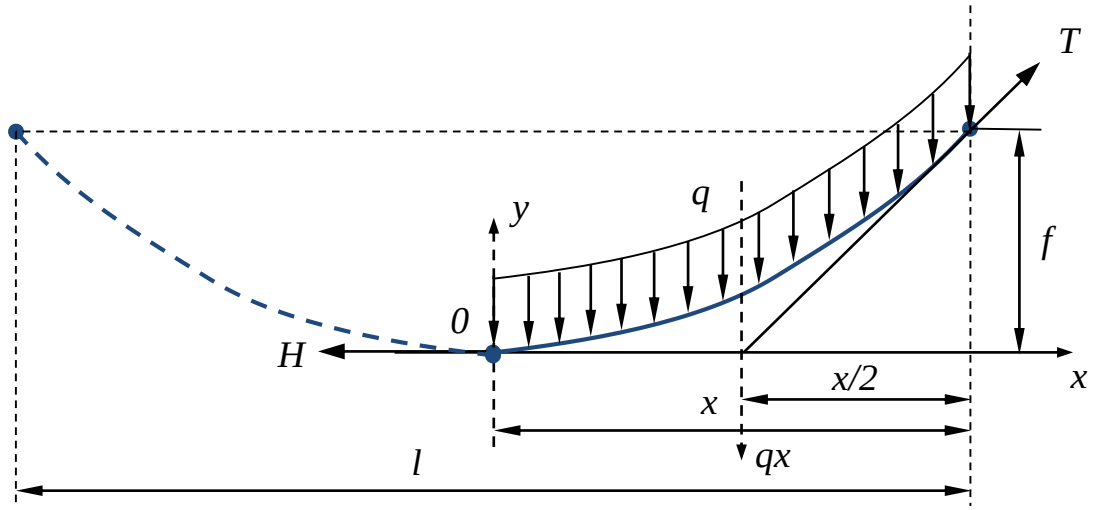

Figure 30. Wire fragment

Once the wire is settled, the sum of moments of forces becomes equal to zero. If we assume that the result of a distributed load q will be qx applied in the middle of x, then the equation of forces of the wire will be:

$$H \cdot y - qx \cdot \frac{x}{2} = 0 \qquad (1)$$

Where H = tensile force,

q = distributed load (weight of the wire),

x = horizontal coordinate,

qx = resultant of the distributed load,

y = vertical coordinate.

Equation (1) can be transformed as:

$$y = \frac{qx^2}{2H} \quad (2)$$

Which means that the curve is parabolic and referred to as the catenary. When both end points are located at the same height, vertical coordinate is equal to catenary f:

$$y = f \quad (3)$$

And resultant of the distributed load is in the middle:

$$x = l/2 \quad (4)$$

Where l = distance between stands (wire fixture points),

Incorporating both into (2), the maximum sag deflection can be derived as

$$f = \frac{ql^2}{8H} \quad (5)$$

Converting mass to force as the following:

$$P = mg = H \quad (6)$$

Where g = 9.81,

Both q and H can be derived from the free weight used in the system and specific weight of the wire. Using the three points (two ends on catenary estimation parameters and one in the middle), a parabolic curve can be fitted to them to be used during straightness measurement.

To validate this catenary estimation method, a test with two different values of counterweight was performed to identify the change of the sag. The wire weight was measured using chemical balance *OHAUS G110* (Appendix B), wire length – with tape measure and counterweight – with conventional 10kg digital scale. The summary is shown in Table 1.

Parameters	Test 1	Test 2
Wire length, m	***1.52***	***1.52***
Wire weight, g/m	***0.016***	***0.016***
Counterweight, kg	***0.73***	***0.55***

Table 1 Catenary estimation parameters

The results of catenary estimation and straightness tests are presented in Figure 31:

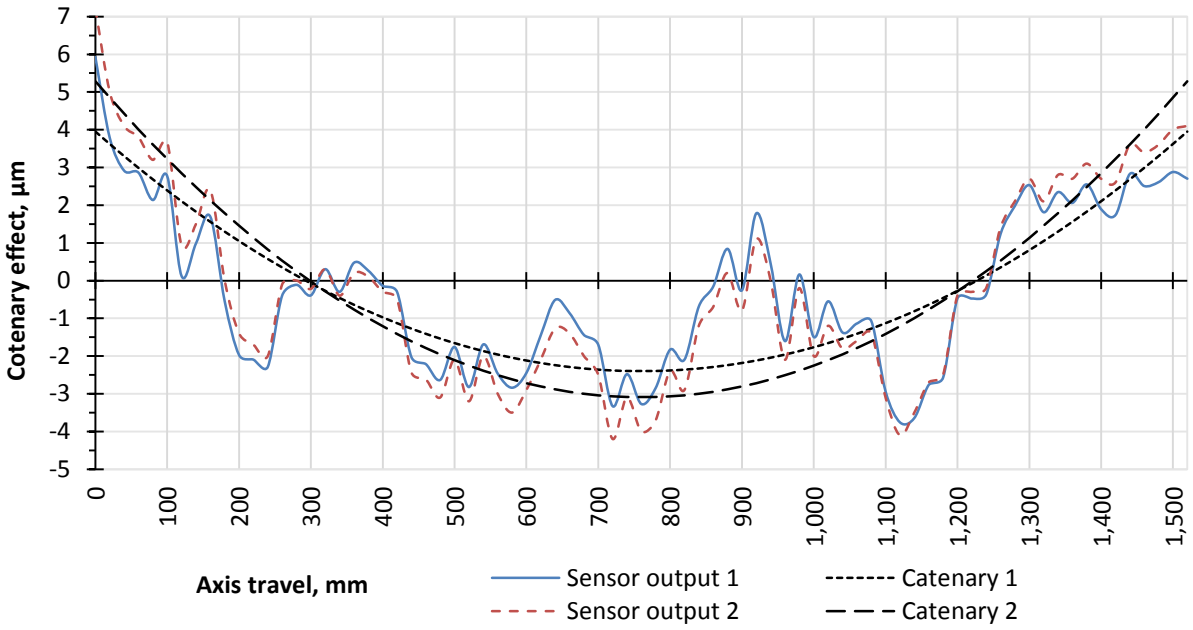

Figure 31. Two examples of catenary estimation

Decreased tensile force resulted in sag increase by 2µm. In both cases the sag can be subtracted from the straightness profile on the stage of data analysis. As before, least squares method was used to obtain the representative line (to position the graphs). Catenary correction was applied after fitting which could be done because the correction does not rotate the graph or move it in vertical direction, it only changes its shape.

3.4 ERROR CANCELLATION TECHNIQUE

The capability of many measuring methods is limited by the accuracy of its reference. The taut wire is no exception as lack of its own straightness always combines with the straightness error of the measured axis. Additionally in this case is the slope error or non-parallelism of the wire to the axis. This can be reduced using good set-up but not eliminated therefore any remaining slope is removed by subtracting linear least square fit or end point

data (not recommended in the related international standards) from the measured straightness profile. The former straightness deviation of the wire itself is more difficult to separate.

It is common practice to use “reversal” techniques, where possible (section 1.2), to compensate the error of a reference but this approach only works with rigid references, such as straightedge artefacts. The wire, being flexible would not retain its shape from any physical reorientation technique. When it is mounted between two points, with tension maintained mechanically to obtain a stable condition, its straightness error remains constant. As soon as the tension force is changed, the surface profile of the wire, read by the indicator, also changes. This change has proved to be random and therefore not predictable. It is obvious that the wire requires a different kind of technique which can be applied to a stationary object, examples of which are discussed in the following section.

3.4.1 Error cancellation importance

The technique of the reference error cancellation during step by step straightness measurements was reviewed in section 2.3 and it was determined that a similar principle could be applied to a taut wire straightness reference. It is not rigid but practically single dimensional and has its own straightness error due to gravity and inconsistency of its diameter over its length (represents two other dimensions). Effect of gravity on the wire, termed its “catenary”, is negligible over range up to 0.5m, however it must be considered for measuring distances associated with machine tool axes and will be discussed in section 3.3. The surface profile of the wire has a certain error which depends on a number of factors, listed below:

1. Wire material.
2. Wire quality.
3. Wire thickness.
4. Tensile force.

The effect of all of those factors, at least once the wire settles between two points, does not vary significantly with time. The shape of its surface profile (in its lateral section) stays the same until the wire is removed or the tensile force changes.

Apart from systematic effects, a number of random factors can affect the wire when it is in the nominally stable condition:

1. Airflow.
2. Vibration.

Those can be tested prior to the measurements using “static tests”, when the measured axis is not moving and readings are taken during a certain time period representative of a typical measurement, such as 5-15 minutes depending on axis length.

In addition to the errors listed, the indicator can have its own imperfections which lead to certain systematic and random errors. All these combine with the straightness of the axis and significantly contaminate the output. To get the desired straightness profile of the axis, it is necessary to determine and/or separate other errors from the result, otherwise it might represent error of the reference but not the measured error. This is particularly important when measured error is as small as few micrometres which is comparable or less than measurement errors including the reference error.

3.4.2 Double sensor

The proposed solution involved switching to a double sensor system which utilises the aforementioned error cancellation principle [67, 68, 69, 70 and 71]. Two identical sensors (used instead of indicators) are mechanically fixed together in the same nominal measuring position with a short offset one from another in the direction of axis travel. The offset distance x should be equal to the step size at which the measurement is performed (when sensor readings are taken at a number of sequential points equally adjacent to each other and covering the full traverse length of the measured axis). The sensor setup and incremental movement is shown in Figure 32:

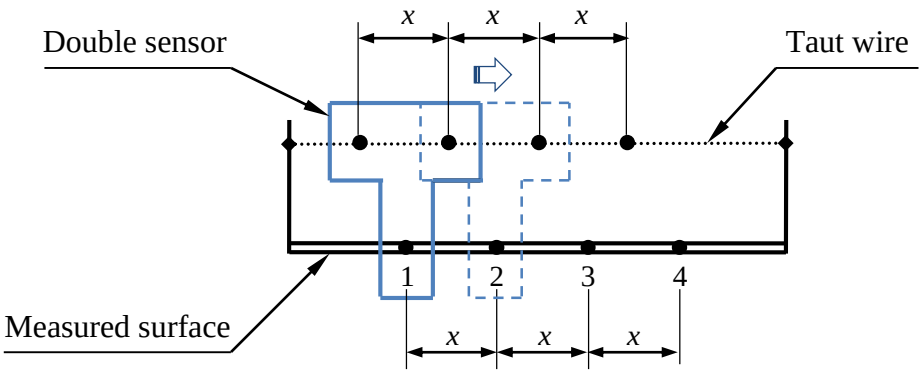

Figure 32. Measurement with the double sensor

Readings from the two sensors will be different because different points of the wire will be measured. At the same time, both sensors will be affected by the same point of axis,

straightness of which is being measured. Repeatability of the machine affects the quality of this repetition but considerably less than if it were two consequent runs. When the axis is moved one step forward, the second sensor takes the same position on the wire that the first one had on the previous step (because the distance between both sensors is equal to the axis movement increment). This way on every step we get two readings every one of which combines measured lateral displacement of the axis guide and wire straightness error along with other errors.

If we subtract reading of one sensor from another, taken on the same step, the result will be a difference between wire errors in its different points because axis errors have been the same and gave zero when subtracted one from another. Repeating for all readings over the length of the axis, we get rate of change of the wire straightness error.

The same result can be obtained with a single sensor doing two measurement runs with a different position of the sensor or the wire (if its tension is maintained constant during reposition). If we move the sensor one step distance forward (using an adjustment carriage, for example) and do a second run, the same values can be obtained. If the sensor remains fixed on the same place on the axis, the wire itself can be moved one step forward giving the same results. All the above implements two-point method, discussed in section 2.3.

In practice, it is very difficult to move the wire or the sensor when both are set up on the machine. Also random errors will be different for two sequential runs and being subtracted from each other will not give zero or a value close to it. That is why using two sensors permanently fixed together on the axis has a potentially higher accuracy and does not require extra runs to measure the error of the axis.

Having obtained rate of change of the measured axis straightness, it is possible to get the actual straightness from it if we conform to the following three conditions:

1. Both the wire and the measured axis have time-invariant surface profiles: errors of both wire reference and the measured axis remain unchanged during the test.
2. Straightness value (error) at the first measured point on the axis has zero value, achieved by simply datuming the result.
3. Measurement time is sufficiently short that no change in straightness of the machine axis will occur.

The first condition is simple to determine using a number of sequential measurements with the machine stationary should give a stable result within a period of time equivalent to the time needed to do a full measurement of the axis.

The third condition states the necessity to perform the measurement within a certain period of time. This is important because nothing is constant in a real world and the condition of measured axis and straightness reference changes over time and ideally should be checked for consistency before and after the measurement takes place. The results of both checks should match, proving the measured objects remained stable during the measurement procedure. To implement that, two quick dynamic (continuous) measurements can be performed.

3.4.3 Error separation procedure

The order of measuring is as follows: every time the machine axis stops, the current error of the axis combined with the error of the wire on the current and the subsequent step are measured. Because the distance between the sensors matches the axial increment, the first sensor repeats the position of the second one on the previous step and measures the same error on the wire but combined with different error of the axis. In Figure 32 it is shown by pairs of readings taken at the same time: 1, 2, …*n*. The subtraction of the second sensor reading of the first pair from the first sensor reading of the second pair (both have the same amount of wire error) gives the difference between the guide errors between the first and the second steps.

Accumulation of these numbers obtained from the full number of steps (starting from 0) gives the measured values. Any deviations due to random effects such as machine repeatability will not be removed.

When two sensors are used simultaneously and readings are taken in every two adjacent points of the wire and the axis, and the distance between points is the same as the machine movement increment, the following calculation separates axis and wire errors (including some random ones) from each other:

$$x_n = x_{n-1} + s_n - c_{n-1} = \sum_{1}^{n} (s_n - c_{n-1}) \qquad (7)$$

Where x = axis error on step n,

c = combined (measured) error from the first sensor,

s = combined error from the second sensor.

According to the first condition $x_1 = 0$, all the other values of x are calculated using this equation which provides the axis straightness motion error on a basis of rate of change accumulation. The calculation takes out not only straightness error of the reference, but in

some cases also its change during the measurement. If, for example, the wire moves slightly due to air turbulence, it changes readings on both sensors at once and by the same amount due to their proximity. Theoretically, every error read by both sensors at the same value, goes after subtraction (as it comes from (7).

3.4.4 Accumulated error

The use of reference error separation results in the accumulation of small errors in each of the readings taken from both sensors. This error contains both systematic and random parts, the latter of which is reduced through averaging and self-cancellation. Most of the first one goes after the reading are being subtracted from each other but the remaining part adds on the top of the same one from the previous step.

The good side of this process is that random errors like electrical noise or vibration get compensated by themselves, the bad side is that other errors with the same sign for adjacent readings get stacked up. The partial solutions proposed are:

1. Increasing accuracy of taking readings.
2. Reducing of systematic error.
3. Reducing number of measurement points over the range.
4. Measuring twice: starting from one side and then from the opposite one.

The number of points required depends on the measured range and is a multiple of the distance between sensors. For longer axes therefore, the accumulated error increases.

The first two solutions depend on the quality of the system components, power source, filters and also on sensor calibration (section 3.5). The third becomes possible if distance between the sensors can be increased. The fourth solution allows reducing accumulation by two times but doubles the time needed for measurement and strongly depends on result repeatability. In any case, bidirectional test runs will clearly show the amount of the accumulated error and a conclusion about the necessity of additional actions will be made.

3.5 SENSOR CALIBRATION

The error compensation technique described in the previous section requires two sensors which need to be identical in a sense that the same input should give the same output in both. Because the input is linear, the output needs to be linear too. Otherwise a sensor output mismatch error can exceed the measured value and even all other errors in total.

Every optical sensor is unique in a sense of its output. Even if average sensitivity value is the same with others, the distribution throughout the sensing area is always different from the one of other sensors. Both light emitter and receiver are silicon crystals which can never be exactly the same as other one; this comes from the technology of their manufacturing.

Practically, optical sensor output slightly differs from sensor to sensor like shown in Figure 33:

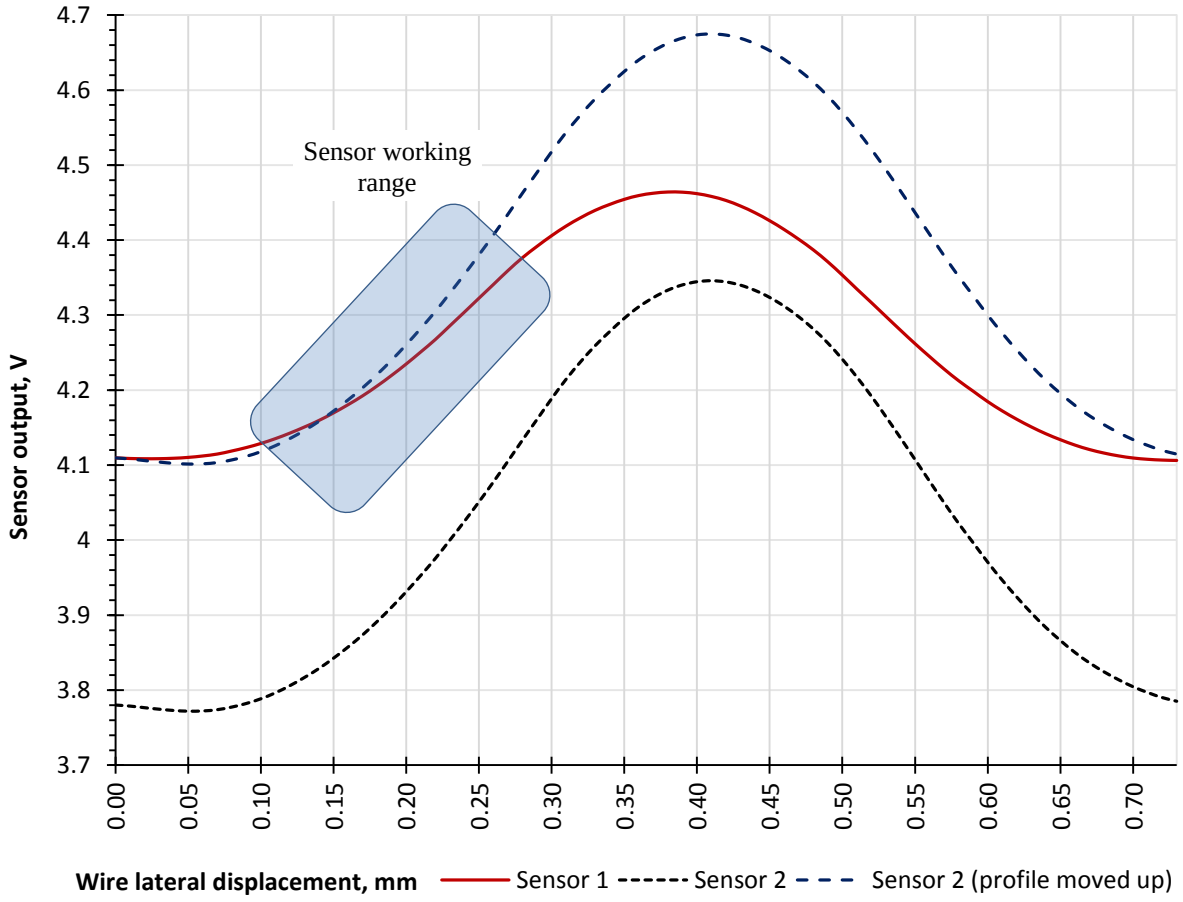

Figure 33. Two sensors detecting the same displacement

3.5.1 Pre-calibration

As discussed before, optical sensors can detect the wire coming in to the sensing area when approaching it from the bottom side or from the top side (left or right in case of measurements in horizontal plane). Each case is represented by a corresponding branch on the sensor sensitivity profile (Figure 33) – left half for one and right half for another.

It is necessary to choose which side will be used for measurements and use it only to avoid confusion. The difference between them is as shown on the graph: left areas are close to each other than the right ones. Even though this effect (Figure 34) can be corrected, it will

always exist more or less and it will be appropriate to choose the side where both graphs are located closer to each other. The reason for that is obtaining the widest combined working range when both sensors start working and stop at the same time. This way intersecting working range will be at its possible maximum.

The choice of work area will determine the direction of sensor readings change relatively to the wire / axis point movement. If moving up wire results in increased values read from sensors or decreased ones. This should be noted.

It is important that both sensors should respond the same direction, otherwise the wire is not installed correctly (extensive slope).

The second objective of pre-calibration is choosing the local area for measurement out of the whole possible range. This can be done, as before, examining the full range sensor response and finding an area of the maximum coincidence. Normally worst expected straightness is known and is less than the value fitting the total work range of sensors and it is desirable to reduce sensor output compensation to its minimum to avoid its own error.

Concluding discussed above it can be said that during pre-calibration a whole sensitivity range of the current wire-sensors system needs to be examined, the direction of the wire entering the system chosen and the best local area of sensor work range determined and corresponding output values noted.

3.5.2 Remaining error

The area where sensors perform similarly is highlighted. It is still not perfect and has certain output mismatch.

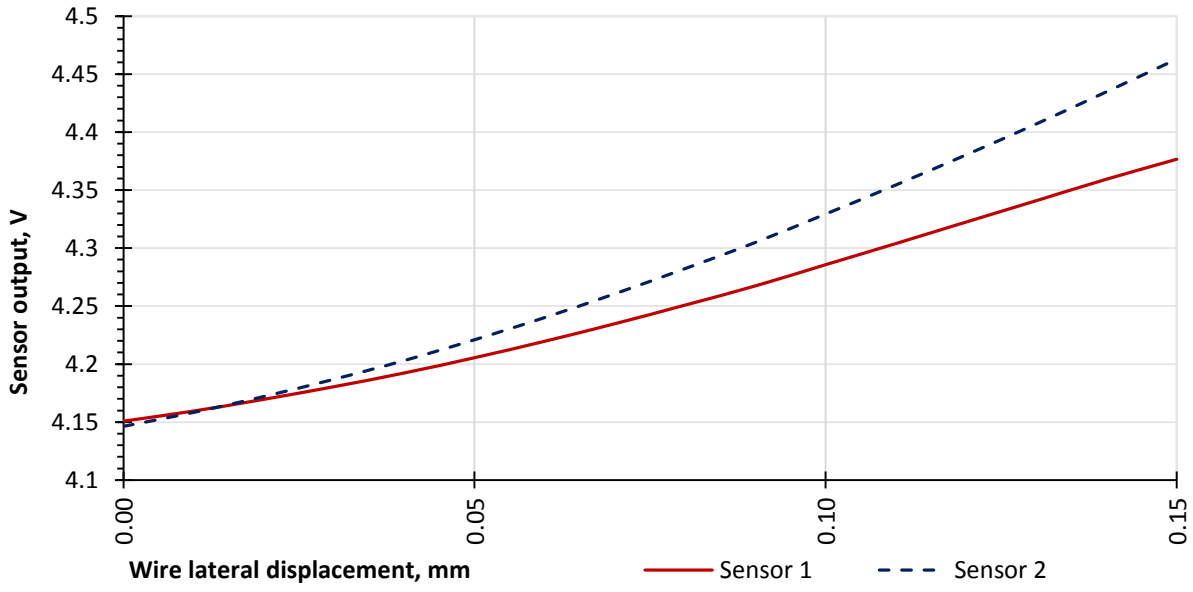

Figure 34. Best match area

Considering sensitivity of 1.6mV/µm and error accumulation, this can lead to a large error. Another possible issue is that working area has been shrunk to 150µm which might not be enough for straightness measurement. Also the sensitivity of sensors can change or they get a different position relatively to the wire resulting in sensitivity profiles move one relatively to another in horizontal direction as show in Figure 35.

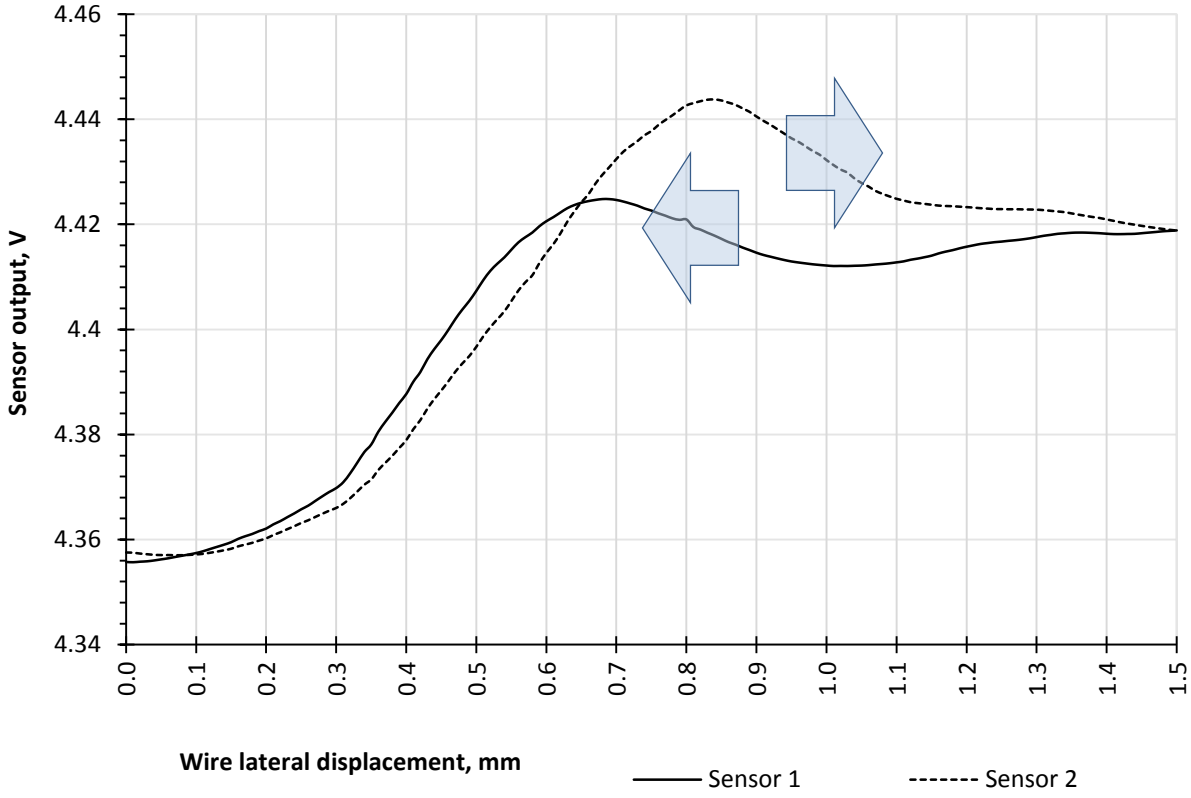

Figure 35. Sensor block tilted

And lastly, both profiles are not linear and even if they were, the area of best match would need to be somehow determined. That is why calibration of sensors, even if only one used, is essential.

3.5.3 Calibration method

Calibration of double sensor system has four aims:

1. Make the output of both sensors linear.
2. Make both outputs equal.
3. Expand the working area to its maximum.
4. Equalize and determine sensitivity of both sensors over all range.

Figure 36 shows outputs of two sensors when the measured axis is moving equal increments in lateral direction only (as discussed in section 3.2.5). The sensors respond slightly differently and both are not linear. Output of the first one is higher than output of the second one. Line in the middle is a desired output of both sensors.

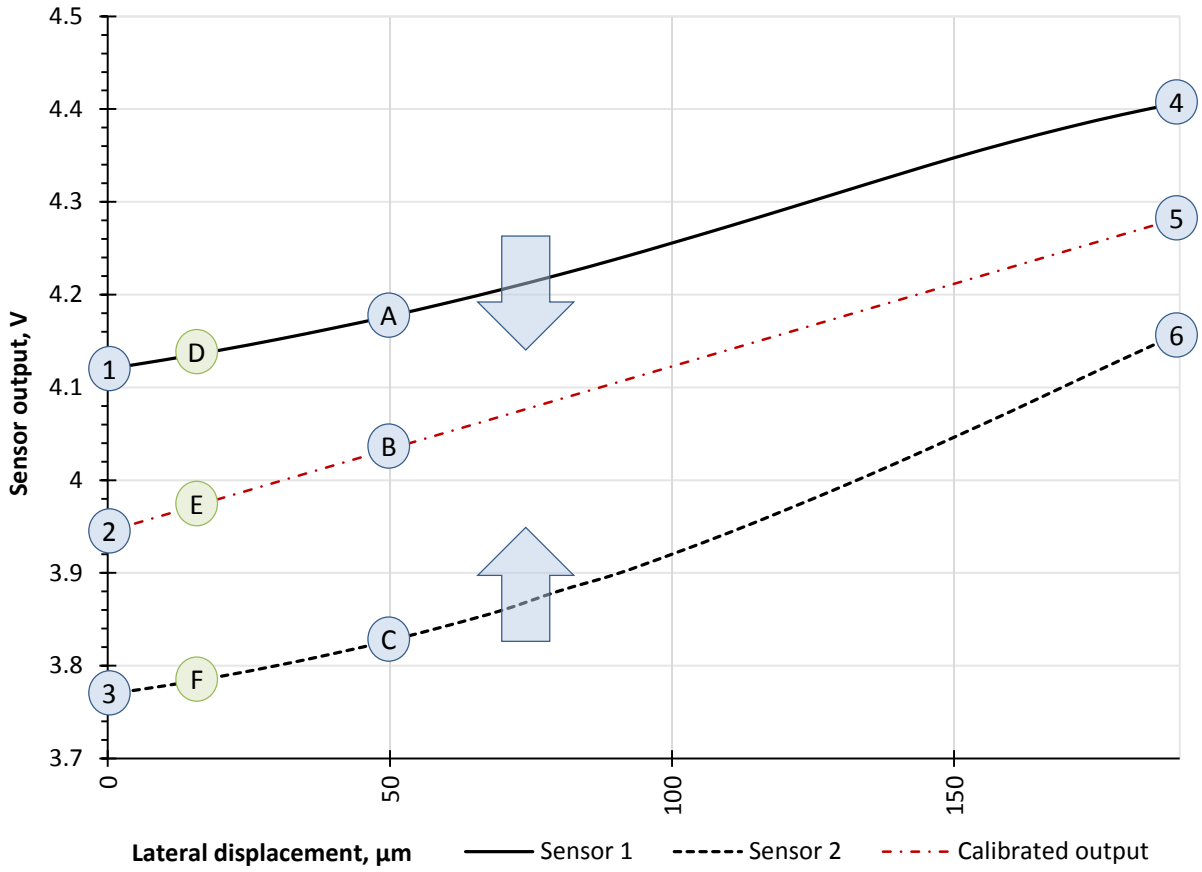

Figure 36. Merging two outputs into one

To linearize and equalize both outputs they need to be corrected accordingly to their values on every step. This means that every point of "native" sensor response needs to have a certain value subtracted from or added to it to bring it exactly on the desired output line from which sensitivity could be easily determined.

The input is known lateral displacement of the axis covering all necessary working range. It can be obtained moving the axis or the sensor head in straightness value measurement direction. The movement should be done using known increments.

Then desired sensitivity line is determined – theoretically it can be located regardless of two sensor output lines but to reduce the amount of correction it is appropriate to locate it in the middle between those, taking two middle points (2) between their left and right ends (1 and 3; 4 and 6).

The next step is to calculate the output differences between desired (B) and actual ones (A and C). This can be done subtracting B from A and C from B on every step, creating a table of correction values. Every of them correspond to a certain output interval of a certain censor.

During the measurement of straightness, values obtained from sensors should be compared against output intervals from the correction table and when it matches one of them, the corresponding correction value needs to be added to or subtracted from it.

3.5.4 Correction enhancement

To increase the accuracy of correction, its amount can be adjusted accordingly to actual output position between two reference points using a linear interpolation.

For example (one sensor), if closest reference outputs are 5 and 6 with corresponding corrections 0.2 and 0.3, the sensor actual output is 5.2, the correction value which could be 0.2 or 0.3 can be adjusted to 0.22 which is more accurate than any of two corrections unadjusted.

3.6 CONCLUSIONS ON MEASUREMENT SYSTEM

A taut wire taken as a straightness reference has been adopted to the measurement. Error separation technique enabled reduction of the wire profile error using dual sensor measurement procedure.

A measuring head incorporating optical sensors and electric circuit has been designed and discussed with a respect to specification requirements. Slotted optical sensors, combining low cost, portability and high sensitivity were chosen to detect measured error.

Different wires have been tested for measurement suitability, a high quality fishing wire which evidenced the lowest diameter variation over the length was chosen for all further experiments.

System setup has also been discussed including choosing the right tension, settling period and size of the axis increment.

Pre-measurement calibration procedure has been described for equalizing and linearizing optical sensors output including all necessary corrections to raw data.

CHAPTER 4 METHODOLOGY FOR STRAIGHTNESS MEASUREMENT USING A TAUT WIRE

It is appropriate to perform experimental measurements on axes of various lengths to help develop the measurement methodology and because increasing distance normally adversely affects the accuracy of measuring systems due to both the magnitude of the errors being measured and straightness reference errors. Since the reference object has a certain length which is ideally not shorter than the traverse length of the measured axis, its own straightness, or other parameters dependent on the wire, may increase with its length.

Variation in the magnitude of the errors being measured in both horizontal and vertical directions can require some differences in measurement approach to consider the change in factors affecting the measurement. Another important reason for testing different axes is a necessity to figure the method's scalability in terms of distance. To see if it is still feasible when the distance is increased and what potential it has.

This chapter will begin by discussing the experimental setup of the system on a precision single-axis test rig, the environment about which can represent either laboratory or improved manufacturing conditions for which the method is proposed (validation under typical manufacturing conditions on a large machine will be covered in Chapter 5).

A number of test results obtained using a measurement procedure will be discussed and validated compared to the results of a commercial laser interferometer system. Both measurement systems were set-up to measure the same error in the same conditions. Additionally, static stability tests, i.e. with the machine stationary, have been completed and are compared as well and all conclusions listed.

4.1 SETUP AND MEASUREMENT

General principle of measurement is as discussed in section 3.2.7: the wire is fixed along the measured axis, the sensors are positioned so that while it moves, the wire passes through their sensing areas. Any lateral displacement of the wire/sensors relative to the axis is detected, reported and recorded.

4.1.1 Measurement procedure

To minimize time and effort needed to perform the measurement and to maintain its efficiency close to maximum, a correct order of actions has to be fulfilled as follows:

1. System setup on the machine.
   1.1 Mounting columns.
   1.2 Mounting measuring head.
   1.3 Mounting the wire.
2. Settling the wire (waiting and monitoring static retraction periods).
3. Adjusting the wire position in main measurement direction (slope removal).
4. Adjusting the wire position in secondary measurement direction (slope removal).
5. Calibration.
6. Measuring straightness of the axis.

The system setup is simple and straightforward, requiring only mechanical adjustment to ensure the wire is parallel to the axis and passes through the optical sensors. It can be done even without monitoring the data from them, visually checking the wire position relatively to the sensors when the axis is either on one end or another. After that the system can be left while the wire settles if it has not been settled in advance. Based on this research, this typically takes between 5 and 10 minutes which can be reduced to 3-6 minutes for pre-stretched wire. The single test run takes 4 minutes for the wire for 1m of axis length which is less than 5 minutes for laser interferometer due to longer stabilization before taking reading.

When continuous monitoring shows that the sensor output stability or a known time interval for settling has passed and the signal drift does not exceed 0.1 mV/minute, the system becomes ready for fine positioning. This includes slope removal by alignment of the wire to the axis in both planes perpendicular to each another, both containing the direction of axis travel and one – straightness value measurement direction. This procedure is described in the following section.

4.1.2 Slope removal

The error, commonly called “slope error” occurs due to minor misalignment of the wire and the axis. This misalignment is always present and the aim of slope error removal is to reduce it to the level where it has negligible effect on straightness measurement.

Slope error makes the reading increase linearly when measuring axis straightness. It may not be an issue by itself as the result can be recalculated by using a simple least square or end point fit.

Practically, however, the slope during a manual setup can be very large, exceeding the measuring range of the sensor system. Also accuracy of a measuring system decreases with increase of the magnitude of measured error, therefore large slope error should be avoided. Even calibration and error cancellation theoretically compensating the abovementioned effect still leave uncertainty that could become significant when it comes to measuring straightness errors in the order of a few microns on precision machines. As a general rule, slope should be minimized to a quarter of the measured error or less prior to making measurements. During this research it was practical to reduce the slope error to within 1-2 microns on the 0.5m axis and to 3-5 microns on the 1.5m axis without requiring too much time. Figure 37 shows an example output with a slope error. It is obvious that the actual sensitive area which was needed for the measurement is few times less compared to the one used.

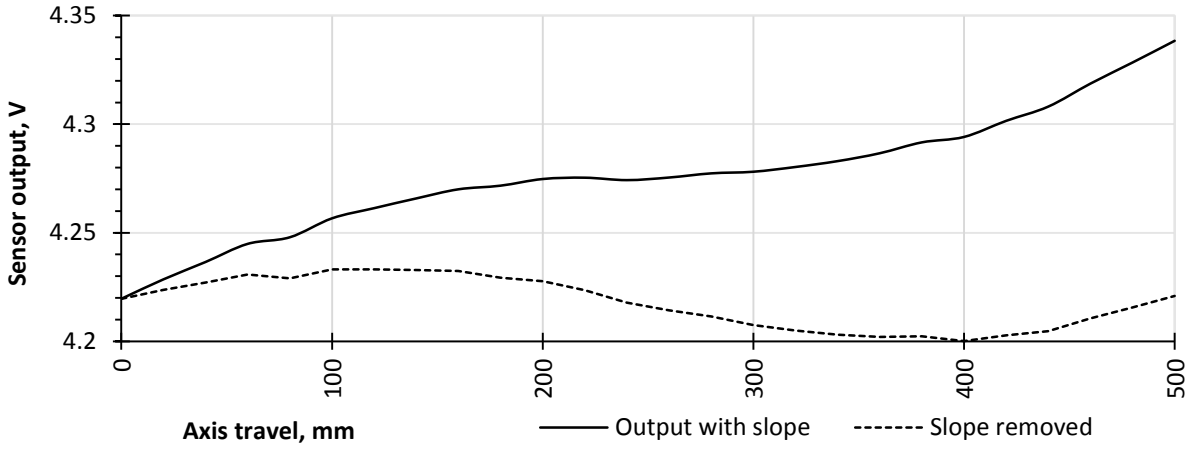

Figure 37. An example of extensive slope error

The method for slope removal is simple and requires moving the axis from one end to the other and checking the change in sensor readings.

Slope removal is an iteration sequence which can be described using an algorithm with three cycles (Figure 38). The procedure begins from setting the head in a position where it can detect the wire when the axis is at its end position. Then the axis is moved to the other end while continuously monitoring sensor readings.

If the slope error is very large, the measuring range may be prematurely exceeded. In this case the wire needs to be adjusted to obtain the reading and the process repeated if necessary. Every time this cycle is performed, the difference between readings at each end is decreased and at some point reaches the value which can be considered negligible, practically few microns as discussed above.

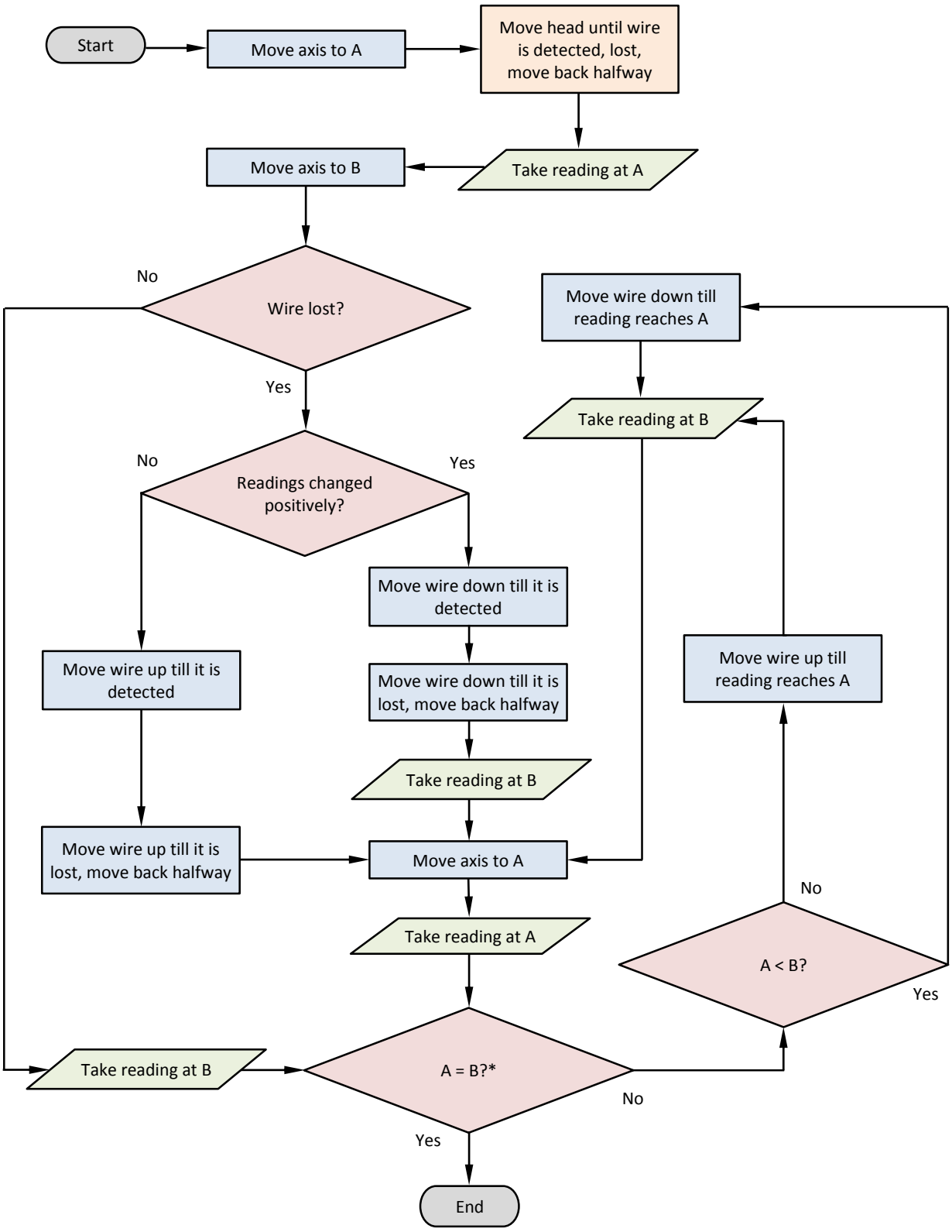

Conditions:

1. Wire position adjustment is done at B
2. Moving the wire up makes the readings go up as well

* - within specified tolerance

Figure 38. Slope removal logic

4.2 TEST RIG STRAIGHTNESS TEST

All straightness tests discussed herein were carried out on a CNC test rig. This is based on a simple but very precise machine tool in as new condition, which provides a horizontal axis having a traverse length of 0.5m which was measured using the taut wire and laser interferometer systems. The setup of both systems is shown in Figure 39.

For mechanical convenience there is a 200mm offset between the two measuring systems. It was therefore necessary to check the contribution of any angular error motion about the vertical axis (yaw error) which could affect the comparisons between the two systems. This was measured using a Renishaw laser interferometer with angular optics and was measured to be less than 1.2µrad which equates to a possible contribution of just 0.24µm to the comparison and therefore deemed negligible for purpose of these tests. The position of both systems in the vertical direction was within 30mm to eliminate any significant contribution from angular motion error about the perpendicular horizontal axis (pitch error).

Laser interferometer consisting of a (V-shaped mirror), Wollaston Prism beam splitter (see Figure 5) and laser head was fixed on the left guide using three magnetic bases.

Taut wire was mounted on two rigid columns along the right guide way, passing through the sensor head (marked orange). Fine adjustment carriages are shown in blue and green colours.

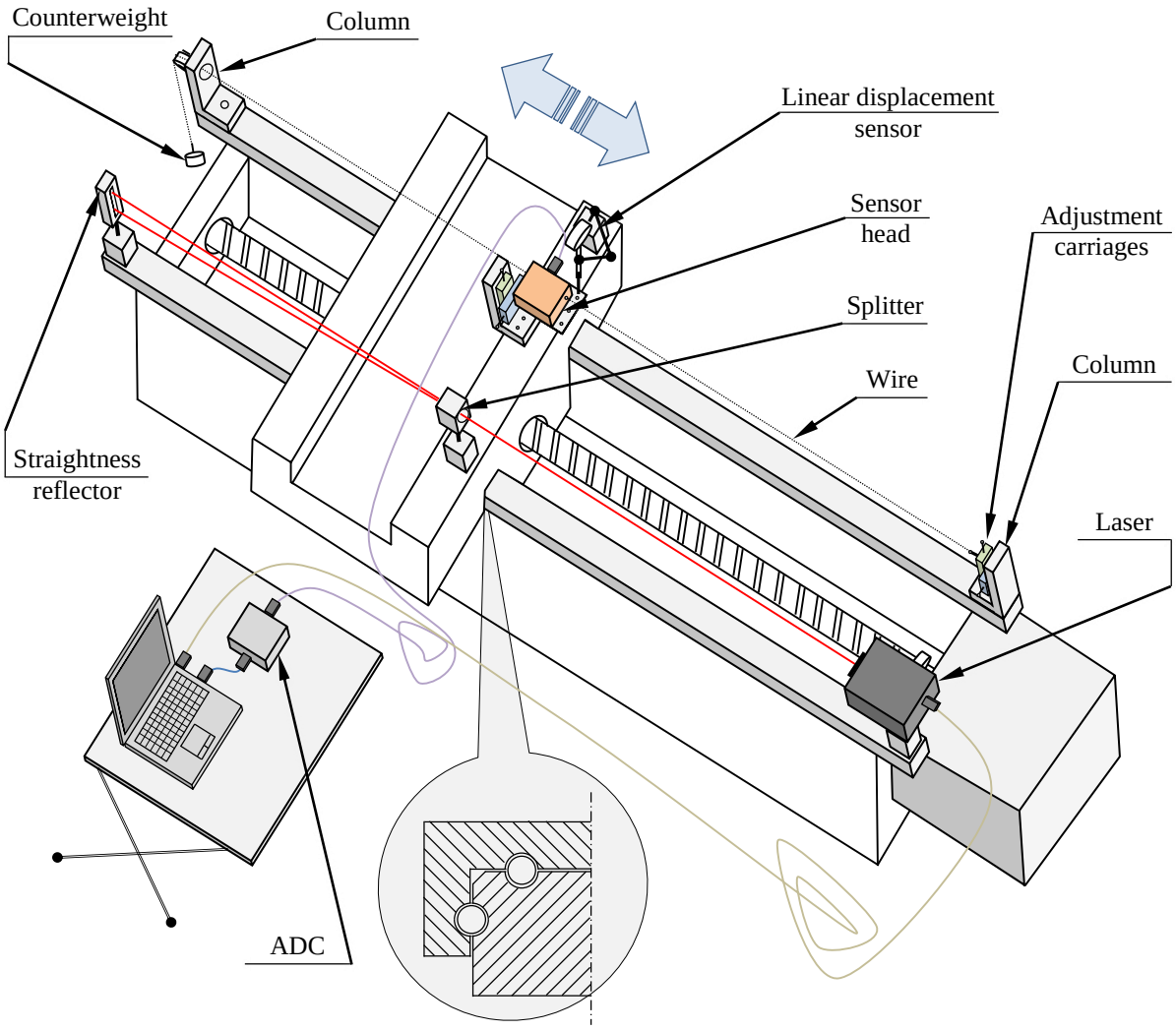

Figure 39. The actual test setup of a ballscrew rig

A linear displacement sensor with 1µm resolution was set up above the head to measure lateral displacement of the head due to vertical carriage operation during calibration. A magnetic base and a rigid clamp were used to keep it permanently fixed on the saddle with a sensitive element on the head plate.

Renishaw laser interferomenter was connected to a laptop computer for data capture using the Renishaw software. The signal cable from the sensor head was connected to the ADC with a USB connection to the same computer.

The test rig uses preloaded rolling element. A magnified section view in Figure 39 shows guideway structure which enables very low friction, repeatable and accurate movement of the saddle and a cast iron bed provides excellent overall stability, therefore the rig is suitable for this experimental work.

4.2.1 Test conditions

The rig was tested while located in both a temperature controlled lab and a typical workshop having normal manufacturing conditions including airflow, temperature gradients, open doors, working machinery, people moving around etc.

In both cases the measurement systems had been static for 30 minutes to complete the heat up stabilization stage. All tests apart from "static" ones were bi-directional and performed 3-4 times to ensure random error elimination. The axis movement speed was set to 5mm/s for measurement runs to reduce axis vibration. Each of them was discrete with a step of 20mm. Every time the machine stopped, a dwell time of 4 seconds followed before taking a reading. The laser was set to long time averaging mode; the wire system used rolling average factor 2. Sampling rate was 50kHz for both systems. The slope of the wire in both planes was always reduced to a value of 1-3µm and did not affect the measurement. The wire used was DAIWA Sensor Monofil 0.26mm diameter chosen during previous research (section 3.2.9).

4.2.2 Calibration considerations

The necessity for calibration was discussed before but in practice there is a question of calibration accuracy. The amount of each step displacement needs to be determined so that it works well but does not require extensive time to capture all data. Conversely, the efficiency of the calibration should be known in order to exclude it from factors affecting further experiments.

For preliminary assessment, the taut wire system was installed on a small high precision CNC machine tool to enable automated vertical movement of the sensor head in 1µm steps. The output from two sensors is as per Figure 40.

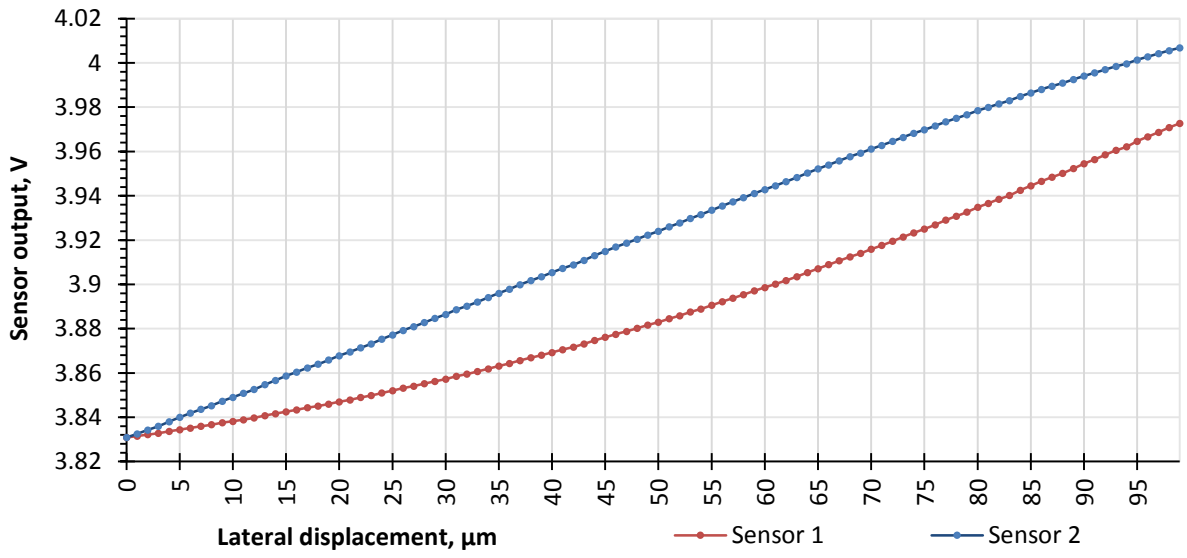

Figure 40. Uncalibrated sensor output captured in hundred 1µm steps

It is clear that both graphs are very smooth and have no spikes or kinks of any kind. This means that the calibration step size can be increased. A simple linear interpolation between calibration points is used therefore based on the largest curvature measured from several of these sensors, a step size of 10µm was determined to provide efficiency with negligible loss of accuracy.

Still, the amount of correction needs to be minimized and therefore the most linear area of the work range should be used. At the same time the maximum sensitivity should be maintained which means the steeper the working area in its used local part, the higher response will be. And the last condition is a necessity to get smooth and linear calibration profiles without any defects which can be controlled manually. These conditions were all met satisfactorily with the optical sensors and taut wire.

The strategy was applied to the set-up on the test rig using a precision linear displacement sensor to validate the procedure. Resulting linear output of both sensors as a response to the controlled lateral displacement is shown in Figure 41:

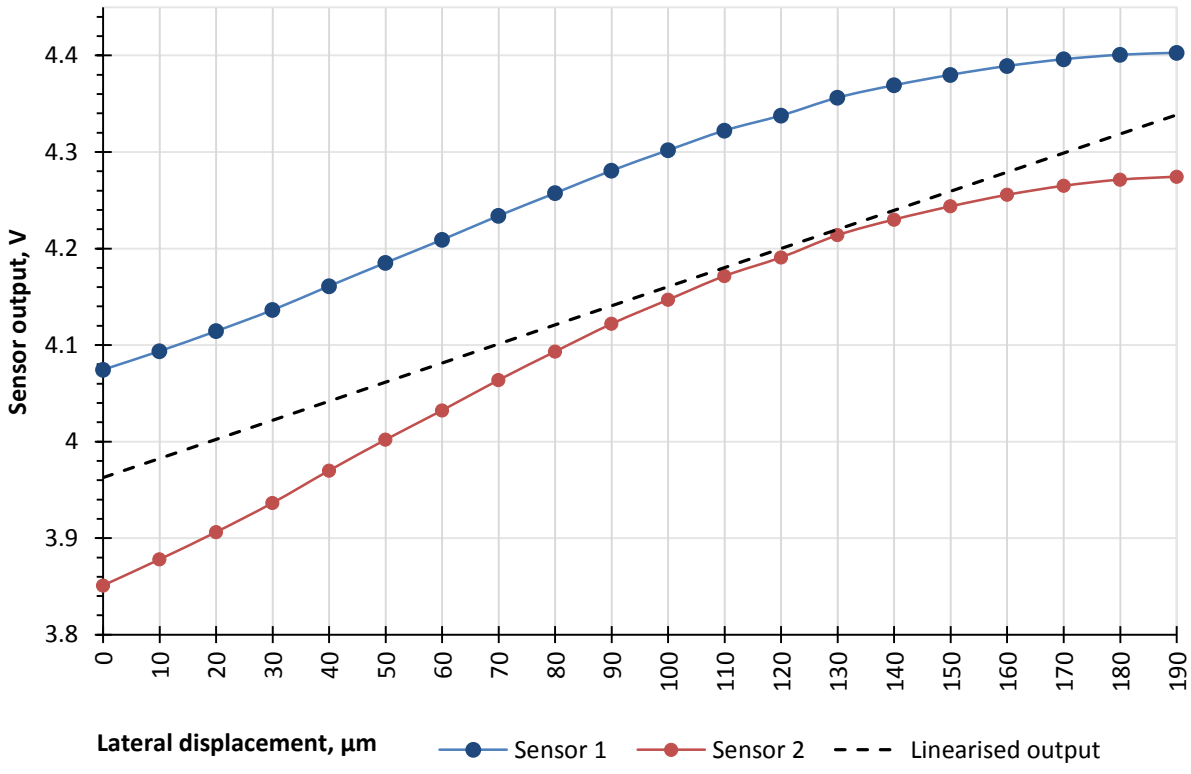

Figure 41. Two sensors linearised

The offsets, calculated from calibration data, will be used to correct the sensor readings during straightness tests.

4.2.3 Laser interferometer repeatability

Straightness measurement using a laser interferometer, a commercial instrument typically used for machine tool error measurement, provides a reference against which to compare the performance of the new taut wire system. Under good operating conditions and over short measuring lengths, a conventional laser interferometer should provide a high level of measurement quality including good accuracy, repeatability and convenience using automated data capture software for short range straightness. Although a mechanical straightedge can have lower uncertainty by using reversal techniques, the difference is small and the convenience and efficiency is lower [77]. In addition, the laser is more flexible in terms of axial range.

This section confirms the performance interferometer. The conditions of the measurement were as follows:

1. Laser model Renishaw ML10, short range straightness kit (0.1m to 4m).
2. The machine, laser and taut wire system were warmed up prior to measurement.
3. The data was taken incrementally, with 20mm steps and 4s dwell time between them.
4. All test runs were bidirectional.
5. Long term averaging (4096 samples during 4s instead of 256 samples in 0.3s) on the Renishaw software was switched on. This is typical for reducing the random fluctuations from air turbulence.
6. Environmental conditions similar to that of a temperature controlled laboratory (±1ºC).

Six sequential tests (three each direction, marked as 1 F – first forward run, 1 B – first run backwards, 2 F – second run forward and so on) were carried out, demonstrating a good repeatable result with a slope less than a micron proving correctness of setup and repeatability of both laser and machine as demonstrated on Figure 42.

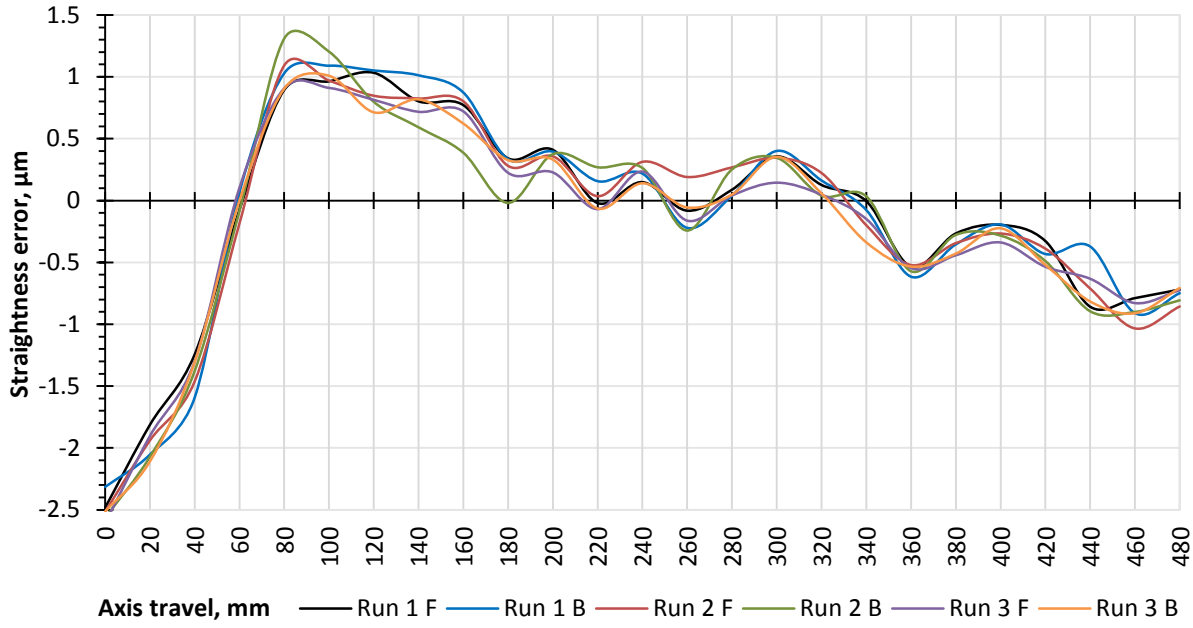

Figure 42. Six laser bidirectional tests of the test rig straightness (vertical plane)

The result was fitted using the least squares method to remove residual slope from the measurement setup and shows repeatability within half of a micron. Taking an average, shown in Figure 43, provides a good result for the comparison.

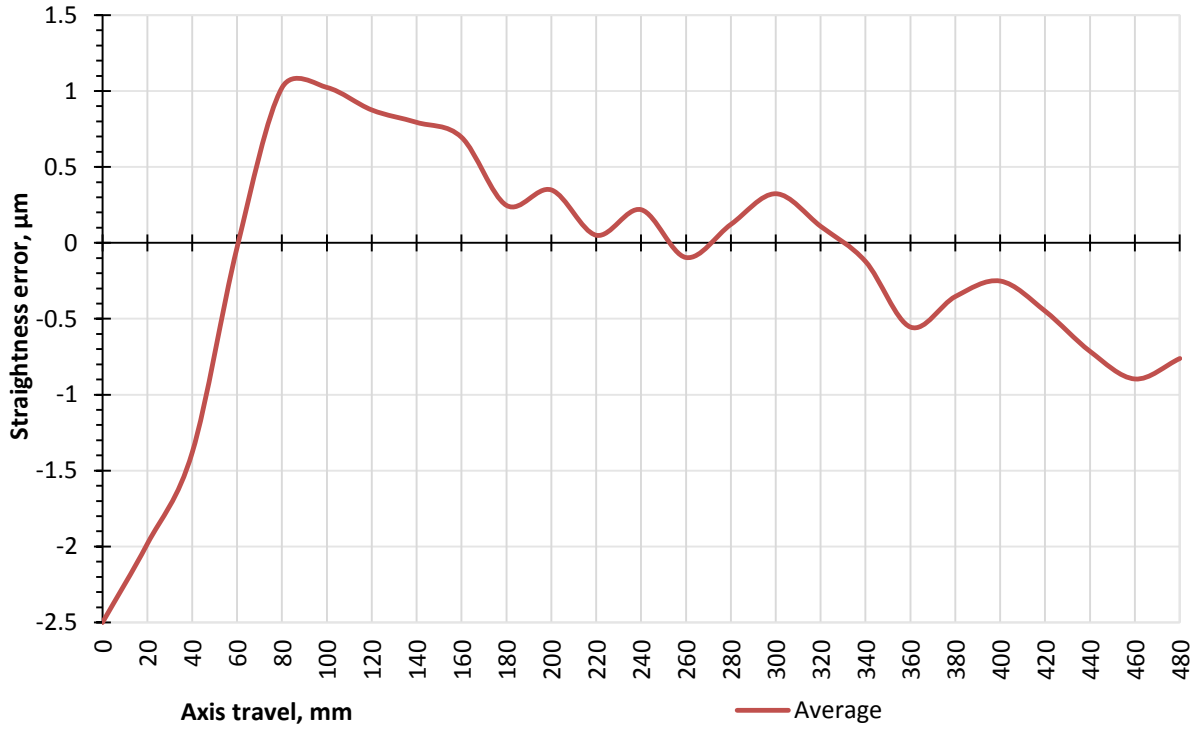

Figure 43. Average of six laser tests

This will be used as a reference for all further tests using a taut wire straightness measuring system.

4.2.4 New sensor and taut wire repeatability

The most basic way to prove repeatability of the system is to measure the same position of the wire repeatedly. Each of those runs can be calculated using the error cancellation technique in both directions as well giving four reading outputs in total. The catenary correction was not used for 0.5m axis because gravity did not have any noticeable effect on such a short range.

Inevitably, random errors such as environmental disturbances, and systematic errors such as electronic drifting and physical transformation of the wire profile as well as step error (mismatch of actual sensor positions with desired locations) will produce variations in the readings which needs to be kept at a sufficiently low level for machine tool error measurement. Any random errors of more than a few hertz can be reduced using averaging.

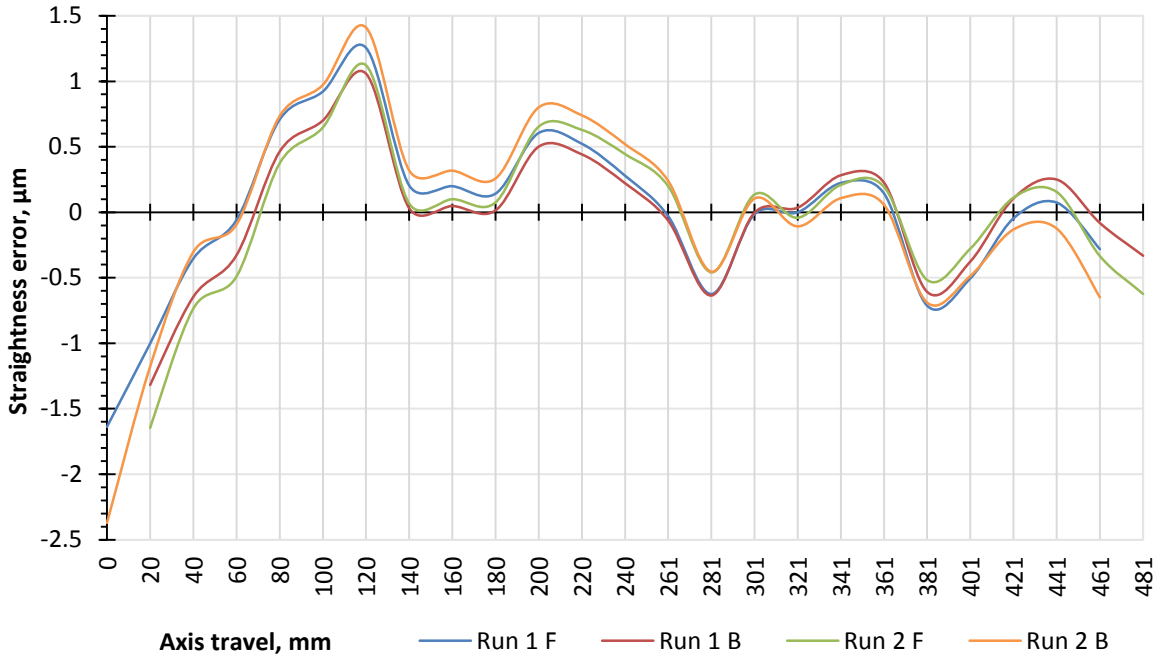

Figure 44. 4-run repeatability of the taut wire system

Figure 44 shows two pairs of outputs: one shifted to the left and one shifted to the right on the graph. This happens because the first point is incomplete (first point of measured axis has only one corresponding point on the wire, therefore its value cannot be corrected using two-point method) and therefore not used in the calculation.

The mismatch between profiles is very slight, and generally within 0.25µm which is confidently acceptable considering included axis reversal error.

All tests which give a straightness error after error cancellation will include an average of all four results and only the average profile will be displayed assuming that no measurement defects (discussion in section 4.2.8) were present.

The next test was supposed to reveal the system's repeatability between measurement runs to get an impression of how many consequent runs are actually needed to get confidence as it is a matter of time.

Figure 45 shows that the difference between runs is always less than 0.5µm, which, taking in to account the magnitude of the measured errors, resulted in the conclusion that three runs is the best compromise of reading improvement through averaging and measuring time.

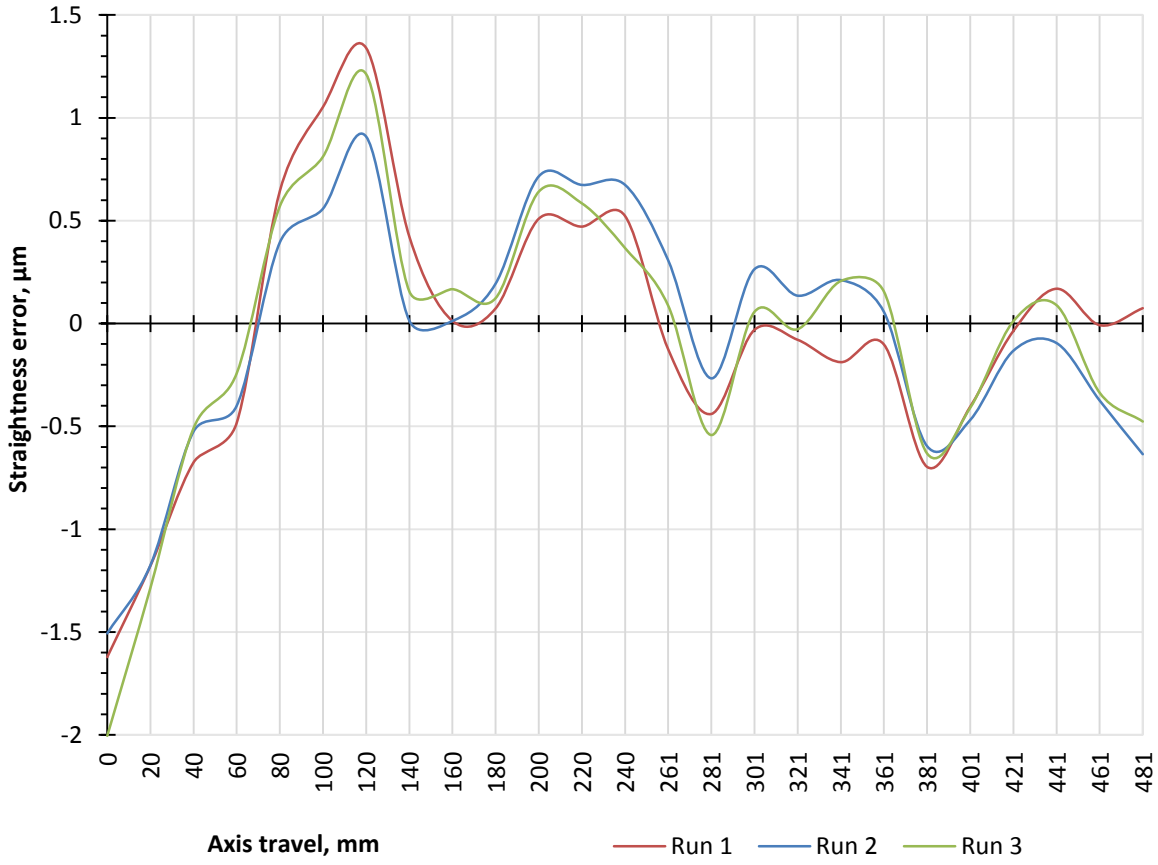

Figure 45. System repeatability within three runs

The results in Figure 44 and Figure 45 approve the error cancellation technique discussed in the next section.

4.2.5 Error cancellation

The error cancellation aims to reduce the difference between different wire profiles therefor three different wires were used to test the machine and validate the methodology under workshop conditions. The results are on Figure 46.

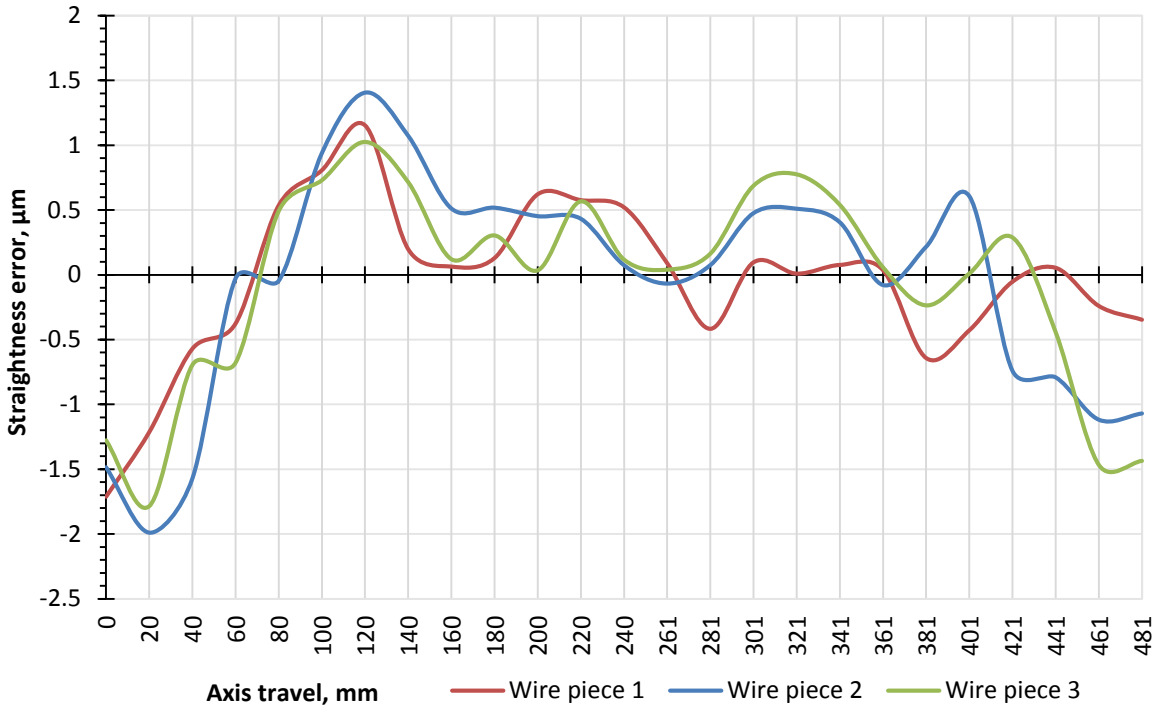

Figure 46. System repeatability with three wire pieces

The mismatch between the runs is wider than measured with only a single wire but is still within a micron and therefore acceptable considering the application of averaging and the target accuracy of 1µm.

In order to show the actual effect of error cancellation the same error was measured using a single sensor results from the same test runs are presented separately (Figure 47).

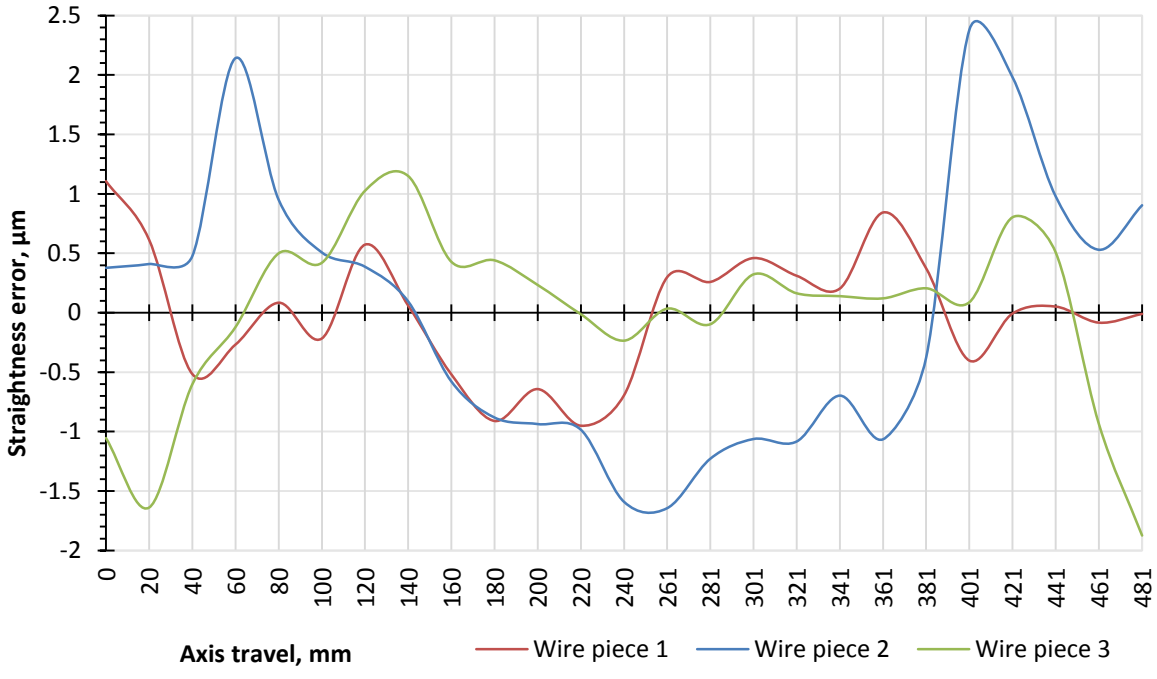

Figure 47. System repeatability with a three wire pieces without error cancellation

These are clearly different profiles which do not represent the straightness of the test rig. It is important to emphasise that the reference error in all three cases is still low and is actually the same as the measured value. But even such a low reference error (which can normally be larger) makes measurement without reference error cancellation unsuitable for precise machines.

4.2.6 Laser interferometer and taut wire comparison

Figure 48 shows the averaged result obtained from the different wire pieces compared against the result provided by the laser interferometer.

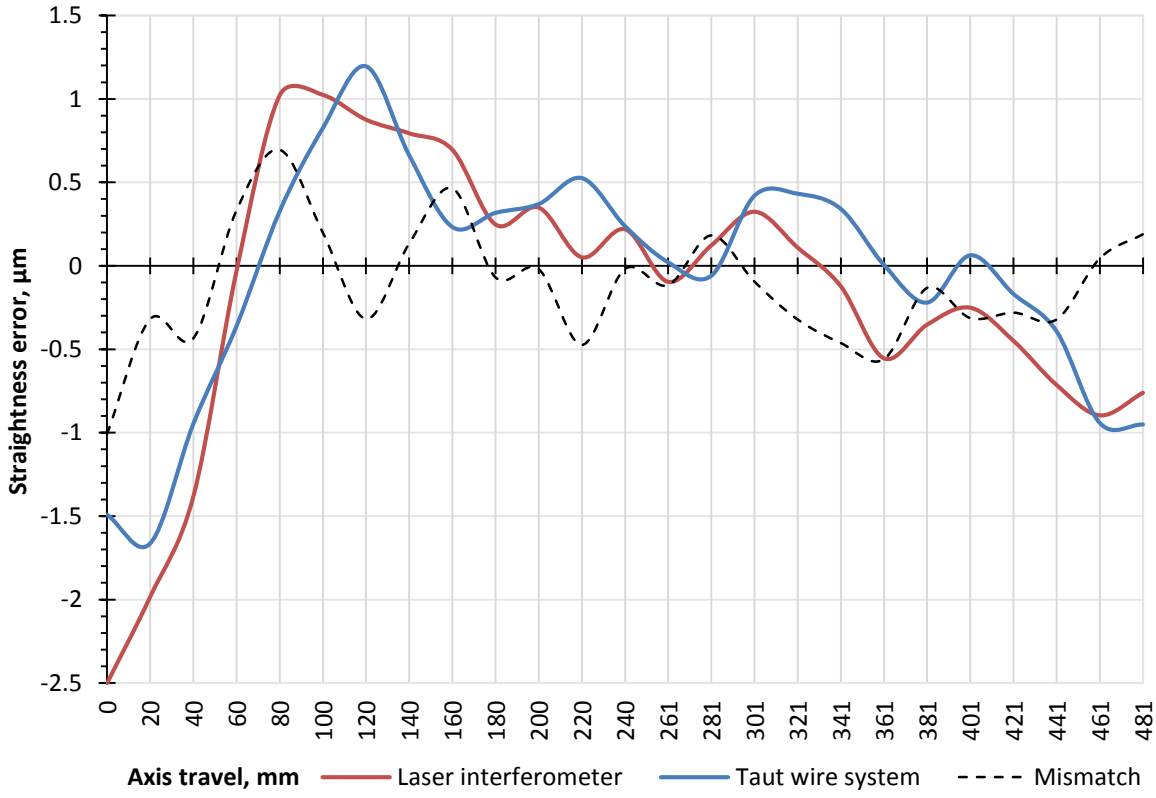

Figure 48. Laser and taut wire measurement results direct comparison

The graph proves a good correlation between the two methods. The mismatch (calculated as a difference between two profiles) is generally within 0.5µm and does not exceed 1µm. Such variation can be accounted for by the calculated uncertainties (section 6.2).

4.2.7 Static stability tests

Static tests are measurements performed as normal but with the measured axis stationary. This enables a better measurement of the system stability, when the machine itself practically does not contribute to the total measurement error.

This kind of test is important to isolate the measuring system stability errors.

As with previous tests, the same dwell times and averaging procedures were used. Error cancellation technique became redundant and worked as a simple error accumulation.

The first test is done using Renishaw ML-10 laser interferometer using the same its setup on the machine.

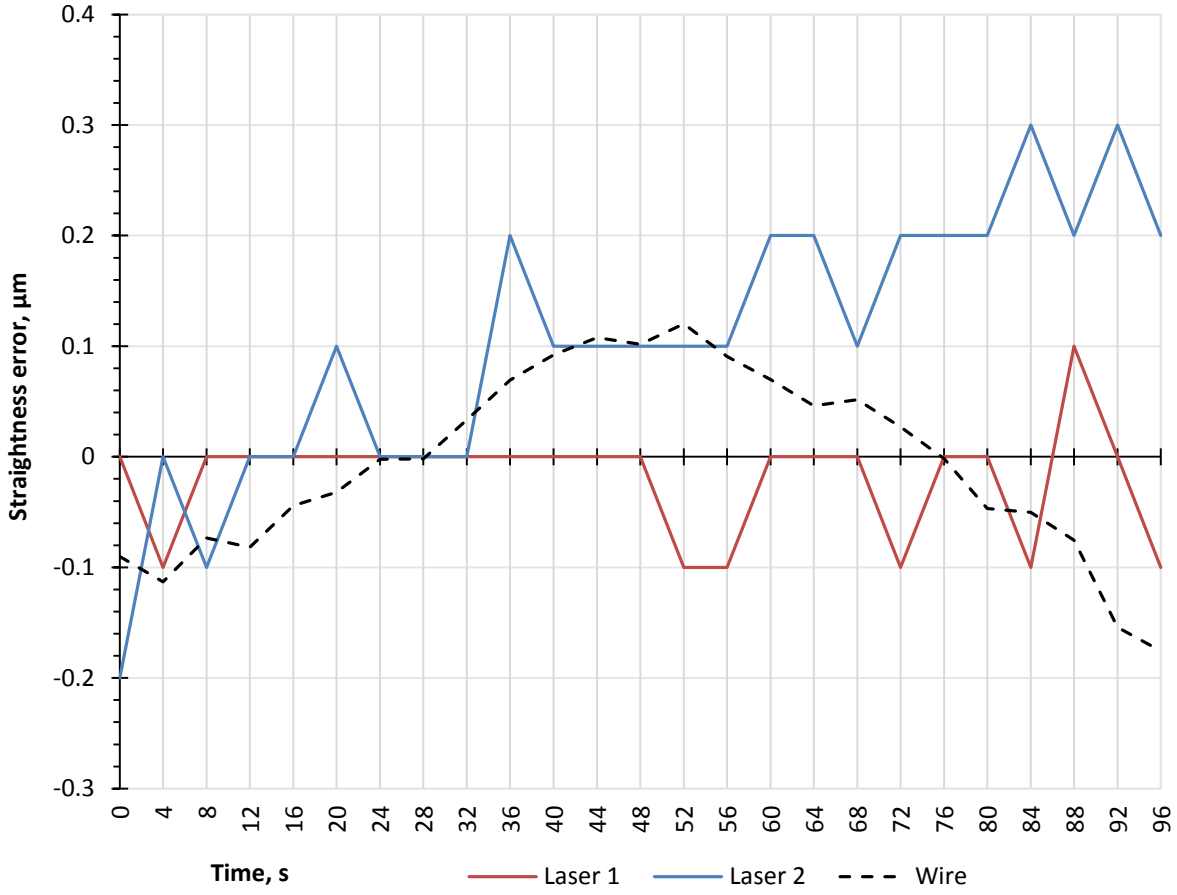

Figure 49. Laser interferometer and wire system static test

The two traces represent “movement” forward and backwards recorded as usual with a dwell time of 4s. Test duration matches the one of a bidirectional straightness measurement run. Stability is within 0.5µm for the laser and 0.25µm for the taut wire.

The maximum drift of the wire system output, shown in Figure 49, is twice less for a typical test duration which can be considered as excellent stability taking into account that this is actually an accumulated error caused by the wire error cancellation method. An additional test was completed to show the stability of the sensor output only as shown in Figure 50. The drift is very low, confirming the negligible effect on the error cancelation method.

Figure 50. Taut wire system in a single sensor mode static test

In this case the stability is within 0.1µm which means that excellent electrical and environmental stability of the system virtually immune to minor disturbances within the sensing system itself as well as external influences such as air turbulence on the wire.

4.2.8 Detecting wire defects

There is the potential for wire defects, such as accidental kinking, to occur which will not be removed by the correction method and generate incorrect output. This means the setup faults need to be corrected which involves either replacing the wire or adjustment of its position relatively to the measured axis.

Detection of such a fault can generally be done comparing results of a number of measurement runs, comparison with an expected profile from previous results or exceeding a maximum rate of change parameter. The system should give a clearly repeating straightness profile, especially in the same working area of the sensors.

A basic investigation of the reasons of a measurement run which failed includes analysis of intermediate data produced within the calculation of straightness error. For example, if the wire has a physical defect the aforementioned kink which result in a spike on the straightness profile which adversely affects the straightness reading, the wire needs to be replaced. This should remove the spike unless it is produced by the measured axis straightness profile.

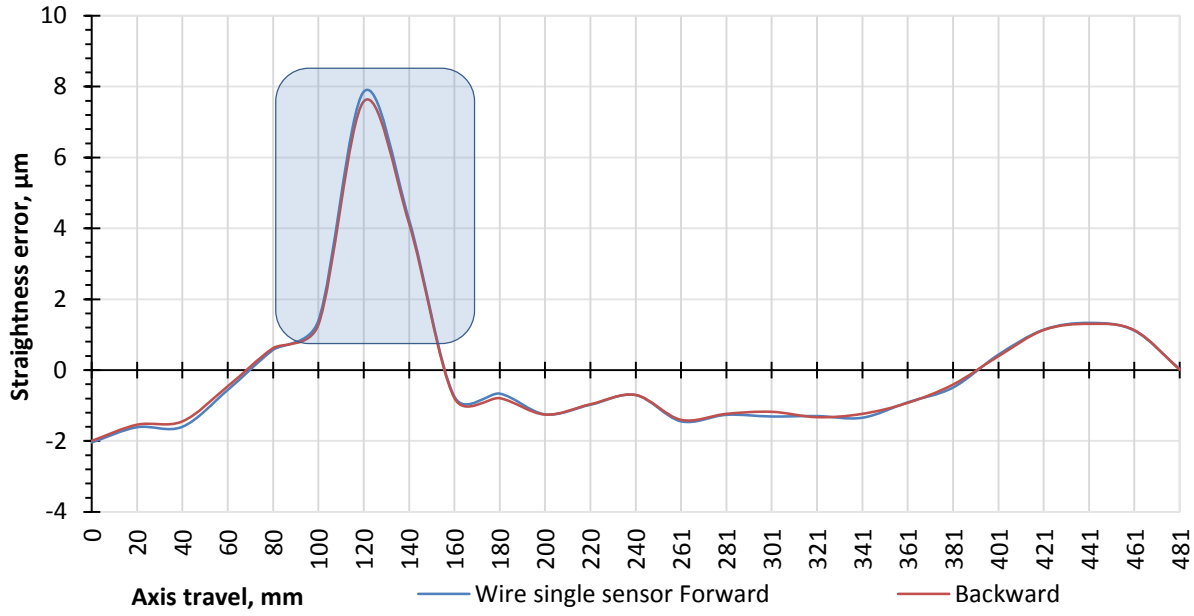

Figure 51. Wire straightness defect

Figure 51 shows the spike (highlighted) which makes the total straightness of this piece double in magnitude leading to a corrupted output as per Figure 52.

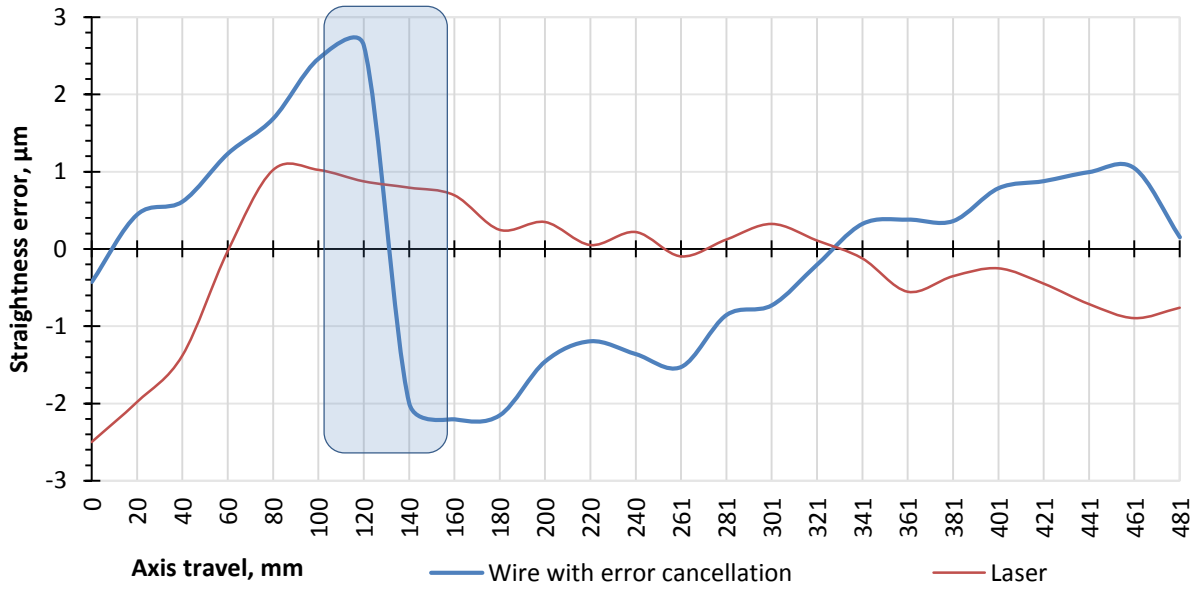

Figure 52. Output corruption caused by a damage of the wire

This happens because local areas of the wire where it is very thin become unstable under tensile force and change their surface profile during measurement.

A general rule is that combined reference and measured error should be not exceed the measured error itself more than two times. Otherwise the chances to get a correct result are greatly decreased.

Similar defects can be caused by an excessive slope in primary or secondary plane containing the wire. This, again, leads to output anomalies or bi-directional inconsistency.

Another issue is “expired” wire which gives all correct intermediate outputs, is stable and even has a normal straightness but gives completely wrong result after error cancellation and loses stability over the working area of the sensors. Figure 53 shows such an example:

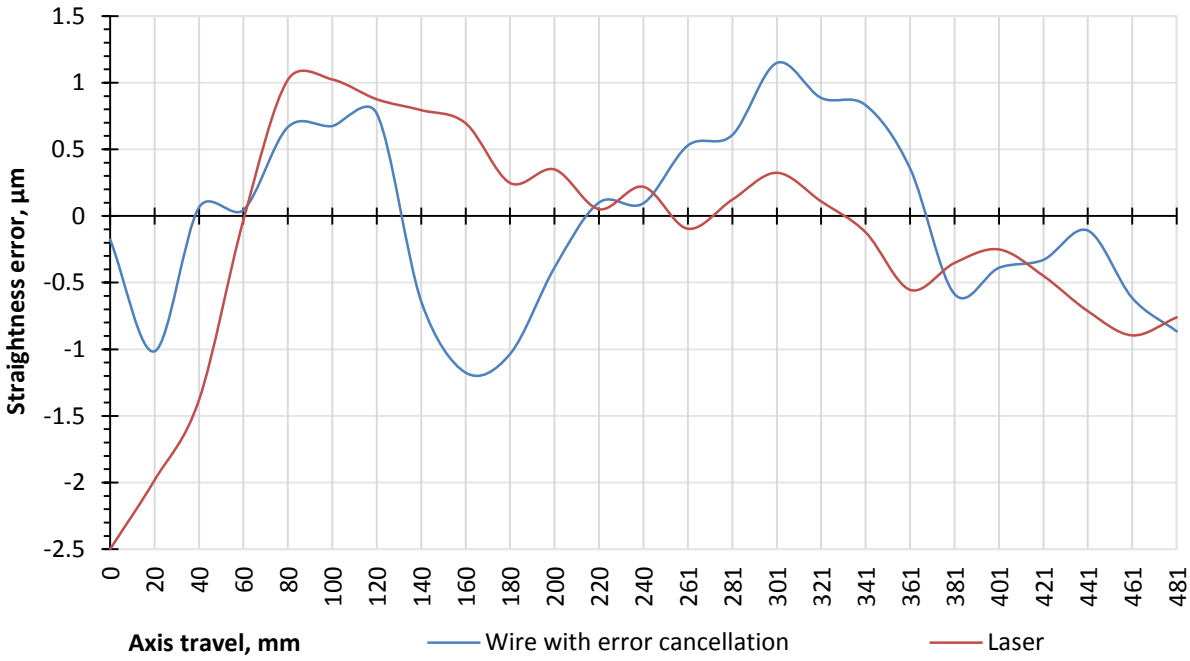

Figure 53. Result obtained using a defective “expired” wire

Research was conducted to obtain more information on this issue. The following factors were considered as its possible reason:

1. Excessive tensile force. This is a force below the rating of the wire, but still sufficient to adversely affect the wire for measurement.
2. Time the wire spent under tension.
3. The rate at which the tension application speed.
4. Existing superficial defects of the wire.

Manipulating these parameters did not highlight any clear pattern or specific reason for wire “expiration” but the probability of it occurring was generally increased by increasing the last three. Therefore, it is recommended to perform measurements soon after the wire stabilises, apply the counter weight gently, and replace the piece of the wire if there are spikes in the output graph.

As a rule, it can be concluded that “expiration” happens when a wire is left stretched for a long time. For this particular wire – if the time exceeds 30-60 minutes. This can be detected through repeated measurements and can be removed by the replacing the wire with another piece of it.

Further investigation into this phenomenon, its physical nature, dependence on the wire properties and installation will be a subject for the future work.

4.3 TEST RIG STRAIGHTNESS TEST IN WORKSHOP CONDITIONS

The same sequence of tests completed in sections 4.2.3-4.2.7, were carried out with the test rig moved to a typical manufacturing environment i.e. with co-located manufacturing machines, uncontrolled environmental effects etc. These tests were repeated to determine any variation compared to the ideal laboratory conditions. This will also provide data for the uncertainty evaluation in section 6.2.

The workshop inner size was approximately 20×10m, with four doors, six machine tools, two of which were operated. Ceiling lights were on, people were passing the workshop during measurements, doors opened and closed. It was winter time, therefore central heating was switched on.

4.3.1 Repeatability

As before, all tests were repeated and the first two test results depict the level of matching between two sequential runs and overall system repeatability within several minutes time.

Figure 54 shows two way outputs (here and after) converted to microns with slope removed using the linear least squares method. The first point of every run is missing due to the error cancellation applied when data from second sensor does not have a matching reading from the first one. The result is repeatable within 0.5μm at maximum and 0.2μm generally. Compared to the measured error of 3.6μm it gives confidence to proceed with the tests.

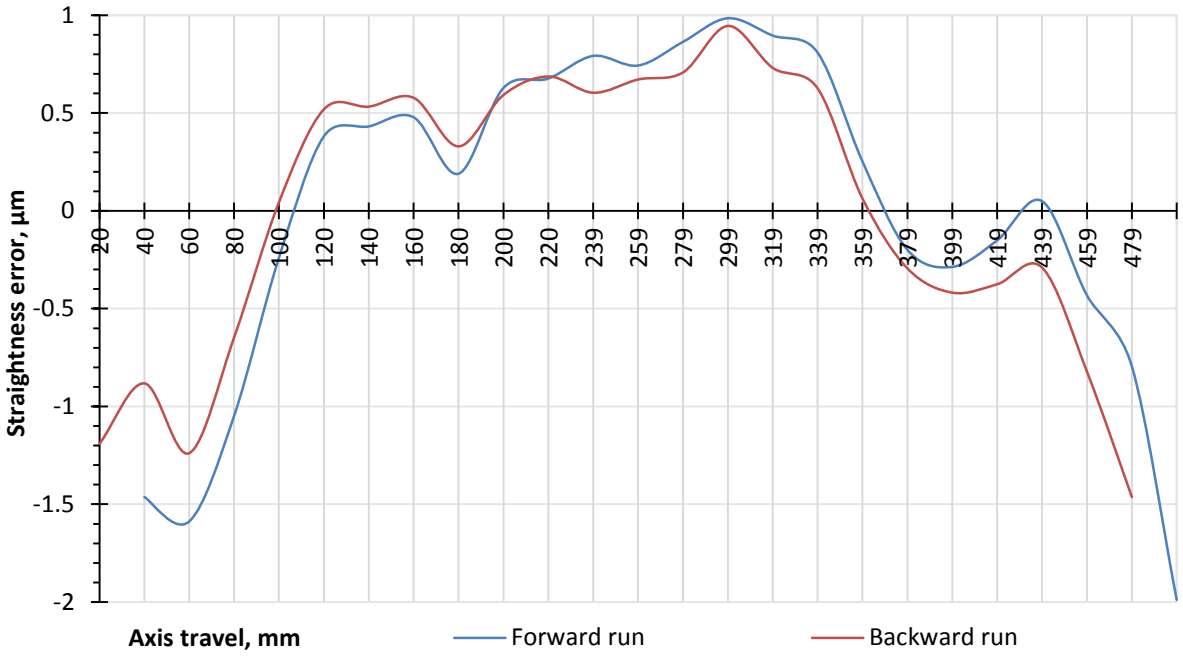

Figure 54. Bidirectional repeatability of the taut wire system

The next step was to check the stability of the wire reference over a longer period of time using three runs evenly spaced having 20 minute intervals.

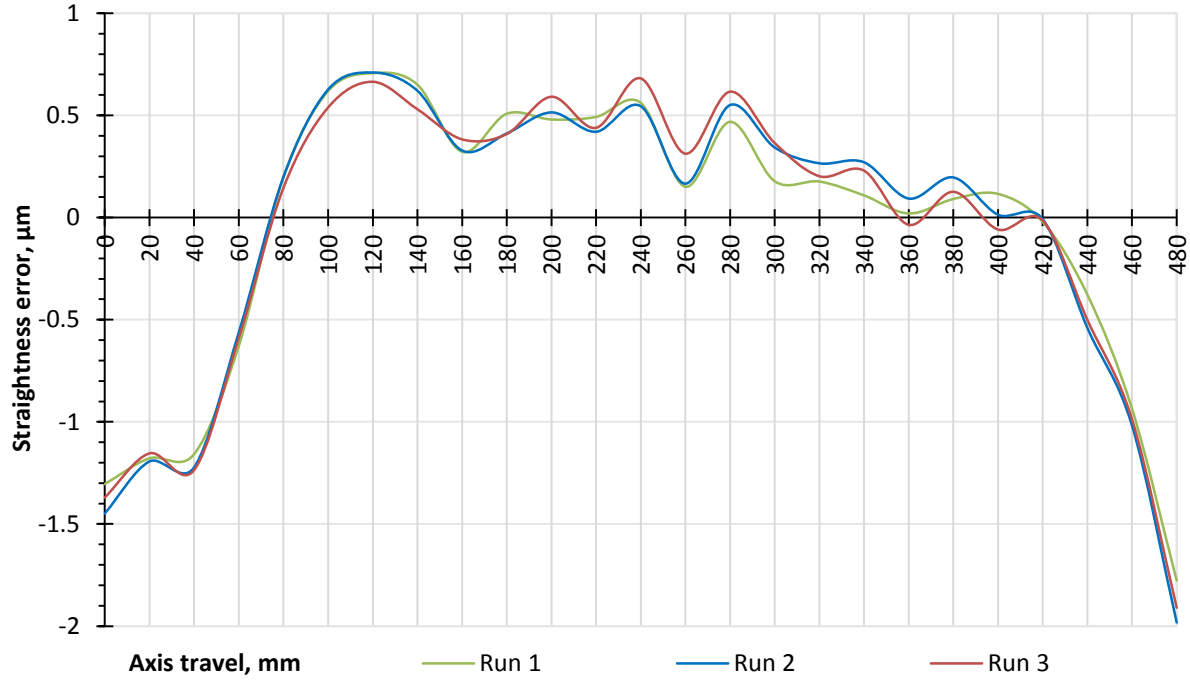

Figure 55. System repeatability within three runs

The same level of stability was demonstrated by the system proving no noticeable drift or noise during a more than sufficient to complete a full straightness test as per Figure 55.

The test was completed again under different workshop conditions to confirm this stability. In addition, another piece of wire was installed.

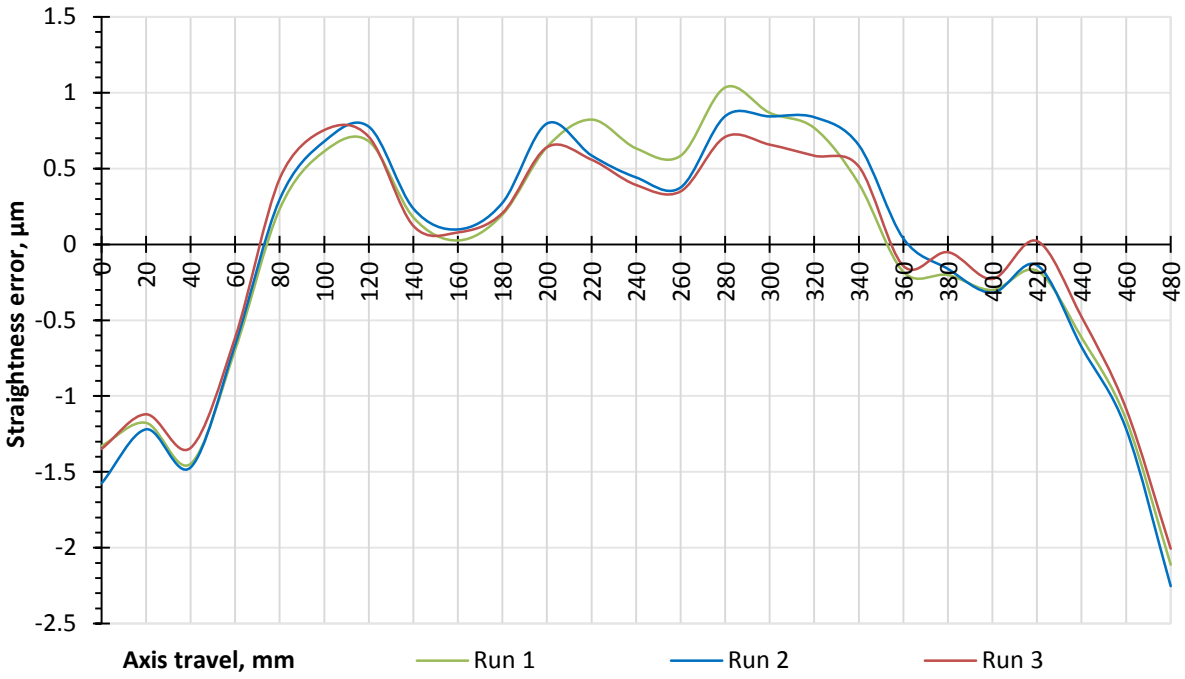

Figure 56. Test repetition with a different piece of the wire

The result shown in Figure 56 confirms the excellent stability of the test rig and taut wire system. Those three test results can be averaged keeping a random error within a 0.1µm which exceeds the one produced by a laser based system (Figure 42).

4.3.2 Error cancellation

The aim of the error cancellation technique discussed previously is to reduce the amount of contamination of the straightness test result by any error in the wire reference. Every piece of wire is unique in terms of its own straightness (diameter irregularity over the range) and is generally unknown.

To see the effect of error cancellation, three tests were performed each using a different piece of the wire used to measure the same axis the same way and during similar conditions. Every test used an average of 3 runs. The result with error cancellation is shown in Figure 57.

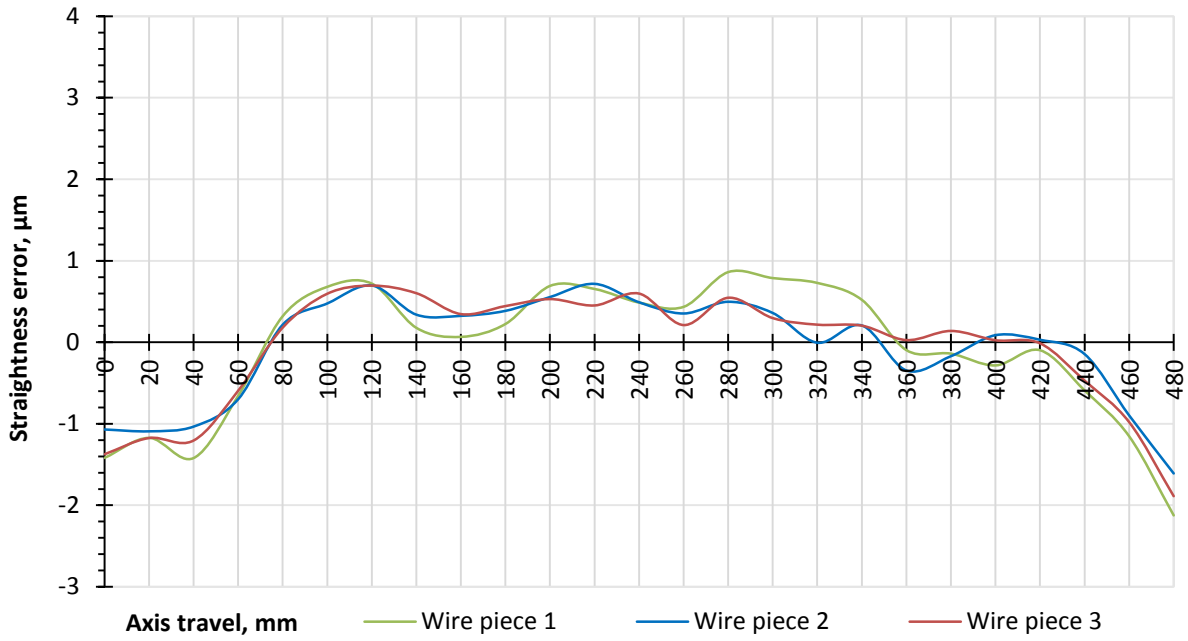

Figure 57. System repeatability with a three wire pieces

All three results are close to each other and the variation does not exceed 0.5µm. To highlight the effect of the error cancellation, the data was processed without it and is shown in Figure 58.

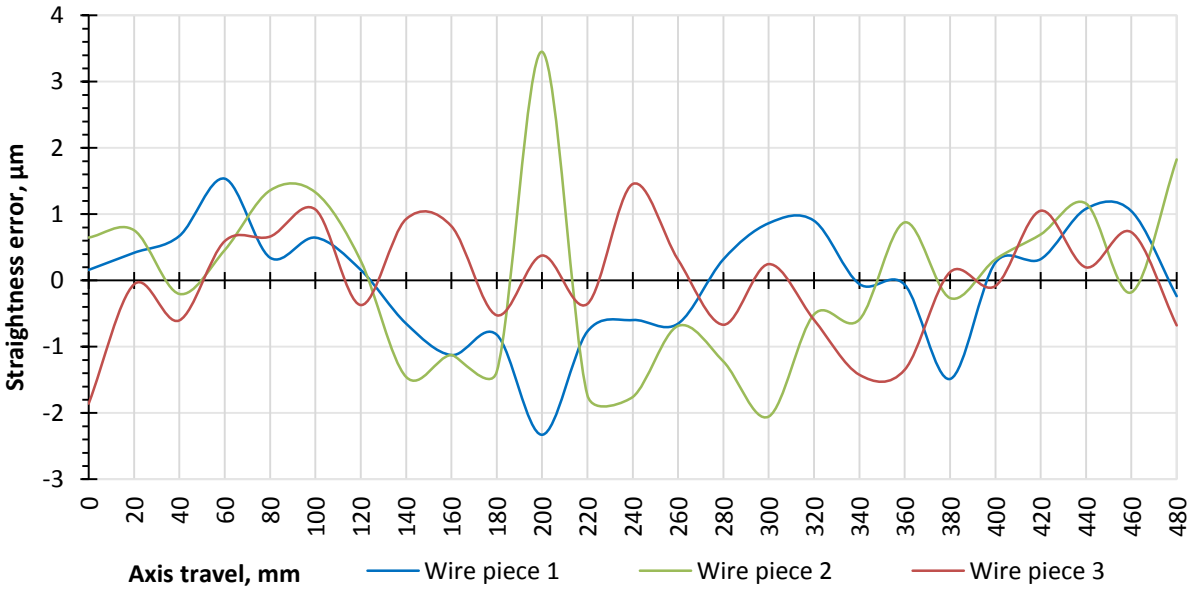

Figure 58. System repeatability with a three wire pieces without error cancellation

Although the variations are quite small, they do not provide a sufficiently consistent output for averaging and does not allow identification of the small straightness error of the test rig.

4.3.3 Laser interferometer and taut wire system comparison

Finally, an average of three different wire pieces was compared to the laser output.

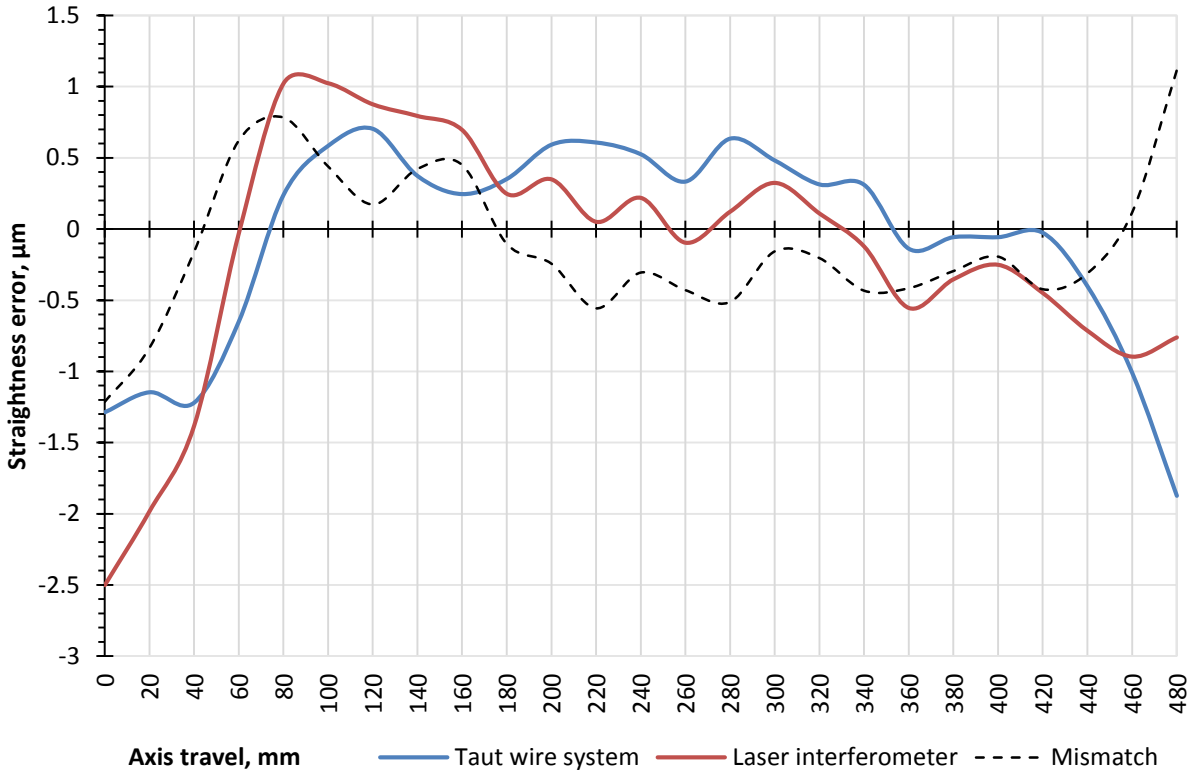

Figure 59. Laser and taut wire measurement results direct comparison

The results, demonstrated in Figure 59 are close to each other within a 1µm which is still persistent and does not contain any significant part of a random error. Considering the very low amount of straightness error of the test rig and completely different measurement principles it is difficult to justify which method delivers the actual picture of measured straightness.

4.3.4 Static stability tests

The new system showed good stability in laboratory conditions. The same tests were completed to determine the stability under typical workshop conditions. One test was carried out with the machine stationary. The same dwell time of 4s was used as before.

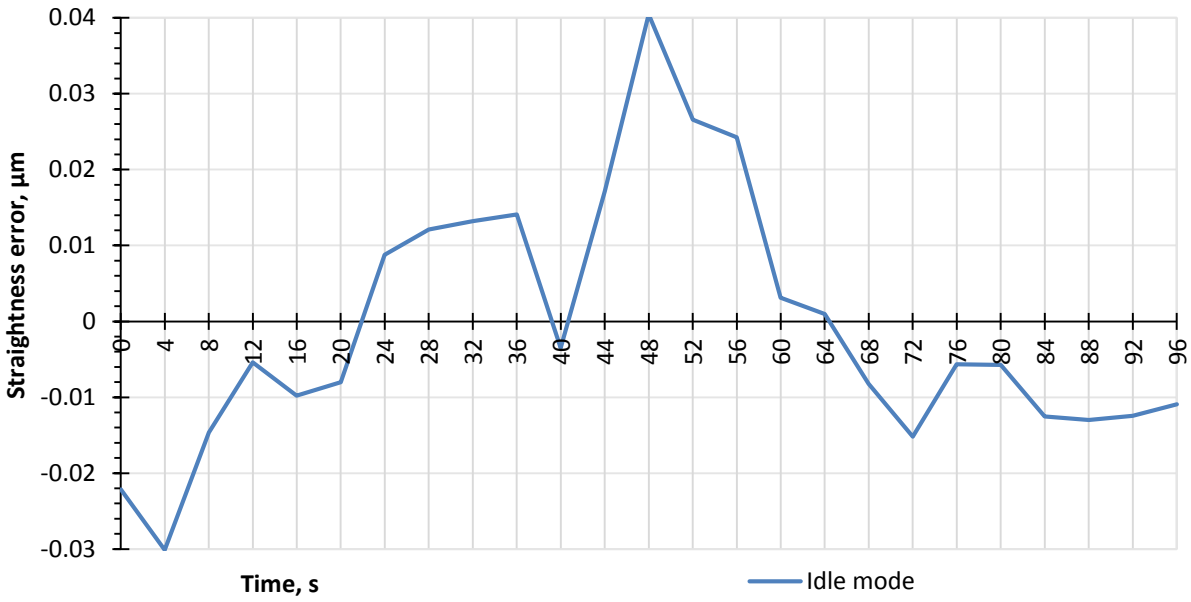

Figure 60. Taut wire static test

The graph in Figure 60 shows very high stability of the system which stayed within less than one tenth of a micron during the time required to do a single bi-directional measurement run. Compared to the result obtained in thermally controlled lab (Figure 49) this one shows even better stability proving that the system is very resistant to environmental conditions.

At the same time in the same conditions the laser interferometer was also tested (Figure 61).

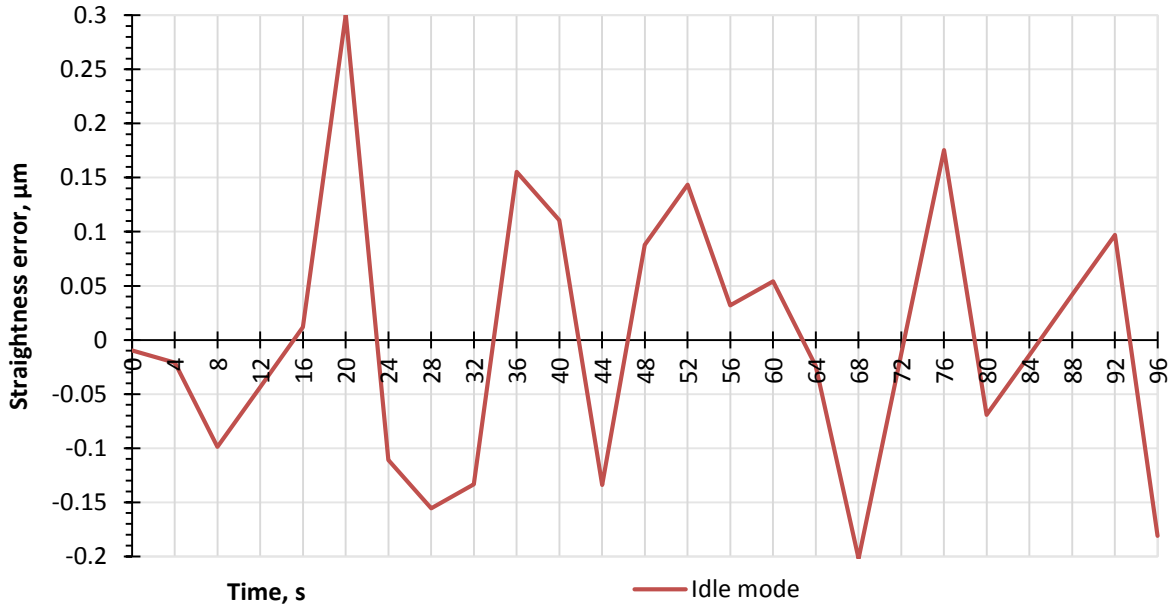

Figure 61. Laser interferometer static test

Compared to the taut wire system, the laser demonstrates almost an order of magnitude larger error even with Long Term Averaging active.

Comparing this result to the one previously obtained in a thermally controlled lab it makes clear that the error is very similar. At the same time, it does not mean resistance to environment as more powerful and newer laser was used (almost new Renishaw XL-80 instead of several years old Renishaw ML10). This makes a considerable difference which will be discussed in the following paragraph.

4.4 LASER INTERFEROMETERS COMPARISON

A comparison between two laser interferometers in the same conditions was completed to determine any difference between two similar laser beam emitter units. This information may be useful for end users whose measurement demands may require consideration of upgrading older measuring systems. The older unit in this test is a Renishaw ML10 Gold system, which has been used actively for several years and a newer Renishaw XL-80 system. Straightness optics remained the same.

The tests were carried out in the same laboratory when no machinery was in use and all doors closed. Same test rig with 0.5m horizontal axis was used, dwell time was set to 1s. Both interferometers were tested in two modes: short term and long term averaging to highlight the behaviour of each system in cases of lower or higher measured error.

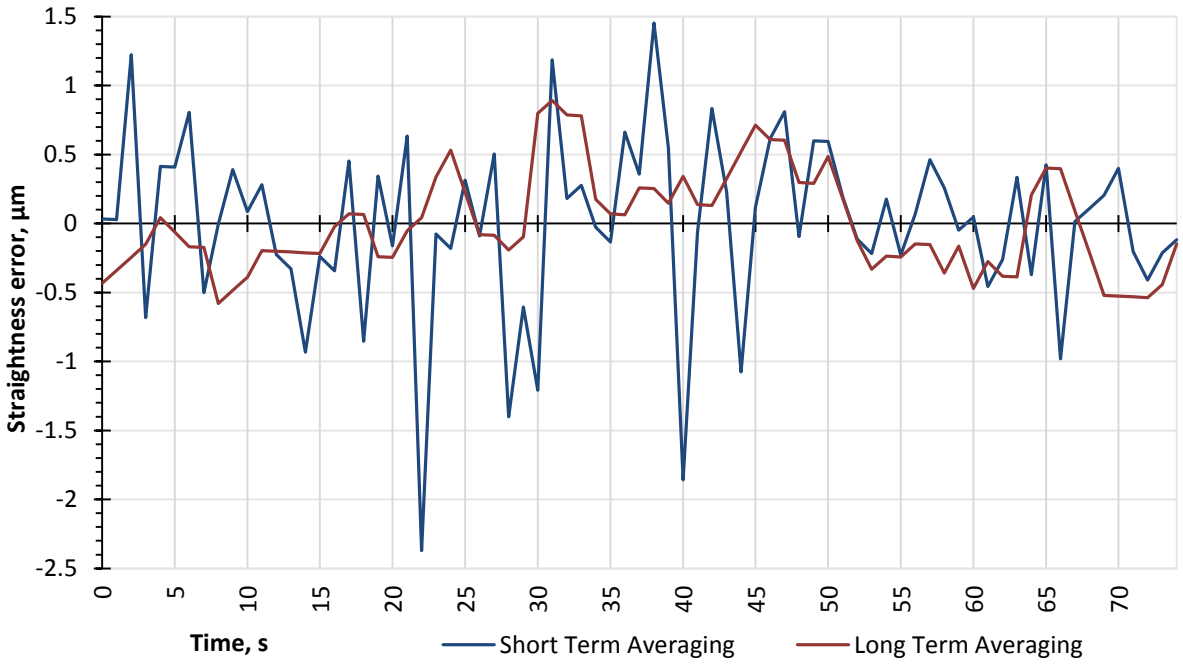

Figure 62. Renishaw ML10 static test

Figure 62 shows stability of the older laser within 4µm and 1.5µm with short and long term averaging respectively. This result is significantly lower than the one obtained using the newer XL-80 system (Figure 61, 0.5µm long term averaging). Increasing the amount of averaging decreases the noise almost three times. To make sure the difference between lasers still exists when shorter dwell time is used, the same was tested using a newer laser.

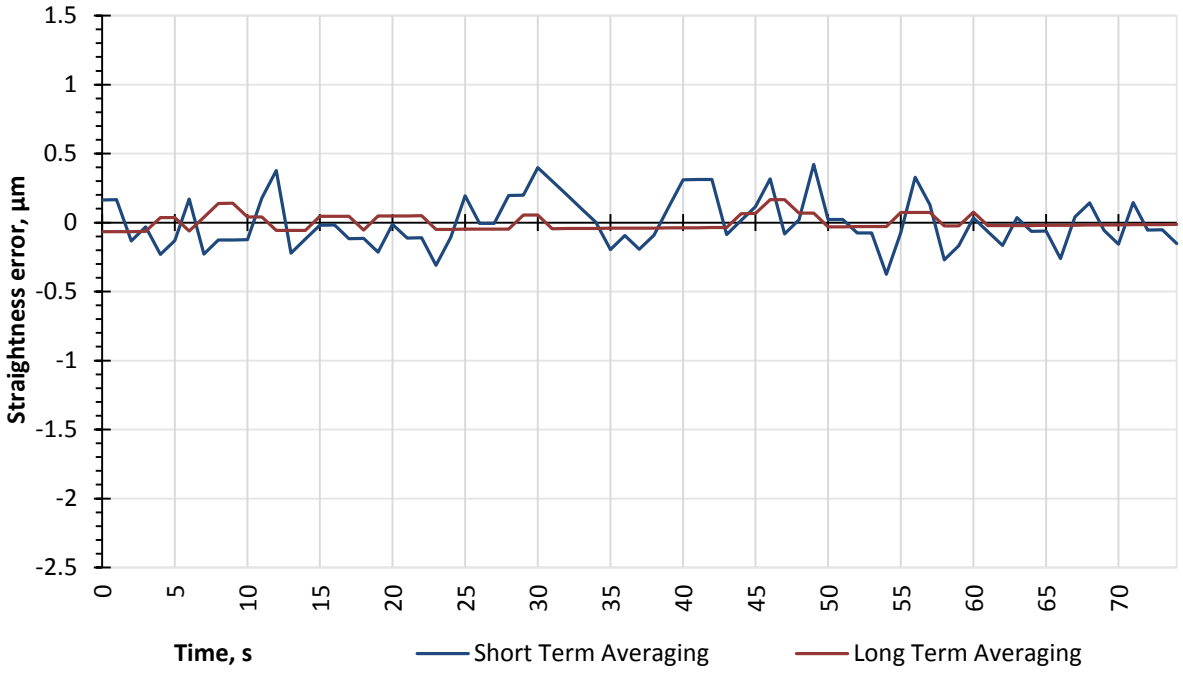

Figure 63. Renishaw XL-80 static stability test

Same scale of the graph in Figure 63 makes obvious the difference between two lasers performance which stands in the order of three times. The effect of switching to a long term averaging is the same.

Although it is logical that the newer system would have an improved performance, it was useful to quantify the variation for this work and potentially many end users.

The tests prove that even within a laser interferometers range can be a considerable difference in terms of accuracy. Even similar models of interferometers from one manufacturer and using the same optic kit have different stability and, consequently, different accuracy or/and take different time to get the same level of accuracy.

There is a question if the older laser had a better stability in the past and if it has degraded due to its age or extensive use. Nevertheless, laser head replacement or upgrade is a matter of additional expenses and time. The taut wire system does not suffer from environment (practically) and even if some part of it needed to be replaced, that could be done quickly and involving very minor additional costs.

In the next chapter “long range” stability tests will be discussed with a respect to the difference between the laser and the wire and comparison continued.

4.5 CONCLUSIONS ON METHODOLOGY AND PERFORMANCE

Taut wire and the new automated measuring system has been applied successfully for the measurement of straightness on a short test rig.

Application of the error cancellation technique to the taut wire used for straightness measurements has enabled a high level of accuracy to be obtained. Simplicity, flexibility and low cost of the method are now combined with elimination of the straightness reference error which has always been present and unpredictable, limiting the minimal error which could be successfully measured.

A number of tests were carried out on the 0.5m long axis of a test rig comprising a high accuracy CNC axis with a straightness error of 3μm which showed a result highly repeatable through a number of runs, a number of wires, a number of setups and even different environmental conditions.

When compared to two conventional laser interferometers, set up on the same machine measured in the same conditions, the method demonstrated a good correlation in results matching each other generally within 0.5μm. Such variations can be described by the uncertainties in the two systems.

Static stability tests of the same machine in both workshop and laboratory conditions showed the taut wire system has excellent stability, lower than that provided by the laser interferometry. Stability was typically within typical 0.2μm during a normal test run time which highlights a good characteristic of the method.

Static stability comparison of two different interferometers revealed a significant improvement between two generations of the laser emitter. It is expected that the simplicity of the taut wire system should help with maintaining long term performance as well the ease with which maintenance can be applied.

At this stage, the system has been validated as a potential solution for straightness error measurement on machine tool axes. However, further validation on a longer axis and under different operating conditions of a 5-axis machine tool is provided in the next chapter. In addition, uncertainty evaluation of the system for such typical measuring conditions is provided in section 6.2.

CHAPTER 5 STRAIGHTNESS MEASUREMENT USING A TAUT WIRE ON A TYPICAL MACHINE AXIS

Tests on a typical machine tool axis having a longer length are necessary because straightness measurement methods strongly depend on the axial range and external influences. These can affect accuracy, choice of equipment, measuring procedure and duration required to complete a measurement. From the literature review, there were two apparent categories based on measuring length. Typically, several short range solutions covering 0.1m to 0.7m, and solutions such as the taut wire and interferometer systems that have a very broad range even exceeding 10m for long machine tool axes.

So far the taut wire system has been tested on a 0.5m axis and the results have been discussed in the previous chapter, validated and proved to be feasible. The next step was to test the system over a longer range using available equipment. That was achieved using a 5-axis machine with a 1.5m horizontal axis, a length which was considered to represent a broad range of machines and to reveal the specific effects of the increased range for both taut wire system and laser interferometer.

This chapter will start by defining the test setup including the measured machine, introducing the new sensor head, redeveloped for higher performance and accuracy. The most significant improvements were making the mounting plate more rigid and with exact 90º angle to reduce instability caused by vibration and make installation simpler, building in a dedicated power stabiliser to reduce noise and drift, adding sensor adjustment knobs for setting the sensors sensitivity close to each other to reduce output non-linearity.

Because of the longer range, other geometric factors such as axis rotational effects can become considerable on a large machine. Its possibly more complicated geometry can require a decision on where to mount the sensor head and how it will be affected by a corresponding combination of angular errors. Those effects are known for laser-based measurements but need to be determined for the taut wire system. The geometry will be discussed and related effects tested separately.

Another consideration on longer axes is gravity affecting the wire, causing it to sag, inducing an error which needs to be tested separately.

Increasing the distance over which the measurement takes place inevitably causes most measurement errors to increase and change the contribution of each one in the total error. This is not necessarily followed by increase in the magnitude of the errors on the machine therefore measurement error components need to be carefully controlled. Among

these is the effect of changing relative wire position in the transverse direction, the magnitude of which could be ignored on the test rig but may become significant in case of a longer and less accurate axis. Although this effect, or contamination, was considered negligible, validation through a normal measurement will be discussed in this chapter as well.

5.1 TEST SETUP

The new sensor and taut wire system were setup on a medium sized 5-axis gantry machine. The longest horizontal axis (X) was chosen for testing. The setup and layout is shown in Figure 64. Like before, the taut wire system and laser interferometer (Renishaw ML10) were both measuring the same axis consecutively. The distance between laser optics attached to the spindle and the sensor head was reduced to 100mm in both the transverse directions (Y and Z) which was the closest possible to minimise differences between the errors measured by the two systems.

Two steel columns held the wire in place in the middle of the workspace of the machine. Two fine adjustment carriages used previously on the test rig to set the head position were substituted by the machines Y and Z axes. Sensor calibration was achieved utilising Z-axis of the machine rather than linear displacement sensor. This made more convenient feedback loop.

The type of wire used remained the same (DAIWA Sensor Monofil 0.26mm) and was stretched by the same force of 15N. Machine axis movement speed was set the same, making one step in three seconds.

The only conditions in which the machine was tested were of an active workshop having no environmental control. Machine’s front doors were shut which minimised air flow from people walking past the machine.

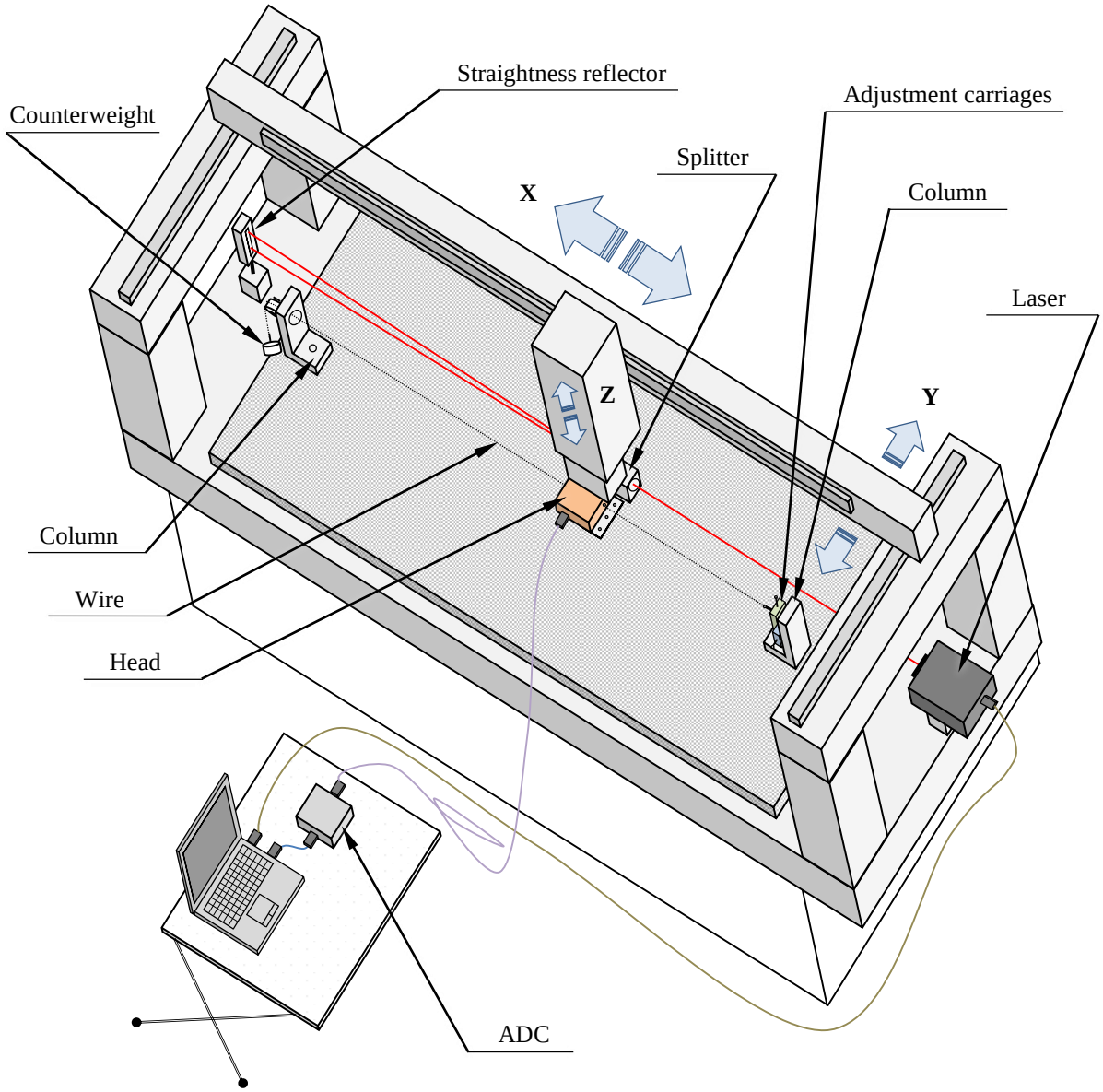

Figure 64. 5-axis machine equipment layout and test setup

Additional two rotary axes not shown on the figure are B and C which provide rotation around the Y and Z respectively. These were also used to emulate angular sensor displacement.

The machine and setup shown in Figure 64 provides good versatility to test the axis and the taut wire system. The new sensor head can be rotated or moved linearly in a precise way and separately from the rest of the machine. This opportunity was useful for measuring the effects of angular motion such as pitch, tilt and yaw errors.

The same computer and ADC unit converted sensor signals and taut wire calculation spreadsheets were modified to fit the new axial range data.

5.1.1 New sensor head

The sensor head used previously was improved and redesigned according to experience obtained from short range measurements tests on the test rig. The improvements are:

1. New mounting plate, more solid and having more precise angle of 90 degrees.
2. New plastic cover, bigger to accommodate two PCB's and adjustable sensor stands.
3. Input voltage stabilizer (no battery power is needed).
4. SMD resistors and capacitors to save space.
5. Additional board with comparator circuit.
6. Interchangeable sensors connected to 4-pin sockets.
7. Sensor stands with extra threaded apertures for sensor position and step size adjustment.
8. Four knobs for sensor input adjustment.
9. More rigid construction.

The mounting plate was made of steel and painted after machining (see

Figure 65). It is heavier than its predecessor but does not bend or change angle due to machine vibration while the axis is moving.

Four sockets were provided for connecting the sensors to facilitate swapping connections which is useful if number of active channels is limited by the signal cable and/or ADC. For example, if only two channels are available, the third sensor normally used for secondary slope measuring can be connected instead of a primary sensor temporarily.

A comparator circuit, assembled on a separate board and shown in Appendix B, can provide the difference between two sensor readings directly without the need to transfer both the signals to the ADC. This reduces the number of ADC channels required and potentially reduces noise in the voltage signals because the wire lengths used significantly reduced. This can be especially useful for simultaneous measurement in two perpendicular planes with four sensors. This simple circuit was added for convenience only. Within this research, the sensor calibration was performed in the data acquisition software therefore all the sensor readings were acquired and used to achieve the experimental results presented. As it will be discussed in section 5.2.3, two point method was found to be unsuitable on the 1.5m axis due to the large measurement error and therefore the two sensors were operating independently and a simple average of the two used. The details are in section 5.2.4.

A signal cable was extended and extra wires for delivery of input current (provided by a standard AC adapter) included.

Circuit diagram for the new device and its PCBs are shown in Appendix B and the top view in Figure 66.

Figure 65. Sensor head assembled with the improved 90° mounting plate

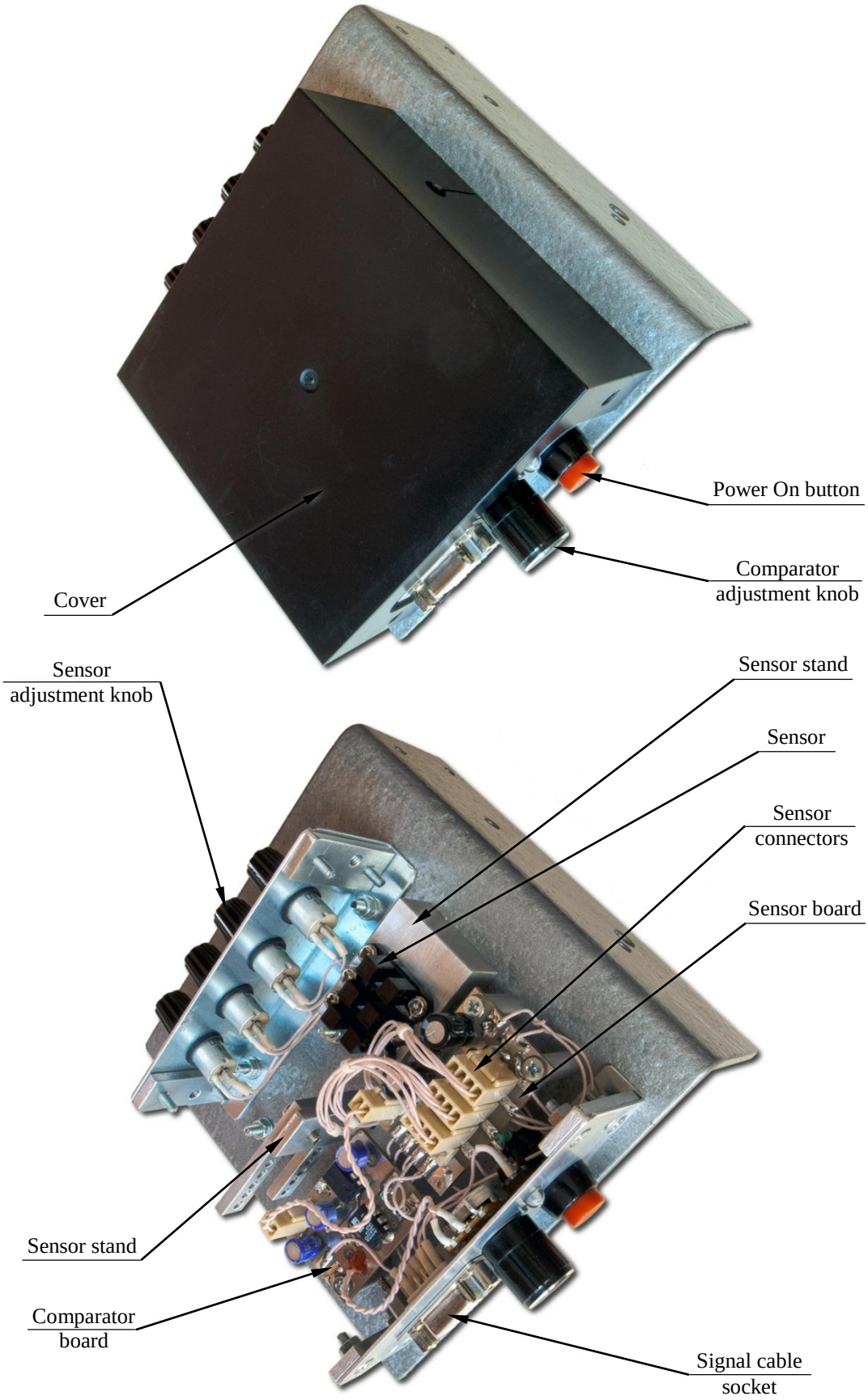

Figure 66. Sensor head with and without plastic cover

5.2 MACHINE TOOL AXIS STRAIGHTNESS TEST RESULTS

Longer range vertical straightness tests (EZX) were carried out on the machine to compare the performance of the new system with the laser interferometer over a more representative measurement distance and under typical operating conditions.

5.2.1 Test conditions and calibration procedure

The machine was located in aforementioned workshop and the tests completed with machine's doors shut, except for a small gap for instrumentation cables, which is standard practice and which also helps to protect the measurement area from airflow (see section 4.2.1). The taut wire system was also set up the same way as that described in section 5.1.

A calibration procedure was completed in accordance with the procedure described in section 3.5, utilising Z-axis of the machine to move in 10µm increments over a 200µm total measuring range. To make sure the calibration is not affected by the position of the sensor head along the wire, different points of the wire were checked to take calibration profile.

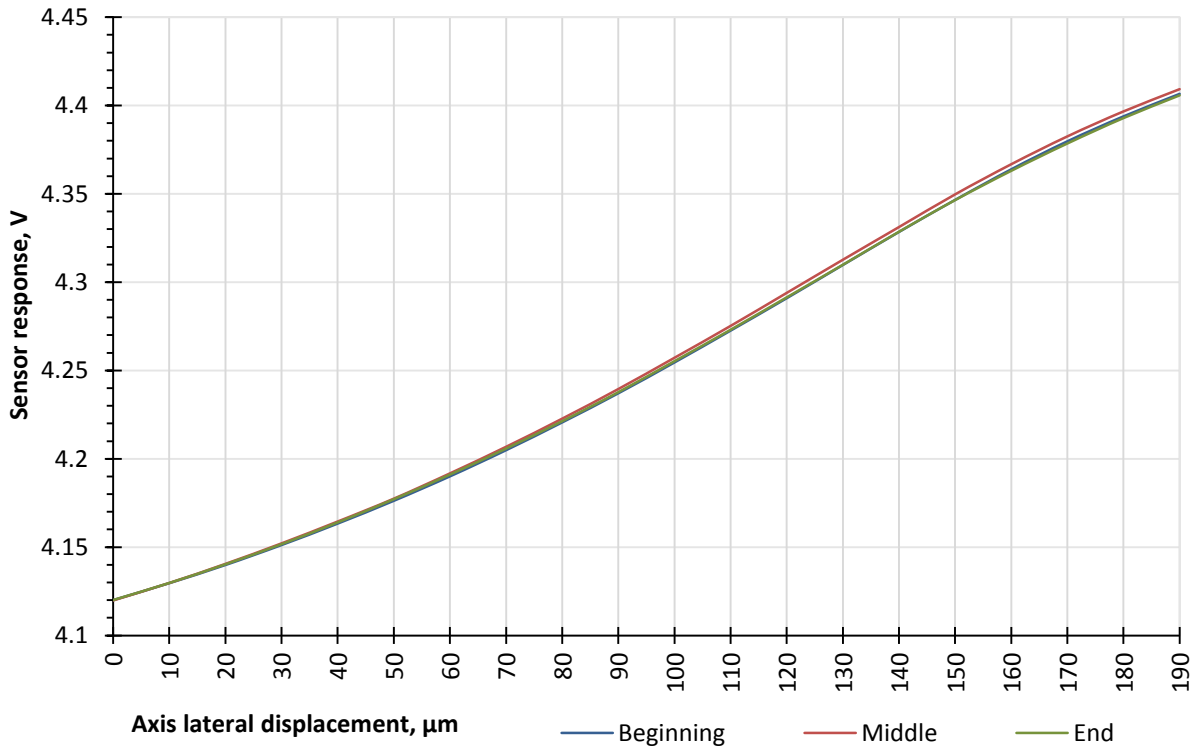

Figure 67. Calibration profiles obtained from different sections of the wire

The maximum difference between all three can be seen in Figure 67, was 3.5mV which equates to only 2µm over the 200µm calibration which is very small.

5.2.2 Laser interferometer test

Renishaw ML-10 Laser interferometer was used to measure the X-axis straightness in the vertical plane (EZX). Six test runs were completed within approximately 45 minutes (each run 76 readings with 4-5s dwell time). The result is shown in Figure 68.

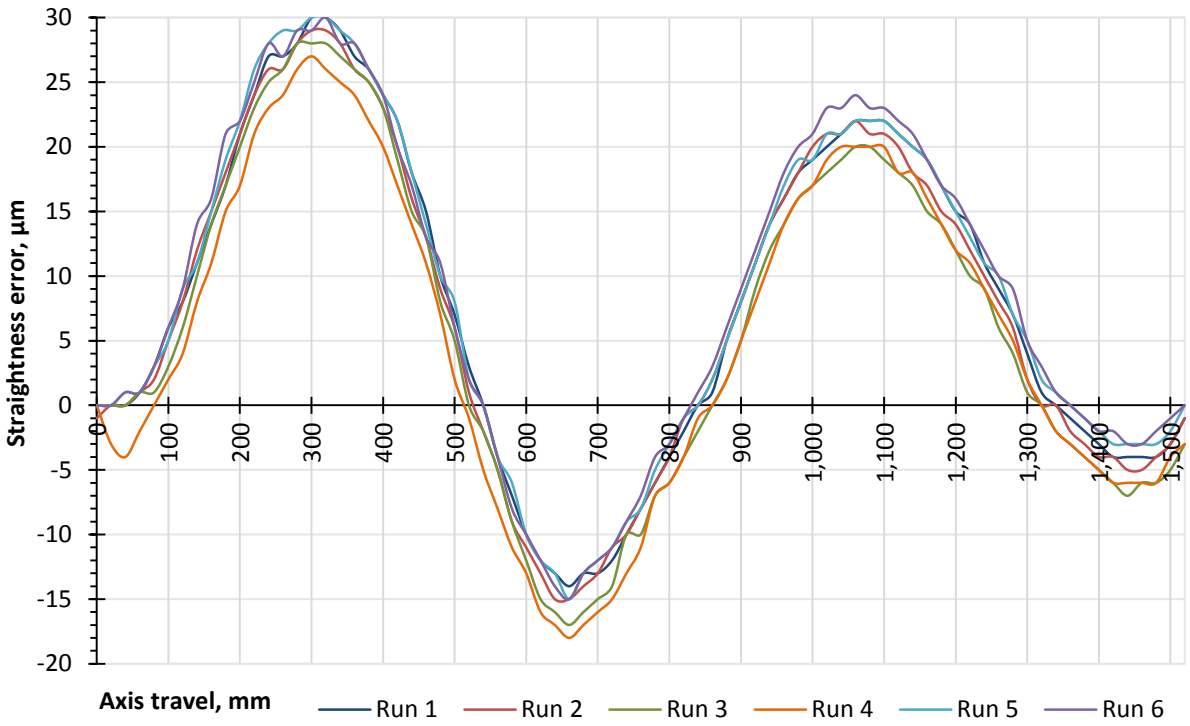

Figure 68. Large straightness error measured using a laser interferometer

Magnitude of the straightness error was measured to be 45µm and the repeatability was 5µm. This value includes repeatability of both the measurement equipment and the machine tool axis. An average of all three forward and three reverse runs was used as a reference error for comparison with the taut wire measurements.

5.2.3 Error cancellation anomaly

The error cancellation technique described in section 3.4.3 and successfully validated for short range measurements was also tested in longer range conditions for measuring 45µm and 5µm straightness errors. The results were as shown in Figure 69.

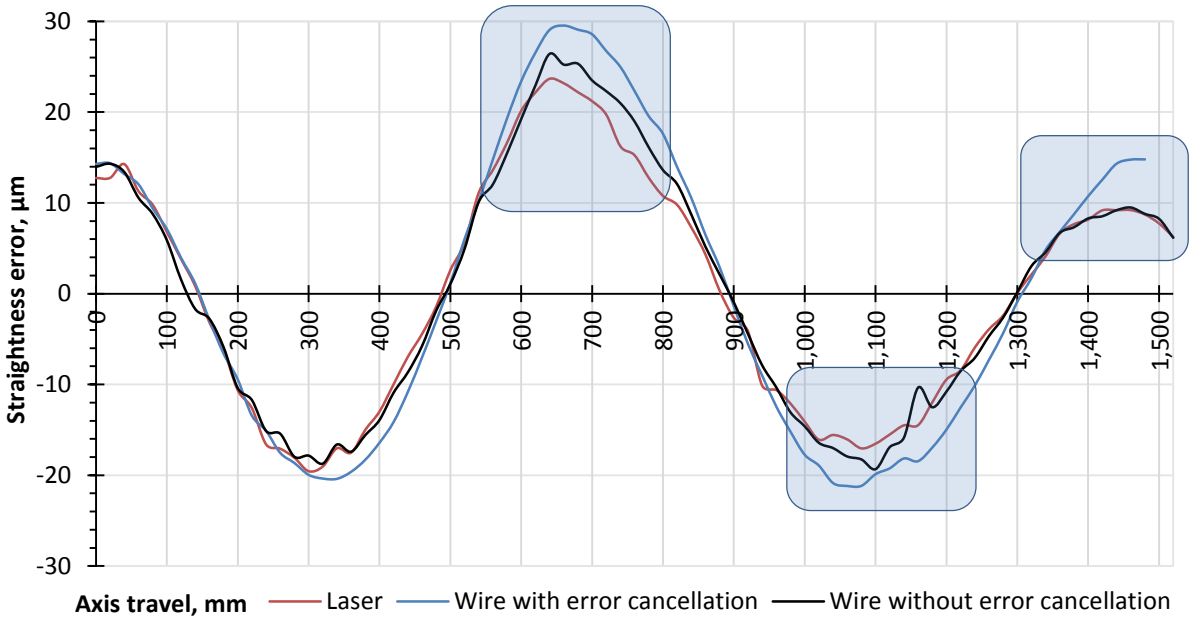

Figure 69. 45µm error measured with error cancellation

And for a smaller measured error as per Figure 70.

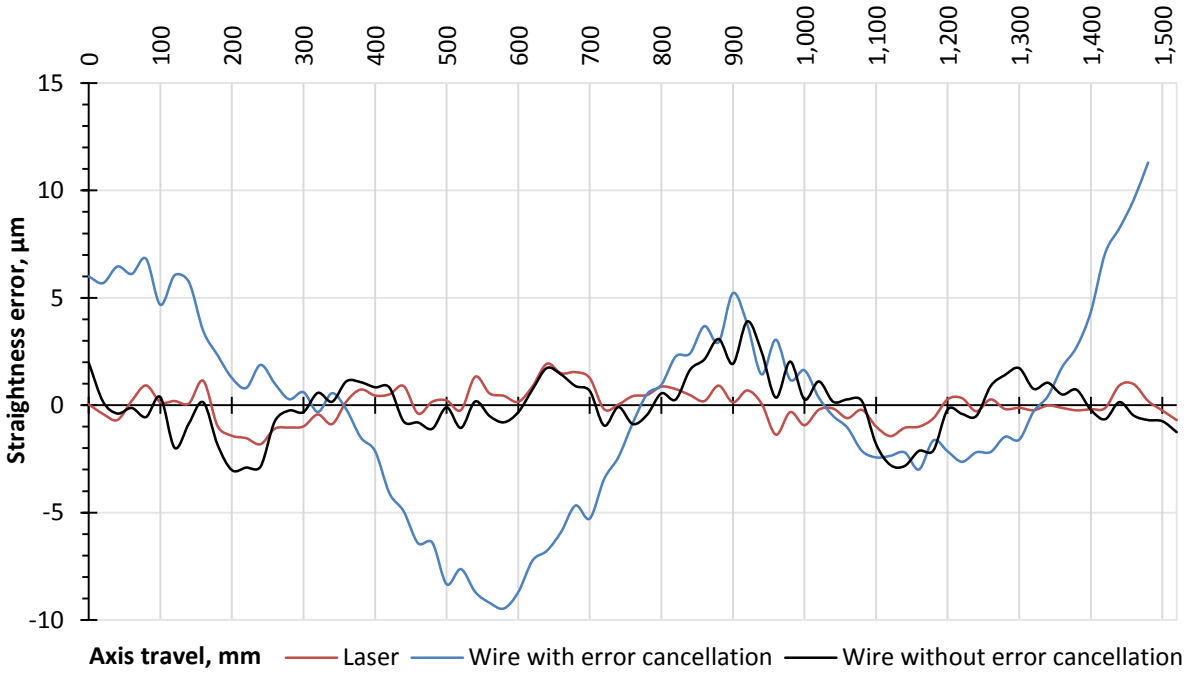

Figure 70. 5µm error measured with error cancellation

Both results show a significantly better correlation with the laser if no error cancellation technique is used. This means that even the straightness of the wire is not the main contributor to the error of measurement. The latter one is mainly accumulated through the axial range progress and at this stage cannot be fully explained.

5.2.4 Multiple sensor method test

Tests on the machine axis showed reduced effectiveness from the error cancellation. An alternative solution was to use a multiple (two or more) sensor measuring method instead of error cancellation for the following reasons:

1. Wire straightness error is limited for every combination of wire material, thickness and tension. Once reached on a certain length, it will not be exceeded by the error of longer wire piece.
2. Longer axes typically have a lower accuracy requirement compared to the shorter ones.
3. Error cancellation involves accumulation getting worse with increased number of reading points.

Considering these factors, it was decided that instead of dual sensor error cancellation technique (including hardware comparison) a single sensor method would be used because error in the wire is lower than the axis straightness measurement accuracy specified in the objectives. Further improvement can also be achieved by reducing the effect of the reference error using two or more of sensors at the same time to get an average of their readings. Due to low cost nature of the sensors, this is feasible and this way the same hardware and testing procedure is used.

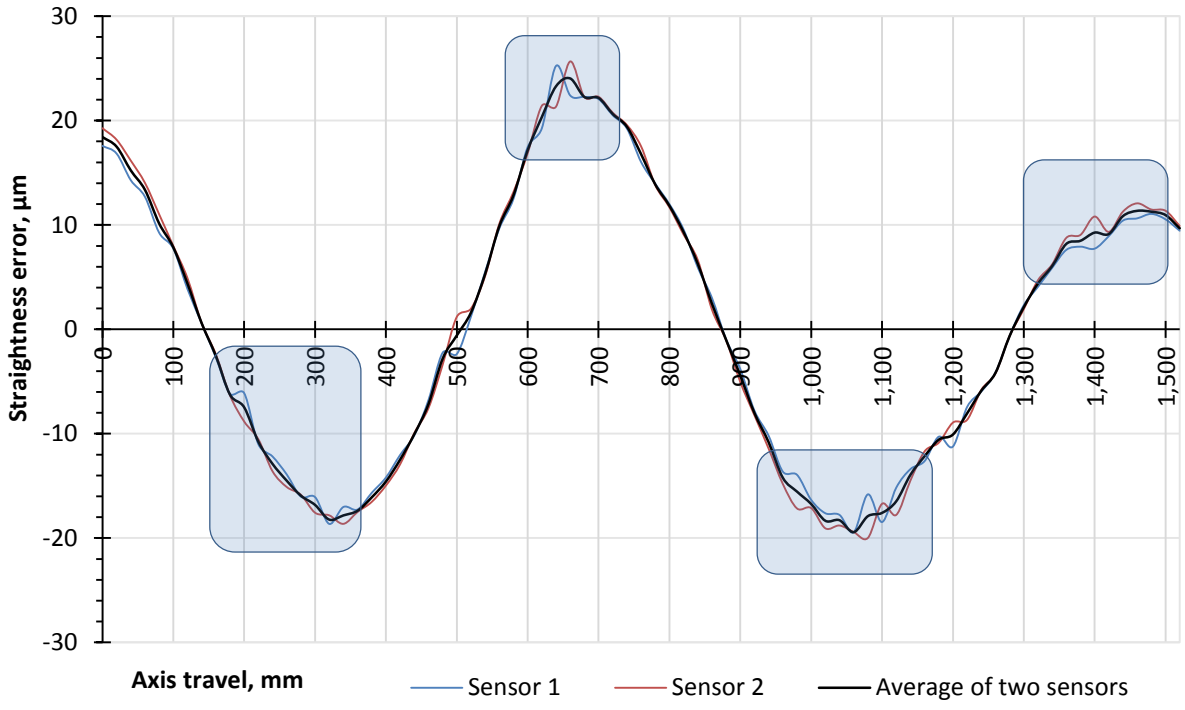

Figure 71. Averaging of two sensor outputs

The result in Figure 71 demonstrates the advantage of two sensor outputs averaged together to reduce the small errors caused by the wire profile imperfections.

The next test was to check repeatability of the wire set up on the machine axis. Three sequential bi-directional test runs had their results averaged on three levels: sensor level (two sensors used together), calculation level (start point on the left and on the right), and run direction level (axis travelling from left to right and vice versa).

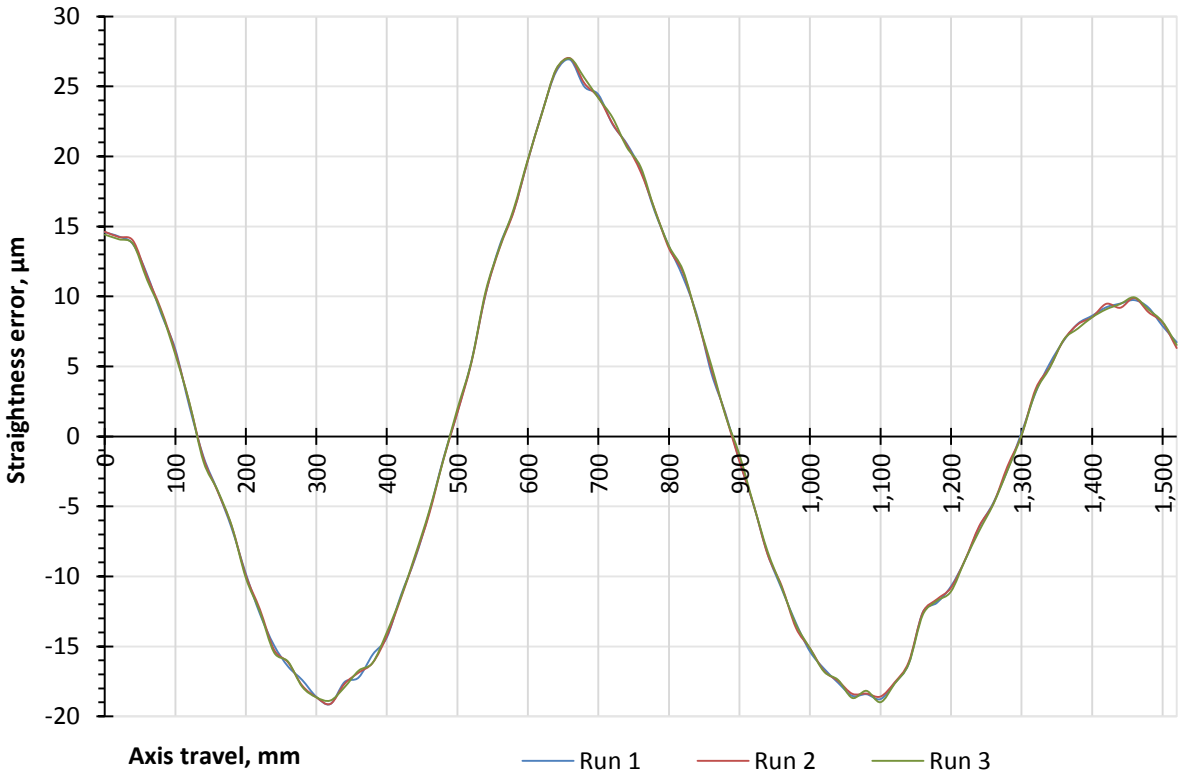

Figure 72. Wire repeatability within three runs

Figure 72 shows an excellent match between the three runs with a maximum difference of less than one micron. There is typically a compromise between increasing the quantity of data to improve the reduction on random effects through averaging and efficiency of the measurement. Based on the results so far, three runs were determined to provide this optimum result.

To check how this stability changes with time, the machine was left for 24 hours and then the same tests were carried out. This duration was chosen so that the machine temperature was as close as possible to minimise its influence on the measurement in order to highlight instability or drift in the new measuring system. The result is shown in Figure 73.

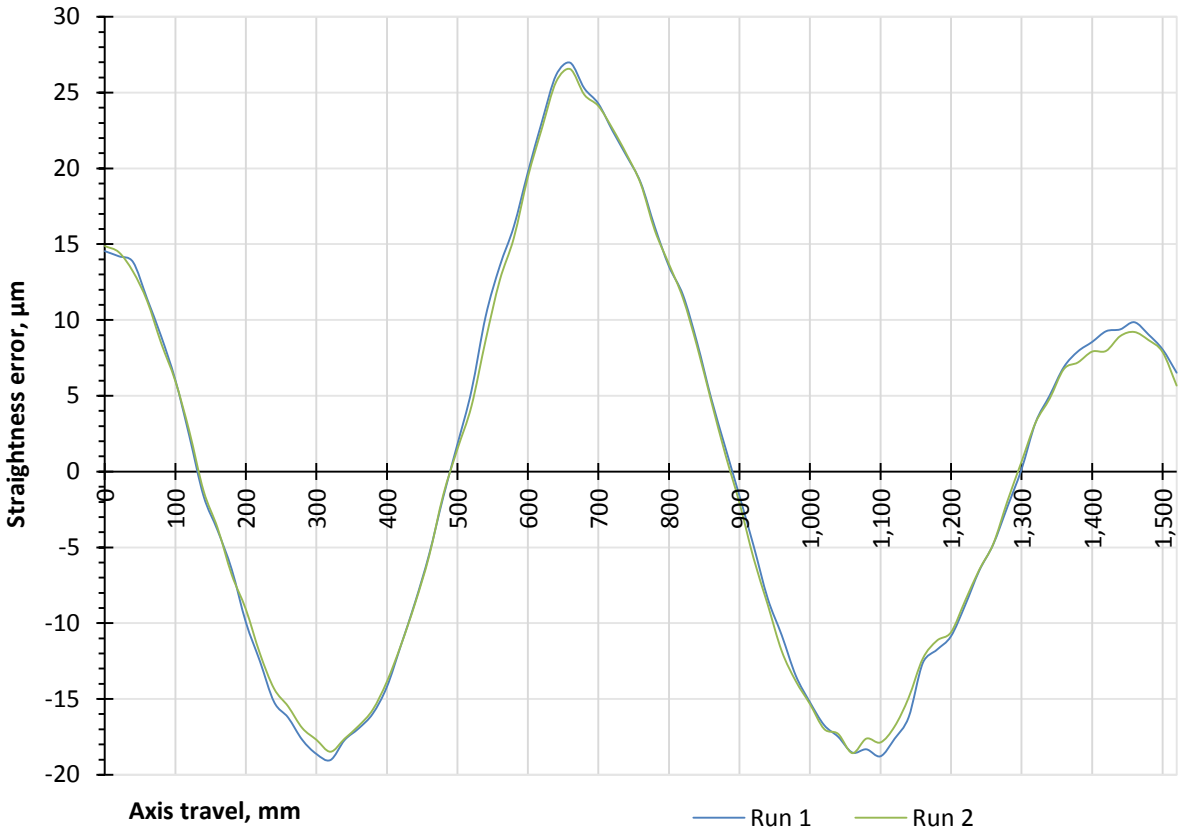

Figure 73. Reading variation over 24 hour period

Both profiles match within 1µm which indicates good stability form the wire and new measuring system.

5.2.5 Compensated error laser interferometer test

The error measured before represented the actual straightness of the axis. To obtain a smaller error for straightness tests, the axis was calibrated in both planes using laser interferometer. A part-program was written for the machine to simulate straight movement of the X-axis adding correction values (laser test result + slope) on Y and Z axes on each travel increment making the axis move along the almost straight line, reducing the straightness error from 45µm to 5µm.

This value represents a very high accuracy and actually makes both straightness measuring methods to reach their capability limits. Catenary compensation as described in section 3.3 was used to eliminate gravity effect on the wire.

After calibration, the axis was measured using the same laser setup three times in both directions each providing six runs in total (Figure 74).

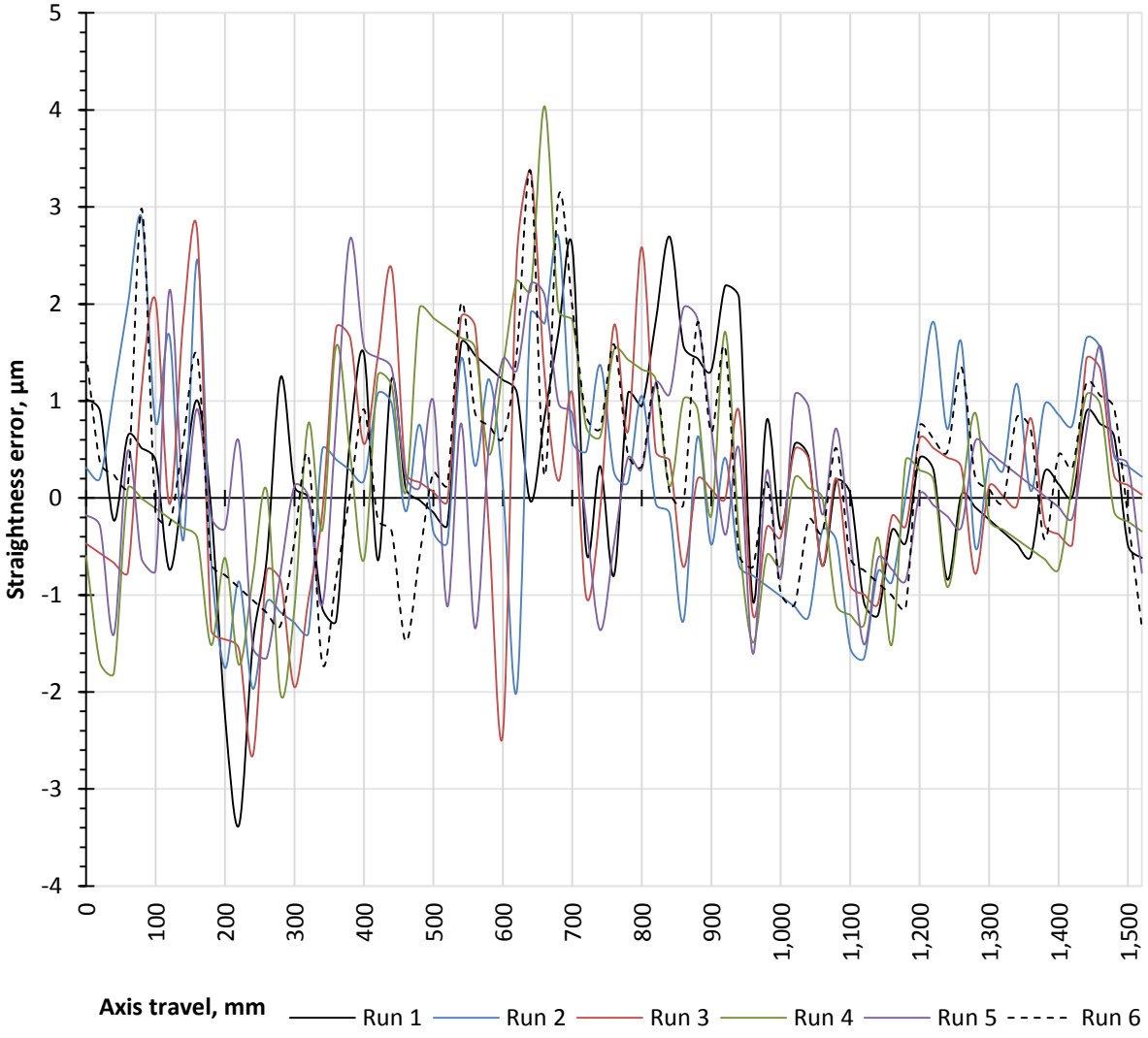

Figure 74. Compensated error measured using a laser interferometer

All six straightness profiles are very different from each other even though the difference generally stays as low as 1-2µm which is generally acceptable for 1.5m range. Averaging here is absolutely necessary and the number of runs needs to be not less than has been the case.

5.2.6 Multiple sensor method repeatability

Like before, three different wire pieces were used to measure straightness to check the contribution of the reference error to the final result. Tests followed one another with the only delay caused by mounting the wire and settling time needed for it to stabilise.

Catenary effect was subtracted from the measured straightness profile to ensure that it does not affect the final result.

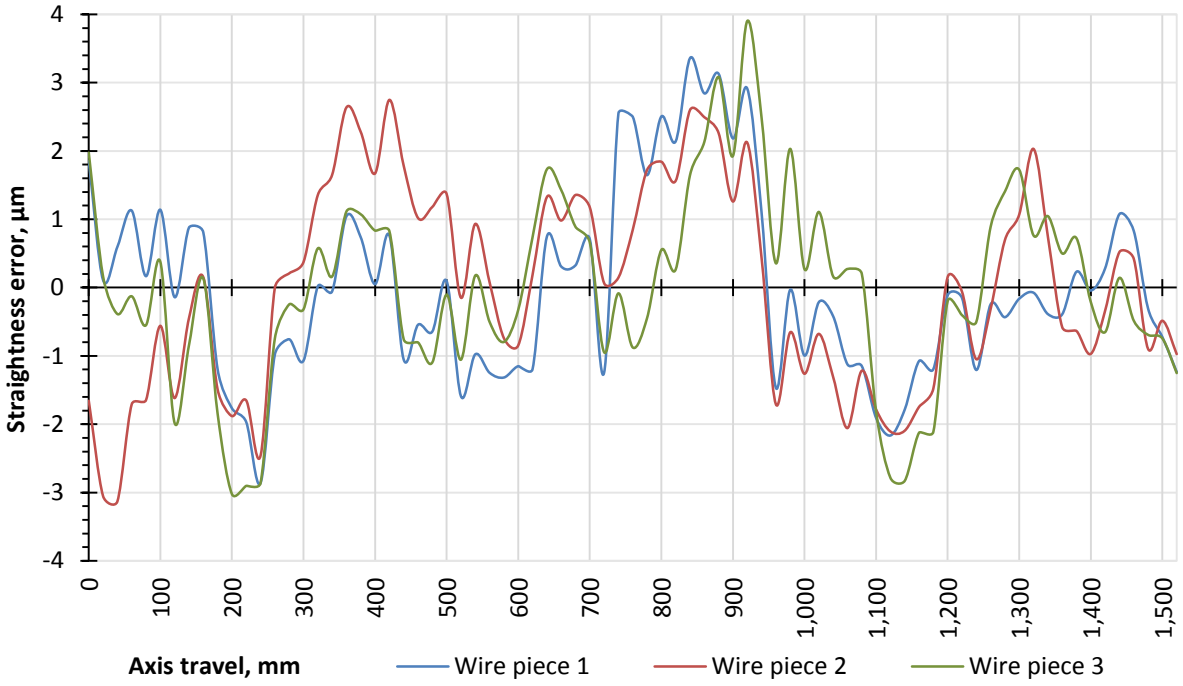

Figure 75. Taut wire system repeatability with three wire pieces

The result in Figure 75 is very similar to the one obtained from the laser and confirms similar mismatch of 1-2µm suitable for averaging.

The next test was to check the dual sensor averaging technique described in the section 5.2.4, which effect it had in case of a better straightness:

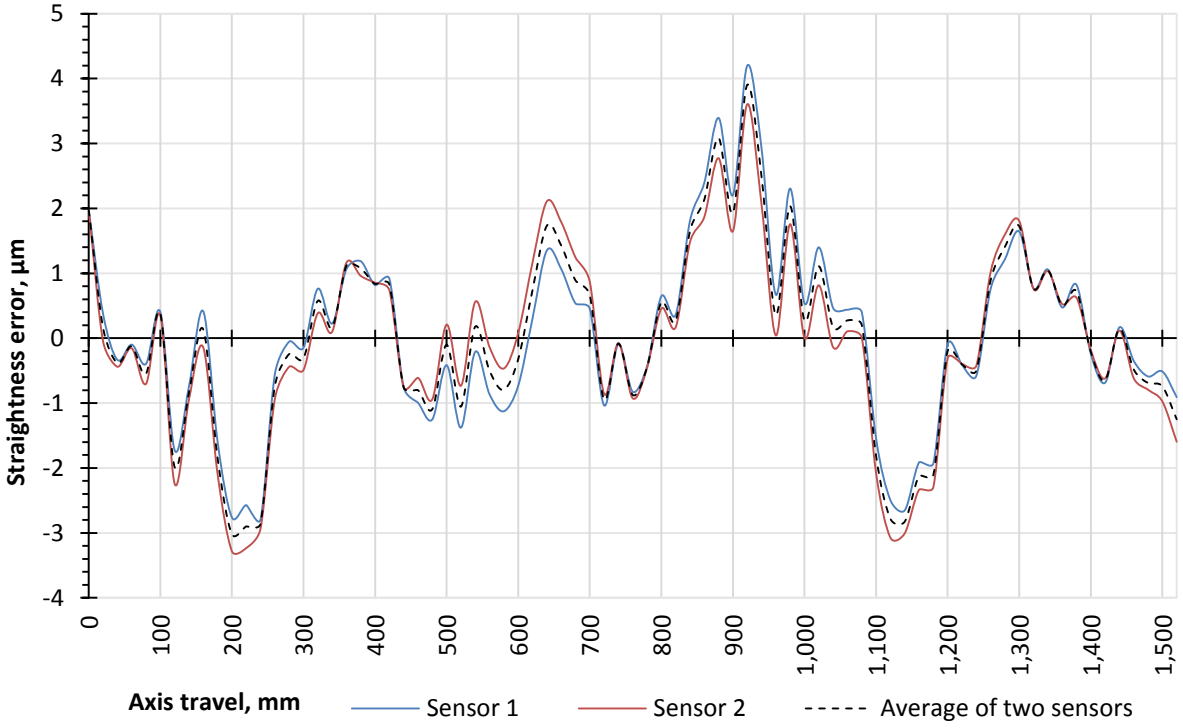

Figure 76. Averaging of two sensor outputs (compensated error)

5.2.7 Laser interferometer and taut wire system comparison

When measuring a 45µm straightness error, both methods provided very consistent results and averaging did not play a big role. When it was applied, the comparison was as per Figure 77.

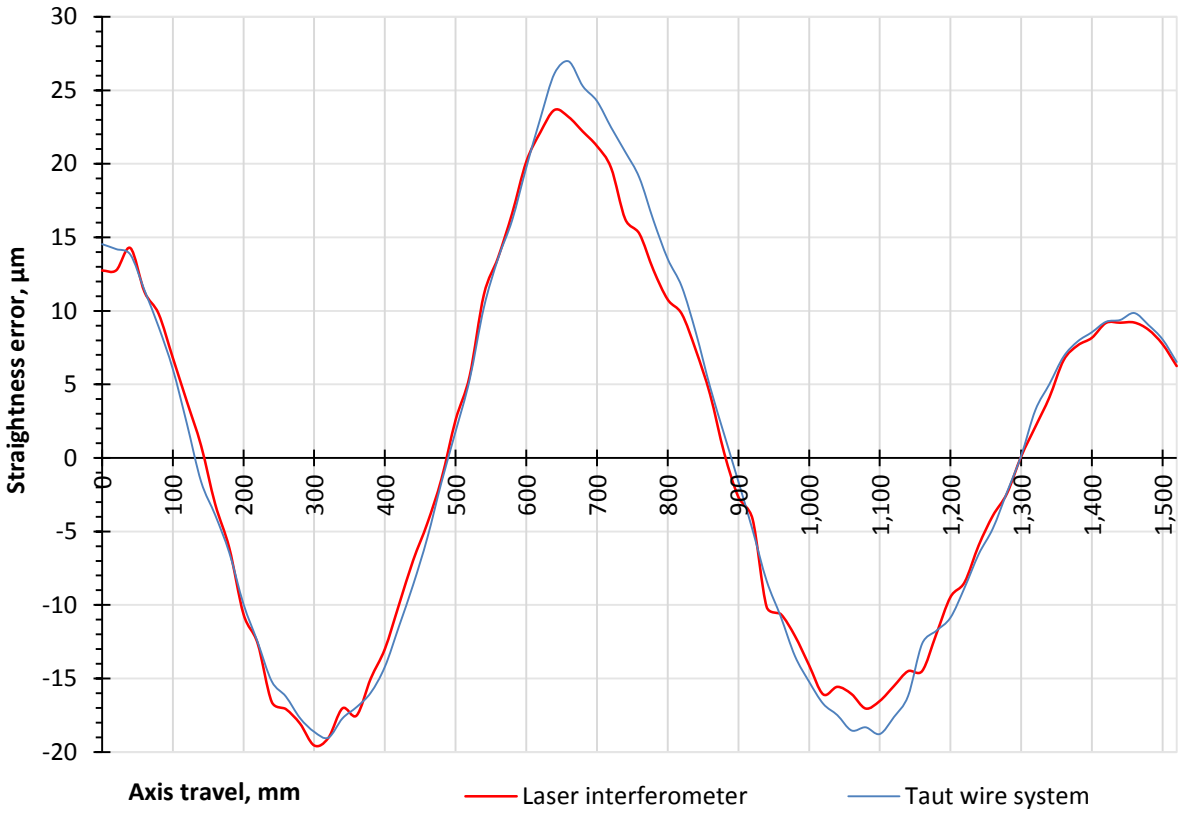

Figure 77. Averaged laser and wire results compared

The difference between two profiles is less than 3µm which is a very good correlation taking into consideration that the wire replacement was not necessary.

The research so far has shown that repeatability values of both laser interferometer and taut wire system, set up for measuring straightness of a 1.5m axis, are similar. When it comes to reducing random influences such as air turbulence, both methods rely on averaging. In addition the taut wire system has a systematic error partially separated by averaging multiple sensors and replacing the wire. The laser data was used to compensate for the straightness error in the X axis and a repeat measurement carried out. The results are shown in Figure 78.

Figure 78. Averaged laser and wire results compared (compensated error)

This time both results are significantly less consistent though absolute mismatch does not exceed 2µm which can be considered normal for such an accurate axis motion.

Figure 79 shows the catenary effect subtracted from the final wire result, calculated using the method described in section 3.3.

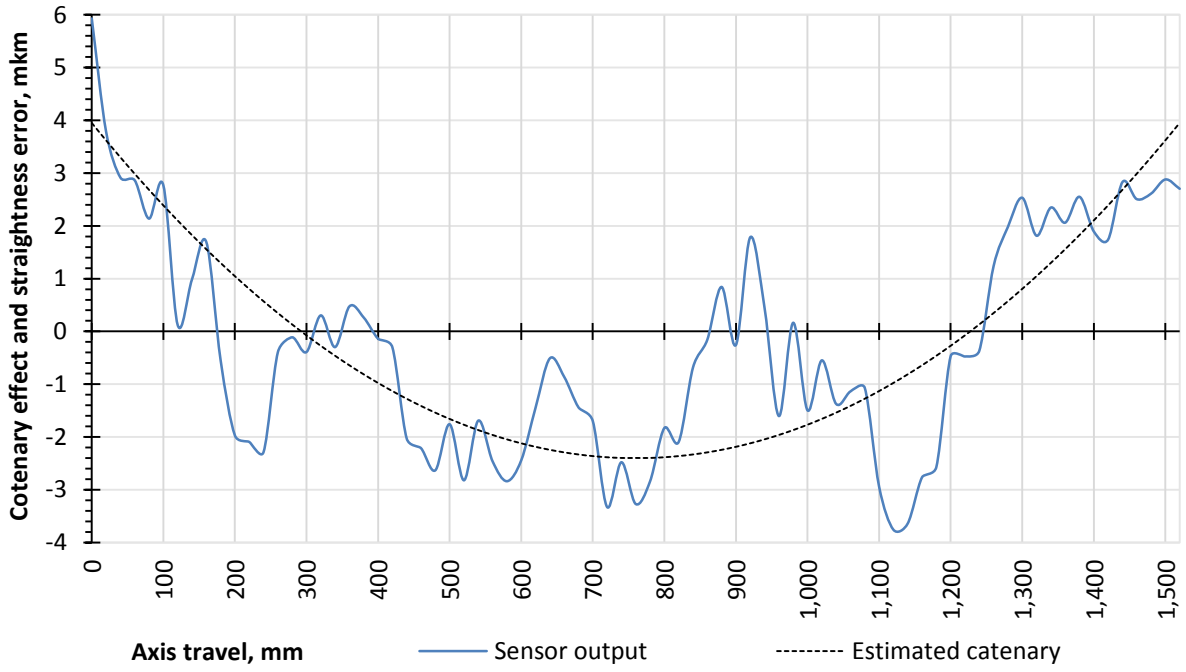

Figure 79. Estimated catenary

Close attention was paid to the accumulation. Longer axis took a larger number of movement increments (which themselves remained unchanged) and therefore the effect of accumulated was expected to increase.

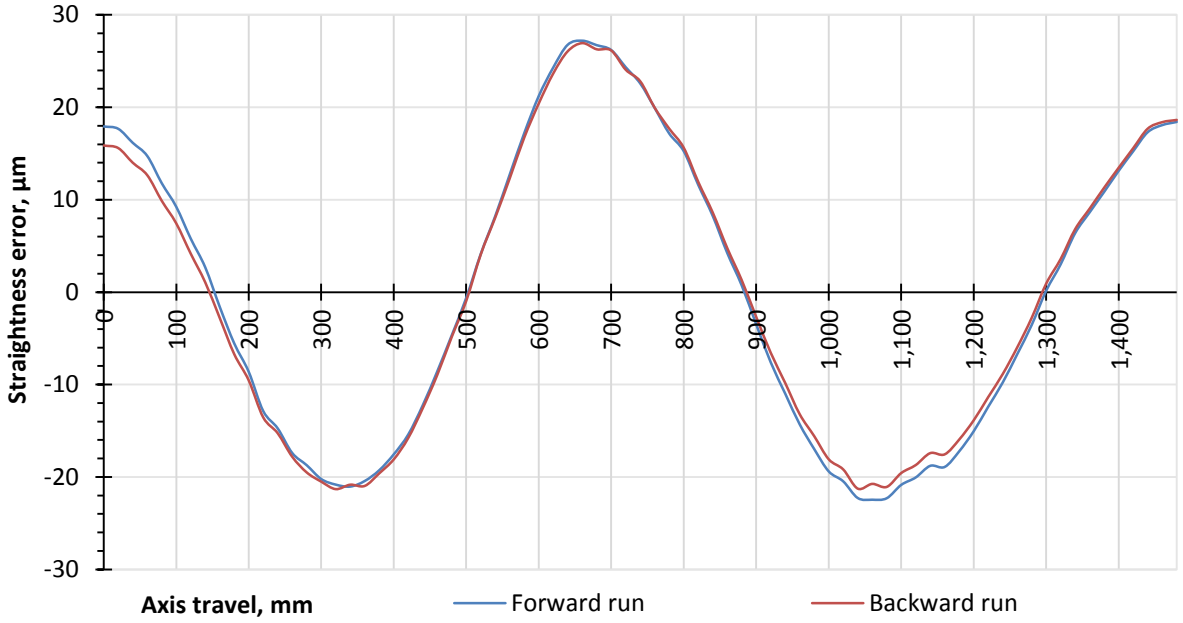

Figure 80. Bi-directional test with error cancellation (large error)

The test (Figure 80) demonstrated a difference never exceeding 2µm containing all of the accumulated error. Similar situation is in case of a smaller straightness error (Figure 81).

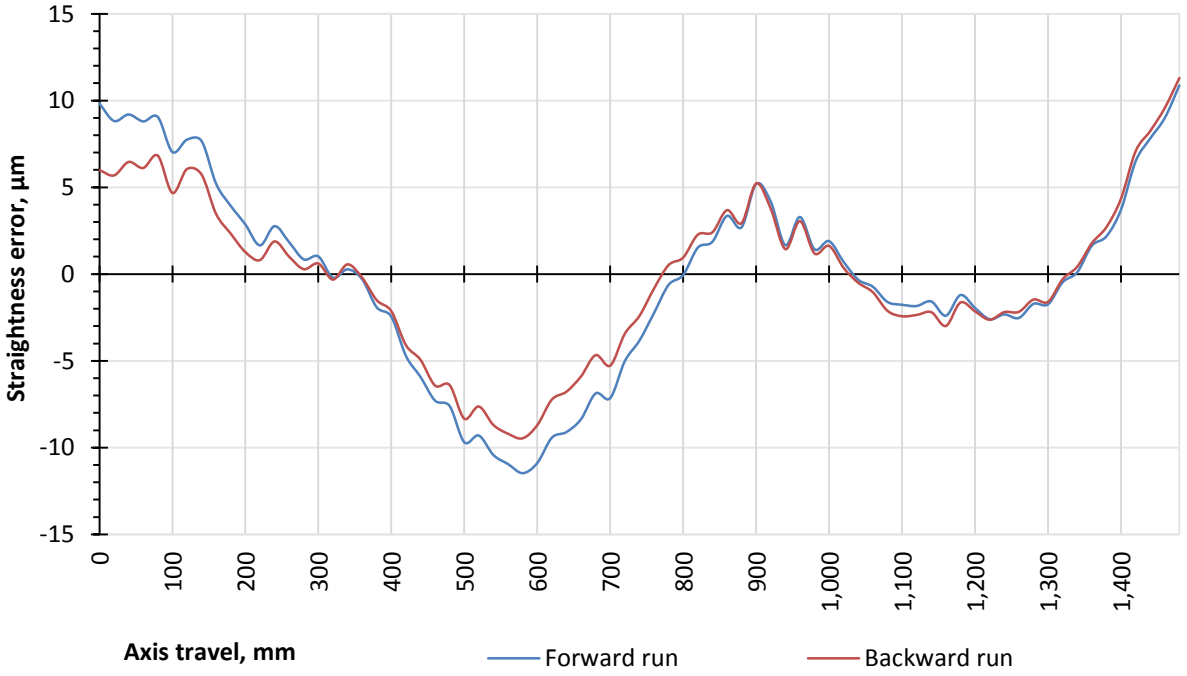

Figure 81. Bi-directional test with error cancellation (compensated error)

Deviation from the laser result is approximately 8μm and does not depend on measured error. A brief research was undertaken on this error cancellation defect. It was found out that the error:

1. Does not depend on the wire transparency (a steel wire gave the same effect).
2. Is systematic within the piece of the wire.
3. Changes with time during wire settling period and shortly after it.
4. Does not affect calibration profile.
5. Does not change the straightness profile read by one sensor separately (affects accumulated result only).
6. Cannot be detected other ways than accumulation.
7. Does not depend on the step accuracy.
8. Is similar to the "wire expiry" effect and possibly has the same nature.
9. Very rarely has a negligible value.
10. Is not affected by secondary slope error and slope error at all.

Nature of this error was not completely clarified, but the effect itself was found to be persistent making the technique of error cancellation not suitable for axis longer than 1m.

This, however, is not an important fact because in practice longer axes have larger straightness error which can be measured successfully ignoring the wire reference error which is limited and stays the same even when the distance between wire mounting points increases.

These considerations were the reason why all long range tests did not implement error cancellation – the wire itself was straight enough to be used as a straightness reference which allowed obtaining a good correlation with the laser-based method. It should be also noted that using multiple sensors simultaneously and/or replacing the wire before each measurement run enables even higher accuracy at a cost of extra time when it is appropriate.

5.3 STATIC TESTS

Stability tests with the machine stationary were carried out under the same conditions as the aforementioned straightness measurements. Duration of the test was 6 minutes.

The results of both measuring methods are shown in Figure 82.

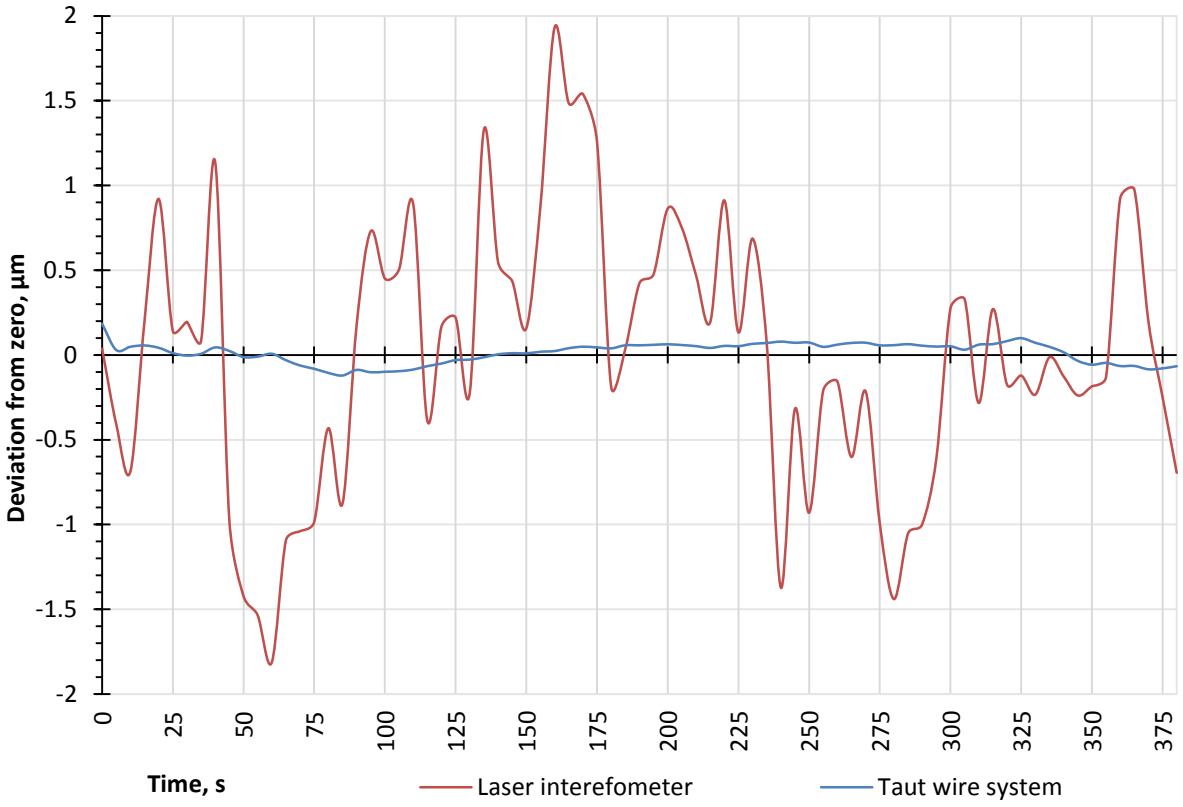

Figure 82. Laser interferometer compared to the taut wire system (static)

Although the laser interferometer was operated using the long term averaging mode provided in data capture software, the random error was measured to be 4 times greater compared to the results obtained on the test rig where laser beam was 2.5 times shorter. The taut wire system stability reduced by only two times under the same conditions (section 4.2.7).

The results confirm that the taut wire system static stability is typically one order of magnitude better than the laser interferometer when applied to the 1.5m machine axis.

5.4 CONCLUSIONS ON TYPICAL AXIS MEASUREMENT

The taut wire system previously validated for short range measurements was tested on a machine tool axis having a traverse length three times greater than the test rig axis used to develop the system and methodology. The redesigned and improved sensor head was set up on the machine together with the laser interferometer with straightness measurement kit and both were tested in close proximity. Both have been measured successfully, with straightness profiles obtained from the taut wire system and laser interferometer having similar shape and magnitude. Summary of the results is in Table 1.

	Error, µm	
Laser	***43***	***4***
Wire	***45***	***6***
Difference		
General	***1***	***1***
Maximum	***3***	***2***

Table 2. Machine tool axis measurement results

The error cancellation technique was replaced by a multiple sensor approach which averages simultaneous readings of two sensors to reduce the reference error (wire straightness).

Static tests showed an order of magnitude difference between the laser and taut wire system signal stability and significantly lower susceptibility of the wire to random noise caused by the environment.

Due to necessity in long term averaging in case of the laser, test runs took longer than in case of the taut wire system less suffering from signal noise. Time required for 1.5m long axis to be measured for straightness error during a single run was 14 and 8 minutes respectively for laser interferometer and taut wire systems.

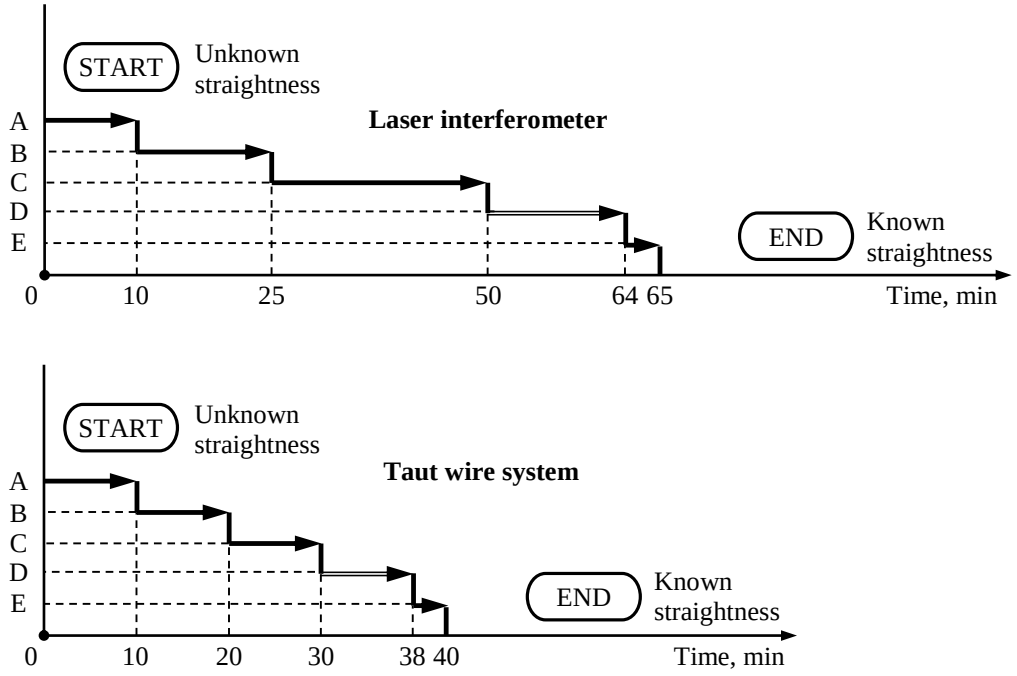

A – Setup on the machine, B – Preconditioning, C – Slope removal, D – actual test run, E – results analysis

Figure 83. Activity diagram for straightness measurements

CHAPTER 6 | UNCERTAINTY AND DATA MANAGEMENT

Commercial instrument have stated accuracies that sometimes include variability based on the magnitude of the reading or other distance factors. However, very few have uncertainty analyses available for different operating conditions etc. Similarly novel instruments published have instrument comparisons usually with some trusted technology similar to that in this thesis. However, a detailed uncertainty analysis is rarely included and therefore true performance in the field is often unknown. One of the potential advantages of the new automated sensor head and taut wire combination is reduced uncertainty over longer measuring distances therefore in addition to the extensive testing already described in chapter 4 and 5, a uncertainty analysis was performed which, according to the literature survey, has not been done yet for the taut wire.

6.1 ASSESSMENT OF THE EFFECT OF LINKED GEOMETRIC ERRORS

Axis straightness is the targeted motion error and ideally the only value to be measured by the taut wire straightness measuring system. All other geometric errors should be separated from straightness in one plane and not be measured together with it. A simple illustration given in the first chapter summarises the errors of any linear axis (Figure 1).

As the X axis moves and straightness is measured in the vertical direction (YZ plane), movement in Z will represent the straightness while the influence of four other components: horizontal straightness in the Y direction, roll, pitch and yaw, will need to be understood. The ISO definition for these error are EYX, EAX, EBX and ECX respectively [9].

Laser interferometer combined with the straightness measuring optics has been designed to be insensitive to all such influences.

Similarly, because those errors are always present on any machine tool axis, the taut wire system should also be insensitive to them.

6.1.1 Cross axis (transverse) sensitivity

The new sensor was set up to measure straightness in the Z axis direction and determine the effect of residual (secondary) slope and error in the machine in the transverse (Y) direction. To check this, the machine was tested twice with a different value of secondary

slope error (Figure 84, 150µm and 5µm), controlled by a special part program that artificially moved the Y axis of the machine during the measurement.

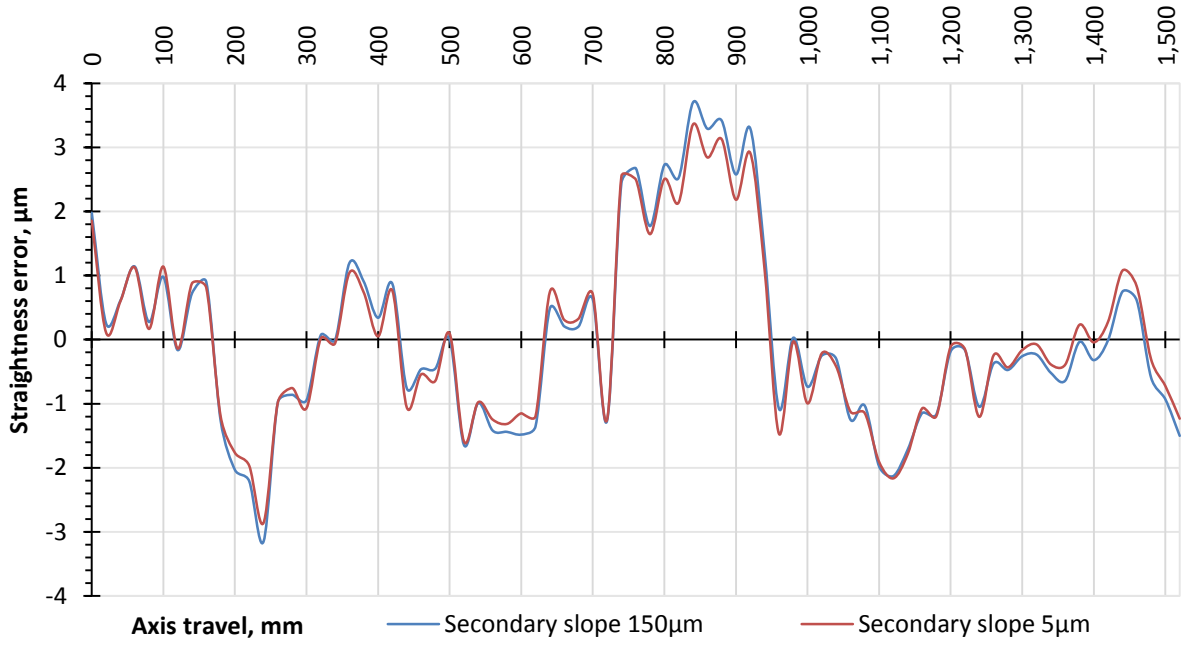

Figure 84. Secondary slope effect

It can be seen in Figure 84 that positioning error in the horizontal plane has a negligible effect on straightness measured in the vertical plane. The mismatch never exceeds 0.5µm and generally stays within 0.2µm.

This validates the method is highly resistant to lateral motion in other than one plane used for measuring straightness.

6.1.2 Pitch (EBX)

Rotational errors can be magnified by the lengths of corresponding axes and result in a combination of three linear motions, the direction of which depends on the axis of rotation and the magnitude of which depends on the effective origin of rotation and offset distance which may be dependent on the Cartesian axis positions or other physical offsets. Conversely, the angular deviation may have a direct influence on the sensor, an example of which is depicted in Figure 85, fortunately in this case, the effect is negligible as described below. For the pitch (rotation about the horizontal Y axis, EBX) error, one of the linear effects is in the measurement direction (Z) and therefore part of the straightness and does not need to be considered. The second linear effect caused by this rotation is in the axial direction and is therefore not detected in the straightness measurement but could affect the error cancellation.

As it was stated in section 3.2.11, the step size (axis movement increment during a straightness test using the taut wire system) does not need to be very accurate due to the physical nature of the wire having a generally even and smooth surface. A tolerance of 0.1mm represents the requirement for linear positioning error along the measured axis. This relatively high value is unlikely to be affected by a linear pitch contribution.

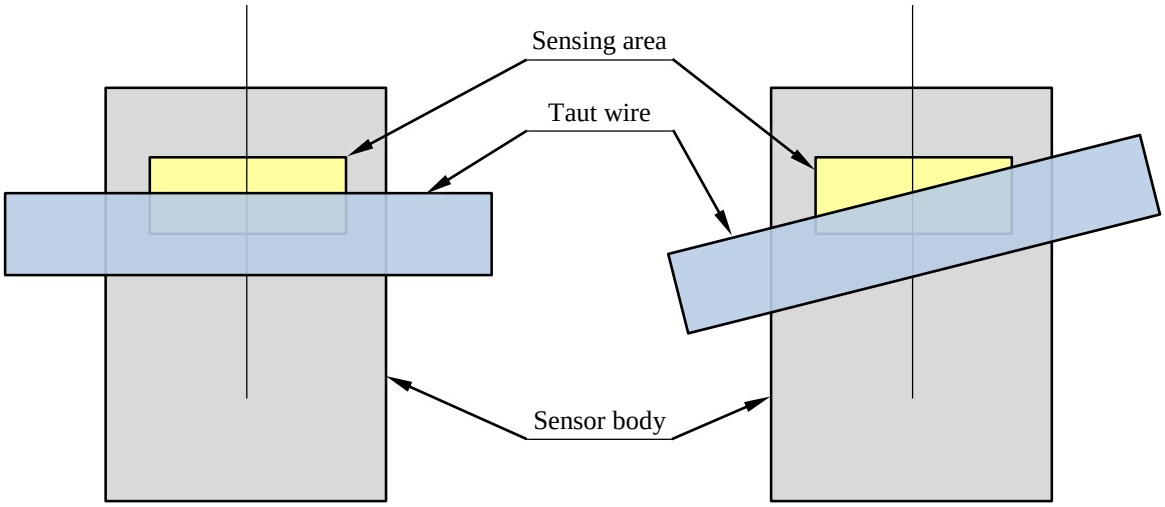

Figure 85. Sensor/wire displacement due to pitch (rotation about the horizontal Y axis, EBX) error

Figure 85 shows how wire and sensor position change due to rotation of one relative to another with linear components subtracted. Sensing area overlapped by the wire remains exactly the same resulting in no change in response of the sensor. Therefore, measured axis pitch error can be considered negligible and not affecting straightness measurement unless the wire comes out of the sensing area which is unlikely to happen because height of the sensing area of a typical sensor is 0.5mm.

6.1.3 Roll (EAX)

Roll error (rotation about the axis parallel to the measured axis) transforms into linear motion along Z and Y and rotation of the sensor around the wire. Because the latter is round, such rotation has only minor effect on the sensor readings as per Figure 86.

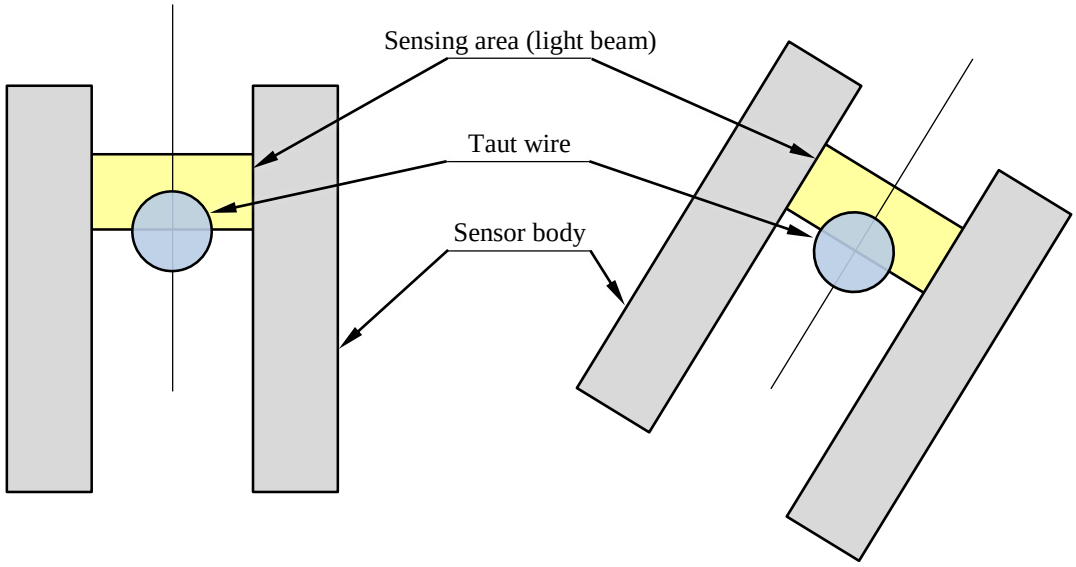

Figure 86. Sensor/wire displacement due to the roll (rotation about the axial X axis, EAX) error

Linear motion in Z is a measured value and linear motion along Y has been discussed in the section 6.1.1 and has negligible effect.

6.1.4 Yaw (EZX)

Yaw error (rotation about the axis parallel to the measured axis) linearly displaces the wire in Y and X directions and its rotation makes the following effect (Figure 87).

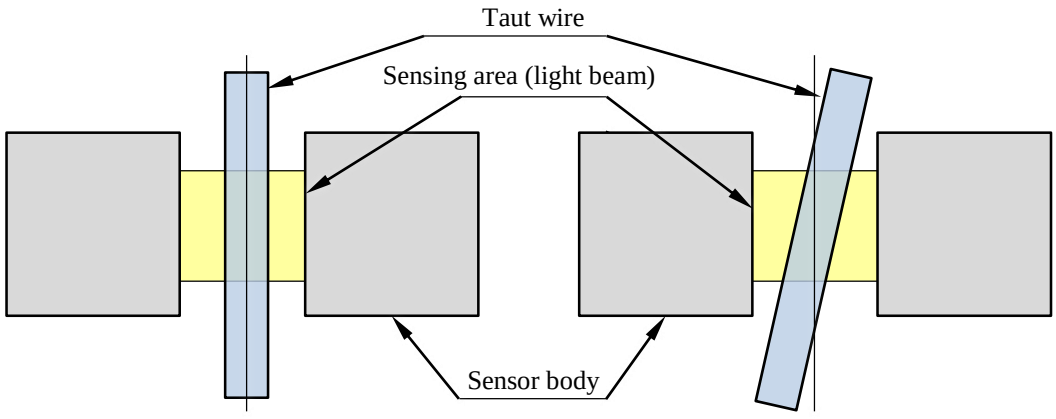

Figure 87. Sensor/wire displacement due to yaw (rotation about the vertical Z axis, ECX) error

The situation here is similar to that found during the pitch analysis. On one side the wire moves closer to light emitter while another – closer to the detector. The net change in light detection is minor. In addition, it has been shown in section 6.1.1 that cross-axis contamination (Y-displacement in this case) has negligible effect.

6.2 UNCERTAINTY ANALYSIS

Measurement uncertainty *U* was determined according to the method presented in technical report ISO230 Part 9 [78], using basic equations applied to uncertainty budget contributors listed in Table 3. The conditions included 1.5m axis, measured for straightness in vertical plane over a 15-minute period using taut wire. All contributors were deemed to be uncorrelated. Their distribution was assumed rectangular because no specific knowledge of them is available and therefore possible overestimation of corresponding uncertainties was considered reasonable. Standard uncertainty of each contributing component was given as:

$$u_i = \frac{a^+ - a^-}{2\sqrt{3}} \quad (8)$$

Where a^- and a^+ are lower and upper limits of distribution respectively. Combined uncertainty u_c was derived as a sum of its contributors:

$$u_c = \sqrt{\sum u_i^2} \quad (9)$$

And with coverage factor *k*, derived from total degrees of freedom, expanded measurement uncertainty *U* was calculated as:

$$U = k \cdot u_c \quad (10)$$

Contributor	Average value	Unit	Sensitivity coefficient	Effect, µm		Uncertainty, µm	Degrees of freedom
				a^-	a^+	u	
Axis pitch	−	mV/deg	0.063	0.01	0.02	0.003	3
Axis roll	−	mV/deg	0.063	0.10	0.50	0.115	3
Axis yaw	−	mV/deg	0.063	0.15	0.80	0.188	3
Horizontal alignment	30	µm/m	0.01	0.20	0.60	0.115	3
Catenary estimation error	0.15	µm/m	2.2	0.2	0.4	0.058	3
Electric noise	1.26	mV	0.063	0.07	0.10	0.009	3
Electronic drift	0.7	mV/h	0.063	0.10	0.20	0.029	3
Wire profile variation	−	µm	**1**	**1.00**	**5.00**	**1.155**	**3**
Wire profile drift	1.7	µm/h	0.25	0.25	0.45	0.058	3
Sensor calibration error	−	µm	1	0.02	0.50	0.139	3

Table 3. Uncertainty budget for straightness measurement using a taut wire system

Table 3 describes factors contributing towards measurement uncertainty. The first three represent angular deviations of the axis during its linear motion. These were measured by tilting the spindle and then separating the vertical lateral displacement from the measured value. It was necessary to quantify the sensitivity of the measuring system to the unwanted rotational movements of the axis during the test runs. All three effects change the position of the wire within the optical sensor slightly moving it forward/backwards (pitch and yaw) or left/right (roll). Horizontal alignment is the uncertainty due to slope in the corresponding plane. It was measured during test runs with different amounts of slope in horizontal plane. The systematic difference in resulting profiles was due to misalignment. Its effect proved to be very small (Figure 84). The wire catenary estimation has an error due to wire length and weight measurement. The latter is determined by the precision of the electronic scale (specification in Appendix B). Electronic noise together with drift were measured while the axis was stopped at its end, minimizing the effect of wire movement. The noise was measured during short period of time (10 seconds) and drift over longer periods (10 minutes). Wire profile variation is represented by the wire profile, unique for each wire piece. Changing the wire and repeating straightness measurements provides data containing the measured and the reference error combined together. First part remains constant, another one changes with every new wire piece installed. This change is the reference error – wire profile variation. The sensor calibration error represents sensor non-linearity approximation during system calibration when the axis moves known intervals incrementally in a vertical direction.

Sensitivity coefficients were obtained from the combined sensitivity value of the optical sensors, which was 16mV/µm. Degrees of freedom were estimated as the number of repeated measurements (n = 4) less one.

The total value of degrees of freedom was derived using a Welch-Satterthwaite equation:

$$\upsilon = \frac{\left(\sum \frac{u_i^2}{n_i}\right)^2}{\sum \frac{1}{n_i - 1}\left(\frac{u_i^2}{n_i}\right)^2} \qquad (11)$$

This gives $\upsilon = 3.41$ which corresponds to coverage factor k = 3.31. The resulting U_{wire} = 4µm could not be compared directly with the accuracy specification of a Renishaw XL-80 laser interferometer (Appendix B), which is 0.86µm, as this does not include a number of uncertainty contributors. Knapp in his paper [58] provides an uncertainty budget for laser interferometer and associated optics and setup for short-range straightness measurement, the

same contributors were calculated to obtain combined uncertainty for our laser system and setup conditions (Table 4).

Contributor	Average value	Unit	Sensitivity coefficient	Effect, µm		Uncertainty, µm	Degrees of freedom
				a^-	a^+	u	
Laser device	2.5	µm	1	0.50	4.50	1.155	3
Thermal drift	1.2	µm	1	1.00	1.40	0.115	3
Air disturbance	0.6	µm	1	0.50	0.70	0.058	3
Δ surface temperature	2	ºC	0.4	0.40	1.20	0.231	3

Table 4. Uncertainty budget for straightness measurement using laser interferometer

This gives U_{laser} = 4µm which is somewhat lower than the value quoted by Knapp (6µm) and is similar to the wire system result mentioned above. The actual results obtained on the machine (Figure 74 and Figure 75) have two standard deviations of 1.5µm for both the laser and taut wire systems. This confirms good performance correlation between both systems.

As can be seen from Figure 75, the main contributor to the taut wire system uncertainty was the unique profile of each piece of wire installed. Consequently, the straightness value depends on quality of the wire, normally does not exceed 4µm and does not depend on wire length being limited by its diameter inconsistency. This allows high stability of the system installed on longer axes to be assumed despite environmental effects normally having a pre-emptive contribution to the uncertainty of other methods. As shown before (Figure 75 and Figure 78), taut wire system uncertainty can be further decreased by the averaging of different wire results in the same conditions at the expense of additional time spent on wire reinstallation and repeated measurement runs.

6.3 DATA MANAGEMENT

The straightness measuring system, discussed in previous chapters, operates on two levels like many metrology systems: hardware and software. Analysis software is necessary because of three reasons:

1. Formatting of the data to produce the final result.
2. Intermediate results and real time indications are required.
3. The software needs to be available for modifications made by the user.

The final result is a straightness profile graph aligned with the horizontal axis using one of the fitting methods. It can be presented as a table of values if necessary or part of it can be used according to the size of target area.

Intermediate results allow verification of the final result, to check its validity and repeatability and thereby avoid poor results.

Also a separate presentation of calibration result should be available to determine the most suitable working area of the optical sensor set and to make sure the procedure has been completed correctly.

Microsoft Excel has been chosen to implement data analysis and reporting functionality. It is readily available and, importantly, is extensible to be adapted to a certain usage scenarios, such as simultaneous measurement of straightness in two planes, replacing the error cancellation with multiple sensor averaging, changing measurement range, axis length, increment values etc.

All the above stipulates the software to be open, user-friendly, easily understandable, convertible and upgradable. This chapter will describe the solution, beginning from the outline of the data flow, showing all necessary operations and corresponding modules, then a platform for those operations will be chosen, crucial calculation techniques will be explained, user interface and its usage demonstrated.

6.4 DATA FLOW

Output from optical sensors in the measuring head is directly affected by the lateral displacements of a moving axis and represents the starting point of the system dataflow. Current from light receivers is filtered by the electronic circuit which incorporates low-pass filters. A multichannel Analogue to Digital Converter (ADC) model NI 9239 (24bit, 4 channels), connected via USB, is used to acquire the data on the PC for processing. Figure 88 shows an overview of the data flow.

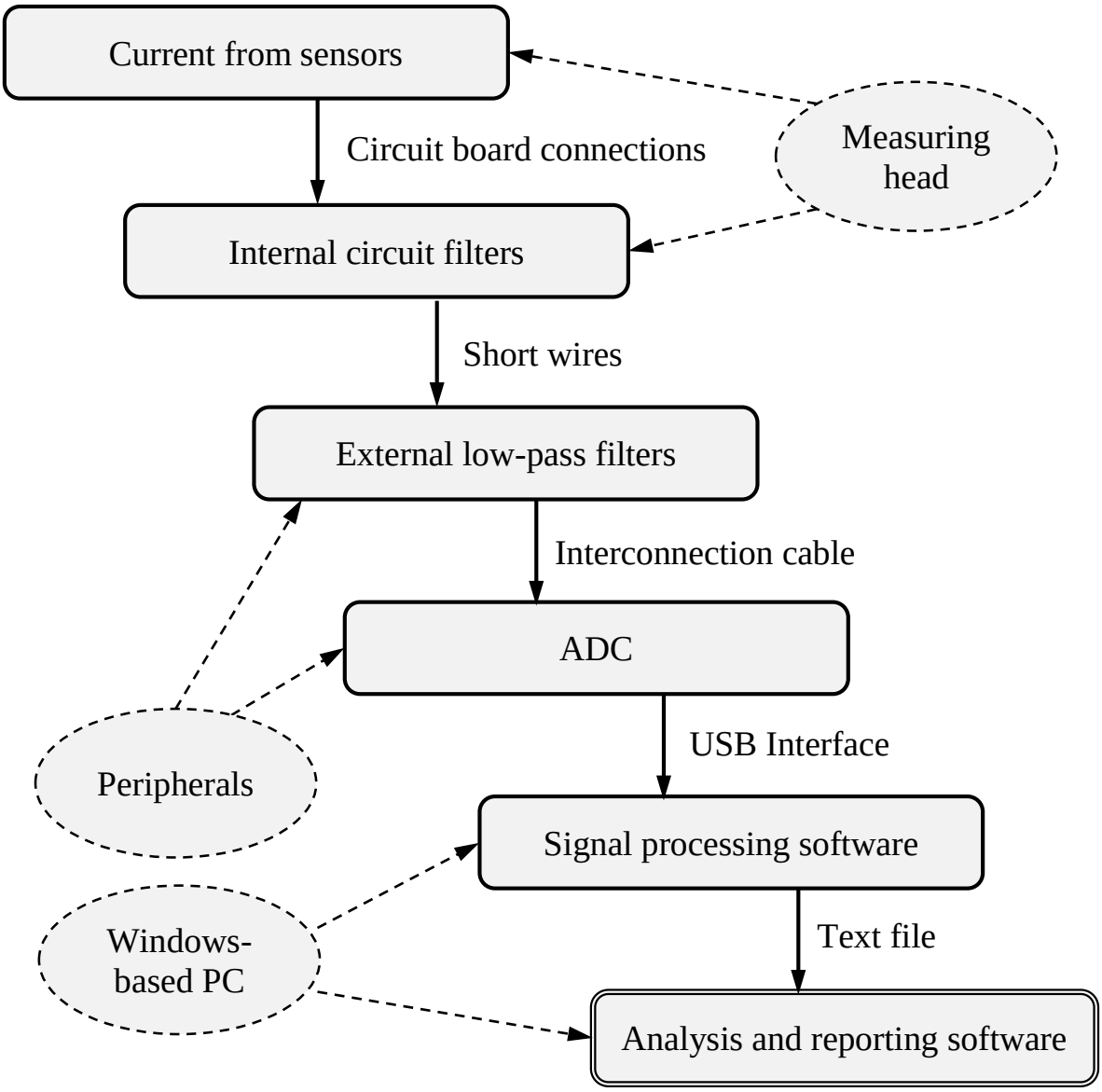

Figure 88. Dataflow diagram

The analysis and reporting block (Figure 89) combines the data from different sources and different measurement stages. It is the most flexible in terms of user control and provides information during the measurement process. Data coming from calibration, setup and measurement runs is processed here and determines the measurement sequence. For example, after completing a calibration run, the results can be checked for suitable working range and sensitivity. Completed runs data can be compared with previous values and repeatability confirmed etc.

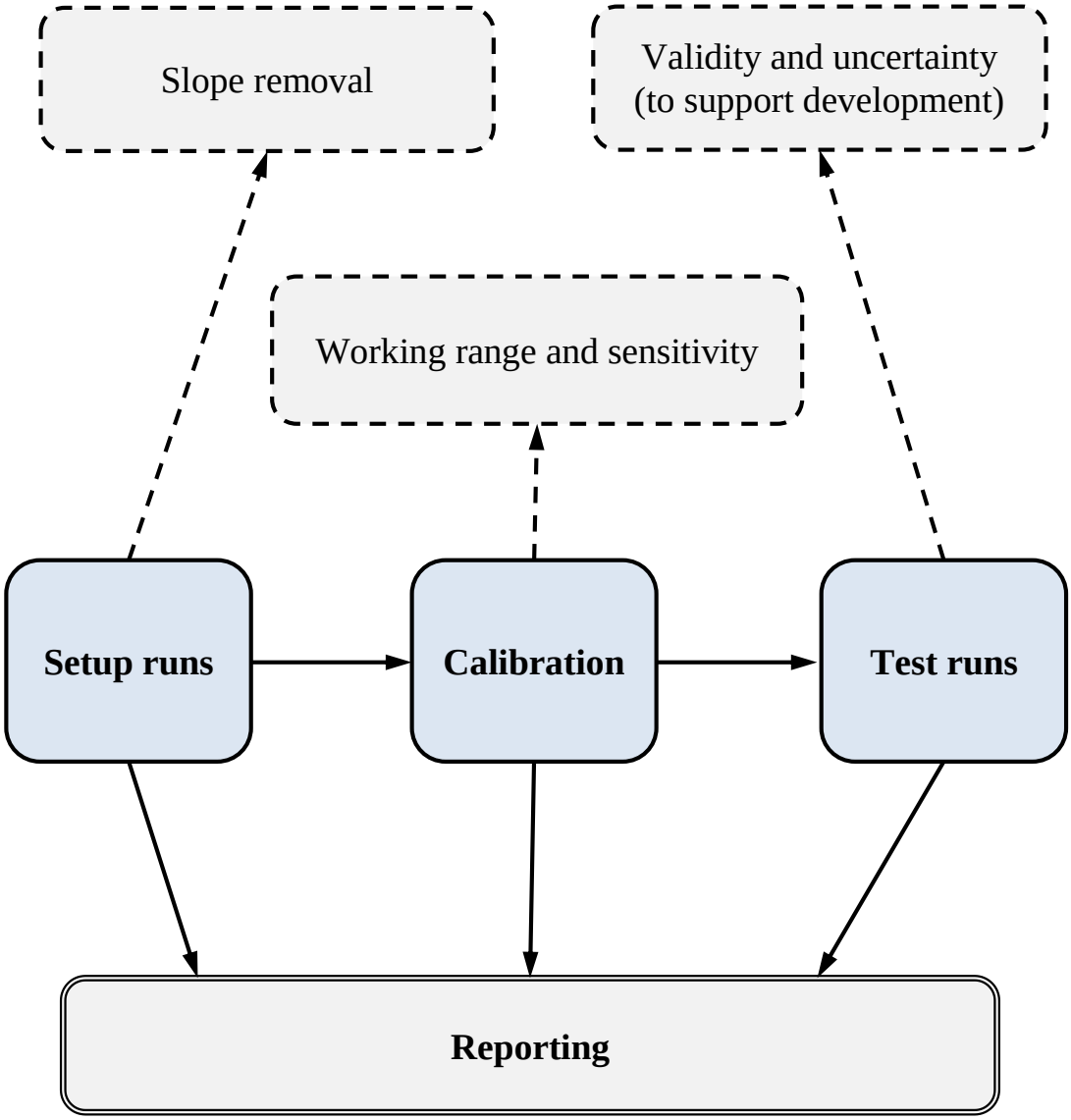

Figure 89. Data analysis and reporting expanded

6.5 SOFTWARE

The software performs two main operations with data: signal processing and reporting.

6.5.1 Signal processing

Driver for the ADC makes the data available to use by other applications. The one used in this project is a custom-built software package produced within the research group. This utility is called “NCDT Logger”; it is universal for a number of data capturing devices and has the following features:

1. Real time monitoring of multiple data channels.
2. Graphical and digital data indication.
3. Manual and time-based automatic data capture.
4. Saving data to an ASCII text file.
5. Incoming data averaging.
6. Dynamic data capture (based on triggering limits and signal stability).
7. Unit conversion.
8. Calibration application.

Not all of the listed above is needed for our purpose and the most important are real-time monitoring, data capture and saving to file. This provides data for the next processing step – calculation, which uses a different software piece.

6.5.2 Straightness calculation and reporting

The input data on this step is an array containing straightness values at each point. The following data processing should be completely open to user and not requiring any programming skills to organize the data the way it is needed to be.

To achieve that, a table processor from Microsoft Excel was chosen as a well-known, powerful, readily available and user-friendly solution. The data file is CSV formatted and therefore easily read.

A capability to build diagrams and table reports suitable for printing and visual presentation of the measurement final and intermediate results as well as on-the-fly editing of the structure producing them is a key-advantage of the chosen table processor.

6.6 CALCULATION

All calculations are done in tables, when input and output data is a sequence of values formatted in a set of table rows. Actually, a sequence of measuring head readings is being passed through a number of transformations each according to a certain logical rule, step by step producing a sequence of axis straightness values.

The process begins from applying the calibration to raw data, then the error cancellation (separation) follows, then – slope removal and averaging. Intermediate results are used for measurement error detection (if it exists) and estimation.

6.6.1 Calibration

The calibration procedure, described in section 3.5, is based on comparison of the new measuring head output (all channels) with a linear lateral displacement achieved by moving the axis or the head separately in the direction of measuring straightness. The output is supposed to be linear therefore any deviation needs to be linearised.

The logic:

1. Get two points to build a reference line: take average of end points of all channels on the left and on the right.
2. Calculate the offsets as differences between each value of the reference line and corresponding values of all channels.
3. For each raw uncalibrated value choose two closest calibration values: one smaller and one larger than itself.
4. Check the position of each uncalibrated value between two adjacent calibration ones and produce a third one taken from the same reference line accordingly (adjusted average).
5. Apply the correction to each raw value producing a calibrated output for further calculations.

Array functions are used to implement this as shown in Figure 90 and Table 5.

	A	B	C	D	E	F	G	H	I	J	K	L	M	N	O	P	Q	R	S	T	U	V
1				Calibration test					Work Readings												Corrected	
2			mkm	V	V	V	V	V	V	V											V	V
3		Point	Travel	S1	S2	Merged_str	Offset1	Offset2	S1	S2	Close_min1	Close_min2	Close_max1	Close_max2	Off_min1	Off_min2	Off_max1	Off_max2	Correction1	Correction2	S1	S2
4		1	0	10	5.2	7.60	2.40	-2.40	11	6	10	5.2	11.2	7.5	2.40	-2.40	2.61	-1.09	2.57	-1.95	8.43	7.95
5		2	1	11.2	7.5	8.59	2.61	-1.09	12.3	8	12	7.5	12.5	8.3	2.41	-1.09	1.92	-1.29	2.12	-1.21	10.18	9.21
6		3	2	12	8.3	9.59	2.41	-1.29	14	7	12.5	5.2	14.6	7.5	1.92	-2.40	3.03	-1.09	2.71	-1.38	11.29	8.38
7		4	3	12.5	8.6	10.58	1.92	-1.98	16.6	9	16.4	8.6	17	9.7	2.84	-1.98	2.44	-1.88	2.71	-1.94	13.89	10.94
8		5	4	14.6	9.7	11.58	3.03	-1.88	12.1	11	12	10.6	12.5	12	2.41	-1.97	1.92	-1.56	2.31	-1.85	9.79	12.85
9		6	5	15.3	10.6	12.57	2.73	-1.97	13.5	8	12.5	7.5	14.6	8.3	1.92	-1.09	3.03	-1.29	2.45	-1.21	11.05	9.21
10		7	6	16.4	12	13.56	2.84	-1.56	15	12	14.6	10.6	15.3	12	3.03	-1.97	2.73	-1.56	2.86	-1.56	12.14	13.56
11		8	7	17	13	14.56	2.44	-1.56	14	13.2	12.5	13	14.6	13.3	1.92	-1.56	3.03	-2.25	2.71	-2.02	11.29	15.22
12		9	8	17.8	13.3	15.55	2.25	-2.25	12	11	11.2	10.6	12	12	2.61	-1.97	2.41	-1.56	2.41	-1.85	9.59	12.85

Figure 90. Calibration spread sheet

Cell	Function / Sub-function	
F4	`AVERAGE($D$4:$E$4)`	
F5	`F4+($F$12-$F$4)/$B$11`	
G4	`D4-F4`	
K4*	`LARGE(IF(uncalibrated1<Sheet1!I4,uncalibrated1),1)`	
	`uncalibrated1`	`Sheet1!$D$4:$D$12`
M4*	`SMALL(IF(uncalibrated2>Sheet1!K4,uncalibrated2),1)`	
	`uncalibrated2`	`Sheet1!$E$4:$E$12`
O4	`VLOOKUP(K4,$D$4:$H$12,4,TRUE)`	
Q4	`VLOOKUP(M4,$D$4:$H$12,4,TRUE)`	
S4	`Q4-(Q4-O4)*(M4-I4)/(M4-K4)`	
U4	`I4-S4`	

Table 5. Key calibration functions

Functions marked with "*" use shortcuts to user-defined sub-functions describing data arrays (available on pressing Ctrl+F3).

6.6.2 Error cancellation

The error cancellation (removal of reference error) is described in section 3.4.3 and practically implemented by the following sequence:

1. Calculation of an offset for each dual-channel reading subtracting one value from another (both corrected, Figure 91, column titled E4).
2. Obtaining an average of all offsets (G2).
3. Moving the second channel profile vertically to make it as close to the first one as possible, subtracting the average offset from every of its values with one step forward shift (to bring both profiles closer horizontally, F4).
4. Subtracting values (3) from the first channel ones and converting the result from volts to microns using sensitivity value obtained on calibration stage (G4).
5. Accumulation of (4) done by adding each value on the top of the previous one starting from zero (J4).

Figure 91 shows a template for implementing the error cancellation:

	A	B	C	D	E	F	G	H	I	J	K	L
1	Taut wire straightness measurement template							-0.0033	480.984	mm	0.44	0.43
2		wire h	4.0	mkm	Offset (average)		-0.0033	V	240.492	20.041	1 mkm =	0.0020
3		Travel,	Captured data, V		Calculation							
4		mm	S1	S2	Offset	S2 (XY)	dS(mkm)	S12 AVG	Basic	Accum	Comp	RepQ
5	0	0	4.1241	**4.1299**	-0.0058			4.1270	-0.8			
6	1	20	**4.1251**	4.1252	-0.0001	4.1266	-0.8	4.1252	-1.7	-0.8	-1.9	0.8
7	2	40	4.1238	4.1302	-0.0064	4.1219	0.9	4.1270	-0.6	0.2	-0.8	0.9
8	3	60	4.1265	4.1289	-0.0024	4.1270	-0.2	4.1277	-0.2	-0.1	-0.9	0.2
9	4	80	4.1276	4.1298	-0.0022	4.1256	1.0	4.1287	0.4	1.0	0.3	1.0
10	5	100	4.1268	4.1299	-0.0031	4.1266	0.1	4.1284	0.4	1.1	0.6	0.1
11	6	120	4.1272	4.1317	-0.0045	4.1266	0.3	4.1295	1.0	1.4	1.0	0.3
12	7	140	4.1273	4.1316	-0.0043	4.1284	-0.5	4.1295	1.1	0.9	0.6	0.5
13	8	160	4.1269	4.1289	-0.0020	4.1284	-0.8	4.1279	0.4	0.1	0.0	0.8
14	9	180	4.1256	4.1298	-0.0043	4.1256	0.0	4.1277	0.4	0.1	0.1	0.0
15	10	200	4.1258	4.1285	-0.0027	4.1266	-0.4	4.1271	0.3	-0.3	-0.1	0.4
16	11	220	4.1262	4.1267	-0.0005	4.1252	0.5	4.1265	0.0	0.2	0.5	0.5
17	12	240	4.1224	4.1291	-0.0067	4.1234	-0.5	4.1258	-0.2	-0.3	0.2	0.5
18	13	261	4.1255	4.1267	-0.0013	4.1258	-0.2	4.1261	0.0	-0.4	0.1	0.2
19	14	281	4.1235	4.1277	-0.0043	4.1234	0.0	4.1256	-0.1	-0.4	0.3	0.0
20	15	301	4.1255	4.1271	-0.0016	4.1244	0.5	4.1263	0.3	0.1	1.0	0.5
21	16	321	4.1234	4.1280	-0.0046	4.1238	-0.2	4.1257	0.1	-0.1	0.9	0.2
22	17	341	4.1241	4.1270	-0.0028	4.1247	-0.3	4.1255	0.2	-0.4	0.8	0.3
23	18	361	4.1223	4.1282	-0.0059	4.1237	-0.7	4.1252	0.1	-1.1	0.2	0.7
24	19	381	4.1240	4.1265	-0.0025	4.1249	-0.4	4.1253	0.2	-1.5	-0.1	0.4
25	20	401	4.1232	4.1263	-0.0031	4.1232	0.0	4.1248	0.1	-1.5	0.0	0.0
26	21	421	4.1233	4.1287	-0.0055	4.1230	0.1	4.1260	0.8	-1.4	0.3	0.1
27	22	441	4.1238	4.1267	-0.0029	4.1254	-0.8	4.1252	0.5	-2.3	-0.4	0.8
28	23	461	4.1212	4.1232	-0.0020	4.1234	-1.1	4.1222	-0.9	-3.4	-1.4	1.1
29	24	481	4.1197	4.1205	-0.0009	4.1199	-0.1	4.1201	-1.9	-3.5	-1.3	0.1

Figure 91. Error cancellation spread sheet

The logic here implements the error cancellation mathematics discussed in section 3.4.3. Average offset is calculated to bring both captured data profiles as close as possible, then the difference between readings from two sensors is obtained (dS column), then this difference is accumulated ("Accum") and then fitted using least squares ("Comp").

6.6.3 Slope removal

Slope removal is achieved using a linear least squares fit which is reliable for comparison of different profiles. Fitting functions for slope removal were built so that they would not depend on input data location on a spread sheet and could be replicated horizontally. The exact implementation is shown in Table 6 (K7) where cell identifiers refer to Figure 91.

Cell	Function / Sub-function
F7	D6+$G$2
G7	(C7-F7)/$L$2
J7	J6+G7
K7	(J7-INTERCEPT(J$6:J$29,ROW(J$6:J$29)-ROW(J$6))- SLOPE(J$6:J$29,ROW(J$6:J$29)-1)*(COUNT(J$6:J7)-1))

Table 6. Key slope removal functions

6.6.4 Averaging

The set of data, obtained from two sensors, can be processed into measured axis straightness four different ways. The difference is in the order of calculation which is based on accumulation. The latter one can start from the first reading and proceed till the last one. This corresponds to going from the top till the bottom of the table in Figure 91 – this is up-down calculation. Going in reverse order is down-up calculation.

Because tests runs were performed in both directions (moving the axis all the way forward and then returning it back the same way), there is additional data to do the calculations in two variants: when considering first physical channel to be the first logically once and once – secondary.

All together there will be four different straightness profiles representing the same axis measured four slightly different ways. The procedure is as follows:

Up-down calculation for both channels is done identically, just using the reverted order of backward run readings (when the first becomes the last and so on). The channels order stays the same.

Down-up calculation is different because steps (4) and (5) of section 6.6.2 are performed from the end of the column to its beginning, this time leaving the last value blank.

Such averaging also gives both end points (each calculated twice during a bi-directional test) making the output profile complete and ready for comparison with other ones obtained using a basic single-point approach (like in case of laser measurements).

Data from the backwards run is processed in both directions the same way as described above and provides another two straightness profiles.

All four results ideally should be identical but in practice they have a difference caused mostly by random measurement errors. Because all four calculations use the same

input data, it takes no time and effort to use all four and take average of them to improve the stability of the final result.

6.7 PRESENTATION

Charts are provided to check of the final result and its validity as well as its comparison with measurement results obtained using other methods or/and in the past.

Along with diagrams, some single-number values are used for quick estimation of measurement quality when the corresponding characteristic is very simple.

6.7.1 Tables

The template (excluding calibration module) designed for straightness measurement is shown in Figure 92. It is its table part designed for bi-directional dual-channel measurements of 480mm axes. Its structural elements are explained in Table 7.

Channel 1	Channel 2	Comment
B5:B29	B31:B55	Axis travel with increment specified in J2
C5:D29	C31:D55	Corrected readings from two channels
I5:I29	I31:I55	Basic (single channel) test result
K6:K29	K32:K55	Dual channel test result (with error cancellation)
K1	K2	Value for repeatability estimation
Q5:Q28	Q31:Q54	Dual channel test result (reversed calculation)
S5:S29		Averaged basic test result
T5:T29		Average bi-directional dual-channel result
L2		Sensitivity after calibration
C2		Actual sensor work range

Table 7. Measurement template elements

	A	B	C	D	E	F	G	H	I	J	K	L	M	N	O	P	Q	R	S	T
1	Taut wire straightness measurement template							-0.0046	480.984	mm	0.47	0.44	RepQ Avg (mkm)							
2		wire h	5.0	mkm	Offset (average)		-0.0043	V	240.492	20.041	1 mkm =	0.0020	V							
3		Travel,	Captured data, V		Calculation									Calculation from the other end					Averages	
4		mm	S1	S2	Offset	S2 (XY)	dS(mkm)	S12 AVG	Basic	Accum	Comp	RepQ		S2 (XY)	dS(mkm)	Accum	Comp		Basic	Comp
5	0	0	4.1947	4.2026	-0.0080			4.1986	-1.1					4.1983	-0.6	-3.6	-1.7		-1.3	-1.6
6	1	20	4.1972	4.1958	0.0014	4.1983	-0.6	4.1965	-2.1	-0.6	-2.7	0.6		4.1915	1.2	-3.0	-2.2		-2.1	-2.2
7	2	40	4.1938	4.2024	-0.0086	4.1915	1.2	4.1981	-1.2	0.6	-1.4	1.2		4.1982	-0.1	-4.2	-0.9		-1.2	-1.0
8	3	60	4.1980	4.2012	-0.0032	4.1982	-0.1	4.1996	-0.4	0.5	-1.3	0.1		4.1969	1.2	-4.1	-0.9		-0.3	-0.9
9	4	80	4.1993	4.2027	-0.0034	4.1969	1.2	4.2010	0.4	1.7	0.1	1.2		4.1985	0.2	-5.3	0.4		0.5	0.4
10	5	100	4.1988	4.2030	-0.0042	4.1985	0.2	4.2009	0.5	1.9	0.4	0.2		4.1987	0.3	-5.5	0.7		0.5	0.6
11	6	120	4.1994	4.2051	-0.0057	4.1987	0.3	4.2023	1.2	2.2	0.9	0.3		4.2008	-0.4	-5.8	1.2		1.3	1.0
12	7	140	4.2001	4.2059	-0.0058	4.2008	-0.4	4.2030	1.7	1.9	0.7	0.4		4.2016	-0.4	-5.5	0.9		1.7	0.8
13	8	160	4.2008	4.2022	-0.0014	4.2016	-0.4	4.2015	1.1	1.5	0.4	0.4		4.1980	0.1	-5.1	0.6		1.0	0.4
14	9	180	4.1982	4.2033	-0.0051	4.1980	0.1	4.2007	0.8	1.6	0.7	0.1		4.1990	-0.2	-5.2	0.8		0.7	0.7
15	10	200	4.1985	4.2021	-0.0036	4.1990	-0.2	4.2003	0.6	1.3	0.6	0.2		4.1978	0.4	-4.9	0.7		0.6	0.5
16	11	220	4.1986	4.1993	-0.0008	4.1978	0.4	4.1990	0.0	1.7	1.2	0.4		4.1951	-0.8	-5.3	1.2		0.0	1.0
17	12	240	4.1935	4.2027	-0.0092	4.1951	-0.8	4.1981	-0.3	0.9	0.5	0.8		4.1984	-0.1	-4.5	0.5		-0.4	0.3
18	13	261	4.1981	4.1996	-0.0015	4.1984	-0.1	4.1989	0.2	0.8	0.6	0.1		4.1953	-0.2	-4.4	0.5		0.1	0.3
19	14	281	4.1949	4.2013	-0.0064	4.1953	-0.2	4.1981	-0.1	0.6	0.5	0.2		4.1970	0.4	-4.2	0.4		-0.1	0.3
20	15	301	4.1978	4.1991	-0.0014	4.1970	0.4	4.1985	0.2	1.0	1.0	0.4		4.1949	-0.1	-4.6	0.9		0.2	0.9
21	16	321	4.1946	4.2006	-0.0060	4.1949	-0.1	4.1976	-0.2	0.9	1.1	0.1		4.1964	-0.4	-4.4	0.9		-0.1	0.9
22	17	341	4.1955	4.2001	-0.0046	4.1964	-0.4	4.1978	0.0	0.4	0.8	0.4		4.1958	-0.9	-4.0	0.5		0.0	0.6
23	18	361	4.1941	4.2020	-0.0079	4.1958	-0.9	4.1980	0.2	-0.4	0.1	0.9		4.1977	-0.3	-3.2	-0.2		0.2	-0.1
24	19	381	4.1971	4.1993	-0.0022	4.1977	-0.3	4.1982	0.4	-0.7	0.0	0.3		4.1950	0.0	-2.9	-0.4		0.4	-0.2
25	20	401	4.1950	4.1999	-0.0050	4.1950	0.0	4.1975	0.1	-0.8	0.1	0.0		4.1957	0.1	-2.8	-0.3		0.1	-0.1
26	21	421	4.1959	4.2021	-0.0062	4.1957	0.1	4.1990	1.0	-0.7	0.3	0.1		4.1978	-1.1	-2.9	-0.1		0.9	0.2
27	22	441	4.1956	4.2004	-0.0048	4.1978	-1.1	4.1980	0.6	-1.8	-0.6	1.1		4.1962	-1.4	-1.8	-1.1		0.6	-0.7
28	23	461	4.1935	4.1962	-0.0027	4.1962	-1.4	4.1948	-0.9	-3.1	-1.8	1.4		4.1919	-0.5	-0.5	-2.4		-0.9	-1.9
29	24	481	4.1910	4.1918	-0.0008	4.1919	-0.5	4.1914	-2.6	-3.6	-2.1	0.5							-2.5	-1.8
30																				
31	0	0	4.1925	4.2012	-0.0087			4.1968	-1.4					4.1967	-0.4	-2.6	-1.5			
32	1	20	4.1958	4.1950	0.0009	4.1967	-0.4	4.1954	-2.1	-0.4	-2.2	0.4		4.1904	1.1	-2.2	-1.8			
33	2	40	4.1925	4.2016	-0.0091	4.1904	1.1	4.1971	-1.1	0.6	-1.0	1.1		4.1971	0.0	-3.3	-0.7			
34	3	60	4.1970	4.2005	-0.0035	4.1971	0.0	4.1988	-0.2	0.6	-0.9	0.0		4.1959	1.2	-3.3	-0.6			
35	4	80	4.1983	4.2022	-0.0039	4.1959	1.2	4.2002	0.6	1.8	0.4	1.2		4.1976	0.0	-4.4	0.7			
36	5	100	4.1976	4.2025	-0.0048	4.1976	0.0	4.2001	0.6	1.8	0.5	0.0		4.1979	0.2	-4.4	0.8			
37	6	120	4.1984	4.2042	-0.0059	4.1979	0.2	4.2013	1.3	2.0	0.9	0.2		4.1997	-0.4	-4.7	1.1			
38	7	140	4.1989	4.2053	-0.0063	4.1997	-0.4	4.2021	1.8	1.7	0.6	0.4		4.2007	-0.6	-4.3	0.8			
39	8	160	4.1996	4.2012	-0.0016	4.2007	-0.6	4.2004	1.0	1.1	0.2	0.6		4.1966	0.2	-3.7	0.3			
40	9	180	4.1970	4.2025	-0.0055	4.1966	0.2	4.1997	0.7	1.3	0.5	0.2		4.1979	-0.4	-3.9	0.6			
41	10	200	4.1971	4.2012	-0.0041	4.1979	-0.4	4.1992	0.5	0.9	0.2	0.4		4.1967	0.5	-3.5	0.3			
42	11	220	4.1976	4.1984	-0.0008	4.1967	0.5	4.1980	0.0	1.4	0.8	0.5		4.1938	-0.8	-4.0	0.9			
43	12	240	4.1923	4.2018	-0.0095	4.1938	-0.8	4.1970	-0.4	0.6	0.1	0.8		4.1972	-0.1	-3.2	0.1			
44	13	261	4.1970	4.1988	-0.0017	4.1972	-0.1	4.1979	0.1	0.5	0.2	0.1		4.1942	0.0	-3.1	0.1			
45	14	281	4.1941	4.2008	-0.0067	4.1942	0.0	4.1974	-0.1	0.4	0.3	0.0		4.1962	0.5	-3.1	0.2			
46	15	301	4.1971	4.1987	-0.0016	4.1962	0.5	4.1979	0.2	0.9	0.8	0.5		4.1941	-0.1	-3.5	0.7			
47	16	321	4.1939	4.2002	-0.0063	4.1941	-0.1	4.1971	-0.1	0.8	0.9	0.1		4.1957	-0.4	-3.4	0.7			
48	17	341	4.1949	4.1995	-0.0046	4.1957	-0.4	4.1972	0.0	0.4	0.6	0.4		4.1950	-0.7	-3.1	0.5			
49	18	361	4.1935	4.2014	-0.0080	4.1950	-0.7	4.1975	0.2	-0.3	0.0	0.7		4.1969	-0.3	-2.3	-0.2			
50	19	381	4.1964	4.1987	-0.0023	4.1969	-0.3	4.1975	0.3	-0.6	-0.1	0.3		4.1941	0.1	-2.0	-0.4			
51	20	401	4.1943	4.1993	-0.0050	4.1941	0.1	4.1968	0.0	-0.5	0.1	0.1		4.1947	0.2	-2.1	-0.2			
52	21	421	4.1951	4.2016	-0.0065	4.1947	0.2	4.1983	0.9	-0.3	0.4	0.2		4.1970	-1.0	-2.3	0.1			
53	22	441	4.1951	4.2000	-0.0049	4.1970	-1.0	4.1976	0.6	-1.3	-0.4	1.0		4.1955	-1.1	-1.4	-0.8			
54	23	461	4.1932	4.1960	-0.0028	4.1955	-1.1	4.1946	-0.9	-2.4	-1.4	1.1		4.1915	-0.2	-0.2	-1.8			
55	24	481	4.1910	4.1918	-0.0008	4.1915	-0.2	4.1914	-2.4	-2.6	-1.5	0.2								

Figure 92. Straightness measurement template (tables)

Intermediate values in Figure 92 are marked grey, forward-run corrected results have blue background, backward-run ones are on red. Basic test results have dark-grey background and final result is on light-violet.

This template can obviously be expanded for different axes.

6.7.2 Graphs

The graphical part of the template consists of one main graph and four subsidiary ones. The main graph contains the averaged straightness profile together with any previous result. It enables clear view of the profiles fitted using least squares method as per Figure 93.

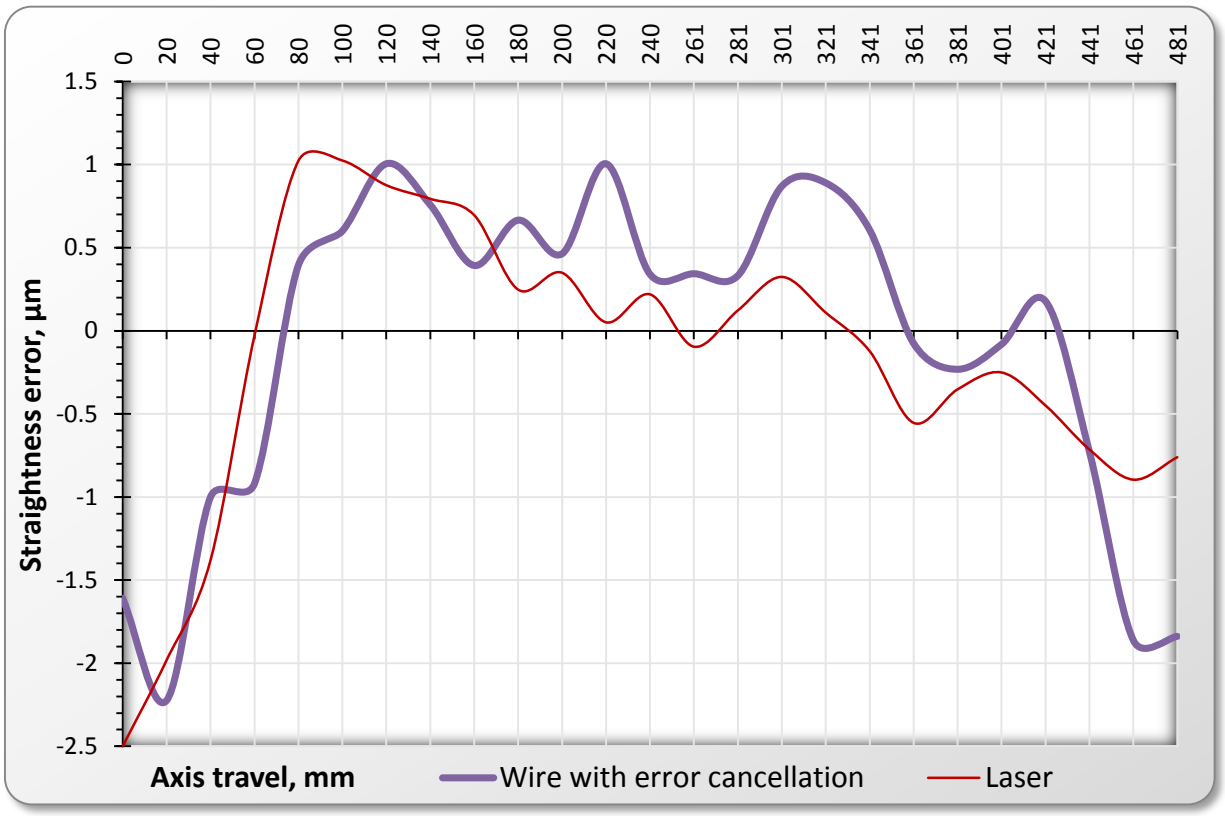

Figure 93. Main graph

Four smaller subsidiary graphs shown in Figure 94 are used to control the measurement: first two display (corrected, not fitted) raw voltage outputs from optical sensors and can be used to determine the amount of physical slope and if there were any significant random errors during a single bi-directional run.

Graph number three displays four error cancelled profiles for averaging and the fourth graph shows the result of bi-directional basic test.

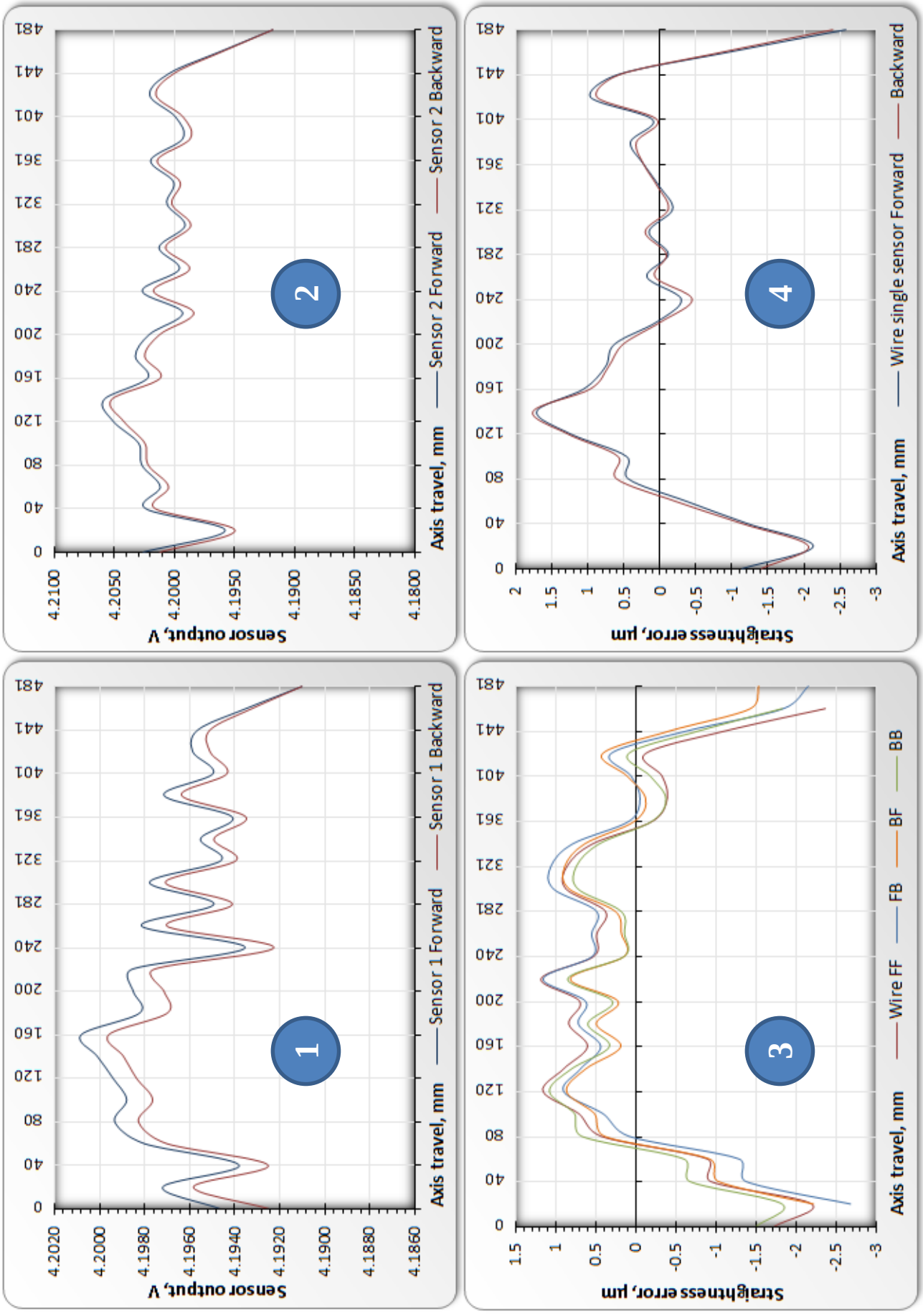

Figure 94. Subsidiary graph set

6.8 INTERPRETATION

The first two graphs show output of both optical sensors without any transformation; this represents the physical quality of system setup including the measured machine itself. This is corrected voltage reading to show repeatability of the whole system within sequential runs, quality of slope removal during the system setup and the quality of the straightness reference.

Both lines on each graph should be as close to each other as possible and ideally both graphs should show the same profile. An example in Figure 94 (1-2) demonstrates almost no slope and slight mismatch of the first sensor readings. This means slight instability of the first channel which is still acceptable as confirmed by experiment.

If the reference wire has a surface defect due to damage during setup, manufacture or overstretching, it is indicated as a spike as indicated in Figure 95.

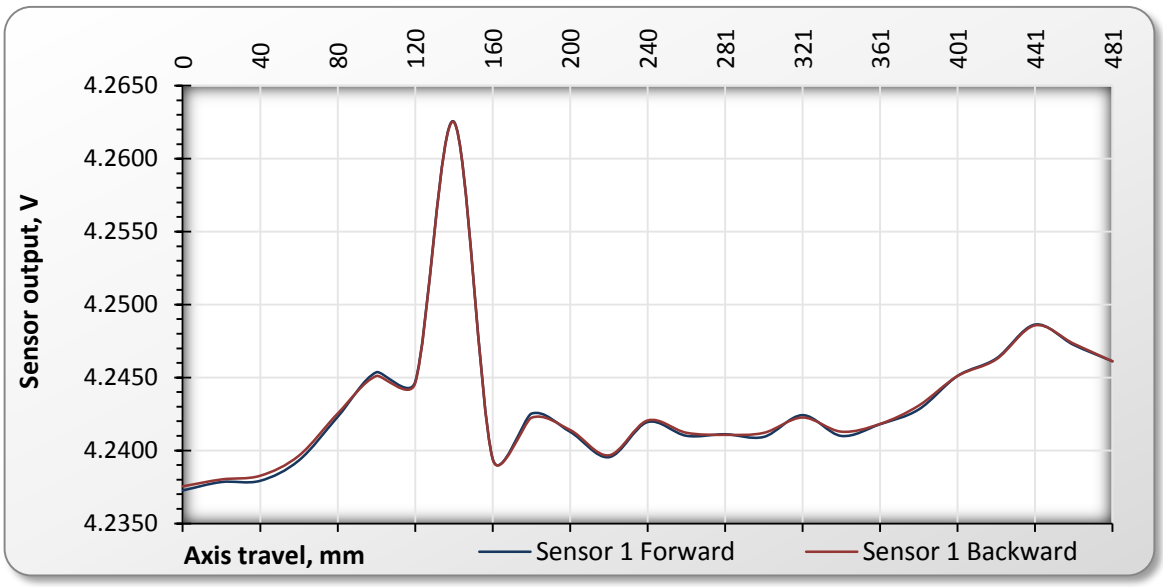

Figure 95. Wire damage indicated

This is normally not acceptable and means that the wire needs to be replaced otherwise the final result will look like in Figure 96.

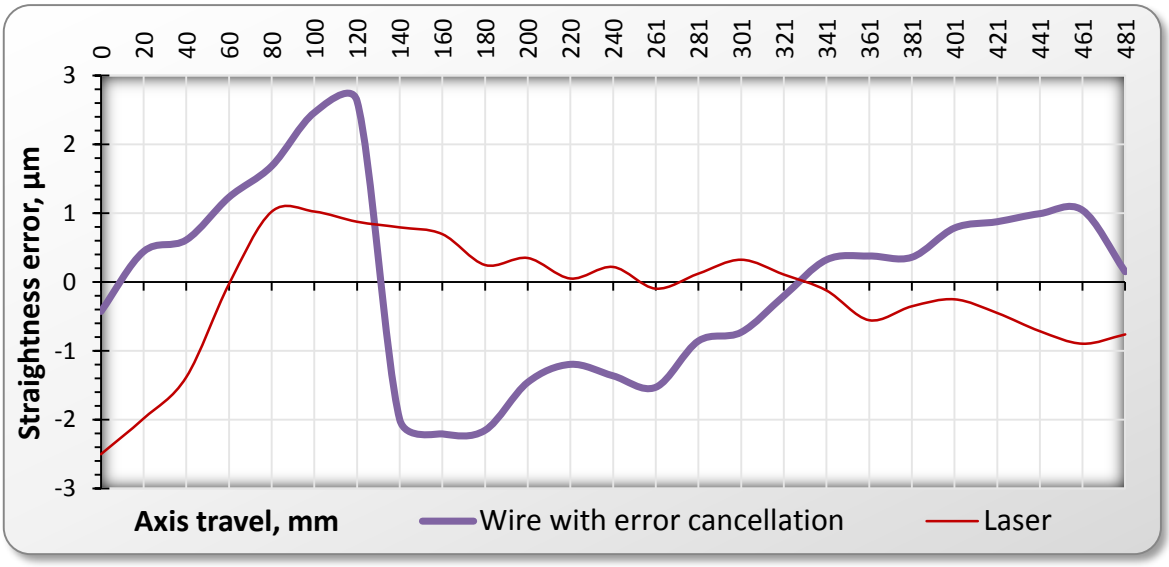

Figure 96. Invalid final result due to the wire damage

The third graph shows level of matching of two bidirectional runs and two directions of error cancellation. Normally all four lines should be close to each other like shown in Figure 94 (3). Significant difference here can indicate step size variability, poor repeatability of the system perhaps due to environmental effects. A typical result with matching outputs is shown in Figure 97.

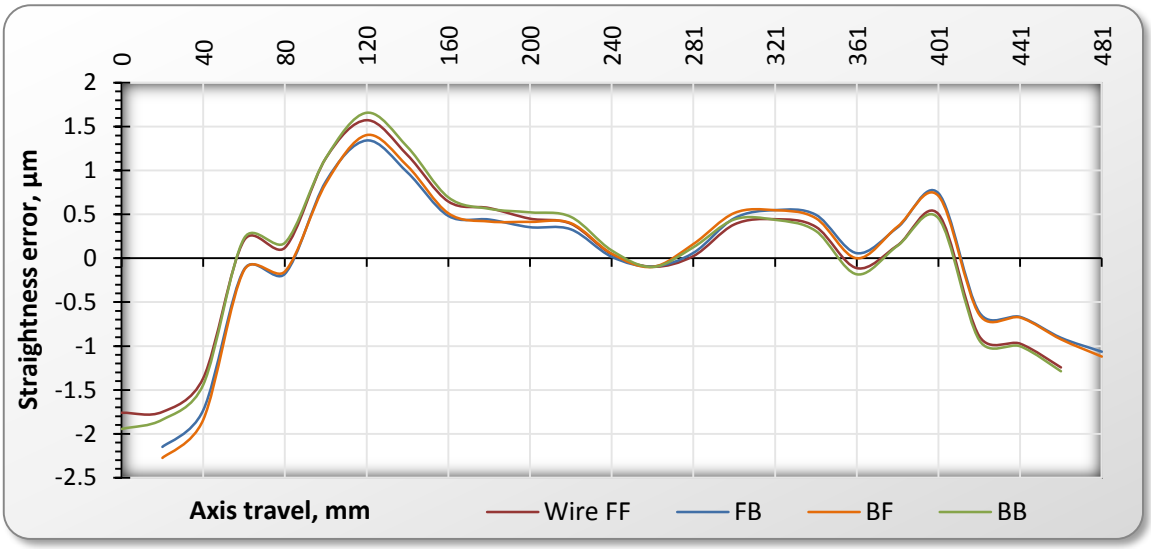

Figure 97. Normal spread of the final result before averaging

Graph number four represents the basic measurement using only one sensor. It allows detection of any problems caused by error cancellation, for example incorrect step size or variation in the velocity of the axis, inadequate number of sampling points, poor reference etc.

This graph becomes a main one in case of long range measurements, when the reference error is negligible compared to the measured one.

6.9 CONCLUSIONS ON DATA MANAGEMENT

Data management during the straightness measurement is based on principles of openness and reconfigurability. It starts from the analogue signal which is then converted to a digital one, transferred over USB interface, processed by data logging utility and then analysed and presented in a spread sheet processor. The entire software solution is flexible, hardware-independent and does not require any special operator skills.

The measurement data is organised in table format, enabling easy manipulation, analysis, storage and presentation. A corresponding template for straightness measurement was designed in Microsoft Excel 2010 where all necessary logic and graphical elements are combined in the same place.

The template provides user-friendly solution helping to visually assess the setup and measurement results, detect faults and validate the final result, full traceability of which ensures clear and reliable data interpretation. Two-channel bi-directional mode is supported throughout the template allowing the use of multiple sensor calibration and reference error cancellation; it can be expanded to a larger number of channels used simultaneously if necessary. The same applies to longer measured axis expansion when no new logic is required for template modification.

CHAPTER 7 | SUMMARY AND CONCLUSIONS

Modern manufacturing industry continues to emphasise the importance of quality in manufactured components. As *quality* is often associated with *accuracy*, tighter dimensional tolerances have to be met as cost effectively as possible. Consequently production machinery, and in particular CNC machine tools, need to become more accurate which can be achieved by improving their design and build quality or through electronic enhancement such as software based error compensation.

In either case various measurement of the machine moving elements are required. Error compensation can be a more cost effective method of improving accuracy as tolerances become difficult to achieve through purely mechanical means. Machine tool axes need to be measured, their imperfections identified and compensating counter-motions applied. This problem has been addressed by a number of volumetric measuring methods developed recently which rely either on direct basic geometric errors measurement or on their estimation.

Due to the fact that modern CNC machine tools have increasing versatility to meet frequent changing of components requirements, increasing complexity of machine configuration and structure, can mean that direct measurement is often the most reasonable solution. Here, however, arise a number of specific problems associated with existing methods. Measurement system utilising laser interferometry and special optics is some of the most commonly used for machine measurement due to the excellent measurement range and good accuracy. However there are issues with the optical beam propagation through the air in workshop conditions, high costs and considerable setup time. These become most significant when using the straightness measuring optics with the laser interferometer.

Research was undertaken to find a straightness reference that had the advantages of optical systems, in particular extensibility, and the advantages of simplicity and low cost of traditional straightedge artefacts. A taut wire, a system typically used on large machines with manual instruments was identified followed by research into a suitable automated measuring system that complemented the wire advantages.

Novel optical system for measuring axis straightness was then developed to address the problems of existing direct measurement methods. Providing a low-cost, simple and efficient solution for measuring straightness motion error of moving axes in any part of the machine workspace. The system fills the void between the high accuracy, but expensive and

environmentally-sensitive laser systems and traditional methods having limited range or portability.

A unique combination of high accuracy, versatility, portability, simplicity, environmental stability and low cost has been established on known taut wire and two-point methods, novel readily available hardware and multi-purpose software means.

The system, consisting of mounting kit, measuring head, data transfer interface and corresponding software has been produced and tested on two different machines in different environments and on axes of different lengths and with different straightness errors. All the test results have been validated using a comparison based on a commercial laser interferometer confirming good correlation even close to the accuracy limits of both methods. Additional performance verification was performed using static stability tests and a detailed uncertainty analysis to provide a more meaningful result for applied measurements.

The measuring procedure has been thoroughly investigated and an optimised methodology explained in detail, including wire preparation, sensor calibration, setup slope removal, number, direction and amount of tests in different conditions. The results show that the system is easy to use; its setup does not change as the measured axis length increases; temperature gradients, airflow and electrical noise do not have a significant effect on it.

7.1 SUMMARY OF NOVEL CONTRIBUTIONS

1. A novel sensing unit employing standard phototransistors capable of measuring the displacement of a cylindrical obscuration object such a wire with high resolution and accuracy.
2. Application of new sensor with traditional taut wire straightness reference to measure straightness error of machine tool axes with performance comparable with existing SoA interferometry method to.
3. The principle of the taut wire method is simple yet very little information existed to quantify the performance of systems utilising such a straightness reference. Wire diameter variation throughout its stretched piece has never been considered. In this thesis, the taut wire method has been investigated quantitatively and uncertainty calculated, testing different wires in different conditions including environment, axis length, straightness errors and linked motion errors including direct comparison with commercial laser interferometers.

4. A unique combination of readily available hardware and software has been proposed as a guarantee of a new level of accuracy and speed of the old taut wire straightness measuring method.

7.2 FUTURE WORK

The system has been developed and a prototype successfully created to validate the performance. During the course of the work, improvements related to performance and efficiency were identified. Future work should be concentrated on research into the method's capability, hardware and software improvements along with further testing with a respect to usability and speed of the system's setup and the measurement itself.

7.2.1 Further research of the method's capability

To rectify the issues with the method, realise the full potential of the method and to improve its capability, a number of research activities are suggested:

1. Looking for alternatives to the fishing wire, stronger and with better diameter consistency.
2. Investigation of the error cancellation behaviour on longer distances.
3. Testing of different distances between the sensors in the measuring head to reduce accumulation.
4. Vertical axes measurement.
5. Microscopic analysis of the wire under tension.

Successful research of second and third objectives would allow to use the method on axes of any length without considerable increase of measurement error due to environmental effects leaving it without alternative .

7.2.2 Implementation

Current implementation aimed to be simple and based on available parts and materials to avoid a no worthy investment. Replacement of hardware parts with specifically manufactured ones would cover the following:

1. Spring clamps holding the wire on both sides.

2. Auto-centering guides for the wire on both sides to prevent its movement in horizontal plane due to length increase and replacement.
3. Set of weights covering the exact range.
4. Lightweight and portable design of the measuring head (electric circuit outside).
5. Fine adjustment carriages with two degrees of freedom built in the stands and the head.
6. Adjustable sensor position (step size).
7. Magnetic base mounting of the measuring head.
8. Basic indication of the sensor catching the wire (a set of lights on the head itself).
9. Wireless interface of the head (rechargeable battery operated).

All listed above will speed up the setup process and make it possible for any kind of a machine and orientation of its axes.

Spring clamps will enable quick fixing and releasing the wire, this will speed up the setting up procedure. Auto-centering guides will keep the wire in place controlled by adjustment carriages only, which will also reduce setup time and associated uncertainty. Weights set will increase portability of the system and make the weight adjustment faster and easier for operator. The electronic circuit moved close to the ADC leaving only the sensors in the measuring head will make it more portable, versatile and easer to mount. Additional and motorised adjustment carriages will enable automatic sensor position adjustment increasing its speed and reliability.

7.2.3 Improving measurement efficiency

Another direction of possible improvement is performance which means more accuracy / less time consumed. This can be achieved by the following measures:

1. Automation of slope removal by using a powered drives for adjustment carriages linked in a loop with sensor feedback.
2. Integrating data capture and data analysis software into the united database tool.
3. Increasing the sensitivity of the head.
4. Integrating an ADC into the control electric circuit.
5. Further research of the “wire expiry” phenomenon.
6. Separate sensor pair’s mounting and fine adjustment for simultaneous two-plane straightness measurement.
7. Faster electric components to enable dynamic measurement.

The most important there are integration and automation measures to simplify the setup procedure and reduce the time spent on it. These improvements will also push the accuracy limit of the system further forward; make the process of measurement more effective and friendly to the end user. Also the result reliability and repeatability will be increased possibly to the level of today's state-of-the-art.

A special attention will be paid to measure five – a number of new tests to separate the affecting factors will be carried out. Other wire diameters and, possibly, materials will be tested with a respect to long term stability. A dual wire design will be tested to use partial reversal implementation. A microscope-based study of wire defects (including those appearing under tension) will also follow.

7.2.4 Multi-degree of freedom system

The high level of sensitivity and stability of the optical system to measure the position of the wire means that it could be possible to use an additional wire aligned parallel and separated by a short distance, for example 50mm, in order to obtain two straightness profiles in two directions. This can be combined with an offset between sensors in the axial direction of 50mm which would provide a measurement of all three angular motion errors of an axis. Additional performance verification would be required to optimize the offset distances etc.

REFERENCES

1. Postlethwaite, S.R., "Electronic based accuracy enhancement of CNC machine tools". PhD thesis, University of Huddersfield, 1992.
2. Schwenke, H., Knapp, W., Haitjema, H., Weckenmann, A., Schmitt, R., Delbressine, F., "Geometric error measurement and compensation of machines – An update", CIRP Annals - Manufacturing Technology, V57, N2, P660-675, 2008.
3. Chen, J.S., Yuan, J.X., Ni, J., Wu, S.M. (University of Michigan), "Thermal error modelling for volumetric error compensation". Sensors and Signal Processing for Manufacturing, V55, P113-125, 1992.
4. Fletcher, S., Longstaff, A.P., Myers, A., "Flexible modelling and compensation of machine tool thermal errors". In: 20th Annual Meeting of American Society for Precision Engineering, Norfolk, VA, 2005
5. Blake, M.D., Ford, D.G., Postlethwaite, S.R., Morton, D., "Analysis of machine tool non-rigid error components", Laser metrology and machine performance II, P297-308, 1995.
6. Ford, D.G., Blake, M.D., Postlethwaite, S.R., "The identification of non-rigid errors in a vertical machining centre", Proceedings of The Institution of Mechanical Engineers, Part B, V213, P555-566, 1999.
7. Bohez, E.L.J., "Compensating for systematic errors in 5-axis NC machining, Computer-Aided Design", V34, N5, P391-403, 2002.
8. Ramesh, R., Mannan, M.A., Poo, A.N., "Error compensation in machine tools - a review: Part I: geometric, cutting-force induced and fixture-dependent errors", International Journal of Machine Tools and Manufacture, V40, N9, P1235-1256, 2000.
9. International Standard ISO 230-1, 'Test code for machine tools – Part 1: Geometric accuracy of machines operating under no-load or finishing conditions', 2012.
10. Oxford English Dictionary: http://www.oed.com accessed at 18 July 2011.
11. Estler, W.T., Edmundson, K.L., Peggs, G.N., Parker, D.H., "Large-Scale Metrology - An Update", CIRP Annals - Manufacturing Technology, **V51**, N2, 587-609, 2002.

12. "University of Huddersfield industrial consultancy report - Geometric error compensation on a large 5-axis gantry machine at GKN Aerospace", University of Huddersfield, May 2009.
13. Yellowhair, J., Burge, J.H., “Measurement of optical flatness using electronic levels”, Opt. Eng., V47, N2, 023604, 2008.
14. Chen, G., Yuan, J., Ni, J., “A displacement measurement approach for machine geometric error assessment”, International Journal of Machine Tools and Manufacture, V41, N1, P149-161, 2001.
15. Soons, J.A., “Analysis of the Step-diagonal Test”, Proceedings of Lamdamap VII Conference, P126-137, 2005.
16. Chapman, M.A.V., “Limitations of laser diagonal measurements”, Precision Engineering, V27, N4, P401-406, 2003.
17. Ibaraki, S., Knapp, W., “Indirect Measurement of Volumetric Accuracy for Three-Axis and Five-Axis Machine Tools. A Review” Int J of Automation Technology, V6, N2, P110-124, 2012.
18. Florussen, G.H.J., Delbressine, F.L.M., van de Molengraft, M.J.G., Schellekens, P.H.J., “Assessing geometrical errors of multi-axis machines by three-dimensional length measurements”, Measurement, V30, N4, P241-255, 2001.
19. Hocken, R.J. and the Machine Tool Task Force, “Machine Acknowledgements Tool Accuracy. Technology of Machine Tools”, Lawrence Livermore National Laboratory, University of California, V5, P1-85, 1980.
20. Schmitz, T.L., Ziegert, J.C., Canning, S.J., Zapata, R., “Case study: A comparison of error sources in high-speed milling”, Precision Engineering, V32, N2, P126-133, 2008.
21. International Standard ISO 230-3, ‘Test code for machine tools – Part 3: Determination of thermal effects’, 2007.
22. Fletcher, S., Longstaff, A.P., Myers, A., “Defining and Computing Machine Tool Accuracy”, Laser Metrology and Machine Performance. Euspen Ltd, Euspen Headquarters, Cranfield University, P77-86, 2009.
23. Huang, P.S., Kiyono, S., Kamada, O., "Angle measurement based on the internal-reflection effect: a new method", Appl. Opt. V31, P6047-6055, 1992.

24. Rahman, M., Heikkala, J., Lappalainen, K., “Modeling, measurement and error compensation of multi-axis machine tools. Part I: theory”, International Journal of Machine Tools & Manufacture, V40, P1535-1546, 2000.

25. Schwenke, H., Franke, M., Hannaford, J., Kunzmann, H., “Error mapping of CMMs and machine tools by a single tracking interferometer”, CIRP Annals - Manufacturing Technology, V54, N1, P475-478, 2005.

26. Pahk, H.J. Kim, Y.S., Moon, J.H., “A new technique for volumetric error assessment of CNC machine tools incorporating ball bar measurement and 3D volumetric error model”, International Journal of Machine Tools and Manufacture, V37, N11, P1583-1596, 1997.

27. Wang S.M., Ehmann, K.F., “Measurement methods for the position errors of a multi-axis machine. Part 1: principles and sensitivity analysis”, International Journal of Machine Tools & Manufacture, V39, P951-964, 1999.

28. International Standard ISO 230-6, ‘Test code for machine tools – Part 6: Diagonal displacement tests’, 2007.

29. Longstaff, A.P., Fletcher, S., Poxton, A., Myers, A., “Comparison of Volumetric Analysis Methods for Machine Tools with Rotary Axes”, Laser Metrology and Machine Performance P87-96, 2009.

30. Lei, W.T., Hsu, Y.Y., “Accuracy test of five-axis CNC machine tool with 3D probe-ball. Part I: design and modelling”, International Journal of Machine Tools and Manufacture, V42, N10, P1153-1162, 2002.

31. Lei, W.T., Hsu, Y.Y., “Accuracy test of five-axis CNC machine tool with 3D probe-ball. Part II: errors estimation”, International Journal of Machine Tools and Manufacture, V42, N10, P1163-1170, 2002.

32. Ibaraki, S., Sawada, M., Matsubara, A., Matsushita, T., “Machining tests to identify kinematic errors on five-axis machine tools”, Precision Engineering, V34, N3, P387-398, 2010.

33. Cho, M.W., Seo, T.I., Kwon, H.D., “Integrated error compensation method using OMM system for profile milling operation”, Journal of Materials Processing Technology, V136, N1-3, P88-99, 2003.

34. Cho, M.W., Kim, G.H., Seo, T.I., Hong, Y.C., Cheng, H.H., “Integrated machining error compensation method using OMM data and modified PNN algorithm”, International Journal of Machine Tools and Manufacture, V46, N12-13, P1417-1427, 2006.

35. Ford, D.G., Postlethwaite, S.J.R., Allen, J.P., Blake, M.D., “Compensation algorithms for the real-time correction of time and spatial errors in a vertical machining centre”, Proceedings of the Institution of Mechanical Engineers. Part B. Journal of engineering manufacture, V214, N3, P221-234, 2000.

36. Fletcher, S., Postlethwaite, S.R., Ford, D.G., “Volumetric compensation through the machine controller”, LAMDAMAP, N5, P321-330, 2001.

37. Longstaff, A.P., Fletcher, S., Myers, A., Ford, D., “Volumetric compensation of machine tools makes geometric errors negligible”, 3rd International Congress on Precision Machining, N3, P209-216, 2005.

38. Sartori, S., Zhang, G.X., “Geometric Error Measurement and Compensation of Machines”, CIRP Annals - Manufacturing Technology, V44, N2, P599-609, 1995.

39. Barakat, N.A., Elbestawi, M.A., Spence, A.D., “Kinematic and geometric error compensation of a coordinate measuring machine”, International Journal of Machine Tools and Manufacture, V40, N6, P833-850, 2000.

40. Chen, J.S., Kou, T.W., Chiou, S.H., “Geometric error calibration of multi-axis machines using an auto-alignment laser interferometer”, Precision Engineering, V23, N4, P243-252, 1999.

41. Ni, J., Wu, S.M., “An On-Line Measurement Technique for Machine Volumetric Error Compensation”, ASME Transaction, Journal of Engineering for Industry, V115, N1, P85-92, 1993.

42. Bridges, B., White, D., “Laser trackers: a new breed of CMM”, A Quality Digest, V18, N2, P41-44, 1998.

43. Lin, C.C., Her, J.L., “Calibrating the volumetric errors of a precision machine by a laser tracker system”, The International Journal of Advanced Manufacturing Technology, N26, P1255-1267, 2005.

44. Balsamo, A., Pedone, P., Ricci, E., Verdi, M., “Low-cost interferometric compensation of geometrical errors”, CIRP Annals - Manufacturing Technology, V58, N1, P459-462, 2009.

45. Bringmann, B., Besuchet, J.P., Rohr, L., “Systematic evaluation of calibration methods”, CIRP Annals - Manufacturing Technology, V57, N1, P529-532, 2008.

46. Bringmann, B., Knapp, W., “Machine tool calibration: Geometric test uncertainty depends on machine tool performance”, Precision Engineering, V33, N4, P524-529, 2009.

47. Fletcher, S., Longstaff, A.P., Myers, A., “Investigation into the accuracy of a proposed laser diode based multilateration machine tool calibration system”, Journal of Physics: Conference Series, N13, P398, 2005.

48. Fan, K.C., Chen, M.J., Huang W.M., “A six-degree-of-freedom measurement system for the motion accuracy of linear stages”, International Journal of Machine Tools and Manufacture, V38, N3, P155-164, 1998.

49. Fan, K.C., Zhao, Y., “A laser straightness measurement system using optical fiber and modulation techniques”, International Journal of Machine Tools and Manufacture, V40, N14, P2073-2081, 2000.

50. HP 5528A Laser Measuerment System Users Manual: https://www.surplex.com/en/m/7/hewlett-packard-hp-5528-a-hp-laser-measuring-system-121597.html accessed at 20 January 2014.

51. Lin, S.T., “A laser interferometer for measuring straightness”, Optics & Laser Technology, V33, N3, P195-199, 2001.

52. Feng, Q., Zhang, B., Kuang, C., “A straightness measurement system using a single-mode fiber-coupled laser module”, Optics & Laser Technology, V36, N4, P279-283, 2004.

53. Kuang, C., Feng, Q., Zhang, B., Liu, B., Chen, S., Zhang, Z., “A four-degree-of-freedom laser measurement system (FDMS) using a single-mode fiber-coupled laser module”, Sensors and Actuators A: Physical, V125, N1, P100-108, 2005.

54. Zhu, L.J., Li, L., Liu, J.H., Zhang, Z.H., “A method for measuring the guideway straightness error based on polarized interference principle”, International Journal of Machine Tools and Manufacture, V49, N3-4, 285-290, 2009.

55. Schwenke, H., Neuschaefer-Rube, U., Pfeifer, T., Kunzmann, H., “Optical Methods for Dimensional Metrology in Production Engineering”, CIRP Annals - Manufacturing Technology, V51, N2, P685-699, 2002.

56. Peggs, G.N., Maropoulos, P.G., Hughes, E.B., Forbes, A.B., Robson, S., Ziebart, M., Muralikrishnan, B., "Recent developments in large-scale dimensional metrology", Proceedings of the Institution of Mechanical Engineers, Part B: Journal of Engineering Manufacture, V223 (B6), P571-595, 2009.

57. You, F., Zhang, B., Feng, Q., "A novel laser straightness measurement method with beam bend compensation", Optik - International Journal for Light and Electron Optics, V122, N17, P1530-1534, 2011.

58. Knapp, W., "Measurement Uncertainty and Machine Tool Testing", CIRP Annals - Manufacturing Technology, V51, N1, P459-462, 2002.

59. Magalini, A., Vetturi, D., "Laser interferometry for straightness measurements in a weakly controlled environment", XVIII IMEKO World Congress, Metrology for a Sustainable Development, Rio de Janeiro, Brazil, P17-22, 2006.

60. Liotto, G., Wang, C., "Straightness measurement of a long guide way comparison of dual-beam laser technique and optical collimator", International Symposium on Precision Mechanical Measurements (ISPMM'2004), Beijing, China, P24-28, 2004.

61. Campbell, A., "Measurement of lathe Z-slide straightness and parallelism using a flat land", Precision Engineering, V17, N3, P207-210, 1995.

62. Lee, J.H., Yang, S.H., "Measurement of geometric errors in a miniaturized machine tool using capacitance sensors", Journal of Materials Processing Technology, V164-165, P1402-1409, 2005.

63. Lee, J.H., Liu, Y., Yang, S.H., "Accuracy improvement of miniaturized machine tool: Geometric error modeling and compensation", International Journal of Machine Tools and Manufacture, V46, N12–13, P1508-1516, 2006.

64. Zang, Y.F., Liu, X.Y., "Method for the straightness measurement of vertical guideways of machine tools using capacitive and inductive sensors", Proc. SPIE 2101, Measurement Technology and Intelligent Instruments, 843, P843, 1993.

65. Pahk, H.J., Park, J.S., Yeo, I., "Development of straightness measurement technique using the profile matching method", International Journal of Machine Tools and Manufacture, V37, N2, P135-147, 1997.

66. Tozawa, K., Sato, H., Komazaki, M., O-Hori, M., "Correlation of the Straightness of Machine Tool with Machined Accuracy", Prep. JSME, P790-17, 1979.

67. Tanaka, H., Tozawa, K., Sato, H., O-hori, M., Sekiguchi, H., Taniguchi, N., "Application of a New Straightness Measurement Method to Large Machine Tool", CIRP Annals - Manufacturing Technology, V30, N1, P455-459, 1981.

68. Tozawa, K., Sato, H., O-Hori, M., "A new method for the measurement of the straightness of machine tools and machined work", Trans ASME J Mech Design, V104, P587–592, 1982.

69. Tanaka, H., Sato, H., "Extensive analysis and development of straightness measurement by sequential-two-points method", Trans ASME J Eng Ind, V108, P176-182, 1986.

70. Yin, Z., Li, S., "High accuracy error separation technique for on-machine measuring straightness", Precision Engineering, V30, N2, P192-200, 2006.

71. Okuyama, E., Akata, H., Ishikawa, H., "Multi-probe method for straightness profile measurement based on least uncertainty propagation (2nd report) - Two-point method considering cross-axis translational motion, pitch motion and sensor's random error", Precision Engineering, V34, N4, P683-691, 2010.

72. Hwang, J., Park, C.H., Gao, W., Kim, S.W., "A three-probe system for measuring the parallelism and straightness of a pair of rails for ultra-precision guideways", International Journal of Machine Tools and Manufacture, V47, N7-8, P1053-1058, 2007.

73. Salsbury, J.G., Hocken, R.J., "Taut wire straightedge reversal artefact", Initiatives of Precision Engineering at the Beginning of a Millennium, V3, P644-648, 2002.

74. Micro Sensing Devices Data Book: http://www.omron.com/ecb/products/pdf/en-ph_micro_info.pdf accessed at 13 December 2013.

75. Micro Sensing Devices Data Book (EE-SX1096): http://www.omron.com/ecb/products/pdf/en-ee_sx1096.pdf accessed at 13 December 2013.

76. Lockwood, E.H., "Chapter 13: The Tractrix and Catenary". A Book of Curves. Cambridge University Press, P122, 1961.

77. Knapp, W., "Measurement Uncertainty and Machine Tool Testing", CIRP Ann-Manuf Technol, V51, N1, P459-462, 2002.

78. International Standard ISO 230-9, 'Test code for machine tools – Part 9: Estimation of measurement uncertainty for machine tool tests according to series ISO 230, basic equations', 2005.

APPENDIX A | LIST OF PUBLICATIONS

1. Borisov, O., Fletcher, S., Longstaff, A.P., Myers, A., "New low cost sensing head and taut wire method for automated straightness measurement of machine tool axes", Optics and Lasers in Engineering, V51, N8, P978-985, 2013.

2. Borisov, O., Fletcher, S., Longstaff, A.P., Myers, A., "Performance evaluation of a new taut wire system for straightness measurement of machine tools", Precision Engineering, V38, P492-498, 2014.

5528A Laser Measurement System

Compensation
Maximum Compensation Update Time: 2.5s Typical
(Combined VOL and Material Temperature Compensation)

Velocity of Light (VOL) Compensation:

Manual: Compensation factor is entered via keyboard Range: 0.0 to 999.9 ppm
Automatic: Requires Agilent 10751A/B Air Sensor. Displays of pressure, temperature, relative humidity setting and computed VOL are provided on the Agilent 5508A.

Material Temperature Compensation:

Manual: User entered via keyboard Range: 0 - 50 degrees C (32 - 122 degrees F)
Automatic: Requires 1 to 3 Agilent 10757A/B/C Material Temperature Sensors.
Display of individual readings and average of all connected sensors is provided on the Agilent 5508A. Average value is used in all calculations.

System Operating Characteristics

Unit Selection: Rear panel switch selects Metric (millimeters, degree C) or English (inches, degree F) units for all displays and data entry.

Update Rates (Nominal):
Measurement data is updated at the following average rates:

Measurement	Auto Record	GPIB Triggered
Distance	40/s	20/s
Velocity	30/s	15/s
Angle, Straightness	25/s	12/s
Not Maximum Resolution	25/s	25/s
Maximum Resolution	5/s	5/s

Maximum data output rate via HP-IB equals the Update Rate for the measurement in process.

Preset Capability:
Measurements can be preset to user selected values within the ranges shown. Presets either add or multiply as indicated.

Measurement	Metric	English	Math Function
Distance	-50000 to +50000 mm	-2000 to +2000 in.	Add
Velocity	-20000 to +20000mm/min	720 to +720 in/min	Add
Angle	0 to 2	0 to 2	Multiply
Straightness	0 to 3	0 to 3	Multiply

Auto Record: Outputs value currently displayed at fixed intervals of time selected by the user.
Range: 0.05 to 12.0 s in increments of 0.05 s, typical

Remote Control Unit:
RESET, RECORD BUTTONS and BEAM STRENGTH indicator for initiating data output from up to 15 m away fromthe Agilent 5508A Measurement Display Unit. Supplied with Agilent 5508A.

Data Smoothing:
Smoothing (averaging) to reduce the effects of vibration and noise is automatically applied to all displayed measurement data. Smoothing can be turned off if desired via keyboard entry.

NI 9229/9239 Specifications

The following specifications are typical for the range –40 to 70 °C unless otherwise noted. All voltages are relative to the AI– signal on each channel unless otherwise noted.

Input Characteristics

Number of channels ..... 4 analog input channels

ADC resolution ..... 24 bits

Type of ADC ..... Delta-Sigma (with analog prefiltering)

Sampling mode ..... Simultaneous

Data rate range (f_s)

Minimum ..... 1.613 kS/s

Maximum ..... 50 kS/s

Data rates (f_s) ..... $\frac{50\text{kS/s}}{n}$, n = 1, 2, ... 31.

NATIONAL INSTRUMENTS

Master timebase (internal)

Frequency ..... 12.8 MHz

Accuracy ..... ±100 ppm max

Operating voltage ranges

	Measurement Voltage, AI+ to AI–		
	Nominal (V)	Typical (V)	Minimum (V)
NI 9229	±60	±62.64	±61.5
NI 9239	±10	±10.52	±10.3

Overvoltage protection ..... ±100 V

Input coupling ..... DC

Input impedance (AI+ to AI–) ..... 1 MΩ

Accuracy, NI 9229

Error	Percent of Reading (Gain Error)	Percent of Range* (Offset Error)
Calibrated max (–40 to 70 °C)	±0.13%	±0.05%
Calibrated typ (25 °C, ±5 °C)	±0.03%	±0.008%
Uncalibrated max (–40 to 70 °C)	±1.2%	±0.55%
Uncalibrated typ (25 °C, ±5 °C)	±0.3%	±0.11%
* Range equals 62.64 V		

Accuracy, NI 9239

Error	Percent of Reading (Gain Error)	Percent of Range* (Offset Error)
Calibrated max (–40 to 70 °C)	±0.13%	±0.05%
Calibrated typ (25 °C, ±5 °C)	±0.03%	±0.008%
Uncalibrated max (–40 to 70 °C)	±1.4%	±0.67%
Uncalibrated typ (25 °C, ±5 °C)	±0.3%	±0.11%
* Range equals 10.52 V		

Input noise

NI 9229 ..... 320 μV_{rms}

NI 9239 ..... 70 μV_{rms}

Stability

Gain drift ..... ±5 ppm/°C

Offset drift

NI 9229 ..... ±150 µV/°C

NI 9239 ..... ±24 µV/°C

Post calibration gain match
(ch-to-ch, 20 kHz)..... 0.22 dB max

Crosstalk (1 kHz)..... –130 dB

Phase mismatch (ch-to-ch)

NI 9229..... 0.045°/kHz max

NI 9239..... 0.075°/kHz max

Phase mismatch (module-to-module, max)

NI 9229..... $0.045°/kHz + 360° \cdot f_{in}/M_{clk}$[1]

NI 9239..... $0.075°/kHz + 360° \cdot f_{in}/M_{clk}$[1]

Phase nonlinearity (f_s = 50 kS/s)..... 0.11° max

Input delay

NI 9229..... $38.4/f_s + 2.6$ µs

NI 9239..... $38.4/f_s + 3$ µs

Passband

Frequency ..... $0.453 \cdot f_s$

Flatness (f_s = 50 kS/s) ..... ±100 mdB max

[1] M_{clk} is the master timebase.

Stopband

Frequency ..... $0.547 \cdot f_s$

Rejection..... 100 dB

Alias-free bandwidth ..... $0.453 \cdot f_s$

–3 dB prefilter bandwidth
(f_s = 50 kS/s)..... 24.56 kHz

CMRR (f_{in} = 60 Hz)

NI 9229..... 116 dB

NI 9239..... 126 dB

SFDR (1 kHz, –60 dBFS)..... –128 dBFS

Total Harmonic Distortion (THD)

1 kHz, –1 dBFS ..... –99 dB

1 kHz, –20 dBFS ..... –105 dB

MTBF ..... 662,484 hours at 25 °C; Bellcore Issue 6, Method 1, Case 3, Limited Part Stress Method

Photomicrosensor (Transmissive)
EE-SH3 Series

■ Dimensions

Note: All units are in millimeters unless otherwise indicated.

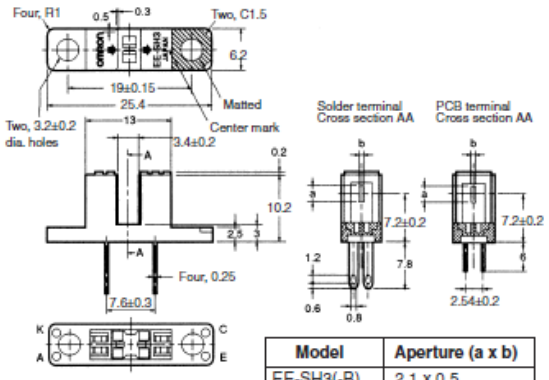

Model	Aperture (a x b)
EE-SH3(-B)	2.1 x 0.5
EE-SH3-C(S)	2.1 x 1.0
EE-SH3-D(S)	2.1 x 0.2
EE-SH3-G(S)	0.5 x 2.1

Internal Circuit

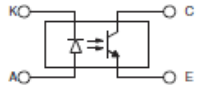

Terminal No.	Name
A	Anode
K	Cathode
C	Collector
E	Emitter

Unless otherwise specified, the tolerances are as shown below.

Dimensions	Tolerance
3 mm max.	±0.2
3 < mm ≤ 6	±0.24
6 < mm ≤ 10	±0.29
10 < mm ≤ 18	±0.35
18 < mm ≤ 30	±0.42

■ Features

- High-resolution model with a 0.2-mm-wide or 0.5-mm-wide sensing aperture, high-sensitivity model with a 1-mm-wide sensing aperture, and model with a horizontal sensing aperture are available.
- Solder terminal models: EE-SH3/-SH3-CS/-SH3-DS/-SH3-GS
- PCB terminal models: EE-SH3-B/-SH3-C/-SH3-D/-SH3-G
- RoHS Compliant.

■ Absolute Maximum Ratings (Ta = 25°C)

Item		Symbol	Rated value
Emitter	Forward current	I_F	50 mA (see note 1)
	Pulse forward current	I_{FP}	1 A (see note 2)
	Reverse voltage	V_R	4 V
Detector	Collector–Emitter voltage	V_{CEO}	30 V
	Emitter–Collector voltage	V_{ECO}	---
	Collector current	I_C	20 mA
	Collector dissipation	P_C	100 mW (see note 1)
Ambient temperature	Operating	T_{opr}	–25°C to 85°C
	Storage	T_{stg}	–30°C to 100°C
Soldering temperature		T_{sol}	260°C (see note 3)

Note: 1. Refer to the temperature rating chart if the ambient temperature exceeds 25°C.
2. The pulse width is 10 μs maximum with a frequency of 100 Hz.
3. Complete soldering within 10 seconds.

■ Ordering Information

Description	Aperture (a x b)	Model
Photomicrosensor (transmissive)	2.1 x 0.5	**EE-SH3(-B)**
	2.1 x 1.0	**EE-SH3-C(S)**
	2.1 x 0.2	**EE-SH3-D(S)**
	0.5 x 2.1	**EE-SH3-G(S)**

■ Electrical and Optical Characteristics (Ta = 25°C)

Item		Symbol	Value				Condition
			EE-SH3(-B)	EE-SH3-C(S)	EE-SH3-D(S)	EE-SH3-G(S)	
Emitter	Forward voltage	V_F	1.2 V typ., 1.5 V max.				I_F = 30 mA
	Reverse current	I_R	0.01 μA typ., 10 μA max.				V_R = 4 V
	Peak emission wavelength	λ_P	940 nm typ.				I_F = 20 mA
Detector	Light current	I_L	0.5 to 14 mA typ.	1 to 28 mA typ.	0.1 mA min.	0.5 to 14 mA	I_F = 20 mA, V_{CE} = 10 V
	Dark current	I_D	2 nA typ., 200 nA max.				V_{CE} = 10 V, 0 *lx*
	Leakage current	I_{LEAK}	---				---
	Collector–Emitter saturated voltage	$V_{CE\ (sat)}$	0.1 V typ., 0.4 V max.		---	0.1 V typ., 0.4 V max.	I_F = 20 mA, I_L = 0.1 mA
	Peak spectral sensitivity wavelength	λ_P	850 nm typ.				V_{CE} = 10 V
Rising time		tr	4 μs typ.				V_{CC} = 5 V, R_L = 100 Ω, I_L = 5 mA
Falling time		tf	4 μs typ.				

■ Engineering Data

Forward Current vs. Collector Dissipation Temperature Rating

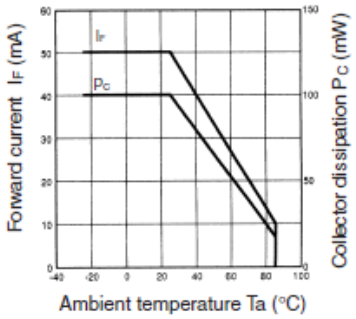

Forward Current vs. Forward Voltage Characteristics (Typical)

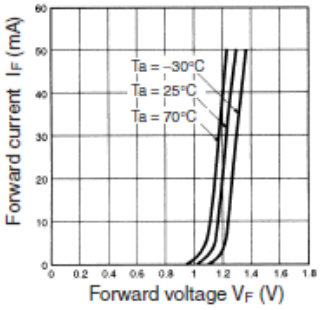

Light Current vs. Forward Current Characteristics (Typical)

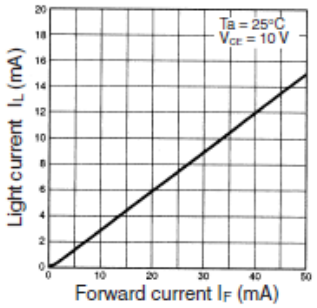

Light Current vs. Collector–Emitter Voltage Characteristics (EE-SH3(-B))

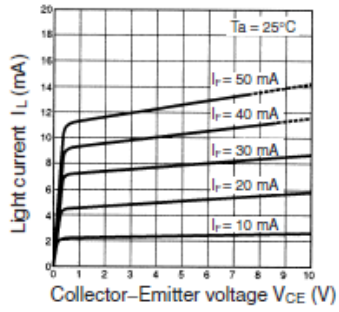

Relative Light Current vs. Ambient Temperature Characteristics (Typical)

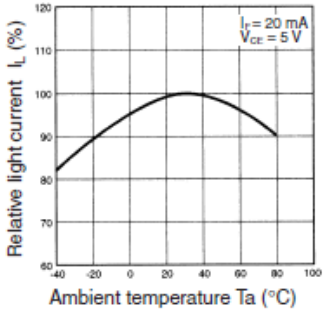

Dark Current vs. Ambient Temperature Characteristics (Typical)

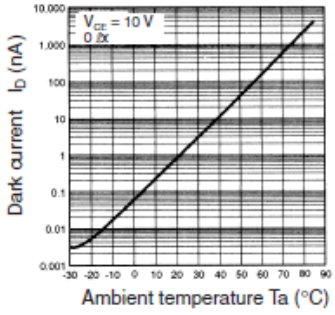

Response Time vs. Load Resistance Characteristics (Typical)

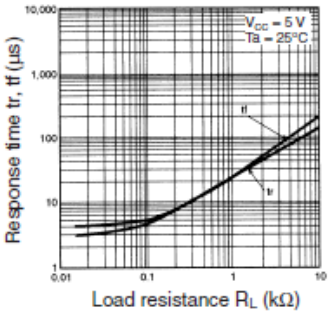

Sensing Position Characteristics (EE-SH3-D(S))

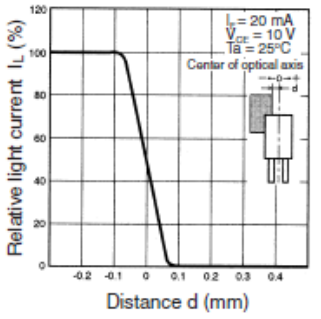

Sensing Position Characteristics (EE-SH3(-B))

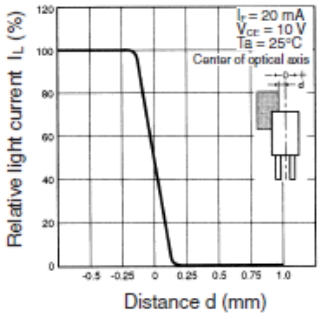

Sensing Position Characteristics (EE-SH3-G(S))

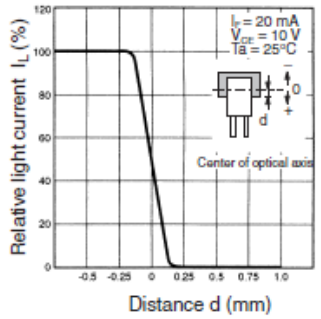

Sensing Position Characteristics (EE-SH3-C(S))

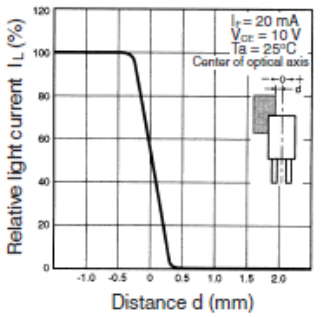

Response Time Measurement Circuit

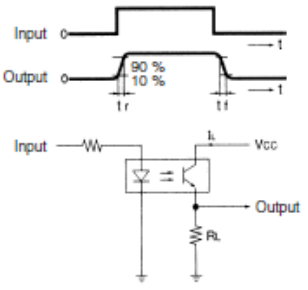

OMRON

Photomicrosensor (Transmissive)
EE-SX1096

⚠ **Be sure to read *Precautions* on page 25.**

■ Dimensions

Note: All units are in millimeters unless otherwise indicated.

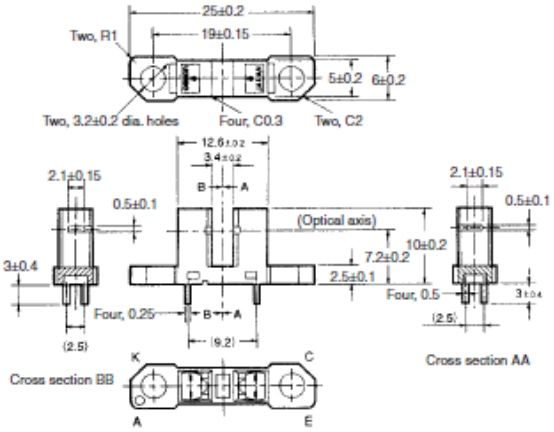

Internal Circuit

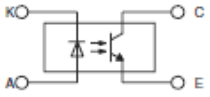

Terminal No.	Name
A	Anode
K	Cathode
C	Collector
E	Emitter

Unless otherwise specified, the tolerances are as shown below.

Dimensions	Tolerance
3 mm max.	±0.3
3 < mm ≤ 6	±0.375
6 < mm ≤ 10	±0.45
10 < mm ≤ 18	±0.55
18 < mm ≤ 30	±0.65

■ Features

- General-purpose model with a 3.4-mm-wide slot.
- Mounts to PCBs or connects to connectors.
- High resolution with a 0.5-mm-wide aperture.
- With a horizontal sensing slot.
- OMRON's XK8-series Connectors can be connected without soldering. Contact your OMRON representative for information on obtaining XK8-series Connectors.

■ Absolute Maximum Ratings (Ta = 25°C)

Item		Symbol	Rated value
Emitter	Forward current	I_F	50 mA (see note 1)
	Pulse forward current	I_{FP}	1 A (see note 2)
	Reverse voltage	V_R	4 V
Detector	Collector–Emitter voltage	V_{CEO}	30 V
	Emitter–Collector voltage	V_{ECO}	---
	Collector current	I_C	20 mA
	Collector dissipation	P_C	100 mW (see note 1)
Ambient temperature	Operating	Topr	–25°C to 85°C
	Storage	Tstg	–30°C to 100°C
Soldering temperature		Tsol	260°C (see note 3)

Note: 1. Refer to the temperature rating chart if the ambient temperature exceeds 25°C.

2. The pulse width is 10 μs maximum with a frequency of 100 Hz.

3. Complete soldering within 10 seconds.

■ Electrical and Optical Characteristics (Ta = 25°C)

Item		Symbol	Value	Condition
Emitter	Forward voltage	V_F	1.2 V typ., 1.5 V max.	I_F = 30 mA
	Reverse current	I_R	0.01 μA typ., 10 μA max.	V_R = 4 V
	Peak emission wavelength	λ_P	940 nm typ.	I_F = 20 mA
Detector	Light current	I_L	0.5 mA min., 14 mA max.	I_F = 20 mA, V_{CE} = 10 V
	Dark current	I_D	2 nA typ., 200 nA max.	V_{CE} = 10 V, 0 lx
	Leakage current	I_{LEAK}	---	---
	Collector–Emitter saturated voltage	V_{CE} (sat)	0.1 V typ., 0.4 V max.	I_F = 20 mA, I_L = 0.1 mA
	Peak spectral sensitivity wavelength	λ_P	850 nm typ.	V_{CE} = 10 V
Rising time		tr	4 μs typ.	V_{CC} = 5 V, R_L = 100 Ω, I_L = 5 mA
Falling time		tf	4 μs typ.	V_{CC} = 5 V, R_L = 100 Ω, I_L = 5 mA

■ Engineering Data

Forward Current vs. Collector Dissipation Temperature Rating

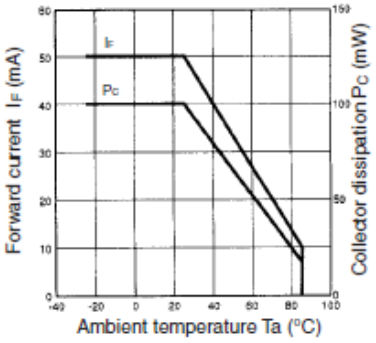

Forward Current vs. Forward Voltage Characteristics (Typical)

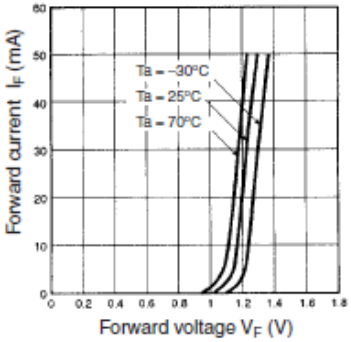

Light Current vs. Forward Current Characteristics (Typical)

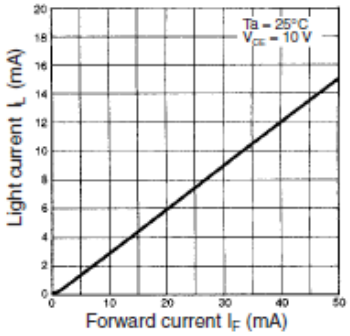

Light Current vs. Collector–Emitter Voltage Characteristics (Typical)

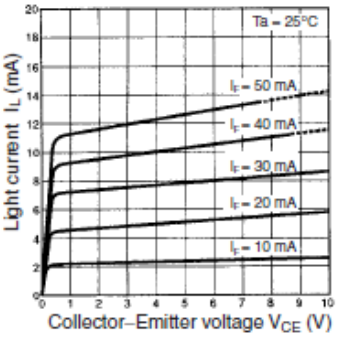

Relative Light Current vs. Ambient Temperature Characteristics (Typical)

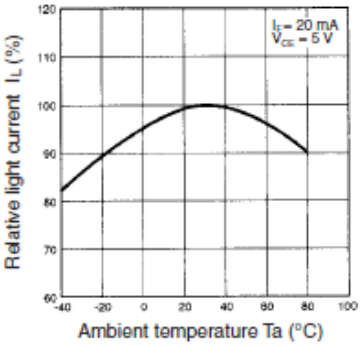

Dark Current vs. Ambient Temperature Characteristics (Typical)

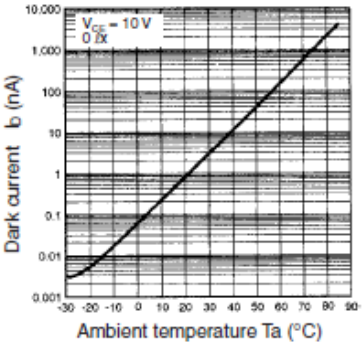

Response Time vs. Load Resistance Characteristics (Typical)

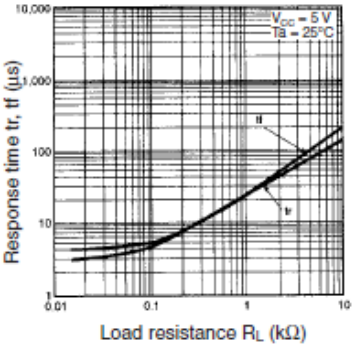

Sensing Position Characteristics (Typical)

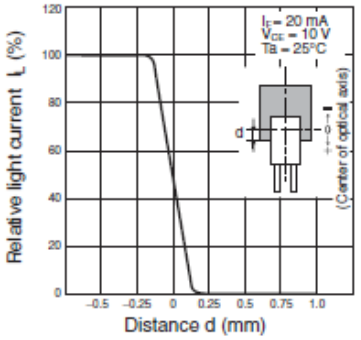

Sensing Position Characteristics (Typical)

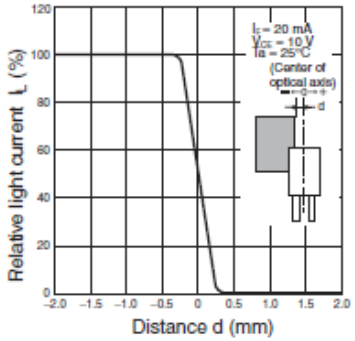

Response Time Measurement Circuit

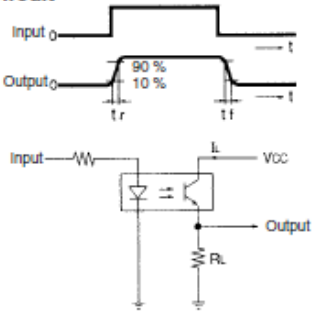

New sensor head circuit diagram

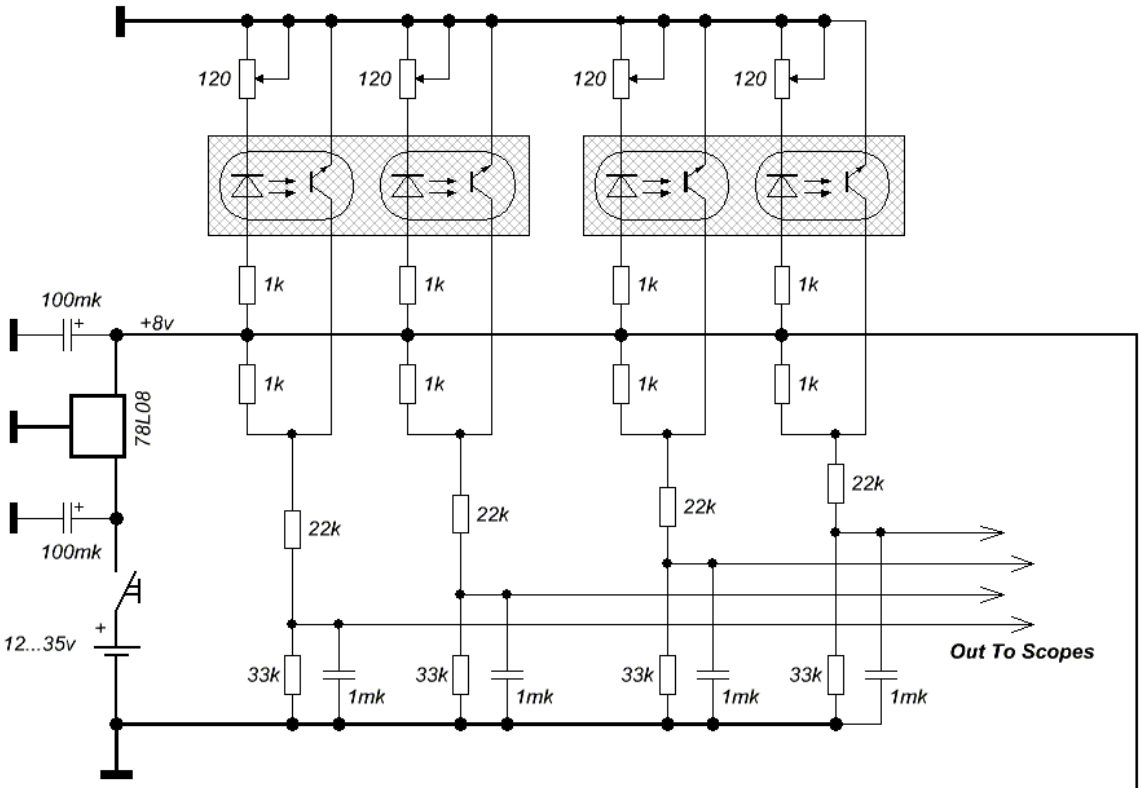

Out C = input A -- input B

Gain = 1+(49.4kOm/Rgain)

(Rgain in kOm)

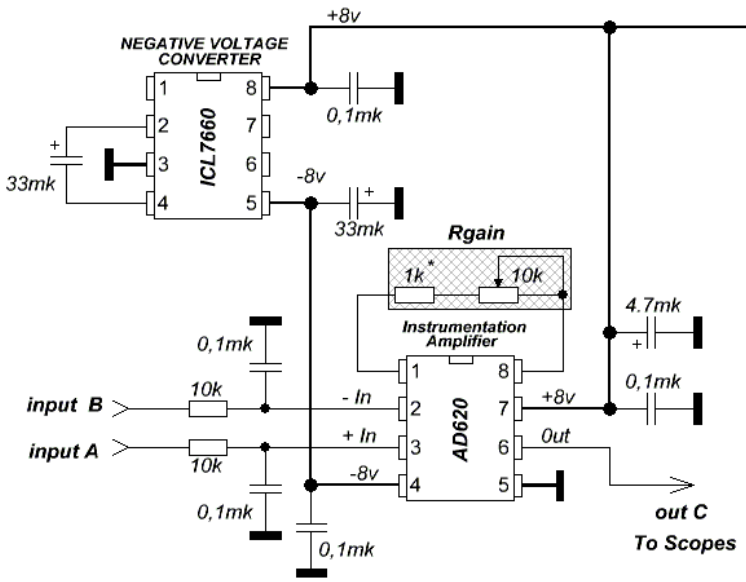

PCB layouts for sensor and comparator boards

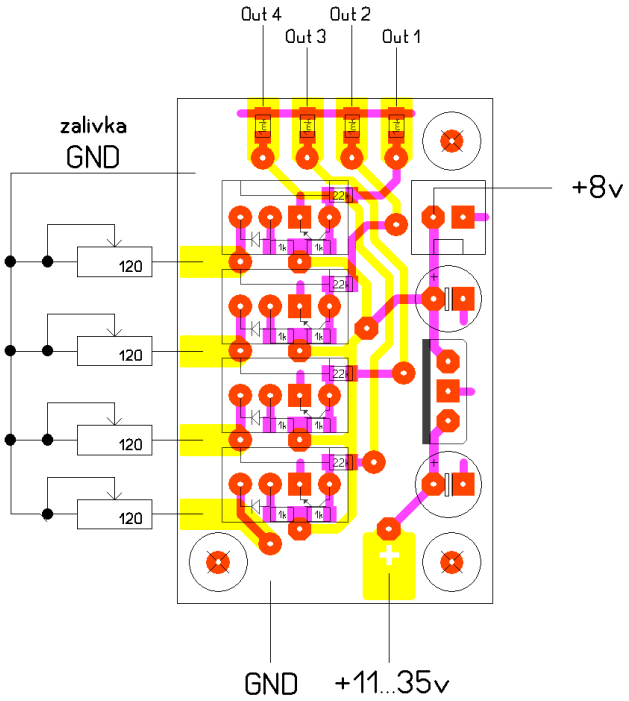

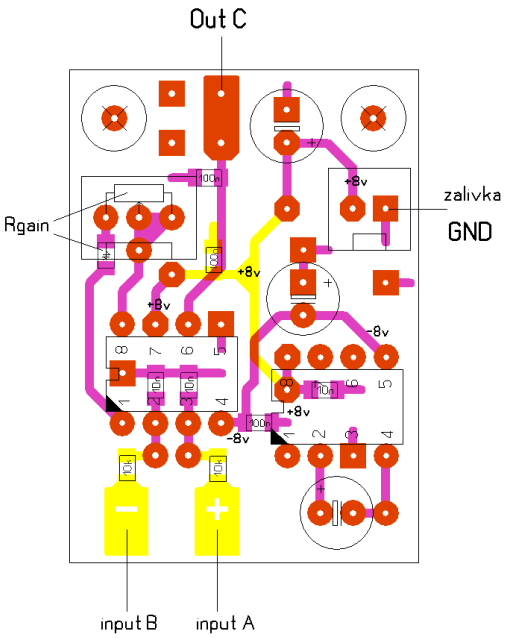

Renishaw XL-80 Specification

Angular

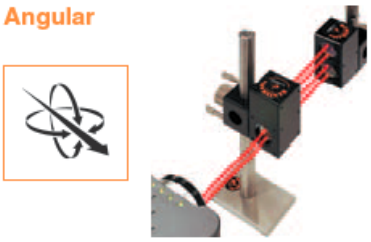

Specification	Metric	Imperial
Axial range	0 m - 15 m	0 in - 590 in
Angular measurement range	±175 mm/m	±10°
Angular accuracy	±0.2%* ±0.5 ±0.1M µm/m	±0.2%* ±0.1 ±0.007F arc sec
Resolution	0.1 µm/m	0.01 arc sec
Where M = measurement distance in metres; F = measurement distance in feet % = percentage of calculated angle * With high accuracy angular optics (± 0.6% with standard optics)		

Rotary

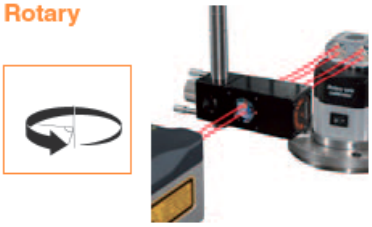

Specification	Metric	Imperial
Angular target range	up to 25 revolutions	
Measurement accuracy (zero at 0°)	±5 µm/m	±1 arc sec
Max axis rotation speed (<5° axis rotation)	Unlimited	
Max axis rotation speed (>5° axis rotation)	10 rpm	
Bluetooth range	Typically 5 - 10 metres	
Orientation	Any	

Flatness

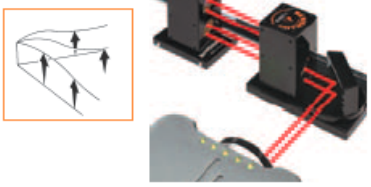

Specification	Metric	Imperial
Axial range	0 m - 15 m	0 in - 590 in
Flatness measurement range	±1.5 mm	±0.06 in
Accuracy	±0.6% ±0.02 M^2 µm	±0.6% ±0.08 F^2 µin
Resolution	0.01 µm	1 µin
Foot spacing	50 mm, 100 mm and 150 mm	2 in, 4 in and 6 in (approx)
Where M = length of the diagonal in metres; F = length of the diagonal in feet; % = percentage of calculated flatness		

Straightness

Specification		Metric	Imperial
Axial range	(short range)	0.1 m - 4.0 m	4 in - 160 in
	(long range)	1 m - 30 m	40 in - 1200 in
Straightness measurement range		±2.5 mm	±0.1 in
Accuracy	(short range)	±0.5% ±0.5 ±0.15 M^2 µm	±0.5% ± 20 ±0.5 F^2 µin
	(long range)‡	±2.5% ±5 ±0.015 M^2 µm	±2.5% ±200 ±0.05 F^2 µin
Resolution	(short range)	0.01 µm	1 µin
	(long range)	0.1 µm	10 µin
Where M = measurement distance in metres; F = measurement distance in feet; % = percentage of displayed value ‡ subject to environmental conditions			

Squareness

Specification		Metric	Imperial
Range		±3/M mm/m	±2000/F arc sec
Accuracy	(short range)	±0.5% ±2.5 ±0.8 M µm/m	±0.5% ±0.5 ±0.05 F arc sec
	(long range)	±0.5% ±2.5 ±0.08 M µm/m	±2.5% ±0.5 ±0.005 F arc sec
Resolution		0.01 µm/m	0.01 arc sec
Where M = measurement distance in metres of the longest axis; F = measurement distance in feet; % = percentage of displayed value			

RK Compact
RK Compact

Ausführung
Version

- **Rechts- *oder* Linksgewinde**
- right *or* lefthand thread

Funktionsprinzip:
Eine Rotationsbewegung der Gewindespindel wird in eine lineare Ausgangsbewegung des Führungsschlittens umgewandelt.

Function:
a rotating movement of the spindle is converted into a linear movement of the guide table.

Standardhübe ab Lager lieferbar
(Rechts-Gewindespindel, Standard)
Standard travel ex stock
(right hand thread, standard)

Type 30: 10, 20, 30, 50 mm
Type 50-120: 25, 50, 75, 100 mm

Code No.	Type	Spindel spindle	Grundlänge* basic length*	Standardhub stand. travel	B1	B2	C	D	F	G	H1	H2
RK Compact mit Gewindespindel RK Compact with metric spindle												
FN_ 3017 TA	30	M5x0,5	59	10,20,30,50	30	16	17	13,5	4,8	M3	8	3,5
FN_ 5023 T_	50	8x1	95	25	50	30,3	23	19	8	M4	13	5
FN_ 8036 T_	80	8x1	144	50 75	80	50,4	36	27	11	M5	20,5	10
FN_ 1246 T_	120	8x1	204	100	120	80,4	46	35	15	M6	26,5	12

Code No.	Type	Spindel spindle	Grundlänge* basic length*	Standardhub stand. travel	B1	B2	C	D	F	G	H1	H2
RK Compact mit Kugelgewindetrieb RK Compact with ball screw spindle												
FO_ 8036 T_	80	8x1	144	–	80	50,4	36	27	11	M5	20,5	10
FO_ 1246 T_	120	8x1	204	–	120	80,4	46	35	15	M6	26,5	12

A = Standard
J = Führungsschlitten m. 1 Klemmhebel
guide table with 1 clamping lever

A = Rechtsgewinde righthand thread
H = Linksgewinde lefthand thread

* Die Grundlänge entspricht der Einheitenlänge ohne Hub.
* The basic length is the length of the unit without travel

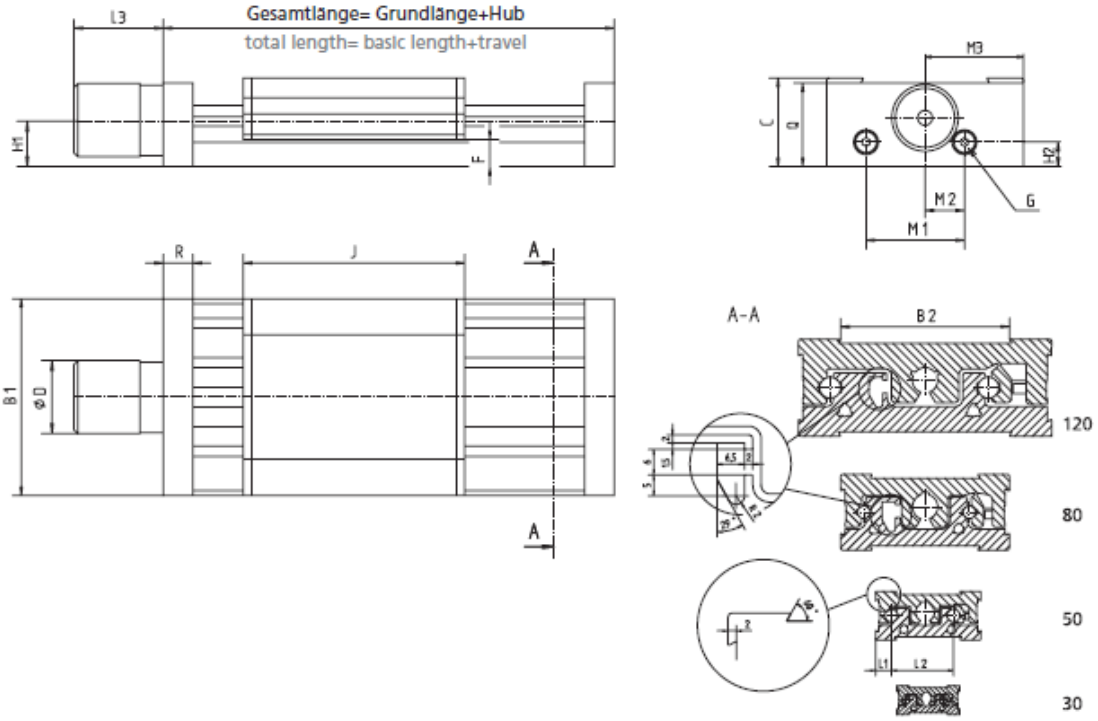

[mm]

J	L1	L2	L3	M1	M2	M3	Q	R	max.Hub max. travel	Masse weight [kg]	
										Grundlänge basic length	pro 100mm Hub per 100 mm travel
45	5	15,8	21	11,6	5,8	17,1	16	7	130	0,08	0,07
75	7,5	29,5	22,5	22	10	26,5	21,5	10	350	0,29	0,18
120	11	50	30,5	40	16	40	34	12	350	0,99	0,33
180	15	75	35,5	61	23	60	44	12	400	2,76	0,67

J	L1	L2	L3	M1	M2	M3	Q	R	max.Hub max. travel	Masse weight [kg]	
										Grundlänge basic length	pro 100mm Hub per 100 mm travel
120	11	50	30,5	40	16	40	34	12	199	0,99	0,33
180	15	75	35,5	61	23	60	44	12	199	2,76	0,67

Bestellbeispiel
RK Compact 50
Rechtsgewinde, ohne Schlittenklemmung
Gesamtlänge 250 mm

Code No. + Länge (Grundlänge+Hub)
FNA 5023 TA 0250

FNA5023TA 0250

Order example
RK Compact 50
Righthand thread, without table clamping
Total length 250 mm

Code No. + length (basic length+travel)
FNA 5023 TA 0250

FNA5023TA 0250

OHAUS Galaxy G110

PERFORMANCE SPECIFICATIONS
(Using External Calibration Procedure)

Weighing Range	0 – 110 g
Readability	0.0001 g
Taring (by subtraction)	0 – 110 g
Precision (std. dev.)	±0.0001 g
Linearity	±0.0002 g
Stabilization Time	3.0 sec
Variable Integration	Selectable
Data Output – RS232	Optional
Pan Size	3.1”
Below Balance Weighing	Standard
Calibration Weight (g)	Built-In
Weighing Chamber	Standard
Dimensions (w × h × d)	7.50“ × 12.90” × 12.75”
Power Supply	100, 120, 220, 240 VAC 50/60 HZ
Weight (net)	21 lb
Operating Temp. Range	10° – 40° C